STRESS-STRAIN RESPONSE OF FABRICS UNDER TWO-DIMENSIONAL LOADING. PART II: LENTICULAR YARN CROSS-SECTION

W. Denney Freeston, Jr., et al

Fabric Research Laboratories, Incorporated

Prepared for:

Army Natick Laboratories

August 1971

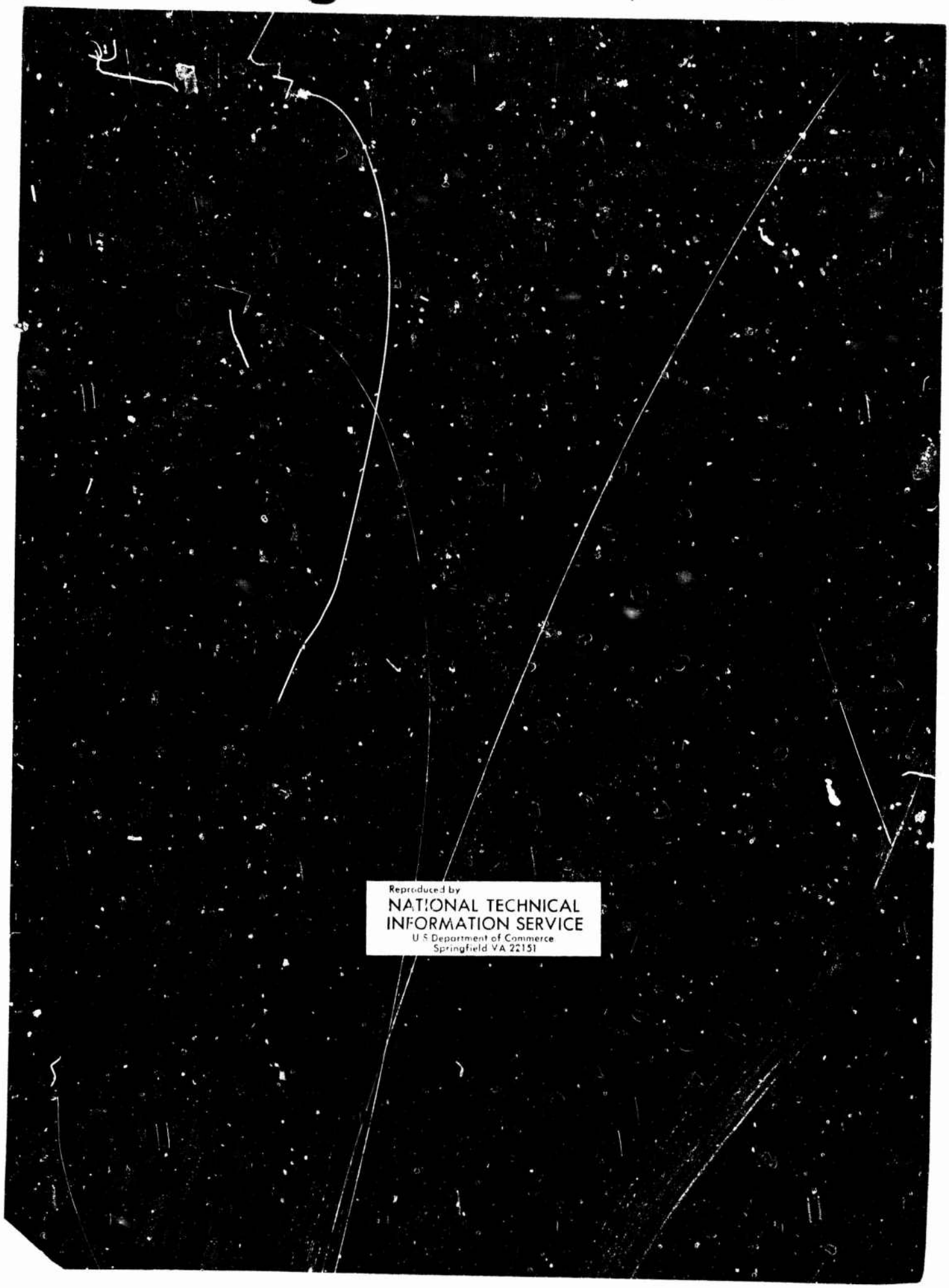

UNCLASSIFIED

Security Classification

DOCUMENT CONTROL DATA - R & D

(Security classification of title, body of abstract and indexing annotation must be entered when the overall report is classified)

1. ORIGINATING ACTIVITY (Corporate author)	2a. REPORT SECURITY CLASSIFICATION
Fabric Research Laboratories, Inc. Dedham, Massachusetts 02026	UNCLASSIFIED 2b. GROUP

3. REPORT TITLE

Stress-strain response of fabrics under two-dimensional loading
Part II: Lenticular yarn cross-section

4. DESCRIPTIVE NOTES (Type of report and inclusive dates)
Technical Report August 1971

5. AUTHOR(S) (First name, middle initial, last name)
W. Denney Freeston, Jr., and Meredith M. Schoppee, Fabric Research Laboratory
Mary Ann Wall, U. S. Army Natick Laboratories

6. REPORT DATE	7a. TOTAL NO. OF PAGES	7b. NO. OF REFS
August 1971	~~195~~ 210	5

8a. CONTRACT OR GRANT NO.	9a. ORIGINATOR'S REPORT NUMBER(S)
DAAG 17-70-C-0030 b. PROJECT NO. 1J662708D503) c. 1J662708DJ40)--36 1J662713DJ40) d.	73-25-GP 9b. OTHER REPORT NO(S) (Any other numbers that may be assigned this report)

10. DISTRIBUTION STATEMENT
Approved for public release; distribution unlimited

11. SUPPLEMENTARY NOTES	12. SPONSORING MILITARY ACTIVITY
Details of illustrations in this document may be better studied on microfiche.	U. S. Army Natick Laboratories Natick, Massachusetts 01760

13. ABSTRACT

A theoretical analysis of the load-elongation behavior of idealized plain-weave fabrics comprised of yarns having a lenticular cross-section and subjected to biaxial stresses is presented. Fabric strains resulting from both crimp interchange and yarn extension are included.

The analytical expressions derived have been solved with a digital computer for both inextensible and linearly elastic materials. Generalized plots of the results are presented for an initial fabric structure with equal crimp distribution in both sets of yarns.

DD FORM 1 NOV 68 1473 REPLACES DD FORM 1473, 1 JAN 64, WHICH IS OBSOLETE FOR ARMY USE.

I-a

UNCLASSIFIED

Security Classification

14. KEY WORDS	LINK A		LINK B		LINK C	
	ROLE	WT	ROLE	WT	ROLE	WT
Evaluation	8					
Tensile Testers	8,9		10		10	
Biaxial	0		0		0	
Measurement	4		8		8	
Strains	4					
Fabrics	4		9		9	
Lenticular Yarns	4		9		9	
Tensile Properties			9		7	
Tensile Strength			9		7	
Armed Forces Equipment			4			
Elasticity					7	
Crimped Yarns					6	
Straight					0	
Yarns					6	

FOREWORD

This report was prepared by Fabric Research Laboratories, Inc. under U. S. Army Contract No. DAAG 17-70-C-0030. The work was carried out under the direction of the U. S. Army Natick Laboratories, with Messrs. Constantin J. Monego and Robert W. Lauder acting as project engineers.

TABLE OF CONTENTS

LIST OF TABLES

LIST OF ILLUSTRATIONS

LIST OF ILLUSTRATIONS (Cont.)

LIST OF ILLUSTRATIONS (Cont.)

LIST OF ILLUSTRATIONS (Cont.)

LIST OF ILLUSTRATIONS (Cont.)

STRESS-STRAIN RESPONSE OF FABRICS UNDER TWO-DIMENSIONAL LOADING

Part II: LENTICULAR YARN CROSS-SECTION

INTRODUCTION

In two previous publications [1,2] theoretical analyses of the load-extension response of idealized, plain-weave fabrics woven from: (1) round yarns; (2) yarns with a racetrack cross-section, and subjected to biaxial stresses were presented. Fabric strains resulting from both crimp interchange and yarn extension were determined. The round-yarn geometry is a good approximation to reality for fabrics woven from monofilaments or high-twist yarns [1]. The racetrack yarn cross-sectional shape is appropriate for many calendered fabrics woven from moderate twist yarns. However, most fabrics for industrial/military applications are comprised of yarns twisted to low-to-moderate levels and are not calendered. Examination of the yarn cross-section in these types of fabrics indicates that they are best described by a lenticular shape.

The analysis developed herein is based on a plain-weave fabric model that incorporates yarns with a lenticular cross-sectional shape. Analytical expressions are developed describing the initial geometry and the geometry after biaxial loading. Fabric strains resulting from both crimp interchange and yarn extension are included. The analytical expressions are solved for infinitely flexible, inextensible yarn and infinitely flexible, extensible, linearly elastic yarn. The inclusion of the effects of fiber and yarn bending rigidity is left to a future publication.

Generalized plots of the results are presented for an initial fabric structure with equal crimp distribution in both sets of yarns. An equal number of warp and filling yarns per unit width before loading is assumed. The fabric extension in both the warp and filling directions is given as a function of the loads applied along the warp and filling axes, a parameter comprised of the yarn cross-sectional area and the number of yarns per unit width in the unloaded fabric, the ratio of the

yarn width-to-thickness, the yarn packing factor, and the filament tensile properties. The results for various loading ratios, fabric constructions and degrees of yarn flattening are compared.

A procedure for predicting the strength and rupture extension of plain-weave fabrics comprised of flattened yarns with a lenticular cross-section and subjected to biaxial loading is also developed.

Assumptions

The analysis developed assumes the following:

1. The fabric is a plain weave.

2. The cross-sectional shape and area of the yarn does not vary along its length nor does it vary with increasing applied loads; the yarns have a lenticular cross-sectional shape.

3. The cross-sectional area of a fiber in the yarn is negligibly small compared to the yarn cross-sectional area.

4. The fibers are homogeneous and either inextensible or linearly elastic.

5. The influences of strain rate, creep and stress relaxation on the response of the fibers are negligible.

6. The yarn twist is sufficiently low that it has a negligible effect on the yarn load-extension response.

7. The axes of the yarns are combinations of circular arcs and straight lines prior to loading. At yarn crossovers each crossing yarn conforms to the cross-sectional contour of the other; between crossovers the axes of the yarns are straight.

8. The warp yarns are initially perpendicular to the filling yarns and remain so during loading.

9. Orthogonal yarns remain in contact during the loading cycle there is no yarn slippage at yarn crossovers.

10. The intrinsic tensile response of the bent yarn is the same as that of the yarn when straight.

11. The yarns are initially relaxed and contain no residual stresses prior to loading.

12. The fabric is loaded in its midplane. The loads are uniformly distributed along the fabric edges. The load on the edges parallel to the filling yarns is parallel to the warp yarns, and the load on the edges parallel to the warp yarns is parallel to the filling yarns.

List of Symbols

The following symbols are used in the analysis:

subscript w - warp yarn or warp direction in fabric,
subscript f - filling yarn or filling direction in fabric,
subscript 1 - value of parameter before application of loads,
subscript 2 - value of parameter after application of loads.

No numerical subscript means the parameter has the same value after application of loads as before. No alphabetic subscript means the parameter is the same for both the warp and filling yarns or in both the warp and filling directions.

A = yarn cross-sectional area

a = one half the thickness of the yarn as it lies in the fabric

b = one half the width of the yarn as it lies in the fabric

E = efficiency by which yarn strength is translated into fabric strength

E_f = fiber modulus of elasticity

E_y = yarn modulus of elasticity

h = distance perpendicular to the fabric plane between yarn cross-section centers at two successive yarn crossovers

L = length along yarn between centers of adjacent crossing yarns

N = number of yarns per unit width of fabric

n_f = number of fibers in yarn

p = yarn packing factor: ratio of the sum of the filament cross-sectional areas to the yarn cross-sectional area

P_y = total axial tensile load on a yarn

r_f = fiber radius

R = yarn radius

s = tensile stress (force per unit area) acting on a fiber

ε = tensile strain in a fiber; fractional fabric extension

ε_y = yarn tensile strain

θ = angle between the yarns and the fabric plane at the mid-point between yarn crossovers; the angle subtended by one half the circular arc over which contact is made between yarns at yarn crossovers

μ = "effective" fabric Poisson's ratio

ν = yarn Poisson's ratio

ρ = radius of curvature of the lenticular yarn cross-sectional contour

σ = external load on the fabric per unit width of fabric

ϕ = the angle subtended by one half the circular arc constituting the lenticular yarn cross-sectional contour.

Fabric Model

The geometry of the fabric model corresponding to the above assumptions is illustrated in Figure 1. As shown, a lenticular yarn cross-section is bounded by two intersecting circular arcs of the same radius of curvature. Eight geometric parameters are required to describe this model: warp and filling yarn cross-sectional area; ratio of yarn cross-sectional width-to-thickness; number of warp and filling yarns per unit length of fabric; angle between warp and filling yarns and the fabric plane at the midpoint between yarn crossovers. The yarn cross-sectional area and yarn cross-sectional dimensions are related to the parameters which specify the bounding circular arcs as follows:

$$A_{lw} = 2\rho_{lw}^{2}(\phi_{lw}-\sin\phi_{lw}\cos\phi_{lw}) \tag{1}$$

$$A_{lf} = 2\rho_{lf}^{2}(\phi_{lf}-\sin\phi_{lf}\cos\phi_{lf}) \tag{2}$$

$$b_{lw} = \rho_{lw}\sin\phi_{lw} \tag{3}$$

$$b_{lf} = \rho_{lf}\sin\phi_{lf} \tag{4}$$

$$a_{lw} = \rho_{lw}(1-\cos\phi_{lw}) \tag{5}$$

$$a_{lf} = \rho_{lf}(1-\cos\phi_{lf}) \tag{6}$$

The lenticular yarn aspect ratios, i.e., ratios of yarn width to thickness, are given by:

$$\frac{b_{lw}}{a_{lw}} = \frac{\sin\phi_{lw}}{1-\cos\phi_{lw}} \tag{7}$$

$$\frac{b_{lf}}{a_{lf}} = \frac{\sin\phi_{lf}}{1-\cos\phi_{lf}} \tag{8}$$

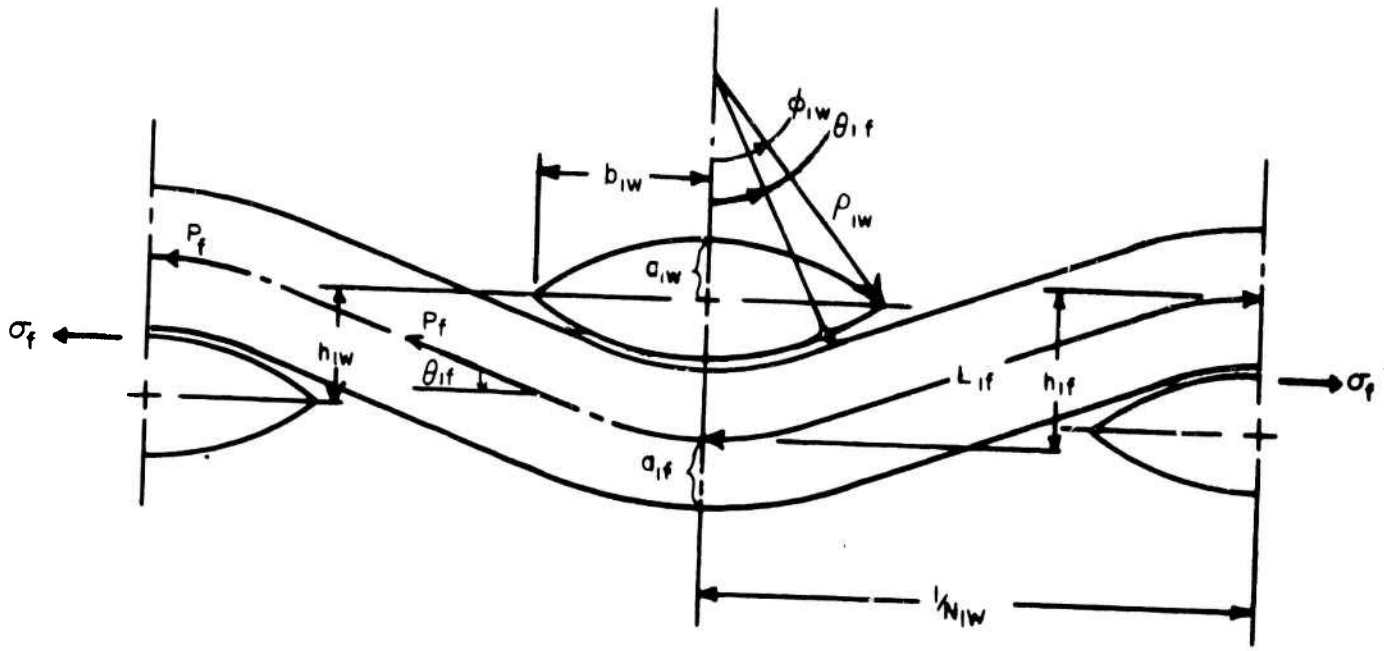

Figure 1. Fabric Model

In addition, it should be noted that

$$\rho_{1w} = \frac{a_{1w}^2 + b_{1w}^2}{2a_{1w}} \tag{9}$$

$$\rho_{1f} = \frac{a_{1f}^2 + b_{1f}^2}{2a_{1f}} \tag{10}$$

The equations describing the geometry before loading of plain-weave fabrics woven from lenticular yarns using the symbols illustrated in Figure 1 and defined in the list of symbols are:

$$\frac{1}{N_{1w}} = [L_{1f} - 2(\rho_{1w} + a_{1f})\theta_{1f}]\cos\theta_{1f} + 2(\rho_{1w} + a_{1f})\sin\theta_{1f} \tag{11}$$

$$\frac{1}{N_{1f}} = [L_{1w} - 2(\rho_{1f} + a_{1w})\theta_{1w})\cos\theta_{1w} + 2(\rho_{1f} + a_{1w})\sin\theta_{1w} \tag{12}$$

$$h_{1w} = [L_{1w} - 2(\rho_{1f} + a_{1w})\theta_{1w}]\sin\theta_{1w} + 2(\rho_{1f} + a_{1w})(1 - \cos\theta_{1w}) \tag{13}$$

$$h_{1f} = [L_{1f} - 2(\rho_{1w} + a_{1f})\theta_{1f}]\sin\theta_{1f} + 2(\rho_{1w} + a_{1f})(1 - \cos\theta_{1f}) \tag{14}$$

$$h_{1w} + h_{1f} = 2(a_{1w} + a_{1f}) \tag{15}$$

Assuming infinitely flexible yarns, these equations also describe the geometry of the fabric after loading with the subscript "1" replaced by the subscript "2". Comparison of the above equations to those in References 1 and 2 shows that the analysis of lenticular yarn fabric differs from the analysis of round yarn fabric and racetrack yarn fabric only by the inclusion of terms expressing the degree and character of yarn flattening. With ρ and a representing the yarn radius, Equations 11 through 15 are identical to the comparable expressions for the round-yarn fabric.

Specification of Initial Parameters

Those geometric quantities describing a fabric structure in the unloaded state that are most easily measured or specified are the number of warp and filling yarns per unit width, N_{lw} and N_{lf}, the yarn cross-sectional areas, A_w and A_f, and the yarn aspect ratios, b_{lw}/a_{lw} and b_{lf}/a_{lf}.

The cross-sectional area of a low-twist yarn can be calculated from the number of filaments in the yarn n_f and the filament radius r_f (assuming an approximately round filament cross-sectional contour) as follows:

$$A = \frac{n_f \pi r_f^2}{p} = \frac{\text{yarn denier}}{\text{fiber denier}} \left(\frac{\pi r_f^2}{p} \right) \tag{16}$$

For a low-twist yarn containing a relatively large number of round filaments packed in cross-section into concentric circular rings the theoretical packing factor p is on the order of 0.750 [3]. In an extreme case of yarn flattening where the filaments are arranged in a rectangular cross-sectional array of dimensions $2r_f \times 2r_f n_f$ the packing factor is the same as that of a circle in a square, namely, 0.785. Since the difference between the packing factors for these two extreme degrees of yarn flattening is not great (<5%) the cross-sectional area of the yarn flattened to any degree can be assumed the same as that of a yarn with a round cross-sectional configuration, i.e., p = 0.750.

The yarn aspect ratio b/a is uniquely determined by the yarn cross-sectional area and yarn width b. The average yarn width b can be calculated from the fabric light transmission and expressions for cover factor. The yarn cross-sectional area can be determined from the yarn denier (using an appropriate packing factor). With these two parameters known, the radius of curvature of the lenticular yarn cross-sectional contour ρ and the angle subtended by the circular arc constituting the lenticular yarn cross-sectional contour ϕ, and thus the yarn thickness a and

aspect ratio b/a can then be calculated. Once N_{1w} and N_{1f}, A_w and A_f, and b_{1w}/a_{1w} and b_{1f}/a_{1f} are specified, the length of yarn between crossovers, L_{1w} and L_{1f}, and the initial warp and filling yarn angles, θ_{1w} and θ_{1f}, can be determined from Equations 1-15 for an initial fabric geometry with equal crimp distribution in both sets of yarns. For other initial fabric geometries one additional parameter must be specified, e.g., either the distance between successive filling yarn cross-section centers perpendicular to the plane of the fabric, h_{1f}, the similar distance between warp yarn cross-section centers, h_{1w}, the filling yarn crimp, or the warp yarn crimp as the yarn lies in the fabric. However, these parameters are not easily determined. One must resort to such methods as imbedding the fabric, sectioning it and examining the section under a microscope.

Fabric Deformation

Referring to Figure 1 and the List of Symbols the equations of static equilibrium become

$$\sigma_w = P_w \cos\theta_{2w} N_{2w} \tag{17}$$

from summing the forces in the warp direction, and

$$\sigma_f = P_f \cos\theta_{2f} N_{2f} \tag{18}$$

from summing the forces in the filling direction. Summing the components of the forces perpendicular to the fabric plane gives

$$P_w \sin\theta_{2w} - P_f \sin\theta_{2f} = 0. \tag{19}$$

Combining Equations 17, 18 and 19

$$\frac{\sigma_w}{\sigma_f} = \frac{\tan\theta_{2f}(N_{2w})}{\tan\theta_{2w}(N_{2f})} \tag{20}$$

which relates the final fabric geometry to the imposed loading

ratio. As was the case for the round yarn and racetrack yarn fabric models, if it is assumed that there is no axial yarn extension ($L_{2w} = L_{1w} = L_w$, $L_{2f} = L_{1f} = L_f$), that the yarn cross-sectional dimensions do not change during loading ($a_{2w} = a_{1w} = a_w$, $b_{2w} = b_{1w} = b_w$), and that the yarns are infinitely flexible; the fabric load-extension behavior consists entirely of an interchange of crimp between the warp and filling yarns. The magnitude of this crimp interchange is governed only by the value of the loading ratio, σ_w/σ_f, and not by the magnitudes of the individual loads σ_w and σ_f. Therefore, in addition to the initial parameters already discussed, only the loading ratio need be specified in this case to characterize the final geometry of the fabric after loading and hence its load-extension response.

If it is desired to include the effects of axial yarn extension in characterizing the response of a fabric to loading, Equations 17 and 18 must be used separately. The functional relationship between the tensile loads P_f and P_w acting on the yarns in the fabric and the yarn construction, filament properties and change in yarn length between crossovers must also be considered.

It is assumed that the load-elongation response of the fabric yarns can be represented by

$$P_y = spA = c+d\varepsilon \qquad (21)$$

where ε = fiber tensile strain, s = tensile stress (force per unit area) acting on a fiber, and c and d are constants. Since the fabric model is composed of flattened yarns, the yarn twist would be low. Therefore, the effect of twist on the tensile response of the fabric yarns is negligibly small and hence the fiber tensile strain is equivalent to the yarn tensile strain, $\varepsilon = \varepsilon_y$. If it is further assumed that the yarn cross-sectional area remains constant during yarn extension ($\nu = 0$) and that the

yarn material is linearly elastic, then c = 0 and

$$P_y = pE_f A\varepsilon_y \tag{22}$$

where E_f is the fiber modulus of elasticity for fabrics woven from continuous filament yarns. (The effects of twist, elasto-plastic stress-strain response, and constant volume extension ($\nu = 1/2$) on the load-extension response of round yarn, are discussed in Reference 1.)

The extension of the filling yarns in the fabric is given by $\varepsilon_y = (L_{2f}-L_{1f})/L_{1f}$, and similarly for the warp yarns by $\varepsilon_y = (L_{2w}-L_{1w})/L_{1w}$. Utilizing these expressions for the strain in the fabric yarns and Equation 22, Equations 17 and 18 can be rewritten in the following form

$$\sigma_w = N_{2w}pE_fA_{2w}\left(\frac{L_{2w}}{L_{1w}} - 1\right)\cos\theta_{2w} \tag{23}$$

$$\sigma_f = N_{2f}pE_fA_{2f}\left(\frac{L_{2f}}{L_{1f}} - 1\right)\cos\theta_{2f} \tag{24}$$

The final warp and filling yarn spacing, N_{2w} and N_{2f}, and the warp and filling yarn angles, θ_{2w} and θ_{2f} can be determined for fabrics woven from infinitely flexible, inextensible yarn ($E_f = \infty$) from Equation 20 and Equations 11-15, with the subscript "1" replaced by the subscript "2", and from these equations and Equations 23 and 24 for fabrics woven from extensible yarn. The resulting fractional fabric extensions in the warp and filling directions are given by

$$\varepsilon_w = \frac{N_{1f}}{N_{2f}} - 1, \tag{25}$$

$$\varepsilon_f = \frac{N_{1w}}{N_{2w}} - 1. \tag{26}$$

Limiting Fabric Geometries

The foregoing discussion of fabric deformation under biaxial loading does not take into account the possibility of geometric limitations on the final fabric configuration imposed by a combination of the initial fabric geometry and the loading ratio. Analysis of the idealized fabric model being considered suggests that there are four possible limiting geometries. (It is assumed that the load applied to the fabric in the warp direction is greater than the load applied in the filling direction, $\sigma_w > \sigma_f$).

1) Warp yarns pulled straight -- If the length of the filling yarns between crossovers is great enough to permit it, the warp yarns can be pulled straight. When this occurs, $1/N_{2f} = L_{2w}$. This limiting geometry, if attained, defines the maximum fabric extension possible from crimp interchange; any further fabric extension requires yarn extension.

2) Maximum filling wrap angle -- As the fabric contracts in the filling direction, the angle θ_{2f} increases. It has reached its maximum value when it equals the angle ϕ_{2w} which defines the contour of the lenticular cross-section of the warp yarns. A value $\theta_{2f} > \phi_{2w}$ violates the assumed fabric model.

3) Maximum filling contraction -- The fabric extension in the warp direction can be limited by the inability of the fabric to contract further in the filling direction. The maximum attainable crimp has been developed in the filling yarns when there are no straight sections between adjacent warp yarn crossovers.

4) Contact between adjacent warp yarns -- Fabric extension in the warp direction can also be limited by contraction in the filling direction if adjacent warp yarns come into contact with each other at the fabric midplane between crossovers [5]. When this occurs $1/N_{2w} = 2b_w$.

That type of limiting geometry which may be achieved at high loading ratios in a particular fabric construction depends upon the length of the filling yarn between crossovers in relation to the yarn cross-sectional width. For $L_{lf} >> 2b_{lw}$ (N_{lw} small), the warp yarns can be pulled straight. For increasingly smaller values of L_{lf}, the maximum filling wrap angle may be achieved or maximum filling contraction reached successively. In order for adjacent warp yarns to come in contact $L_{lf} \cong 2b_{lw}$ (N_{lw} large). Detailed discussion of these limiting geometries is presented in later sections.

ANALYTICAL RESULTS

The analytical expressions derived above for the load-extension behavior of idealized plain-weave fabrics subjected to biaxial stresses have been solved for various combinations of initial fabric geometries and filament properties. The Newton-Raphson iterative method for the solution of simultaneous non-linear algebraic equations and a digital computer were used to obtain the solutions (see Appendix). Descriptions of the cases solved and the results obtained are given below.

Solutions are given first for the case of incompressible yarn and no axial yarn extension ($E_f = \infty$) during fabric loading. Only the contribution of crimp interchange of the load-extension response of the biaxially stressed fabrics is considered. Results are given for initial fabric structures with equal crimp distribution and an equal number of warp and filling yarns per unit width before loading. As noted previously, the results for this case are a function only of the loading ratio σ_w/σ_f and not of the magnitudes of the imposed loads.

I. Square Fabric, Inextensible, Infinitely Flexible Yarn

For an initially square, plain-weave fabric with the same infinitely flexible, incompressible, inextensible yarn in both directions

$$N_{1w} = N_{1f} = N_1$$

$$\theta_{1w} = \theta_{1f} = \theta_1$$

$$L_{1w} = L_{1f} = L_{2f} = L_{2w} = L$$

and assuming the yarn cross-sectional dimensions do not change during loading

$$\phi_{1w} = \phi_{1f} = \phi_{2f} = \phi_{2w} = \phi$$

$$\rho_{1w} = \rho_{1f} = \rho_{2f} = \rho_{2w} = \rho$$

$$b_{1w} = b_{1f} = b_{2f} = b_{2w} = b$$

$$a_{1w} = a_{1f} = a_{2f} = a_{2w} = a$$

$$b_w/a_w = b_f/a_f = b/a.$$

These assumptions allow considerable simplification of the equations describing the initial and final fabric geometries. Equations 1-15 reduce to the following seven expressions:

$$A = 2\rho^2(\phi - \sin\phi\cos\phi) \tag{27}$$

$$b = \rho\sin\phi \tag{28}$$

$$a = \rho(1-\cos\phi) \tag{29}$$

$$b/a = \frac{\sin\phi}{1-\cos\phi} \tag{30}$$

$$\rho = \frac{a^2+b^2}{2a} \tag{31}$$

$$N_1\rho = \frac{\sin\theta_1}{2(2-\cos\phi-\cos\theta_1)} \tag{32}$$

$$L/\rho = \frac{2(2-\cos\phi)(\cos\theta_1+\theta_1\sin\theta_1)-2}{\sin\theta_1} \tag{33}$$

Insight into the interdependence of one initial parameter upon another in determining the initial fabric geometry is more difficult to achieve in this case than in the case of the circular or racetrack yarns; more parameters and hence more equations are necessary to completely fix the initial geometric configuration.

The variation of ϕ with b/a (Equation 30) is shown in Figure 2. Unless the dependence of ϕ on the radius of curvature ρ of the lenticular contour is understood, the fact that ϕ decreases with increasing aspect ratio might seem unexpected. This dependence is not directly apparent from Equations 28-30. An increase in aspect ratio can result from an increase in "b", a decrease in "a", or both. Equation 31 shows that ρ increases with both increasing "b" or decreasing "a"; in order to preserve the equalities of Equations 28 and 29 a decrease in ϕ with increasing aspect ratio is required.

The functional relationship described by Equation 32 is illustrated in Figures 3, 4, and 5 in which the dimensionless parameter $N_1\rho$ is plotted in various ways as a function of θ_1 and ϕ and associated aspect ratios b/a. The curves in Figure 3 have been terminated at the point where $\theta_1 = \phi$ since $\theta_1 < \phi$ is an obvious geometrical limitation implied by the model construction. However, it is apparent from this figure that a maximum value of $N_1\rho$ is reached at a lower value of θ_1 than that given by $\theta_1 = \phi$. To further investigate the maximal values of the variables, coincident mappings of the two functions $(2N_1\rho\cos\theta_1 + \sin\theta_1)$ and $2N_1\rho(2-\cos\phi)$ are presented in Figure 4. These expressions when equated result in an equivalent form of Equation 32; individually plotted, they serve to illustrate the separate behavior of θ_1 and ϕ for particular values of $N_1\rho$. Since b/a is specified initially, the dominant parameter is ϕ. The corresponding values of ϕ and θ_1 are readily apparent for each value of $N_1\rho$ represented; the pairs of maximum values of ϕ and θ_1 for a particular value of $N_1\rho$ are defined by the largest value of θ_1 for which simultaneous values of the two functions can be found. These maximum values are plotted in Figure 5 versus $N_1\rho$; this figure may also be interpreted as showing a maximum value of $N_1\rho$ for particular values of ϕ (or b/a). Thus the solution space for Equation 32 is the area under the curves in Figure 5.

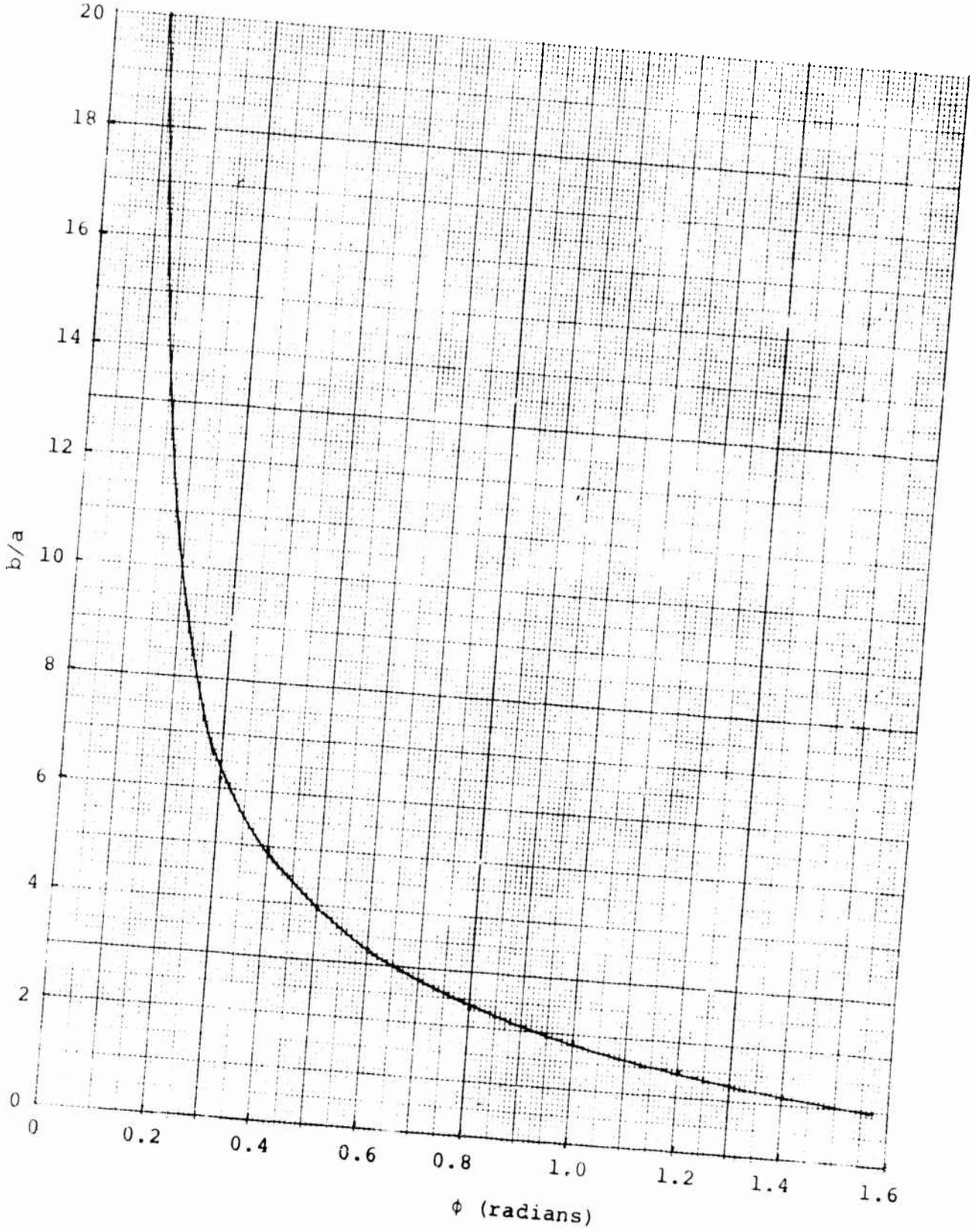

Figure 2. Aspect Ratio, b/a as a Function of the Lenticular Contour Arc Angle ϕ

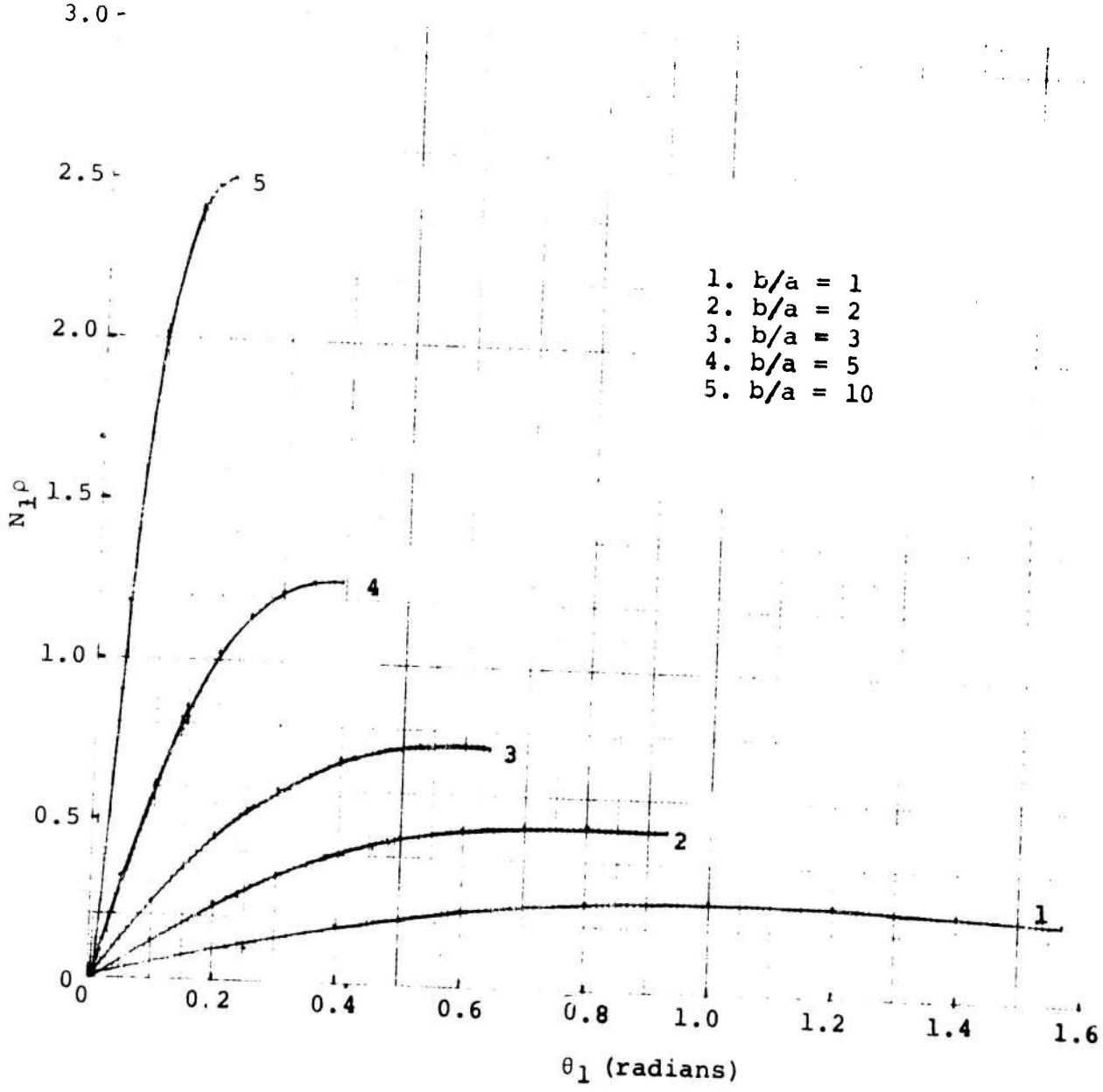

Figure 3. $N_1\rho$ as a Function of θ_1 for Various Aspect Ratios

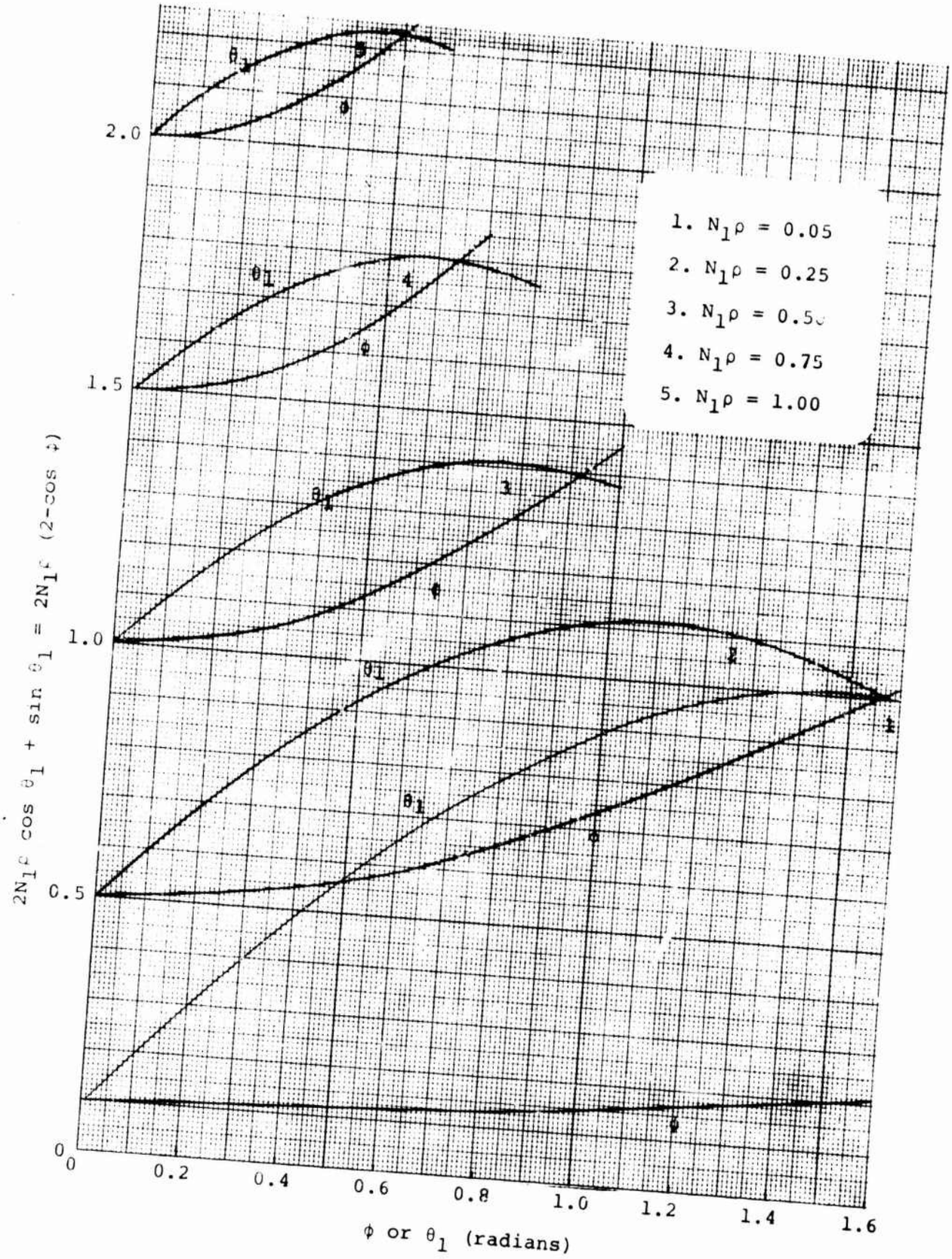

Figure 4. θ_1 and ϕ as Simultaneous Functions of $N_1\rho$

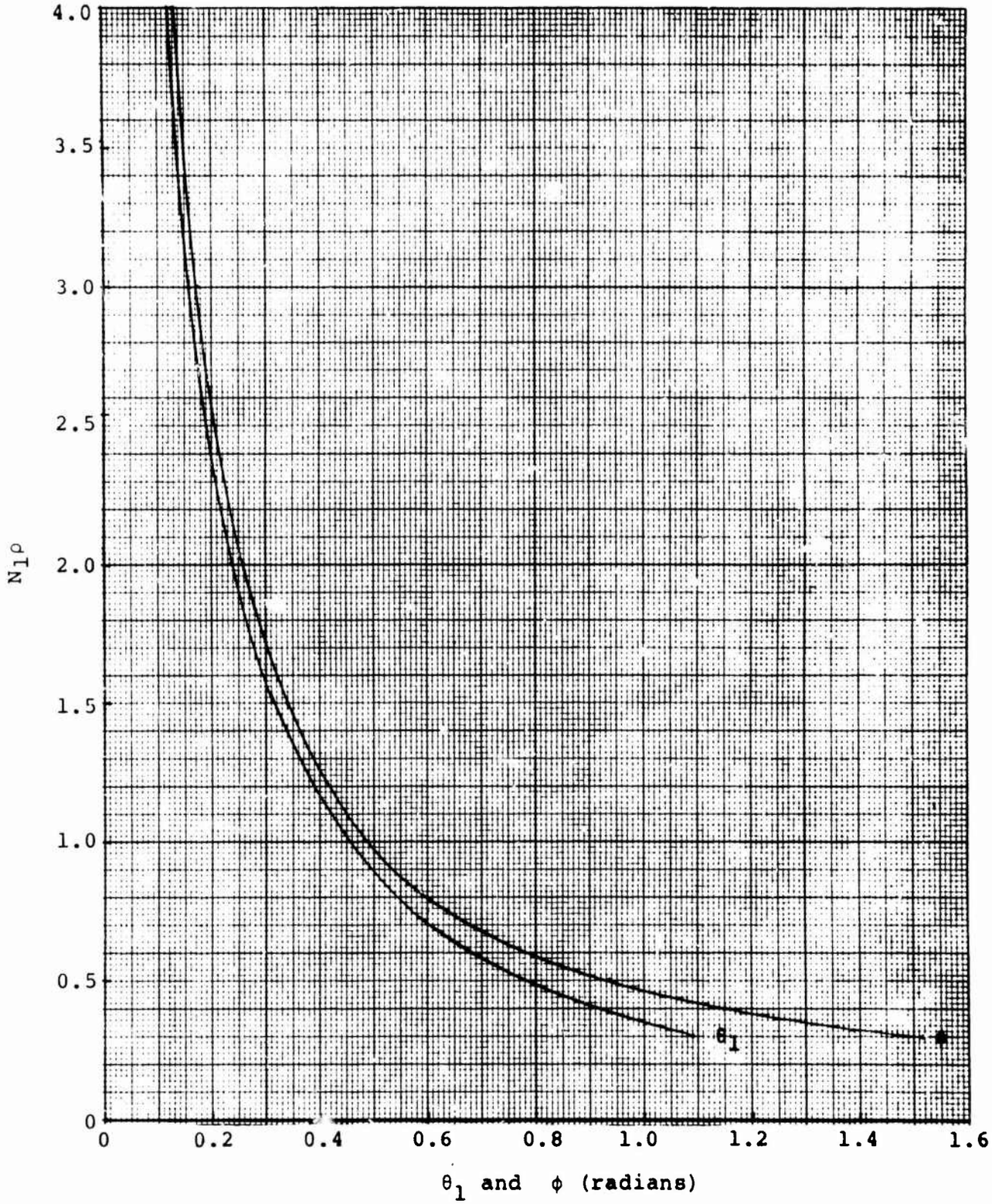

Figure 5. Solution Space of Equation 32

Of more value than the foregoing, however, would be a similar analysis from which maximum achievable aspect ratios could be predicted for various combinations of number of yarns per unit width and yarn cross-sectional area. Substitution of the parameter $\sqrt{A/\pi}$ for ρ similar to the substitution made in the analysis of the racetrack-yarn fabric [2], not only permits comparisons with the round-yarn analysis ($\rho = \sqrt{A/\pi}$ when $b/a = 1$) but allows a more versatile interpretation of the geometrical relationships in Equations 32 and 33. The basis of the substitution is the following:

$$\sqrt{A/\pi} = \rho[2(\phi-\sin\phi\cos\phi)/\pi]^{1/2} \tag{34}$$

Table 1 contains values of the factors necessary to make the substitution for various degrees of yarn flattening.

TABLE 1

AREA NORMALIZING FACTORS FOR LENTICULAR YARNS

b/a	$[2(\phi-\sin\phi\cos\phi)/\pi]^{1/2}$
1	1.000000
2	0.533626
3	0.322627
5	0.159100
10	0.057750

Figures 6 and 7 are analogous to Figures 3 and 5 with $N_1\rho$ replaced by $N_1\sqrt{A/\pi}$. Each of the curves in Figure 6 has been terminated at the maximum value of $N_1\sqrt{A/\pi}$ possible for the appropriate value of ϕ, as determined from the maximum value of $N_1\rho$ in Figure 5. The curves in Figure 6 show for a range of aspect ratios the way in which the crimp angle θ_1 increases with: (1) increasing number of yarns per unit width N_1 for any specified yarn cross-sectional area A or; (2) increasing yarn cross-sectional area A for any specified number of yarns per unit width. For a given crimp angle, maximum achievable values of N_1 for any A or of A for any N_1 are also apparent for various yarn aspect ratios.

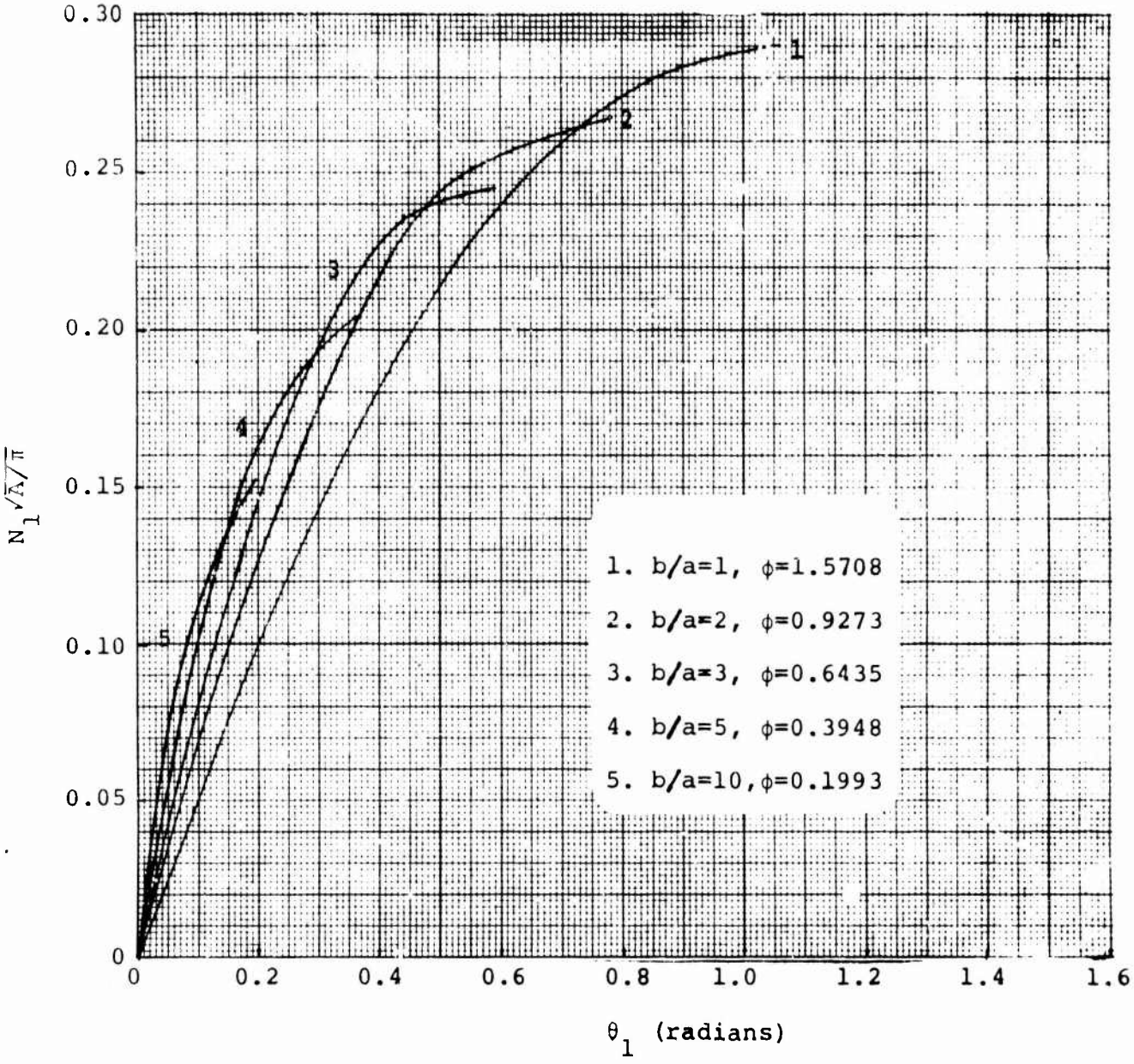

Figure 6. Variation of θ_1 with Weave Tightness

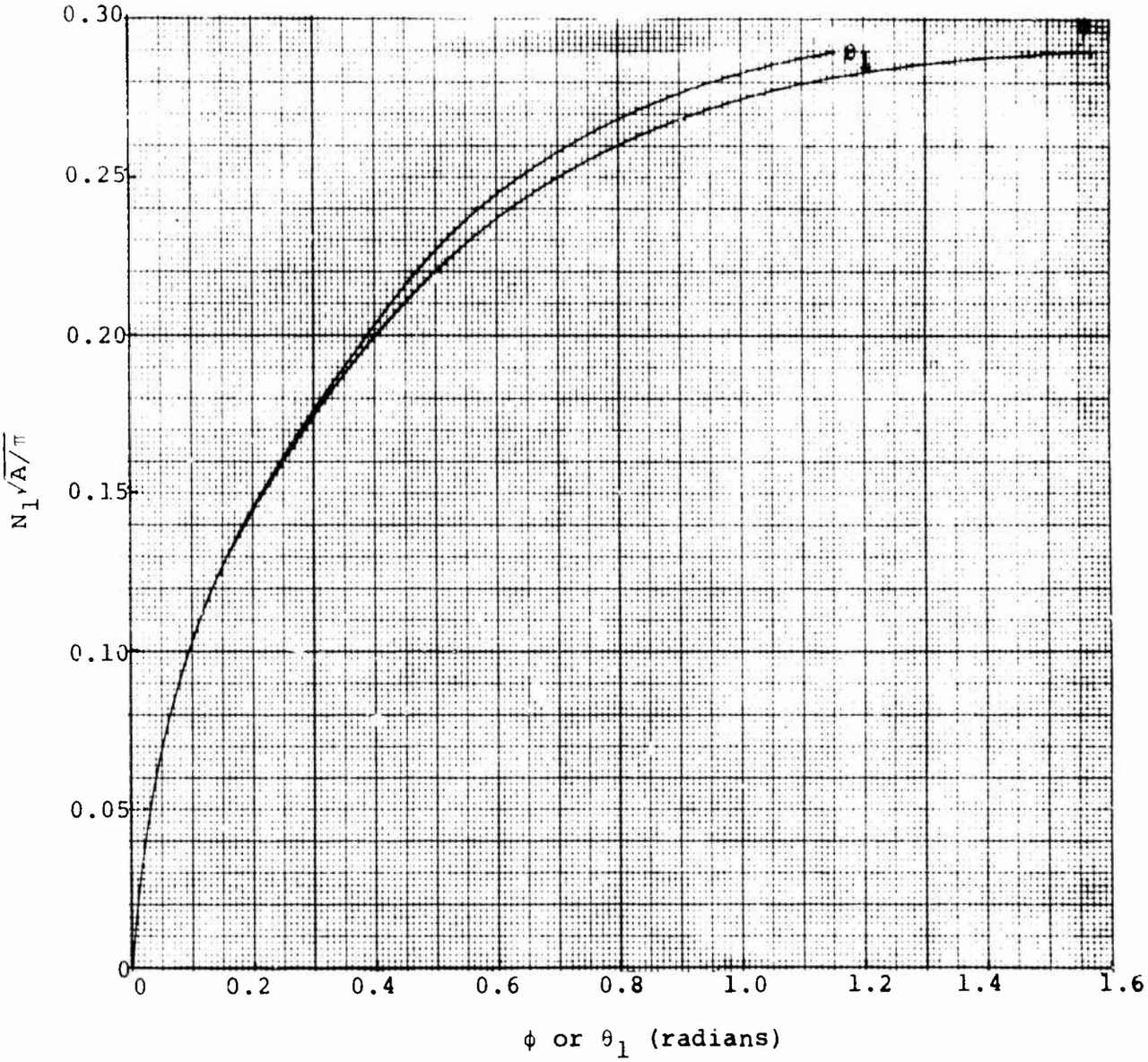

Figure 7. Solution Space for Eq. 32 Normalized for Yarn Cross-Sectional Area

As would be expected, the more open fabrics (low values of $N_1\sqrt{A/\pi}$) can accommodate a greater degree of yarn flattening. Another interesting fact shown in Figure 6 is that in the more open fabrics the crimp angle is greatest when the aspect ratio is lowest; while above a critical value of tightness, which differs for each aspect ratio, the trend is somewhat reversed. The lower the aspect ratio, the thicker the yarn and thus the greater the angle the crossing yarns must make with the plane of the fabric at their midpoint between yarn crossovers in order to pass over one yarn and then under the next in the plain-weave construction (see Figure 1). However, in a more tightly woven fabric the higher the yarn aspect ratio, the closer the fabric is to a jammed construction and thus the greater the yarn angles must be.

Figure 8 is an alternate way of presenting the information given in Figure 7; in both figures the solution space for Equation 32 is the area under the curve or curves. The maximum amount of yarn flattening which can occur in a particular initially square fabric construction is easily determined from Figure 8 while it would be much less than straightforward to extract this information from Figure 5.

Also given graphically in Figure 9 is the relationship, normalized with respect to yarn cross-sectional area, between the number of yarns per unit width in the fabric N_1 and the length of yarn between crossovers L for various aspect ratios. As was the case with the racetrack-yarn fabrics [2] for comparable values of $\sqrt{A/\pi}$, the yarn length L is quite insensitive to changes in the degree of yarn flattening; its value is determined predominantly by the number of ends per unit width in the fabric in relation to the yarn cross-sectional area, i.e., by the tightness of the fabric construction. In addition, the set of curves for the lenticular yarns almost exactly match the curves for racetrack yarns except that the end points differ.

It is interesting to examine graphically the various components of yarn length between crossovers for different degrees of

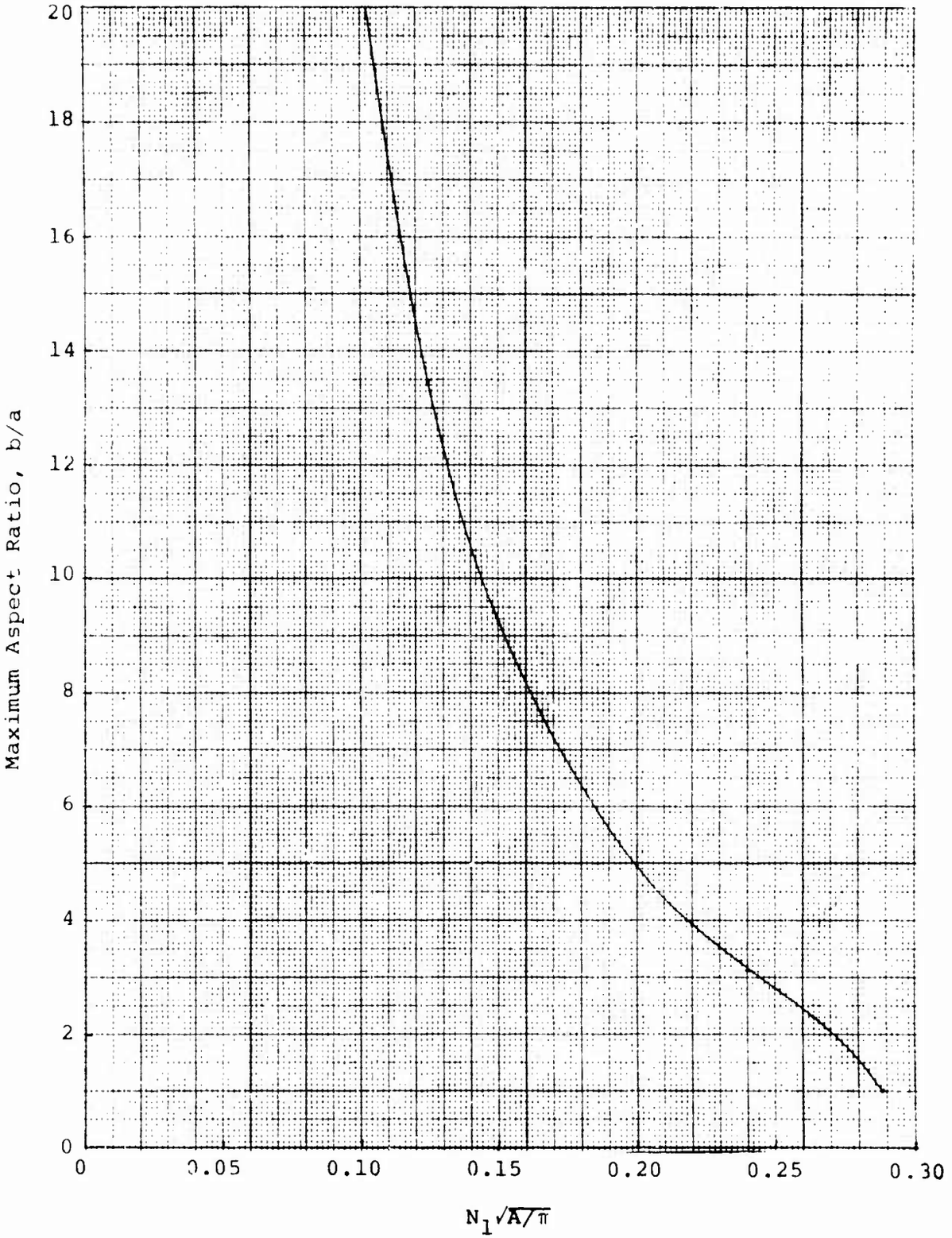

Figure 8. Maximum Degree of Yarn Flattening Accommodatable as a Function of Weave Tightness

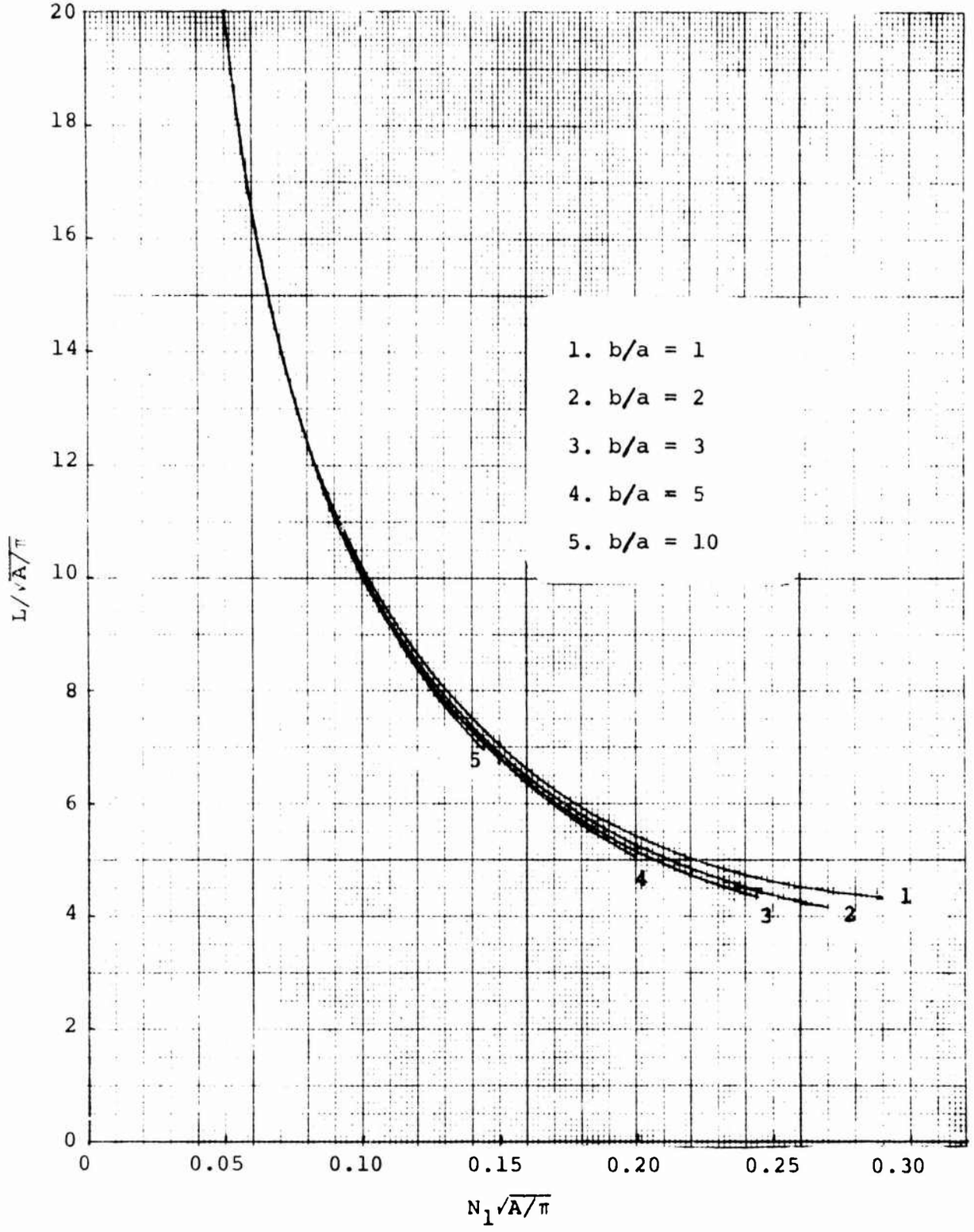

Figure 9. $L/\sqrt{A/\pi}$ vs $N_1\sqrt{A/\pi}$ for a Square Fabric with Inextensible Yarn

yarn flattening. For this purpose the total length L of yarn between crossovers may be divided into two components; L_I, the length of the straight section between points of contact with adjacent crossing yarns, inclined at an angle θ_1 to the plane of the fabric; and L_{II}, the wrapped portion of length conforming to the contour of the crossing yarn which is also defined by the angle θ_1. The magnitudes of these two components can be expressed as follows:

$$L_I = L - L_{II}$$

$$L_{II} = 2(\rho+a)\theta_1 = 2\rho(2-\cos\phi)\theta_1 \tag{35}$$

or normalized for yarn area,

$$\frac{L_{II}}{\sqrt{A/\pi}} = \frac{2(2-\cos\phi)\theta_1}{[2(\phi-\cos\phi\sin\phi)/\pi]^{1/2}}. \tag{36}$$

These component lengths are plotted in normalized form versus $N_1\sqrt{A/\pi}$ for various aspect ratios in Figures 10-14. As shown, the total yarn length L between crossovers and the length L_I of the straight section decrease with increasing fabric tightness while the length L_{II} of the wrapped portion increases. Additionally, the total yarn length L does not vary greatly with increasing aspect ratio. However, L_I decreases and L_{II} increases more rapidly with increasing fabric tightness at the higher yarn aspect ratios. Consequently, the wrapped portion of the yarn length L_{II} becomes a greater portion of the total yarn length L with increasing yarn aspect ratio for any specific value of $N_1\sqrt{A/\pi}$.

A particularly pertinent piece of information relevant to the lenticular-yarn fabric model is evident in Figures 3, 4, and 7, namely that in many of the theoretically possible initial fabric geometries the angle θ_1 is much less than ϕ. Ideally, the fabric model describes a fabric in which each yarn flattens at crossovers to conform to the contour of the crossing yarn.

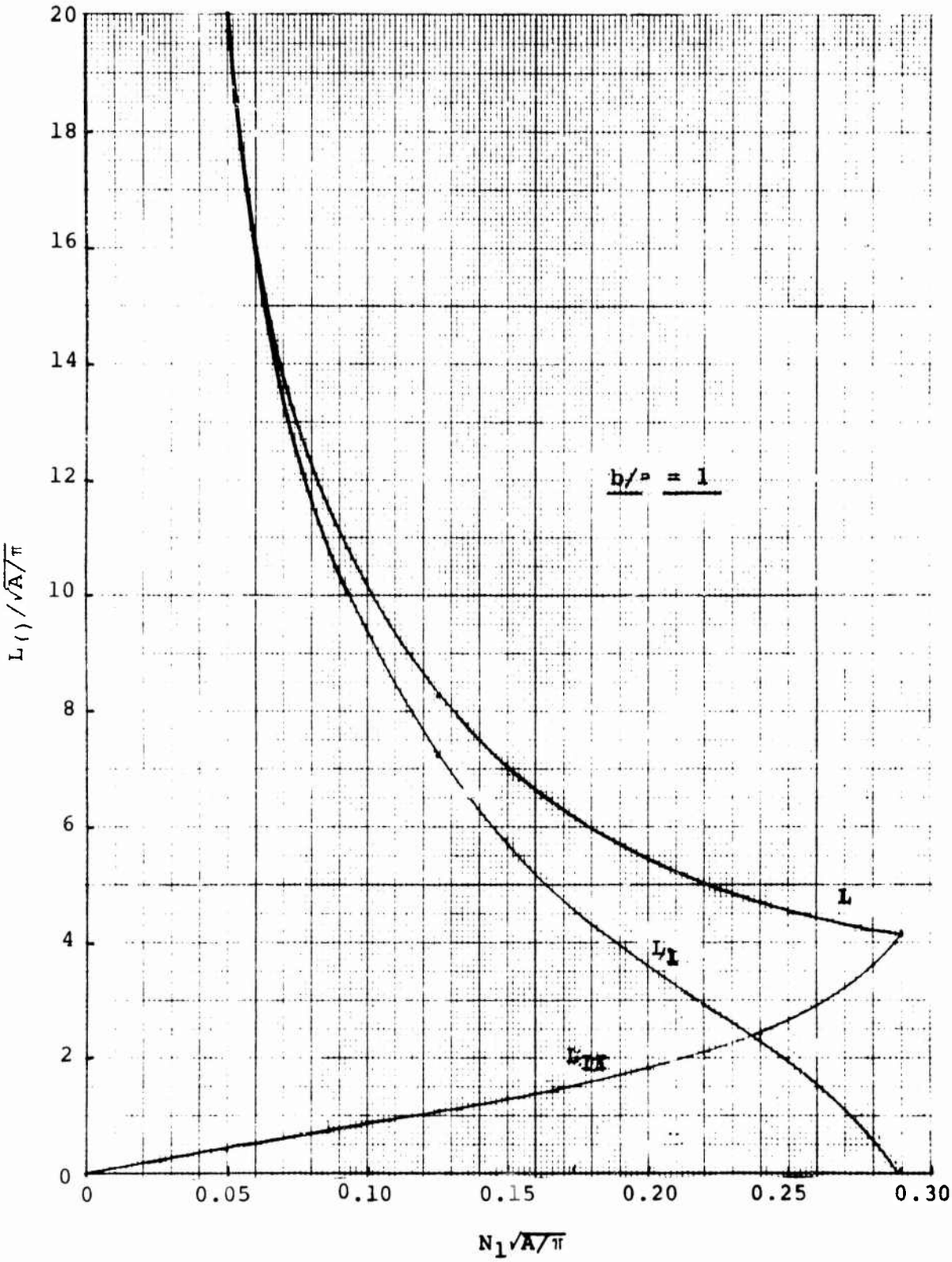

Figure 10. Components of Yarn Length Between Crossovers (Aspect Ratio = 1)

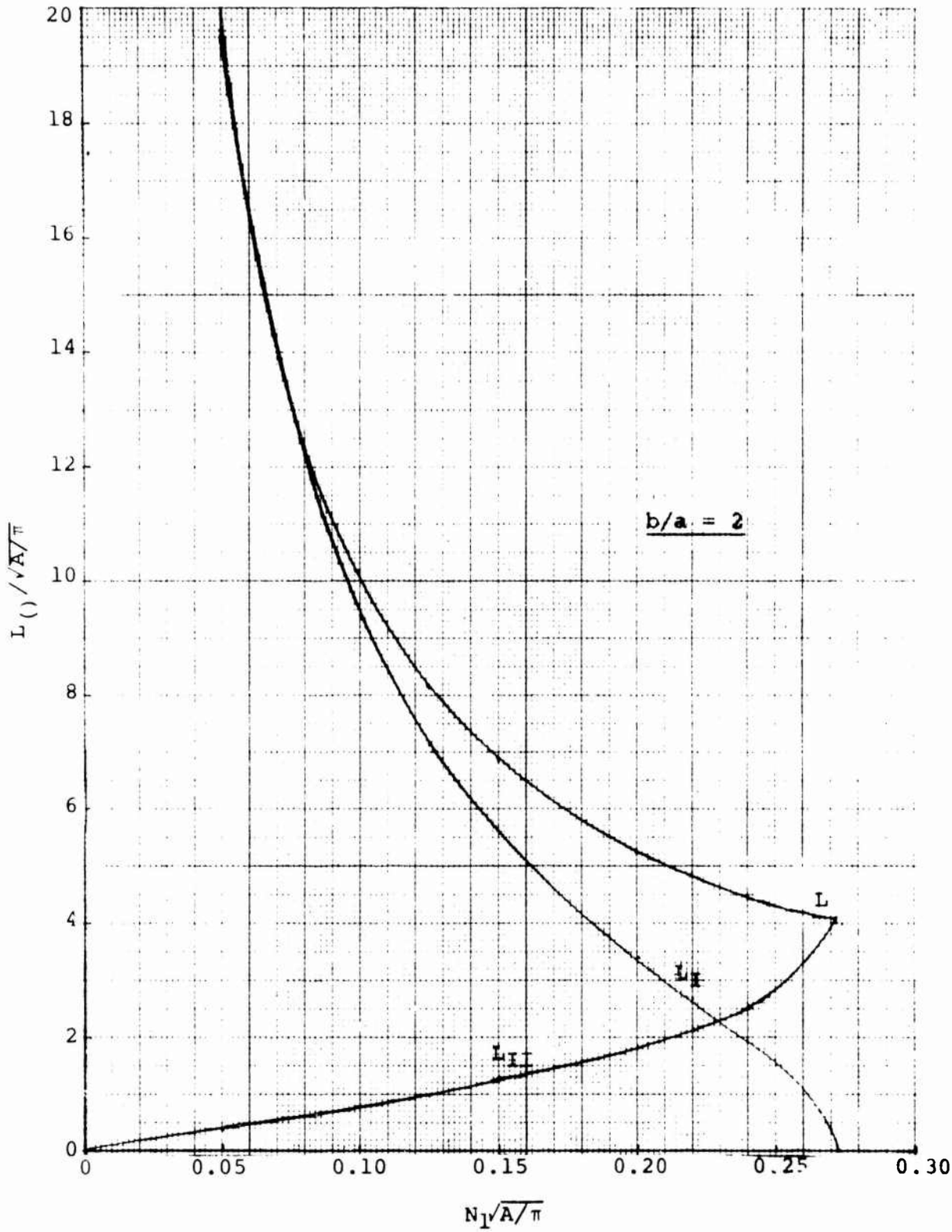

Figure 11. Components of Yarn Length Between Crossovers (Aspect Ratio = 2)

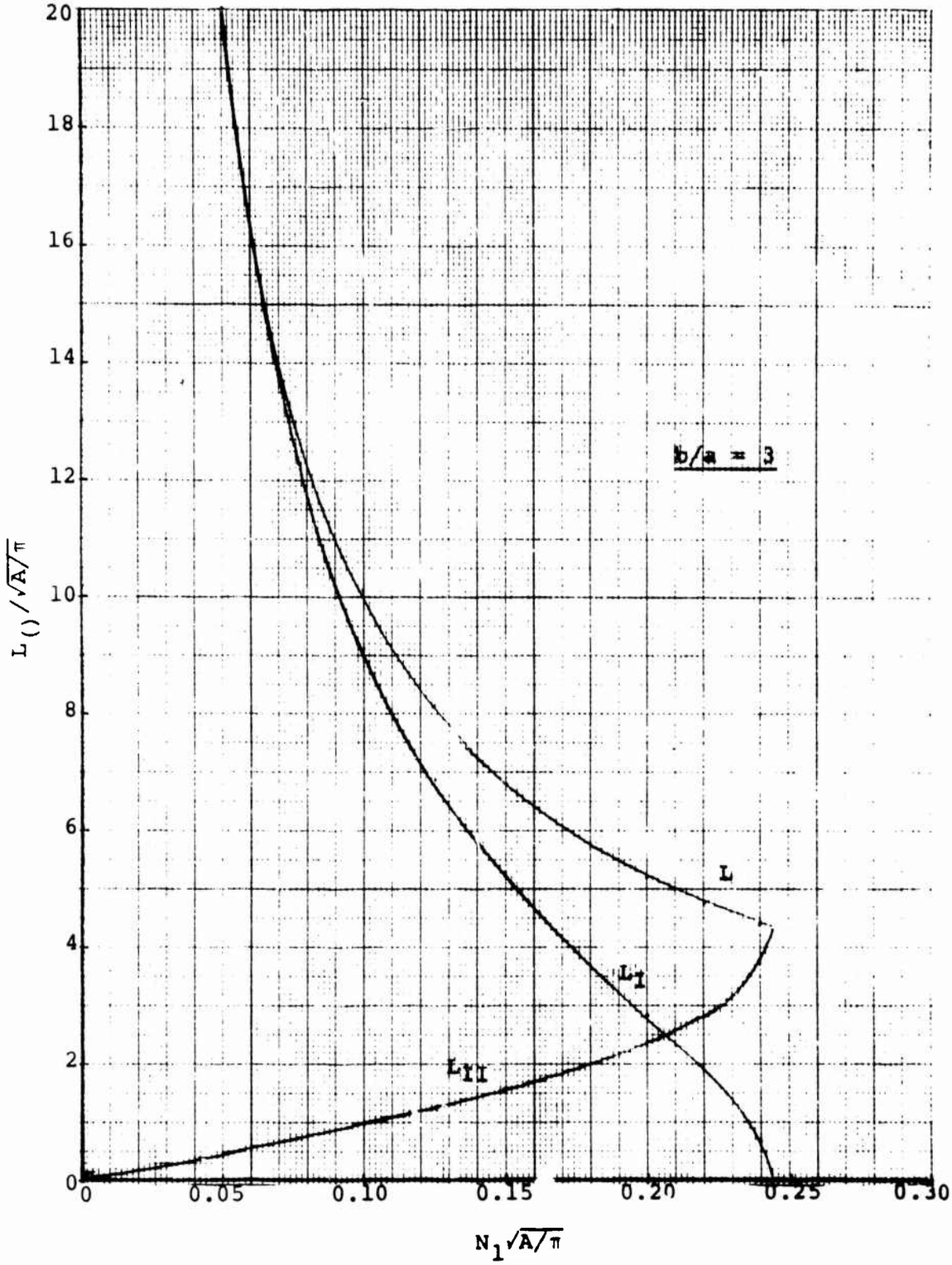

Figure 12. Components of Yarn Length Between Crossovers (Aspect Ratio = 3)

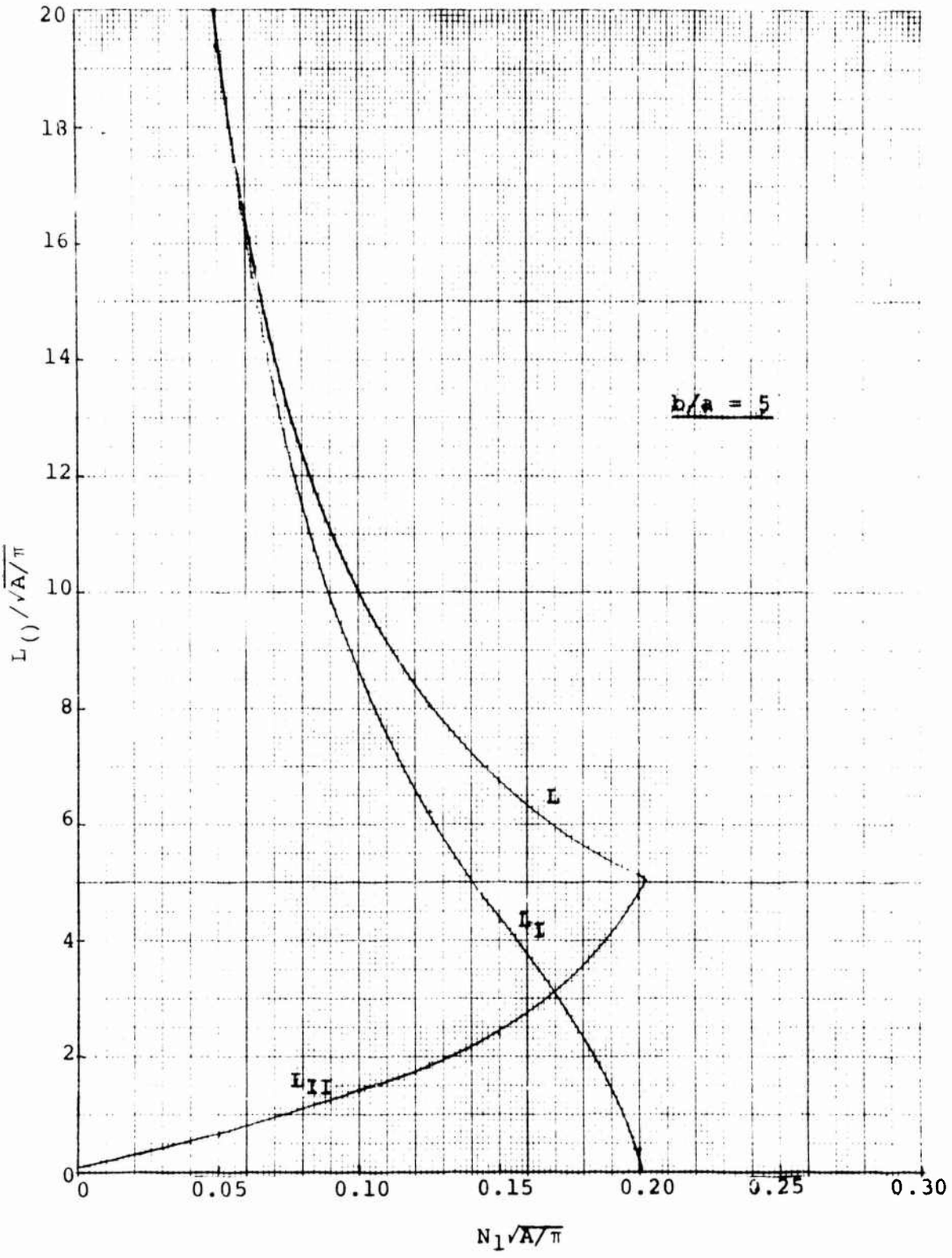

Figure 13. Components of Yarn Length Between Crossovers (Aspect Ratio = 5)

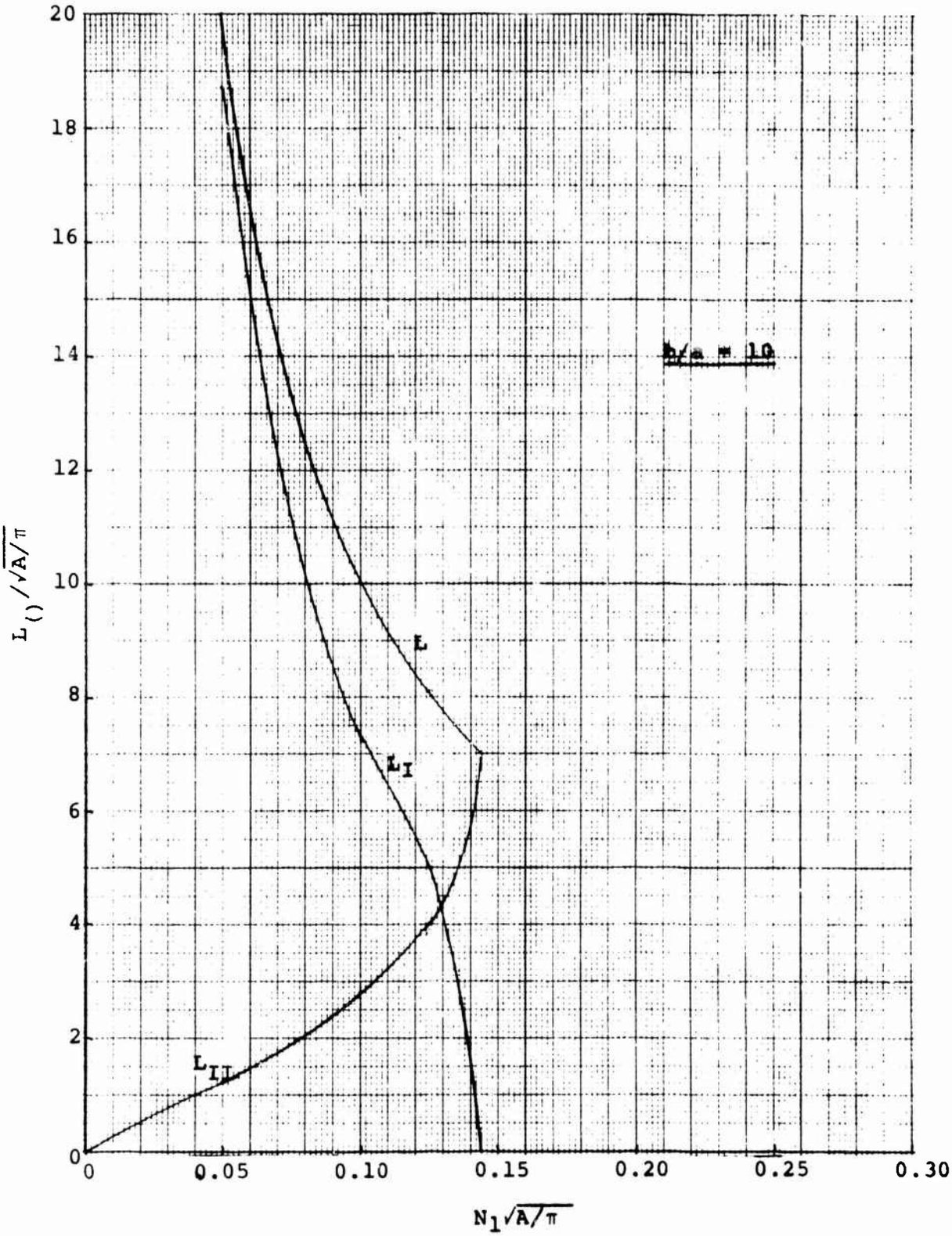

Figure 14. Components of Yarn Length Between Crossovers (Aspect Ratio = 10)

If this is the case, the angle θ_1 defining the arc over which contact is made between crossing yarns should be very nearly equal to the angle ϕ describing the contour arc of the lenticular cross-section. If instead $\theta_1 << \phi$, a geometrical configuration will occur, consistent with the fabric model in which there is a significant separation or gap between the node of the lenticular cross-section and the boundary of the crossing yarn, (see Figure 15). Such a configuration is not likely to occur in a real fabric composed of low twist yarns.

The magnitude of this separation can be defined in a number of ways, one of which is illustrated in Figure 15 and given analytically by the following expression for initially square fabrics.

$$(GAP)_1 = \frac{1-\cos(\phi-\theta_1)}{(1-\cos\phi)\cos(\phi-\theta_1)} \tag{37}$$

This equation defines a distance along the radius vector of the lenticular cross-section between its node and the boundary of the crossing yarn expressed as a fraction of half the yarn thickness a. This separation is plotted in Figure 16 as a function of $N_1\sqrt{A/\pi}$ and b/a. As shown, the gap decreases with increasing values of $N_1\sqrt{A/\pi}$ for each aspect ratio and decreases with increasing aspect ratio for a particular value of $N_1\sqrt{A/\pi}$. As the aspect ratio approaches its maximum achievable value for a particular value of $N_1\sqrt{A/\pi}$, the gap decreases to a minimum value, a value very near zero for aspect ratios of three and greater.

Thus it appears that the lenticular-yarn fabric model closely approximates the geometry of real fabrics containing low-twist yarns only for those initial configurations for which the yarn aspect ratio is very near its theoretically maximum value.

(As an alternate method of defining the gap, the distance perpendicular to the fabric plane between the node of the lenticular cross-section and the crossing yarn could be used, again expressed as a fraction of one half the yarn thickness. While the

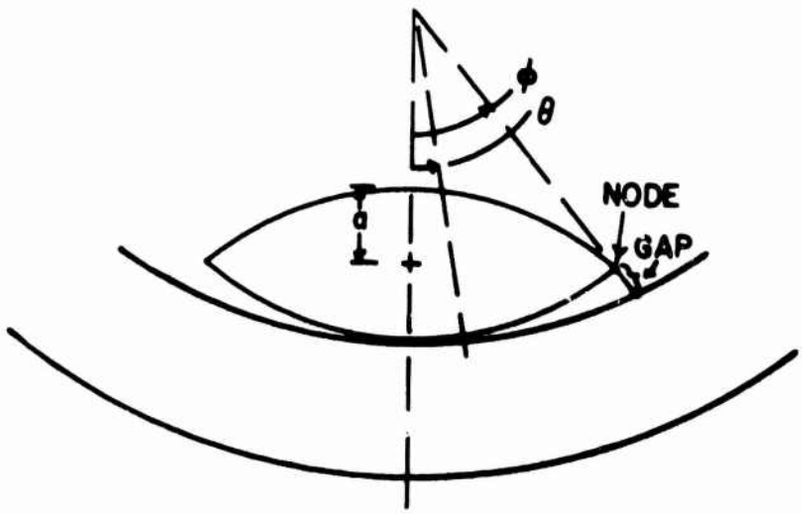

Figure 15. Radial Separation Between the Node of the Lenticular Cross-Section and the Crossing Yarn

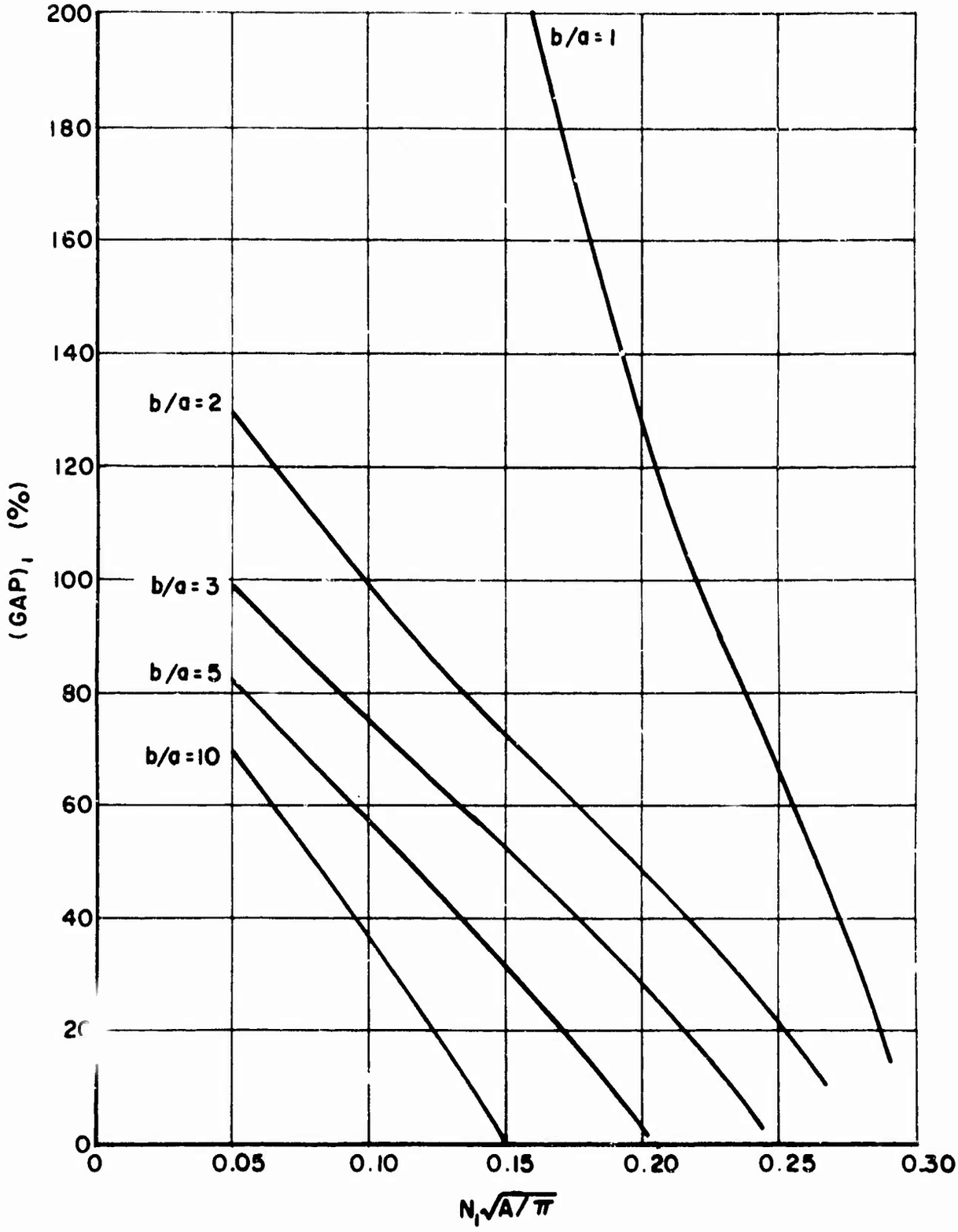

Figure 16. Initial Radial Separation Between the Node of the Lenticular Cross-Section and the Crossing Yarn for Square Fabrics

observed trends using this definition would be the same as with the other, there would be the advantage of normalizing the magnitude of the gap for each value of ϕ to a scale between 0 and 1, i.e., the largest gap would be equal to "a" for all values of ϕ).

After loading the yarn geometry of an initially square fabric composed of infinitely flexible, incompressible, inextensible lenticular yarns, i.e., taking into account only crimp interchange ($L_1 = L_2 = L$), is given by the following four equations:

$$\frac{\sigma_w}{\sigma_f} = \frac{\cot\theta_{2w}[2(2-\cos\phi)(\sin\theta_{2w}-\theta_{2w}\cos\theta_{2w})+(L/\rho)\cos\theta_{2w}]}{\cot\theta_{2f}[2(2-\cos\phi)(\sin\theta_{2f}-\theta_{2f}\cos\theta_{2f})+(L/\rho)\cos\theta_{2f}]} \tag{38}$$

$$2(2-\cos\phi)(\theta_{2w}\sin\theta_{2w}+\cos\theta_{2w}+\theta_{2f}\sin\theta_{2f}+\cos\theta_{2f}) - (L/\rho)(\sin\theta_{2w}+\sin\theta_{2f})-4 = 0 \tag{39}$$

$$\frac{1}{N_{2w}\rho} = 2(2-\cos\phi)(\sin\theta_{2f}-\theta_{2f}\cos\theta_{2f})+(L/\rho)\cos\theta_{2f} \tag{40}$$

$$\frac{1}{N_{2f}\rho} = 2(2-\cos\phi)(\sin\theta_{2w}-\theta_{2w}\cos\theta_{2w})+(L/\rho)\cos\theta_{2w}. \tag{41}$$

Equation 39 is derived from Equation 20; Equation 39 is derived by combining Equations 13 and 14 as specified in Equation 15, in each case with the subscripts "1" replaced by subscripts "2". These equations were solved with the aid of a digital computer for the various values of b/a and $N_1\rho$ given in Table 2 and σ_w/σ_f = 2, 3, 4, 5 and 10. The solutions obtained for $\sigma_w/\sigma_f > 1$ may also be applied to cases where $\sigma_w/\sigma_f < 1$ by simple reversal of subscripts "w" and "f". The set of values of $N_1\rho$ associated with each particular value of b/a correspond to the same set of values of $N_1\sqrt{A/\pi}$ as at b/a = 1.

TABLE 2

VALUES OF PARAMETERS USED TO DETERMINE GEOMETRY AFTER LOADING

ϕ (radians)	b/a	$N_1\rho$	$N_1\sqrt{A/\pi}$
$\pi/2$	1	0.050	0.050
		0.100	0.100
		0.125	0.125
		0.150	0.150
		0.200	0.200
		0.220	0.220
		0.240	0.240
0.9273	2	0.094	0.050
		0.187	0.100
		0.234	0.125
		0.281	0.150
		0.375	0.200
		0.412	0.220
		0.450	0.240
0.6435	3	0.155	0.050
		0.310	0.100
		0.387	0.125
		0.465	0.150
		0.620	0.200
		0.682	0.220
		0.744	0.240
0.3948	5	0.314	0.050
		0.628	0.100
		0.786	0.125
		0.943	0.150
		1.257	0.200
		1.383	0.220
0.1993	10	0.867	0.050
		1.733	0.100
		2.166	0.125
		2.600	0.150
		3.466	0.200

The solutions proceeded in the following manner. The value of ϕ corresponding to each value of b/a was determined from Equation 30 by a simple iterative procedure. The value of θ_1 corresponding to a particular value of ϕ and $N_1\rho$ was then found from Equation 32. The appropriate set of values of θ_1 and ϕ were substituted in Equation 33 giving a set of values of L/ρ for each desired value of ϕ. Substitution of the appropriate values of L/ρ and ϕ were made in Equations 38-41. The Newton-Raphson iterative method for solving nonlinear simultaneous equations numerically was used to determine values of θ_{2w} and θ_{2f} from Equations 38 and 39 (see appendix) subject to the following limiting conditions:

$$0 \leq \theta_{2w} \leq \theta_1 \leq \theta_{2f} \leq \phi.$$

With the values of θ_{2w} and θ_{2f} fixed, $N_{2w}\rho$ and $N_{2f}\rho$ were found from Equations 40 and 41. The fabric strains corresponding to each set of initial conditions and each value of imposed loading ratio were then found using Equations 25 and 26. Values of each parameter were determined to six significant figures.

The results of the computations are presented graphically in Figures 17 through 26. Fabric extensions in the warp direction and contractions in the filling direction are plotted versus the loading ratio, σ_w/σ_f, for various degrees of initial fabric tightness, $N_1\sqrt{A/\pi}$, and various amounts of yarn flattening, b/a. The fabric extensions in both the warp and filling directions are also given as a function of $N_1\sqrt{A/\pi}$ for various loading ratios and yarn aspect ratios. Limiting fabric extensions are also given for $\sigma_w/\sigma_f \to \infty$, i.e., as uniaxial loading is approached. These extension values represent the maximum fabric extensions possible from crimp interchange. Their derivation is discussed below. Figures 17 and 18 which show the response of the initially square, round-yarn fabric (b/a = 1) are reprinted from Reference 1.

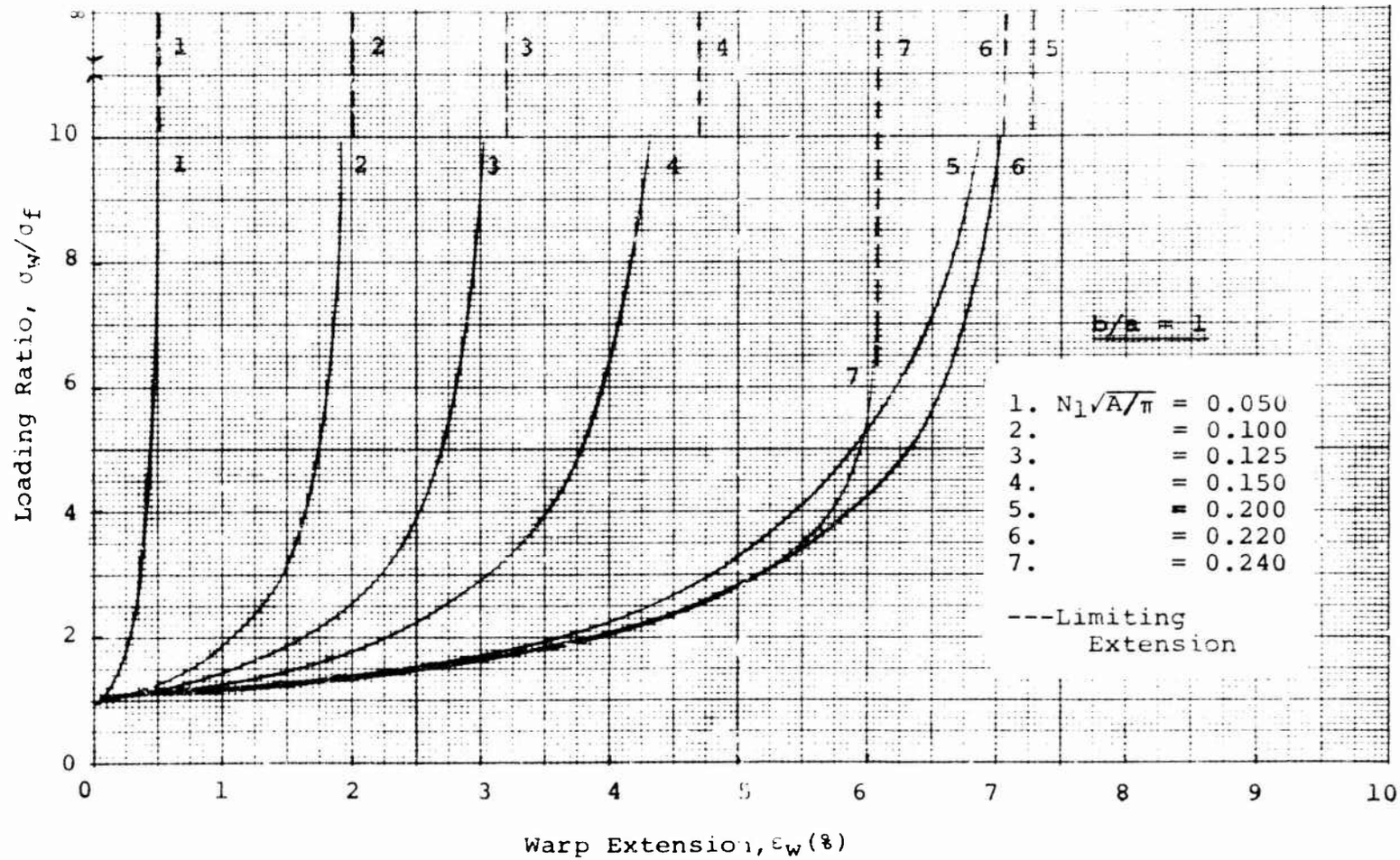

Figure 17(a). Fabric Extension in the Warp Direction: (Aspect Ratio = 1. Inextensible Yarn

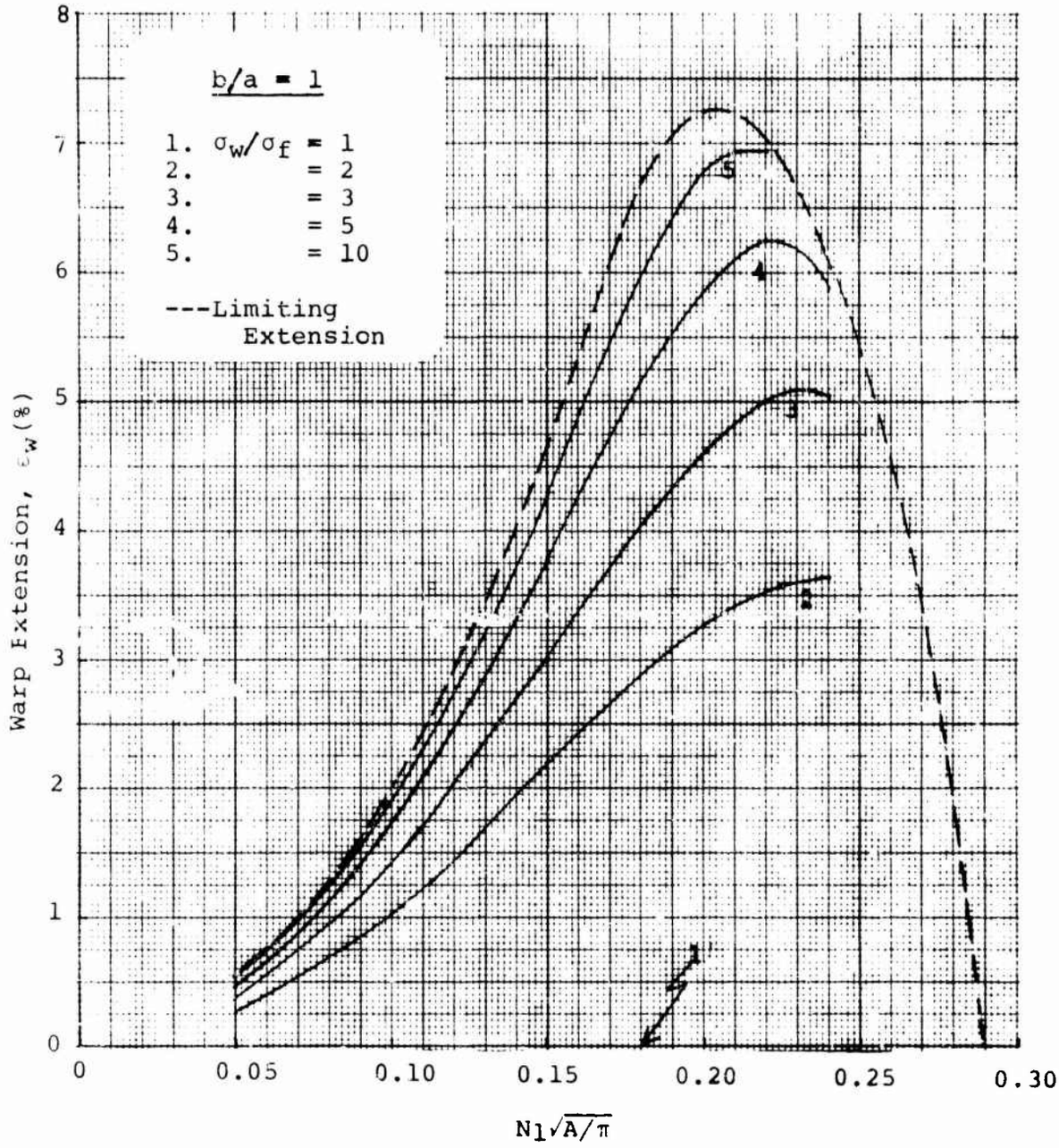

Figure 17(b). Fabric Extension in the Warp Direction: (Aspect Ratio = 1) Inextensible Yarn

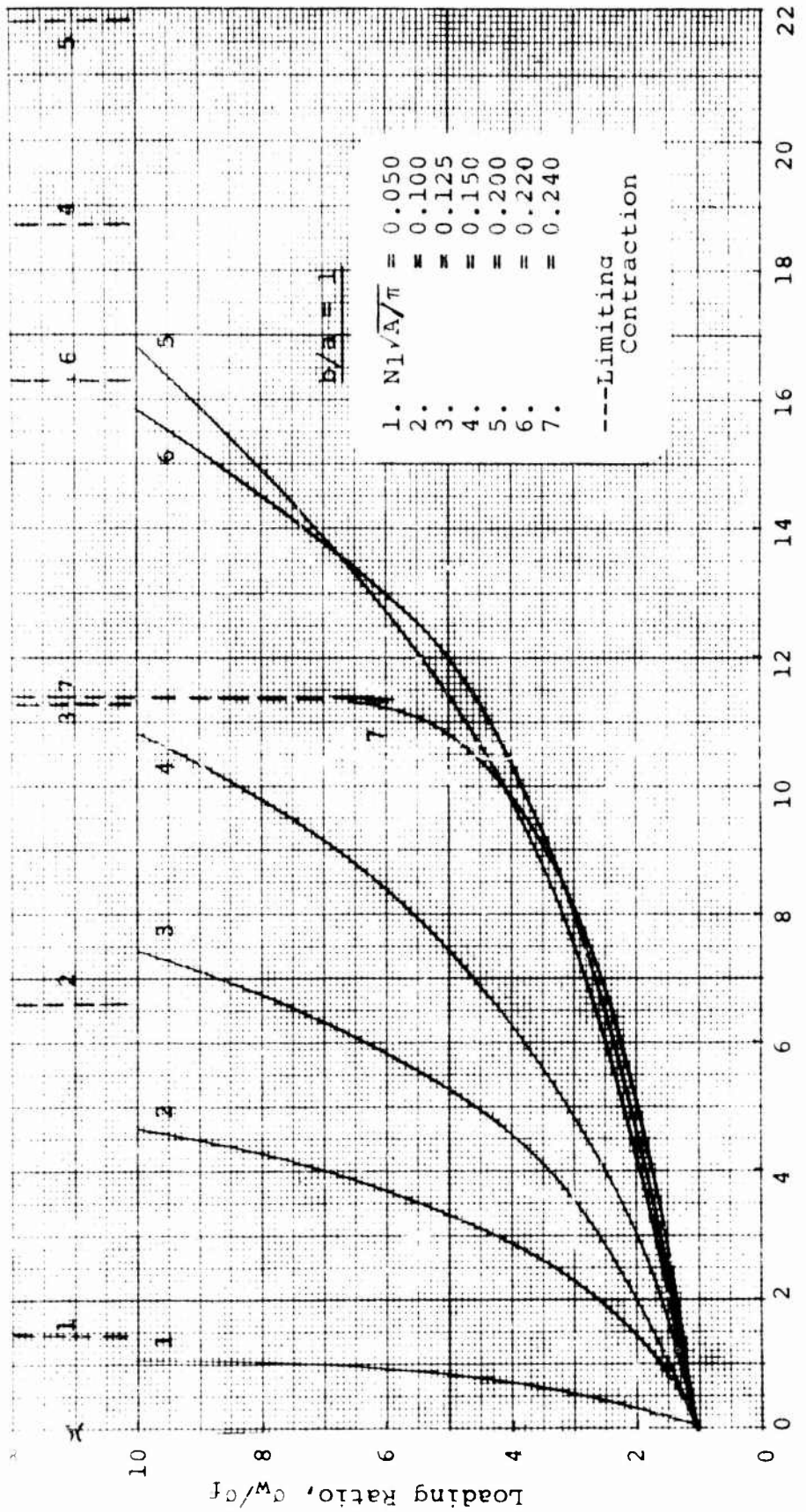

Figure 18(a). Fabric Contraction in the Filling Direction: (Aspect Ratio = 1) Inextensible Yarn

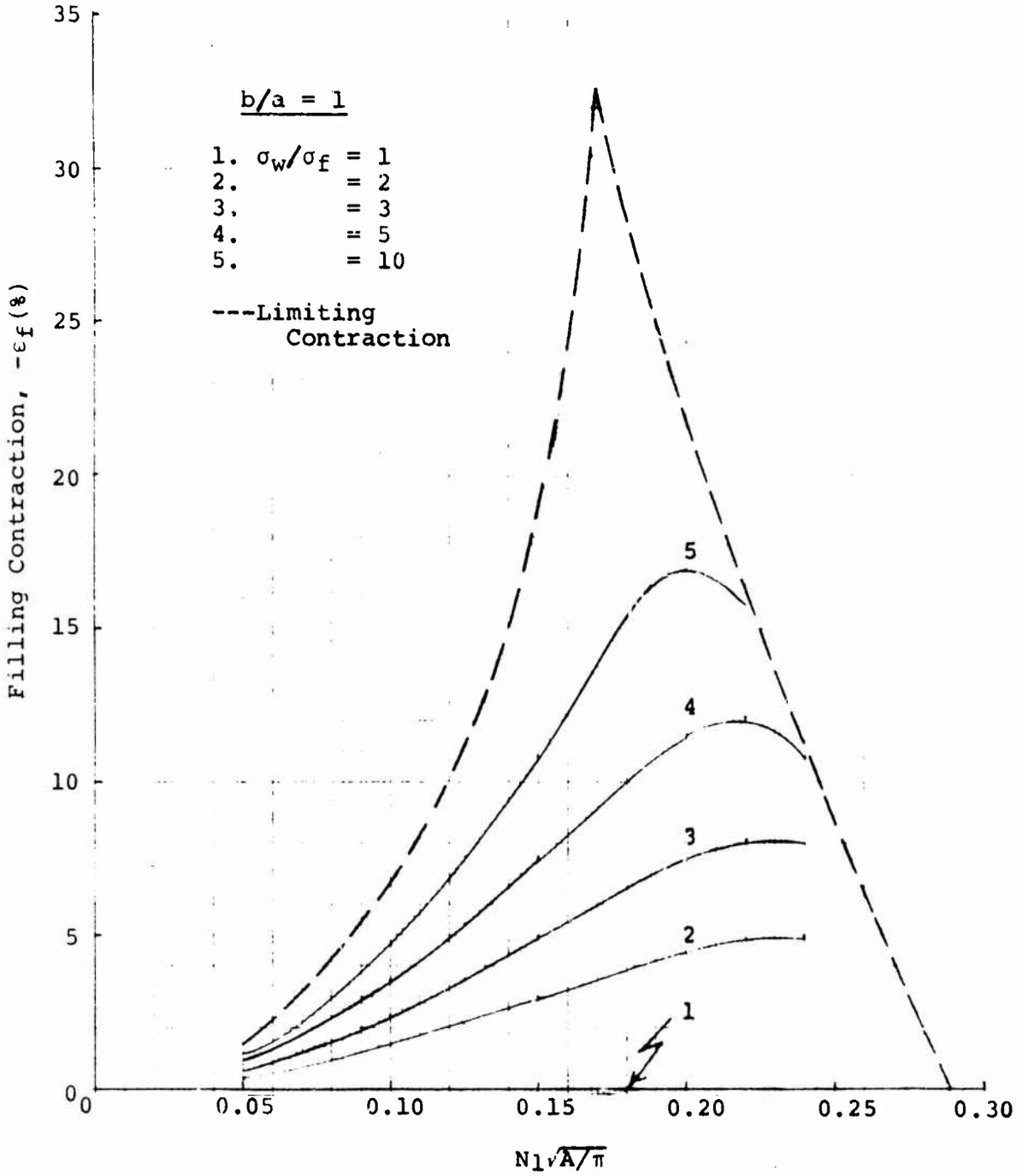

Figure 18(b). Fabric Contraction in the Filling Direction: (Aspect Ratio = 1) Inextensible Yarn

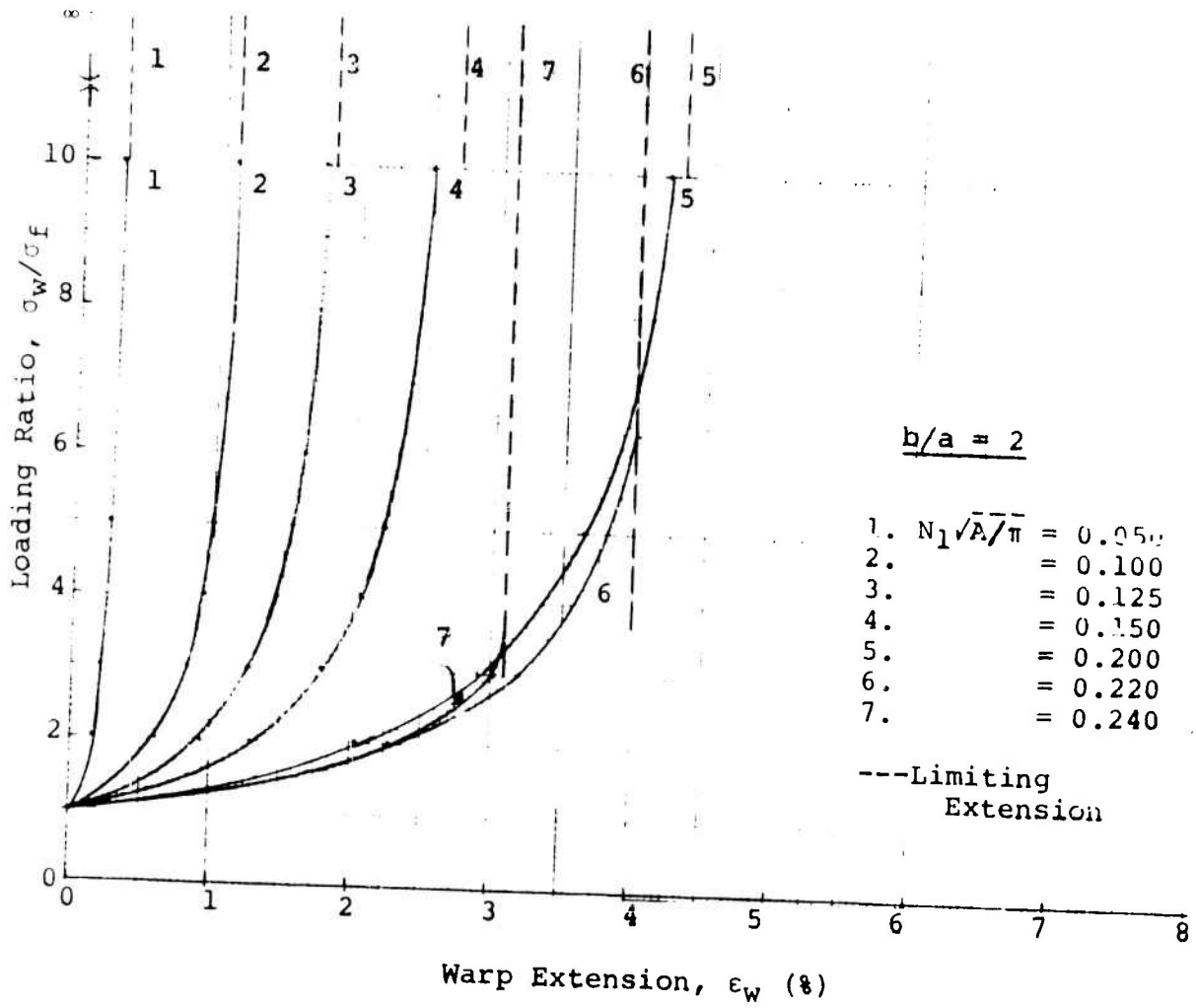

Figure 19(a) Fabric Extension in the Warp Direction: (Aspect Ratio = 2), Inextensible Yarn

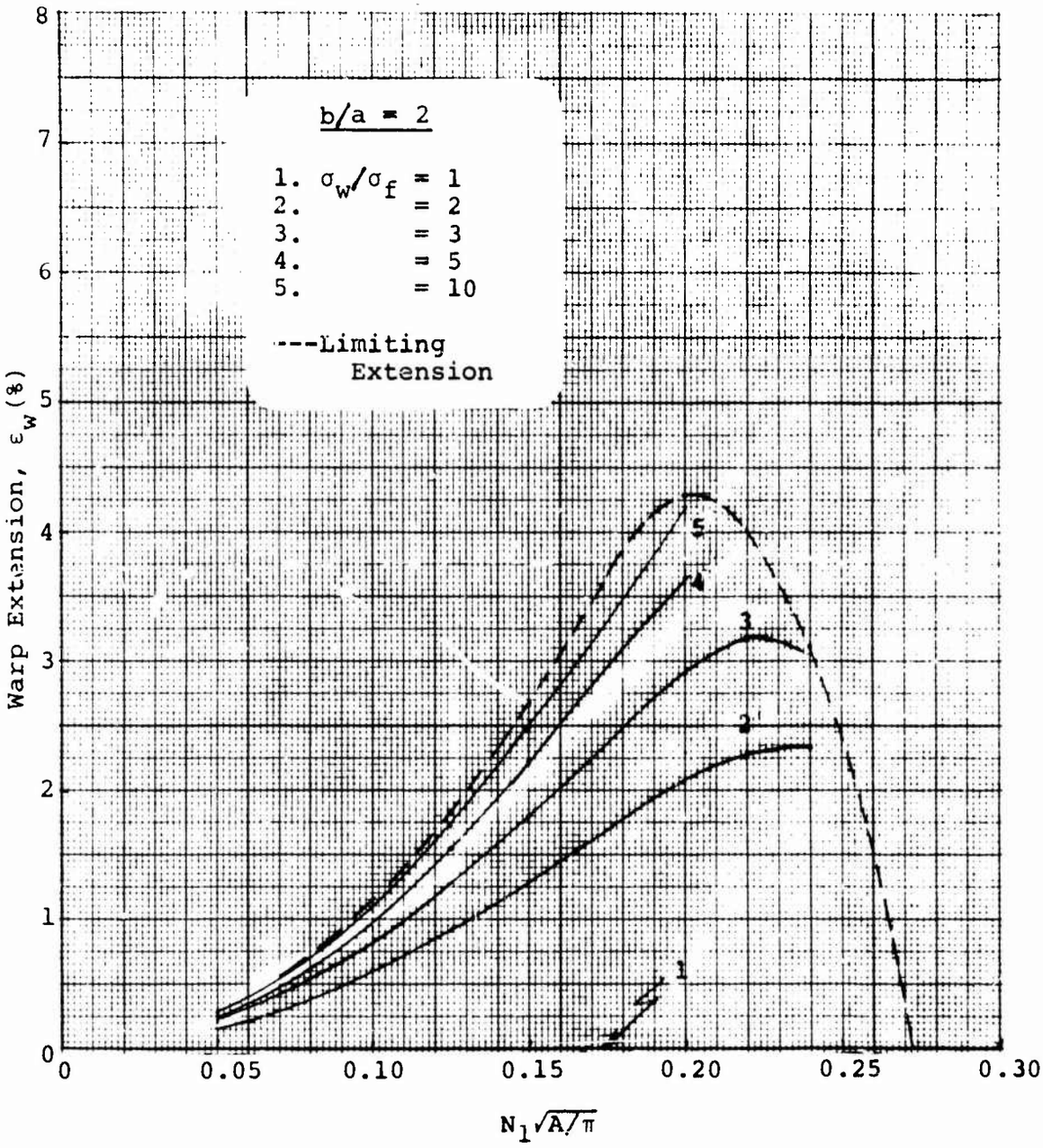

Figure 19(b). Fabric Extension in the Warp Direction: (Aspect Ratio = 2), Inextensible Yarn

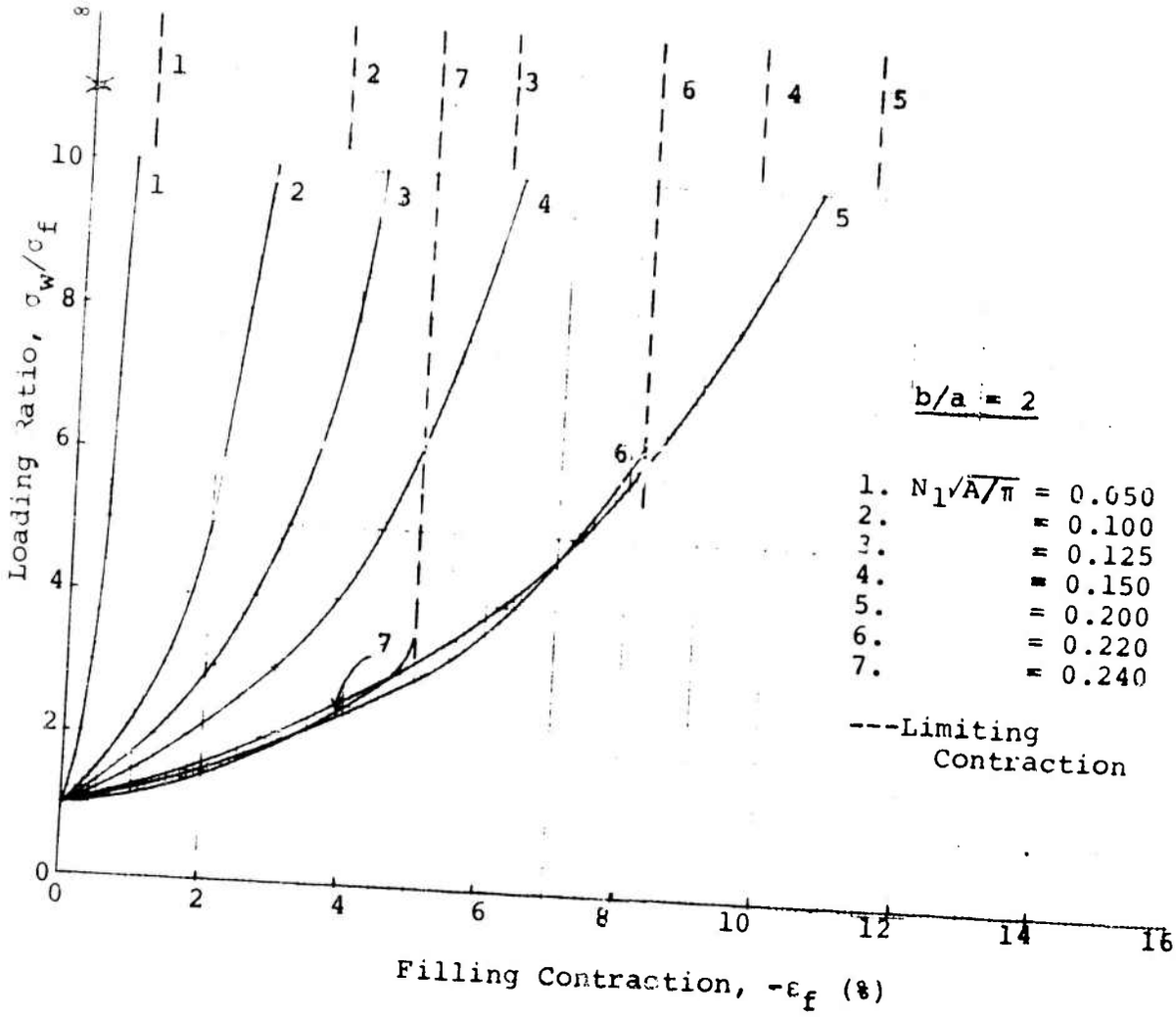

Figure 20(a). Fabric Contraction in the Filling Direction: (Aspect Ratio = 2), Inextensible Yarn

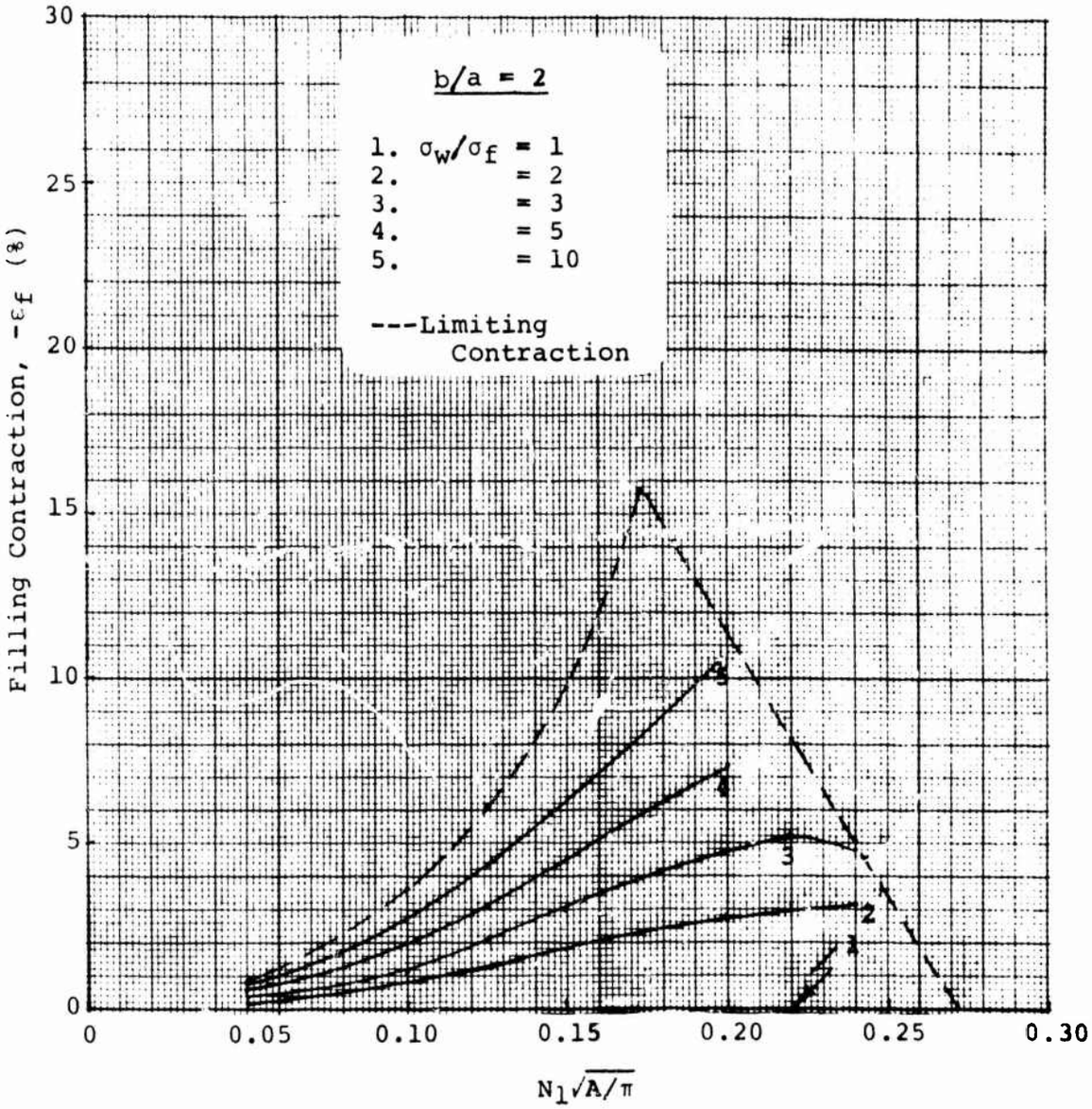

Figure 20(b). Fabric Contraction in the Filling Direction: (Aspect Ratio = 2), Inextensible Yarn

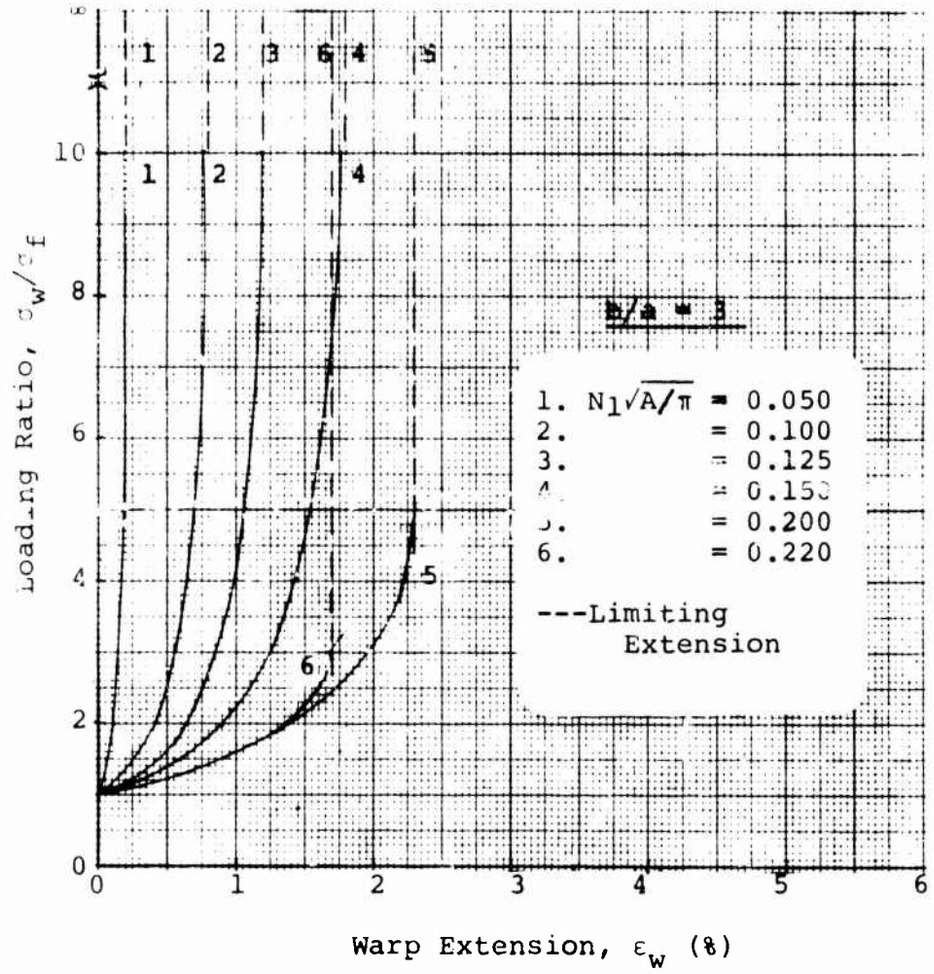

Figure 21(a). Fabric Extension in the Warp Direction: (Aspect Ratio = 3), Inextensible Yarn

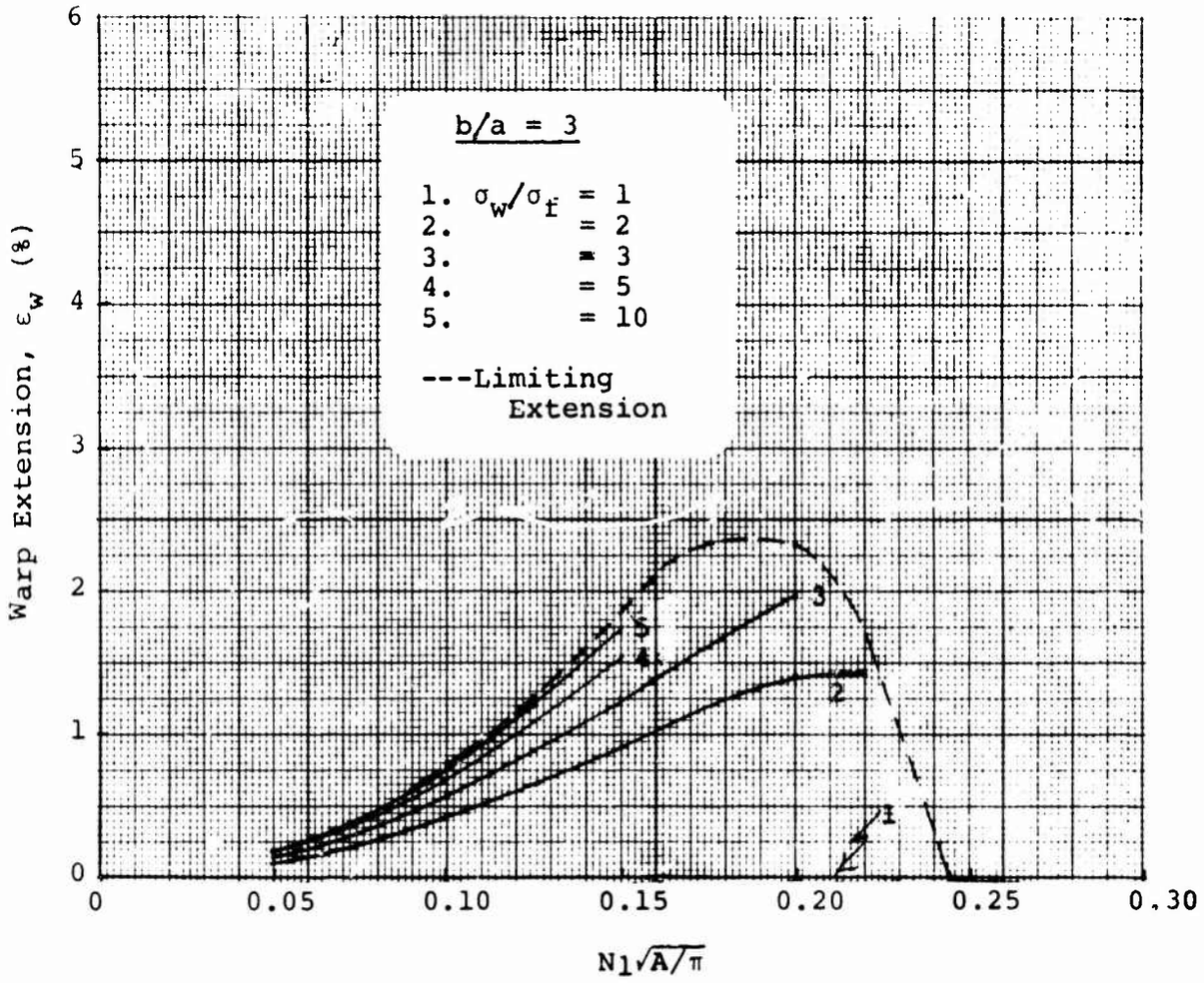

Figure 21(b). Fabric Extension in the Warp Direction: (Aspect Ratio = 3), Inextensible Yarn

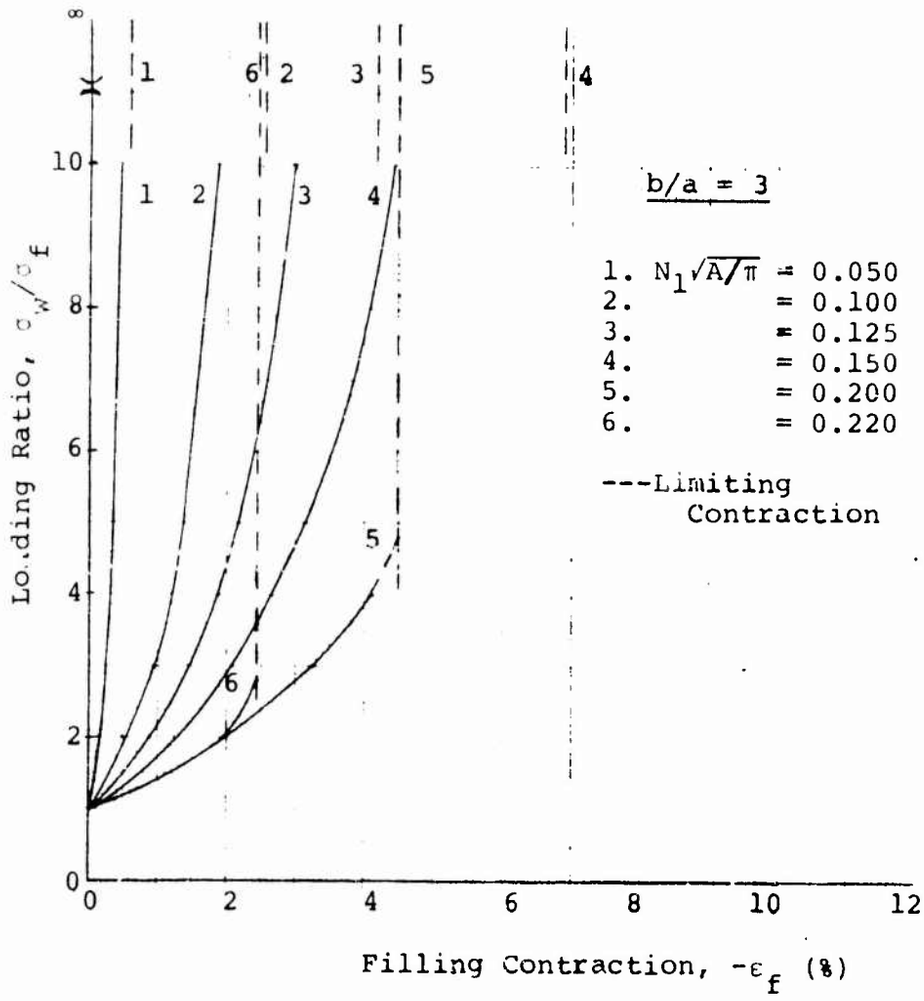

Figure 22(a). Fabric Contraction in the Filling Direction (Aspect Ratio = 3), Inextensible Yarn

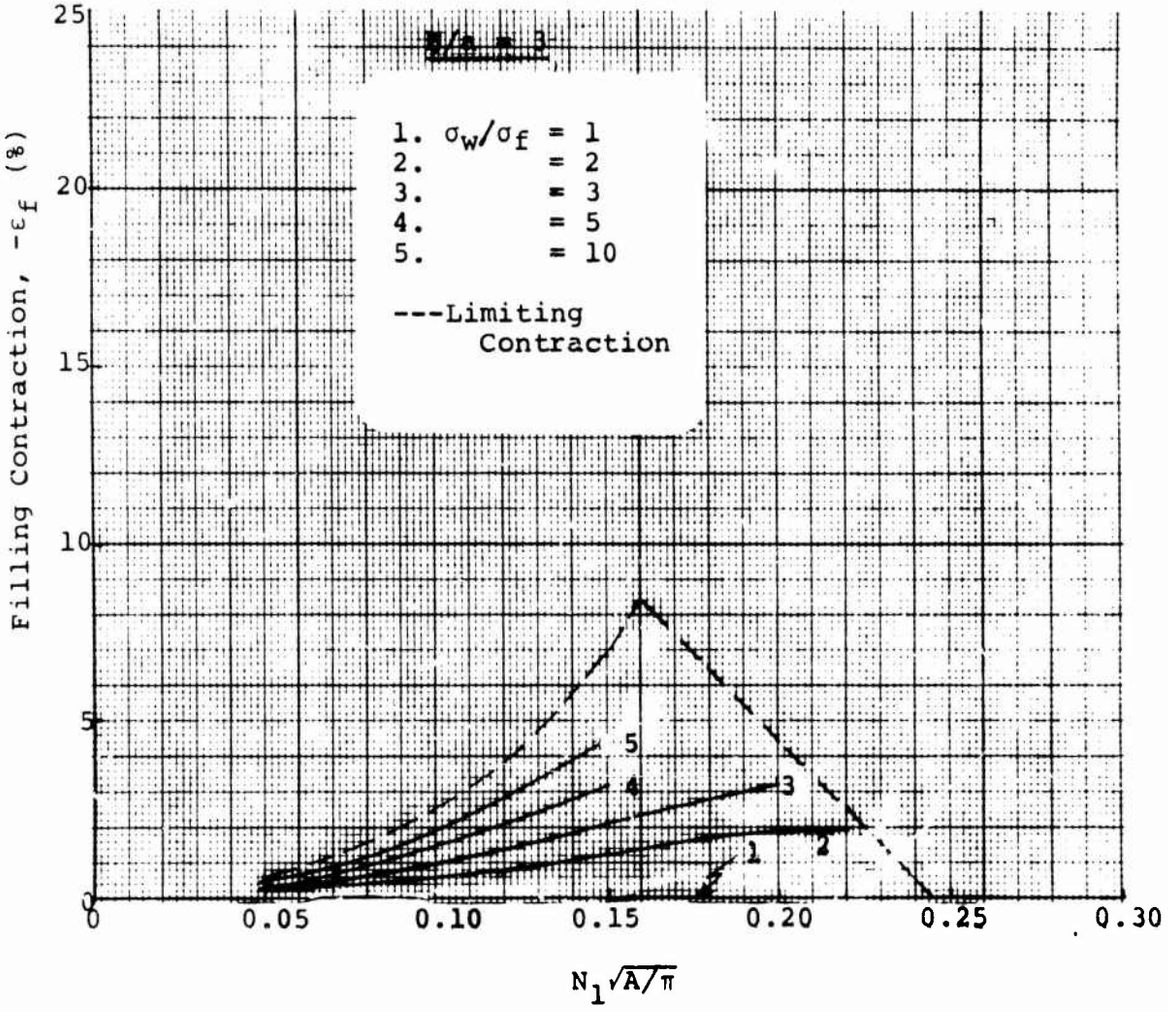

Figure 22(b). Fabric Contraction in the Filling Direction: (Aspect Ratio = 3), Inextensible Yarn

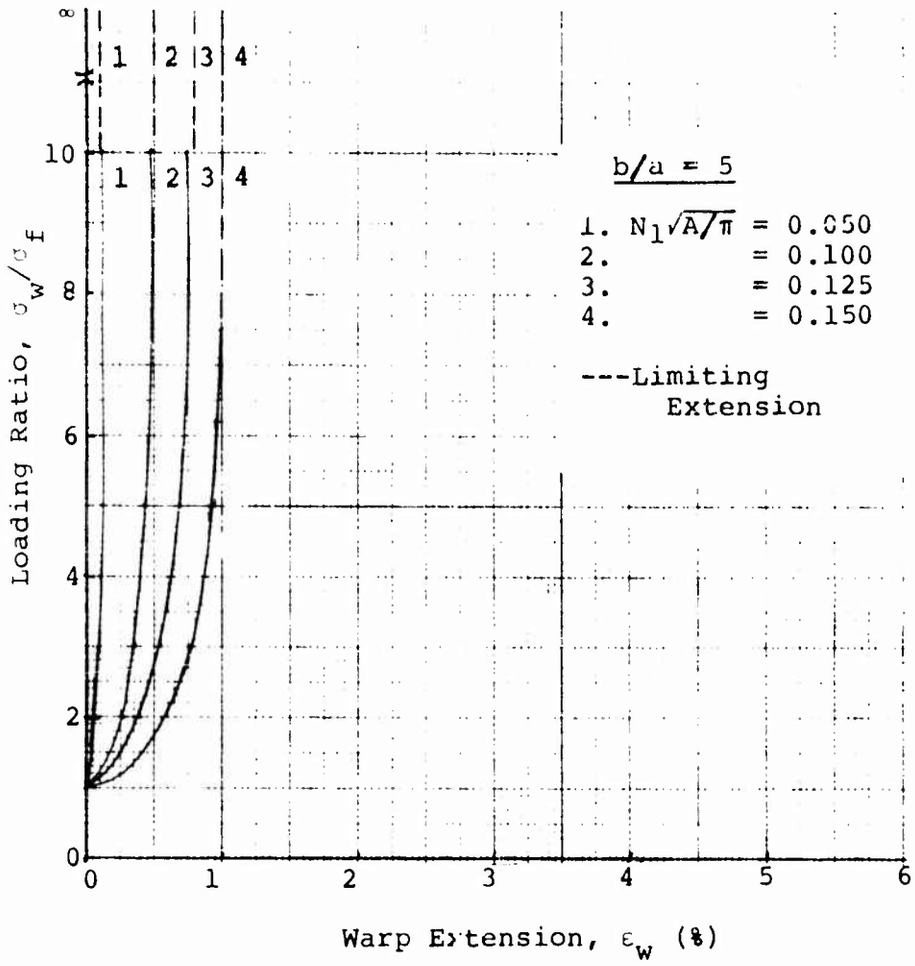

Figure 23(a). Fabric Extension in the Warp Direction: (Aspect Ratio = 5). Inextensible Yarn

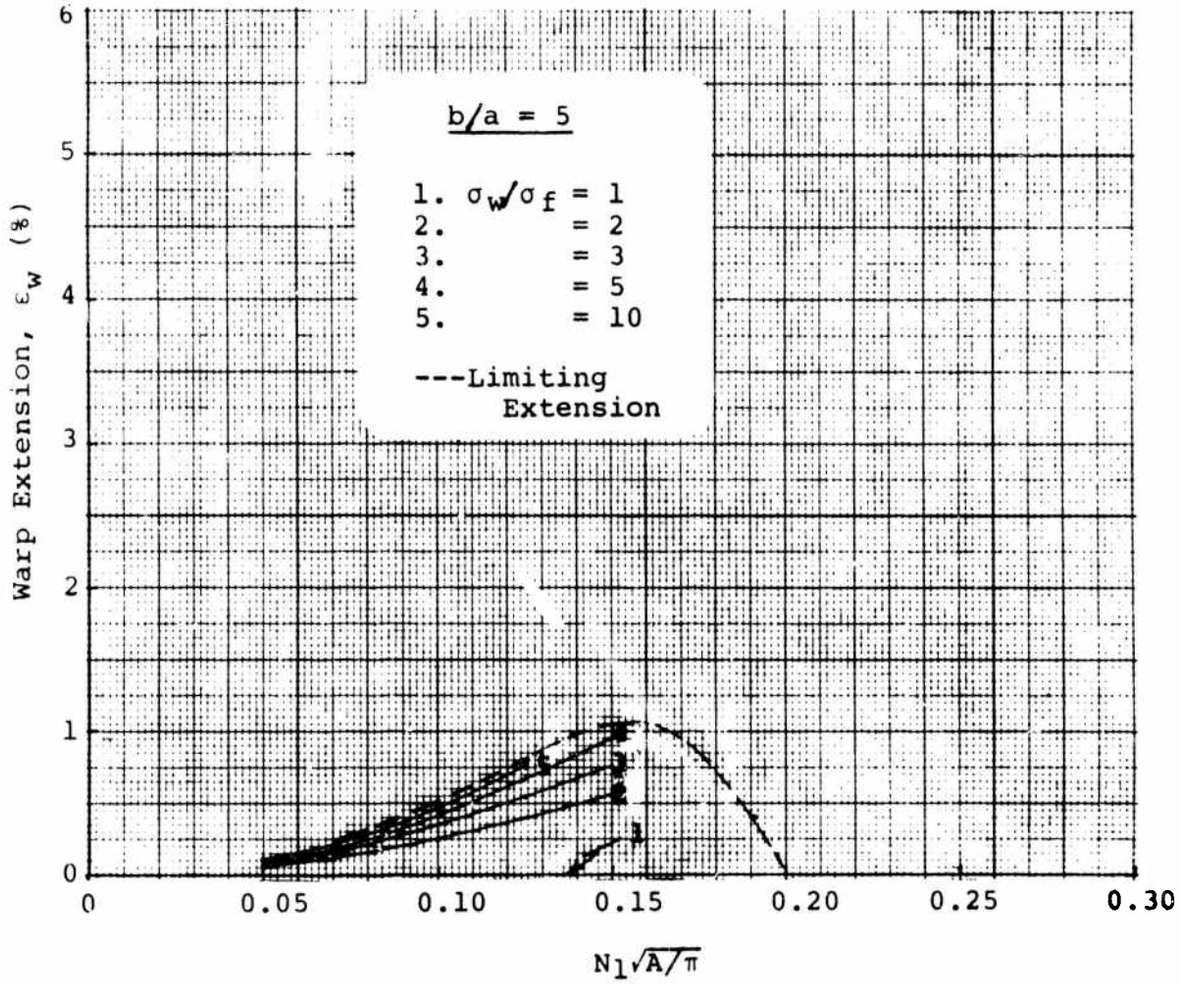

Figure 23(b). Fabric Extension in the Warp Direction (Aspect Ratio = 5), Inextensible Yarn

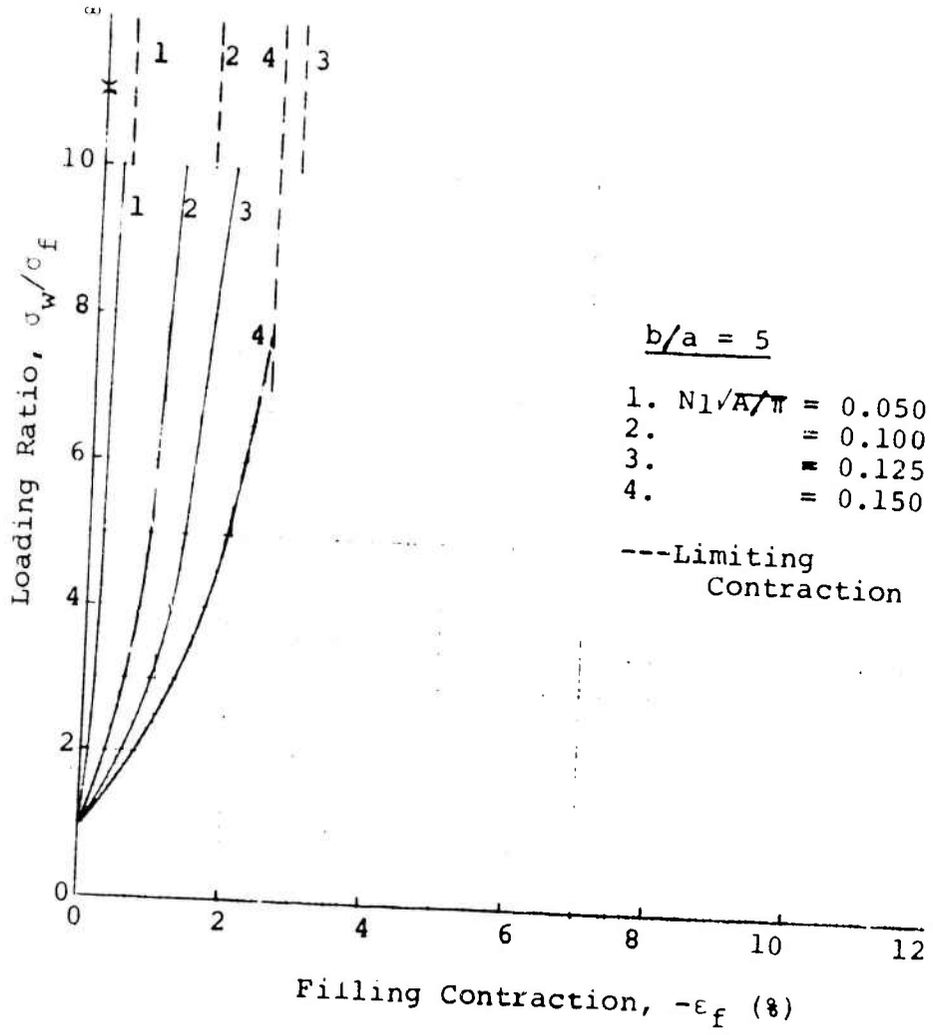

Figure 24(a). Fabric Contraction in the Filling Direction: (Aspect Ratio = 5), Inextensible Yarn

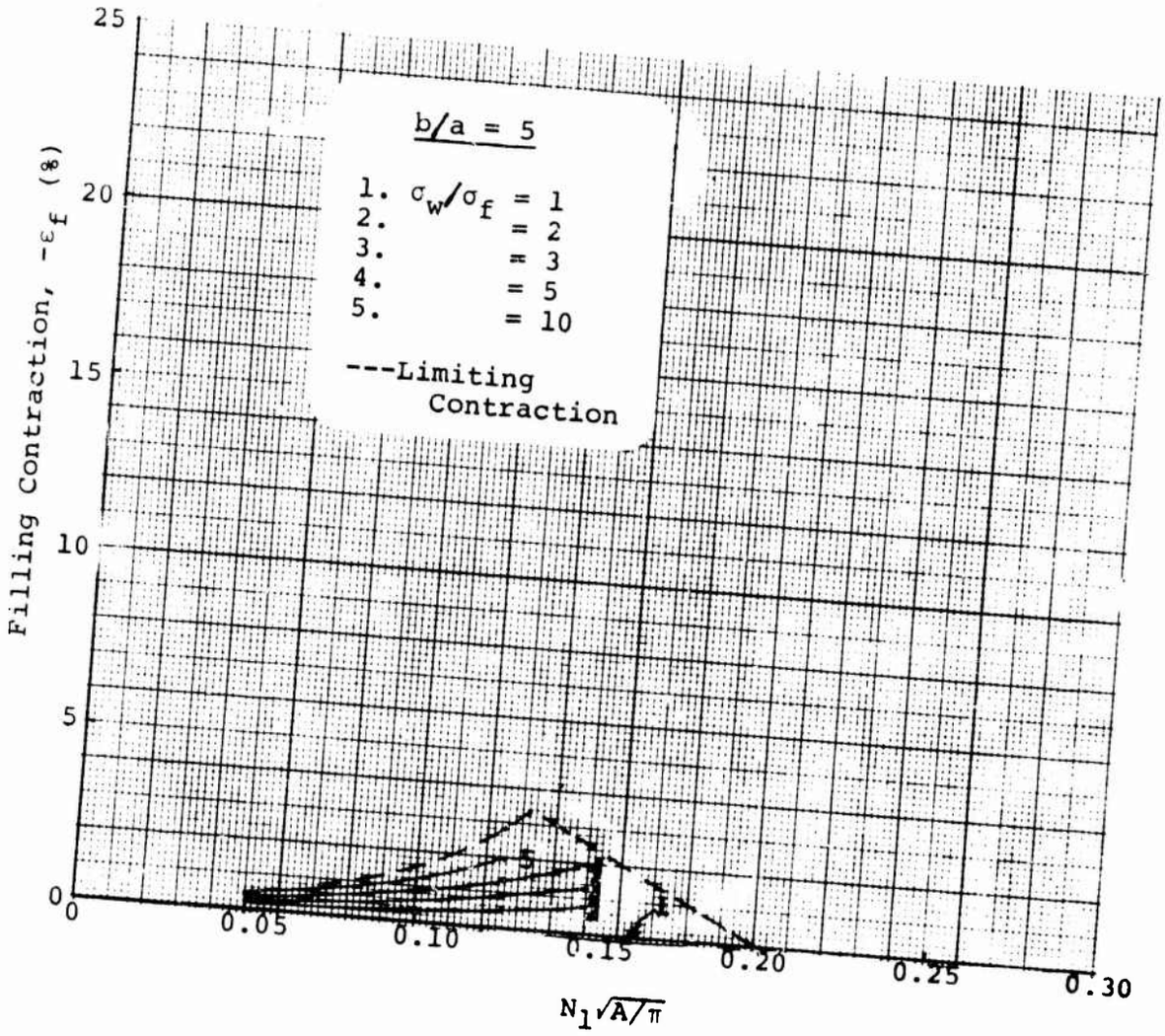

Figure 24(b). Fabric Contraction in the Filling Direction: (Aspect Ratio = 5), Inextensible Yarn

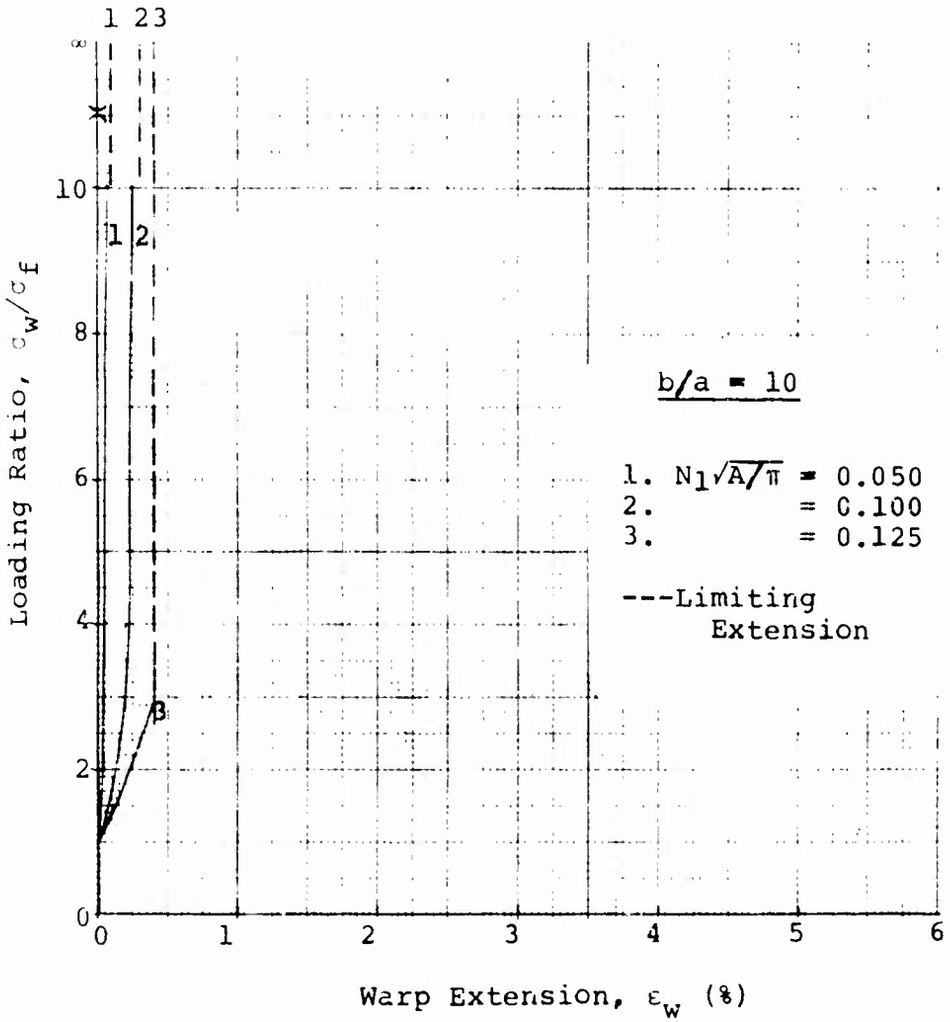

Figure 25(a). Fabric Extension in the Warp Direction: (Aspect Ratio = 10), Inextensible Yarn

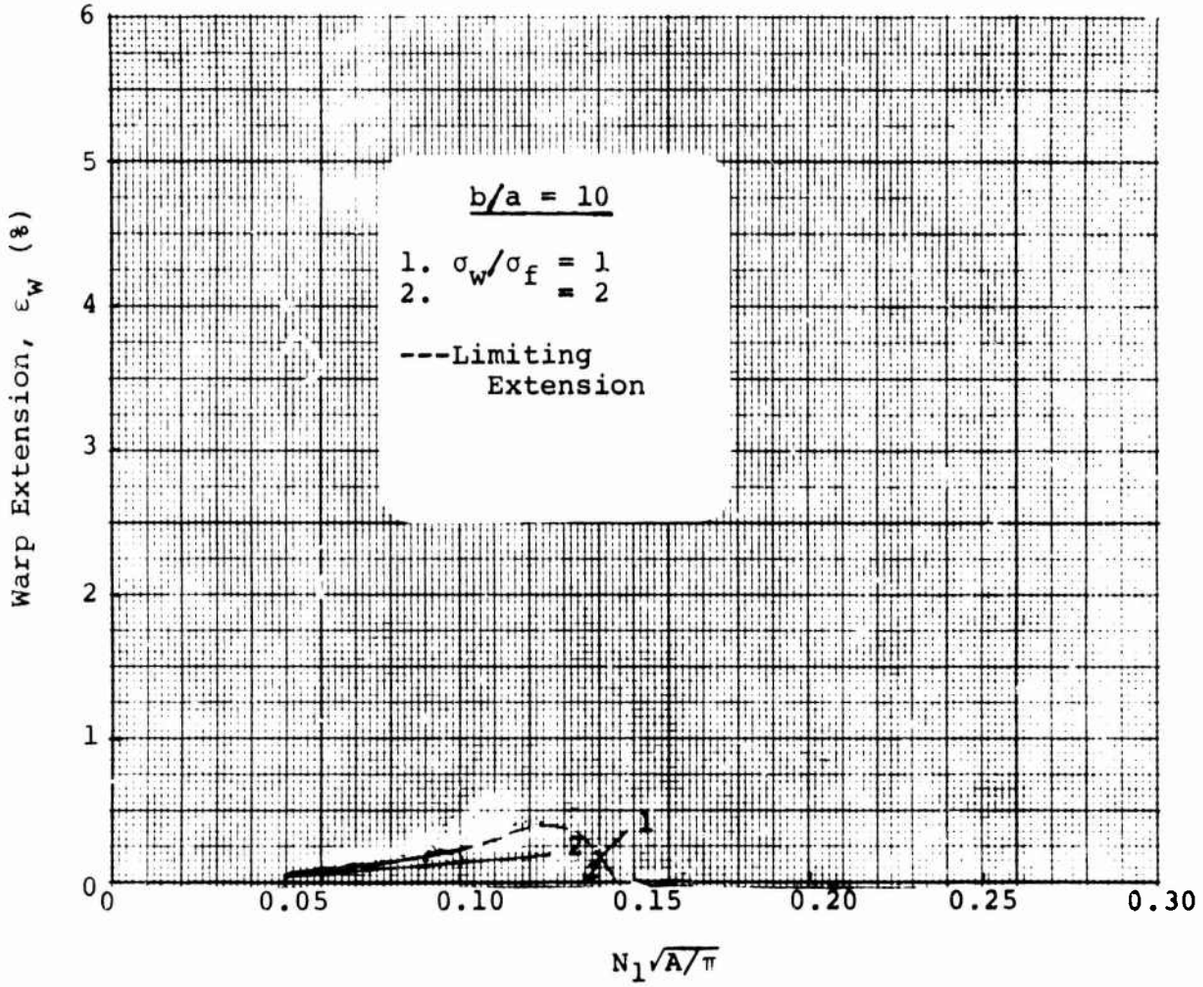

Figure 25(b). Fabric Extension in the Warp Direction: (Aspect Ratio = 10), Inextensible Yarn

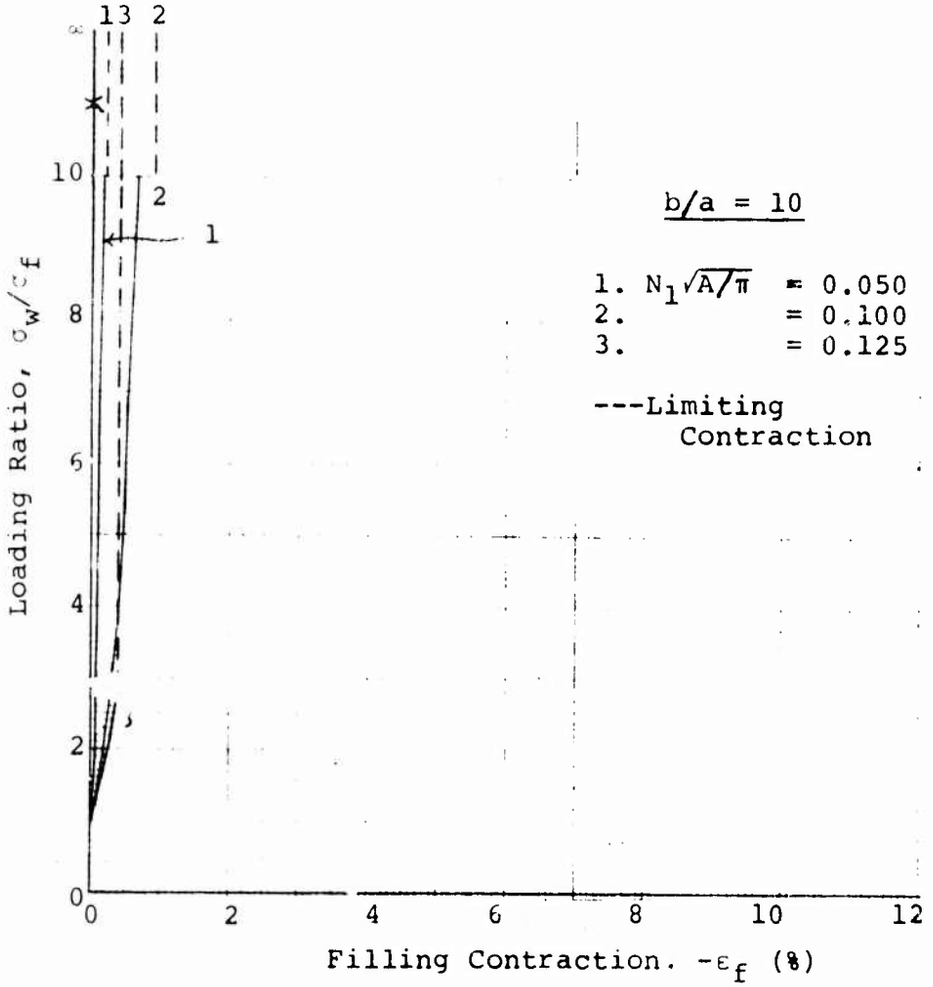

Figure 26(a). Fabric Contraction in the Filling Direction: (Aspect Ratio = 10), Inextensible Yarn

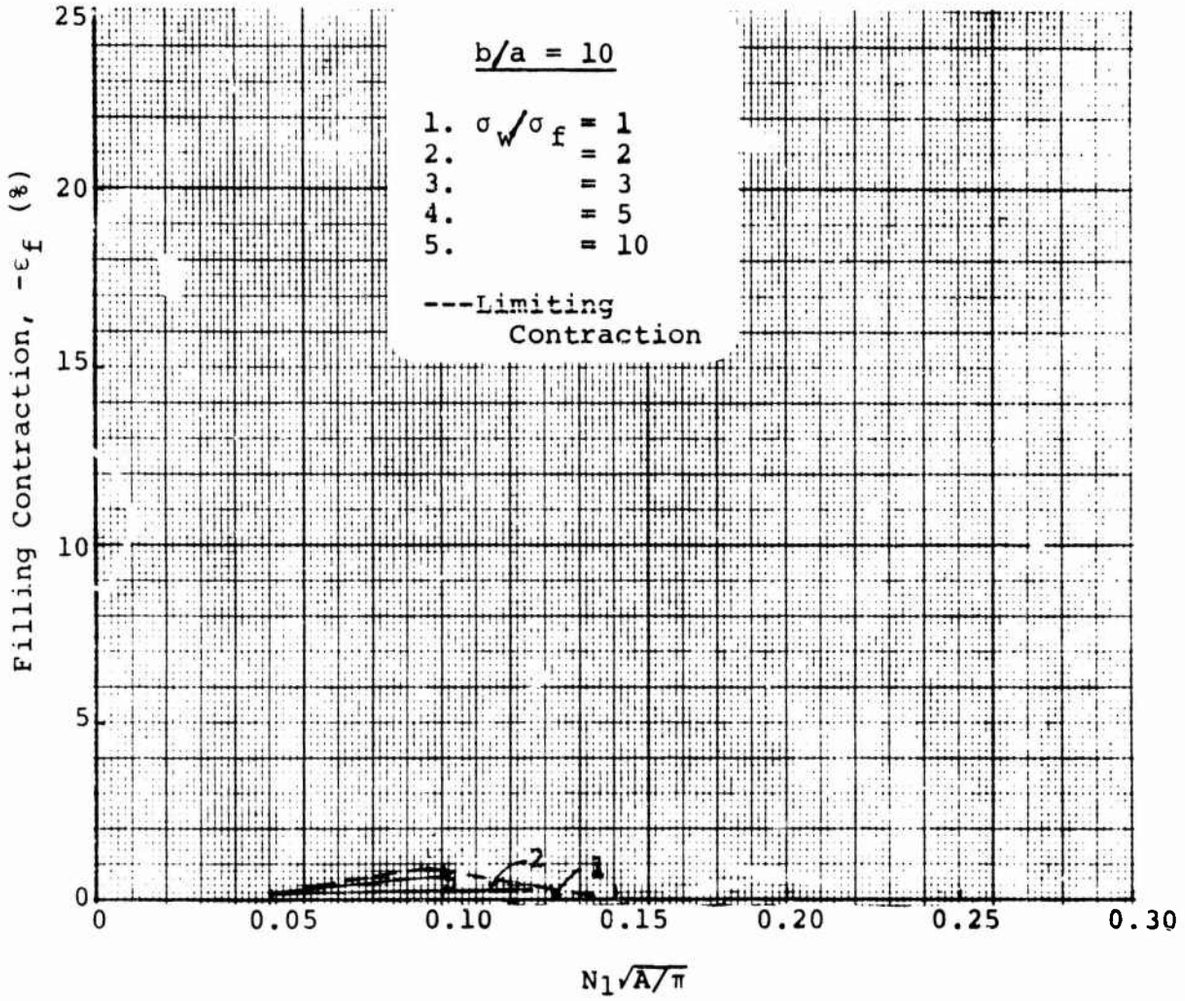

Figure 26(b). Fabric Contraction in the Filling Direction: (Aspect Ratio = 10), Inextensible Yarn

Examination of Figures 17 through 26 shows that the amount of extension or contraction achieved in the fabric as a result of crimp interchange increases with both increasing loading ratio and in general with increasing weave tightness, i.e., $N_1\sqrt{A/\pi}$. This latter effect occurs even though the length L of yarn between crossovers decreases with increasing number of ends per unit width N because the ratio of L to the yarn spacing $1/N_1$ increases. However, a limiting geometry is reached at lower levels of the loading ratio for those fabrics characterized by higher values of $N_1\sqrt{A/\pi}$, as indicated by the curves which are terminated at loading ratios lower than 10 (see Table 5).

No fabric extension occurs for a loading ratio of one. Since the fabric is initially square, i.e., containing an equal number of ends and equal crimp in both the warp and filling directions, no crimp interchange can take place under conditions of equal loading in both directions. For loading ratios greater than one, the fabric elongates in the warp direction and contracts in the filling direction. The magnitudes of these extensions increase with increasing values of the loading ratio, approaching the limiting extension asymptotically. Additionally, the fabric contracts more in the filling direction than it extends in the warp direction.

Comparison of Figures 17, 19, 21, 23 and 25 and also Figures 18, 20, 22, 24 and 26 indicate that, generally, as the yarn aspect ratio increases, the fabric becomes stiffer in tension, i.e., the amount of extension or contraction resulting from the application of a particular loading ratio decreases as the degree of yarn flattening increases. This decrease in crimp interchange is primarily attributable to the small, but nonetheless significant, decrease in total yarn length between crossovers and decreasing level of initial crimp with increasing aspect ratio for particular values of $N_1\sqrt{A/\pi}$.

Comparison of Figures 17 through 26 with comparable data in Reference 2 for fabrics comprised of yarns with a racetrack cross-section shows that at low values of $N_1\sqrt{A/\pi}$ the load-elongation response of fabrics containing lenticular yarns is very nearly identical with the response of racetrack yarn fabrics for the same degree of yarn flattening; at higher values of $N_1\sqrt{A/\pi}$, however, the racetrack yarn fabrics show considerably greater extension than the fabrics containing lenticular yarns under the same conditions.

The magnitude of the radial separation or GAP between the node of the lenticular cross-section and the crossing yarn after loading is illustrated in Figures 27-30 for yarn aspect ratios of 2, 3, 5 and 10. The analytical expressions describing the gap in the warp and filling directions respectively after loading are as follows:

$$GAP_{2w} = \frac{1-\cos(\phi-\theta_{2f})}{(1-\cos\phi)\cos(\phi-\theta_{2f})} \tag{46}$$

$$GAP_{2f} = \frac{1-\cos(\phi-\theta_{2w})}{(1-\cos\phi)\cos(\phi-\theta_{2w})} \tag{47}$$

As expected the separation increases between the node of the filling yarn and the crossing warp yarn and decreases between the node of the warp yarn and the crossing filling yarn with increasing loading ratio.

Limiting Geometries

(1) Warp yarns pulled straight -- If the length L of yarn between crossovers is sufficient, as the loading ratio σ_w/σ_f increases, eventually all of the crimp will be pulled out of the warp yarns, $\theta_{2w} = 0$, with an appropriate increase in the filling yarn crimp. Figure 31 illustrates this limiting configuration.

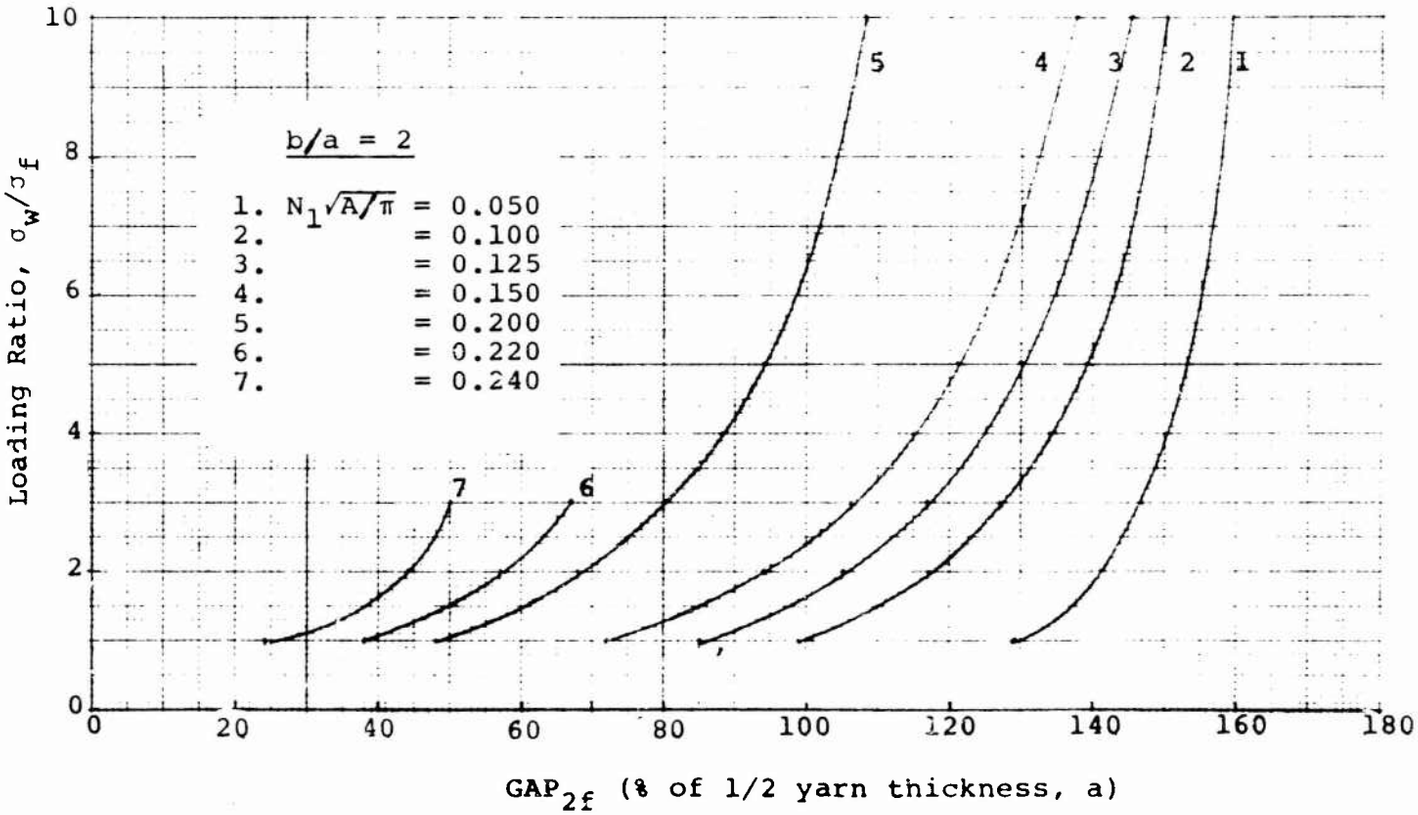

Figure 27(a). Radial Separation Between the Crossing Warp Yarn and the Node of the Filling Cross-Section (Aspect Ratio = 2), Inextensible Yarn

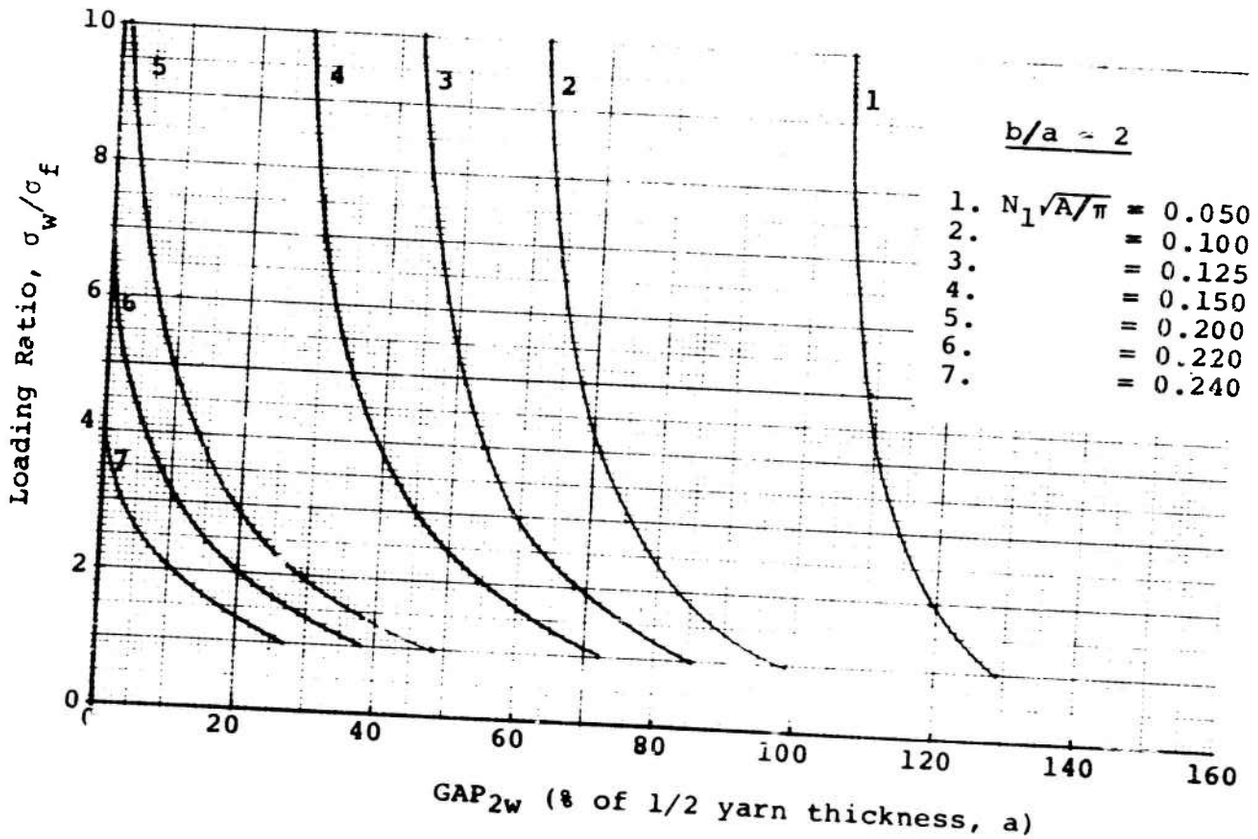

Figure 27(b). Radial Separation Between the Crossing Filling Yarn and the Node of the Warp Cross-Section (Aspect Ratio = 2), Inextensible Yarn

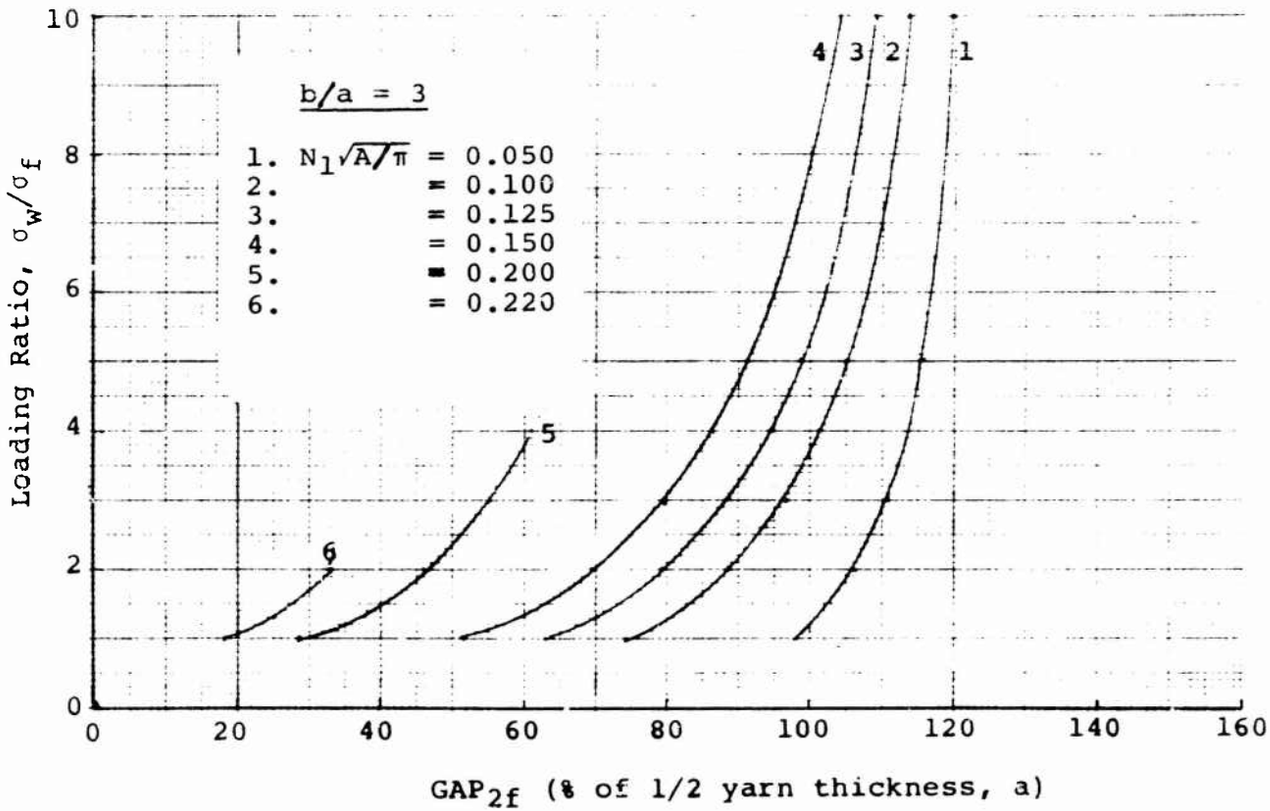

Figure 28(a). Radial Separation Between the Crossing Warp Yarn and the Node of the Filling Cross-Section (Aspect Ratio = 3), Inextensible Yarn

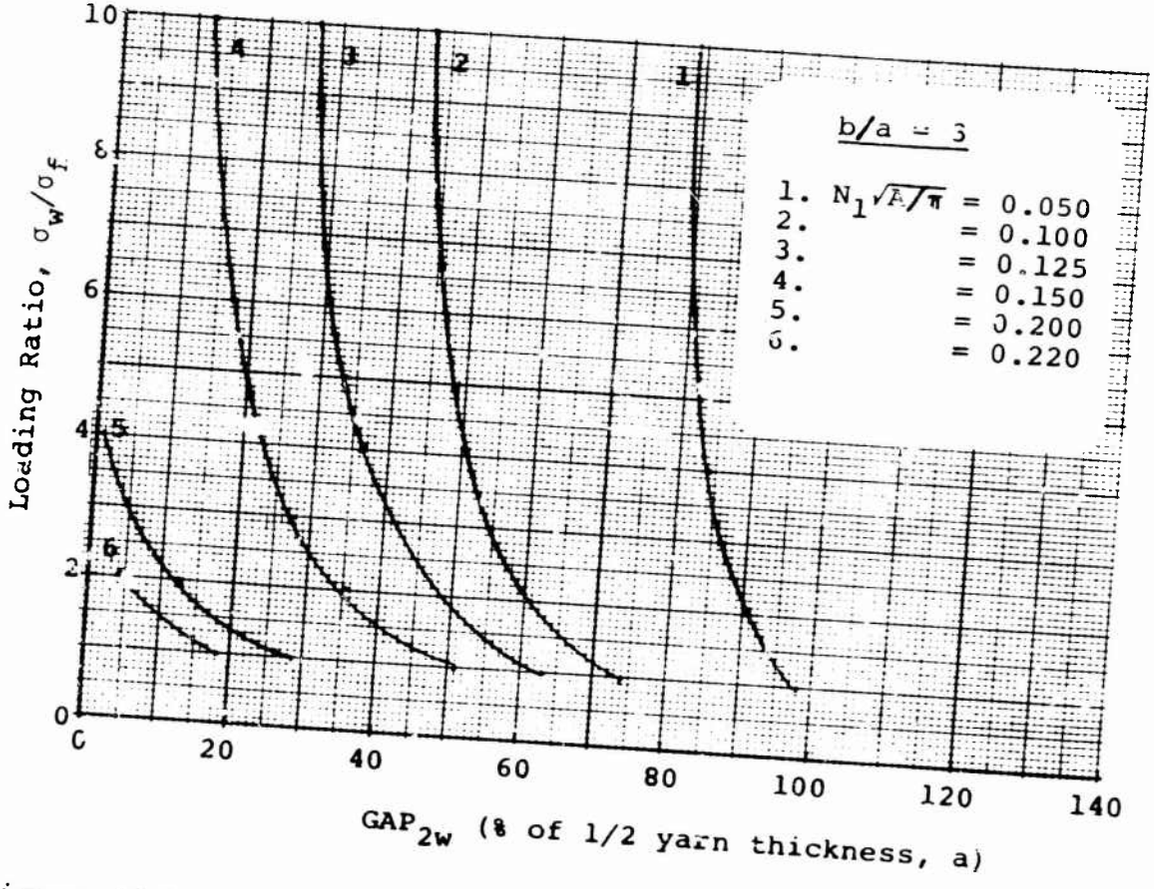

Figure 28(b). Radial Separation Between the Crossing Filling Yarn and the Node of the Warp Cross-Section (Aspect Ratio = 3), Inextensible Yarn

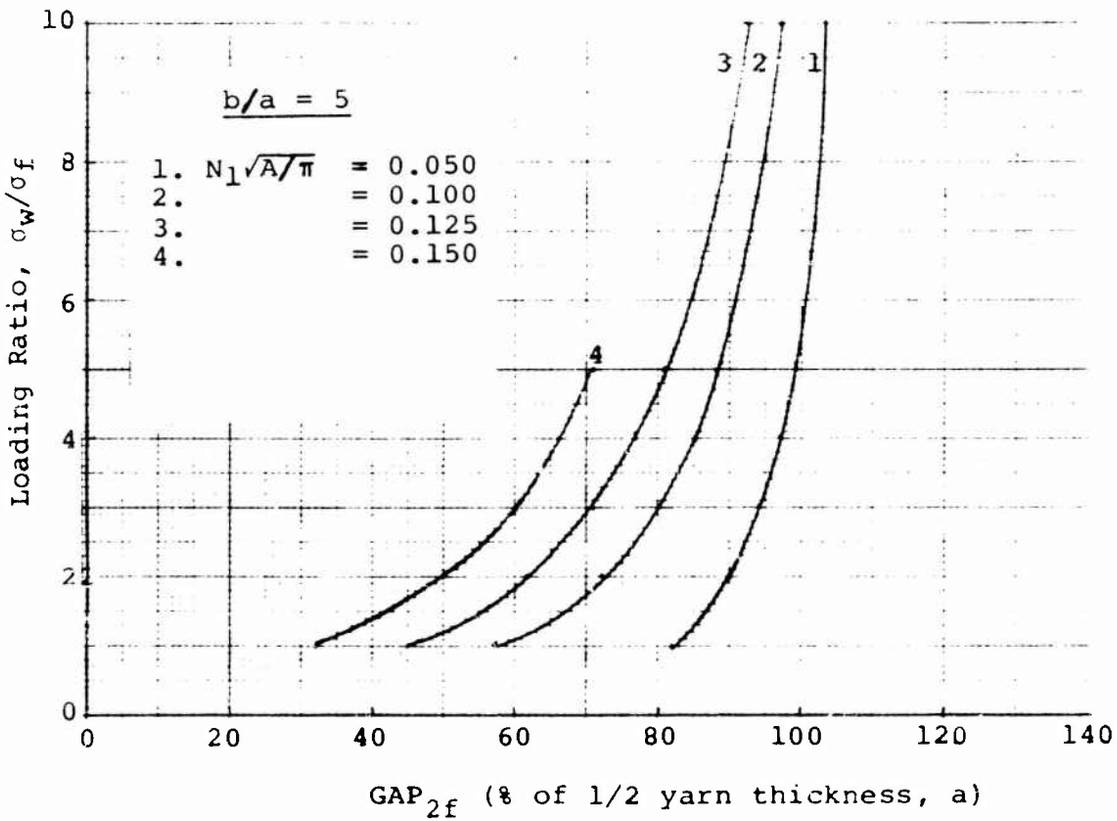

Figure 29(a). Radial Separation Between the Crossing Warp Yarn and the Node of the Filling Cross-Section (Aspect Ratio = 5): Inextensible Yarn

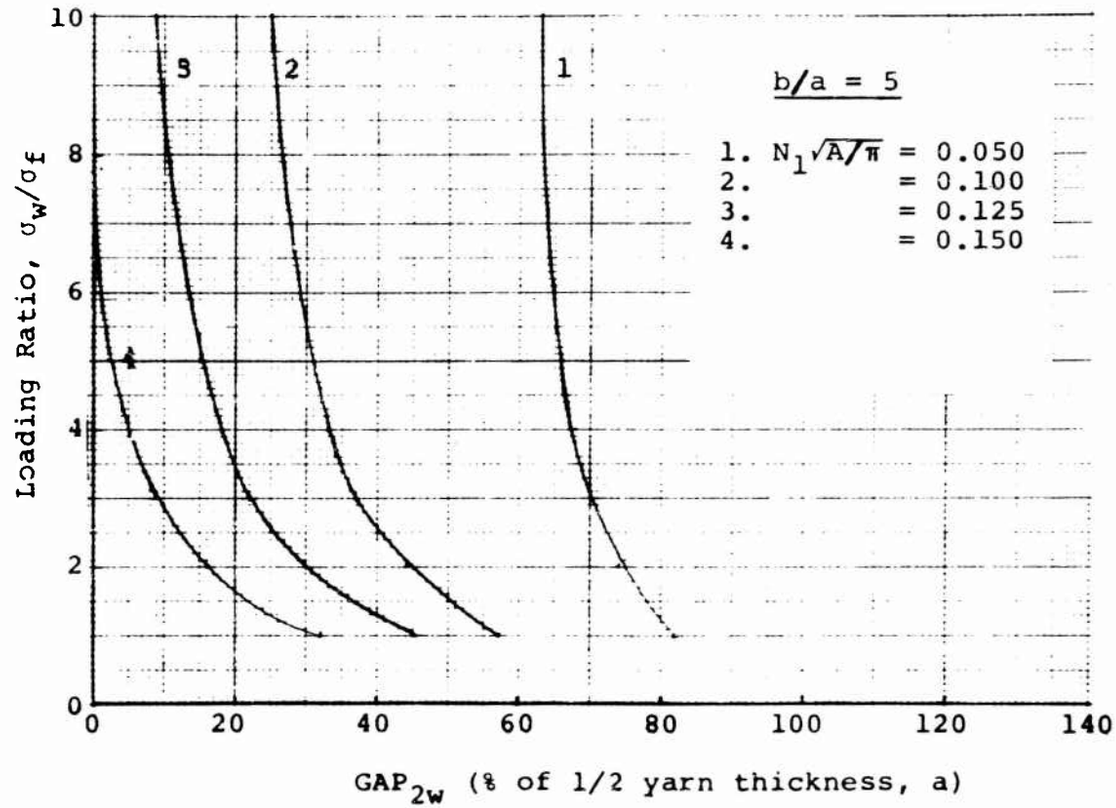

Figure 29(b). Radial Separation Between the Crossing Filling Yarn and the Node of the Warp Cross-Section (Aspect Ratio = 5), Inextensible Yarn

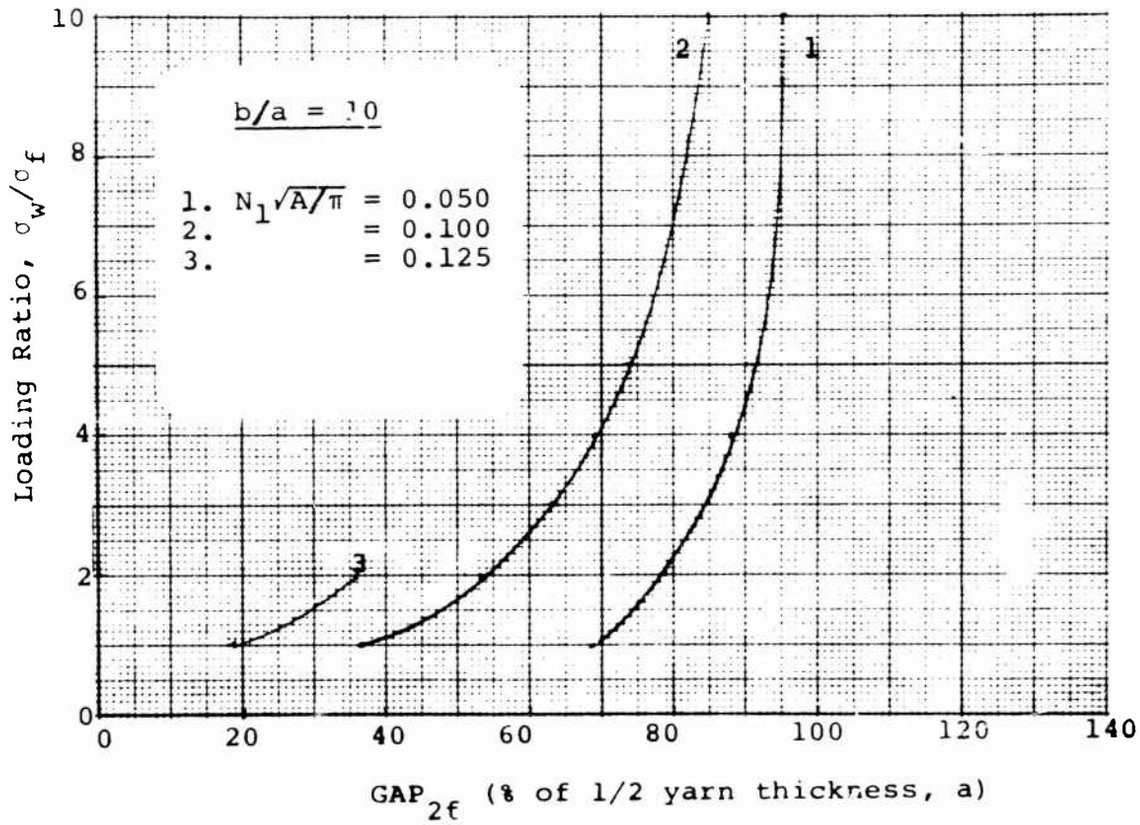

Figure 30(a). Radial Separation Between the Crossing Warp Yarn and the Node of the Filling Cross-Section (Aspect Ratio = 10), Inextensible Yarn

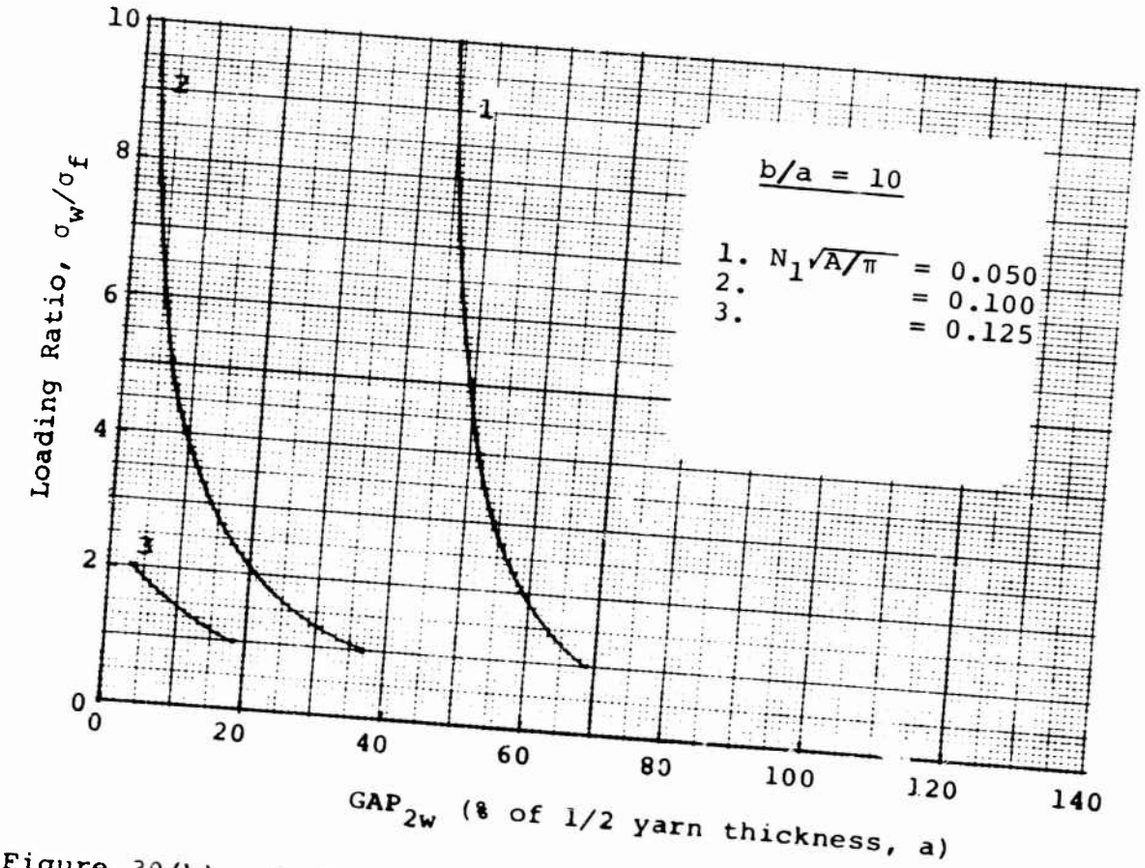

Figure 30(b). Radial Separation Between the Crossing Filling Yarn and the Node of the Warp Cross-Section (Aspect Ratio = 10). Inextensible Yarn

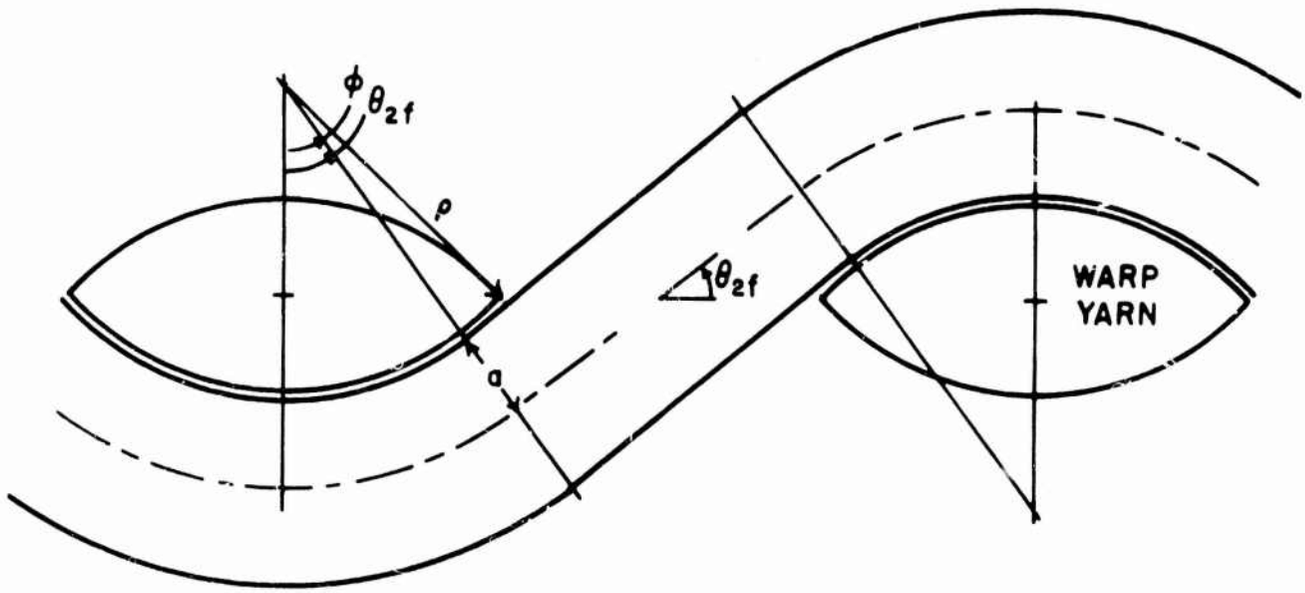

Figure 31. Warp Yarns Pulled Straight

(2) Maximum filling wrap an -- As the filling yarn crimp increases upon loading, a value $\theta_{2f} = \phi$ may be reached which defines the maximum wrap angle consistent with the requirements of the assumed fabric model. This type of limiting geometry is shown in Figure 32.

(3) Maximum filling contraction -- For certain initial constructions a degree of filling yarn crimp may be achieved upon loading such that there is no straight length of yarn - no component L_I of the length of yarn L - between crossovers. When this occurs, the fabric cannot contract further in the filling direction. This condition is described by the relationship

$$L = 2(\rho+a)\theta_{2f} = 2\rho(2-\cos\phi)\theta_{2f}$$

which may be seen from Figure 33.

(4) Contact between adjacent warp yarns at the fabric midplane -- This type of limiting geometry can conceivably be achieved only for those initial fabric constructions where $L \approx 2b$. If it is achieved, then

$$\frac{1}{N_{2w}} = 2b.$$

Figure 34 illustrates this configuration.

In order to predict those fabric constructions which are subject to a particular type of limiting configuration it is necessary to consider the boundaries between successive types: (1) Warp yarns pulled straight - maximum filling wrap angle: -- The two requirements necessary for these configurations to occur simultaneously are $\theta_{2w} = 0$ and $\theta_{2f} = \phi$. Substituted into Equation 39, the following relationship is defined:

$$L/\rho = 2[\phi(2-\cos\phi)+\cot\phi(1-\cos\phi)] \qquad (48)$$

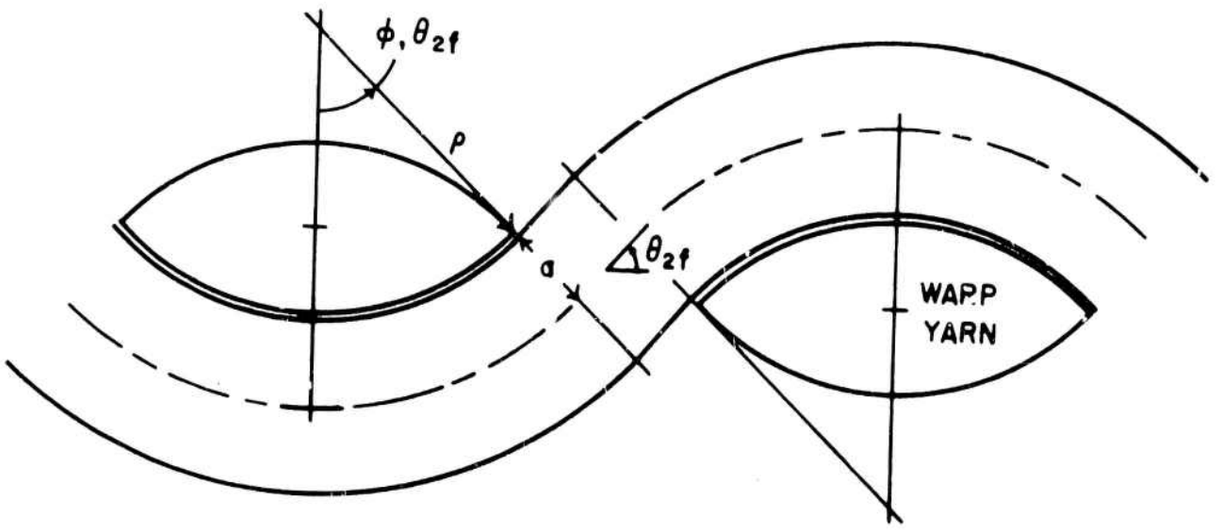

Figure 32. Maximum Filling Wrap Angle

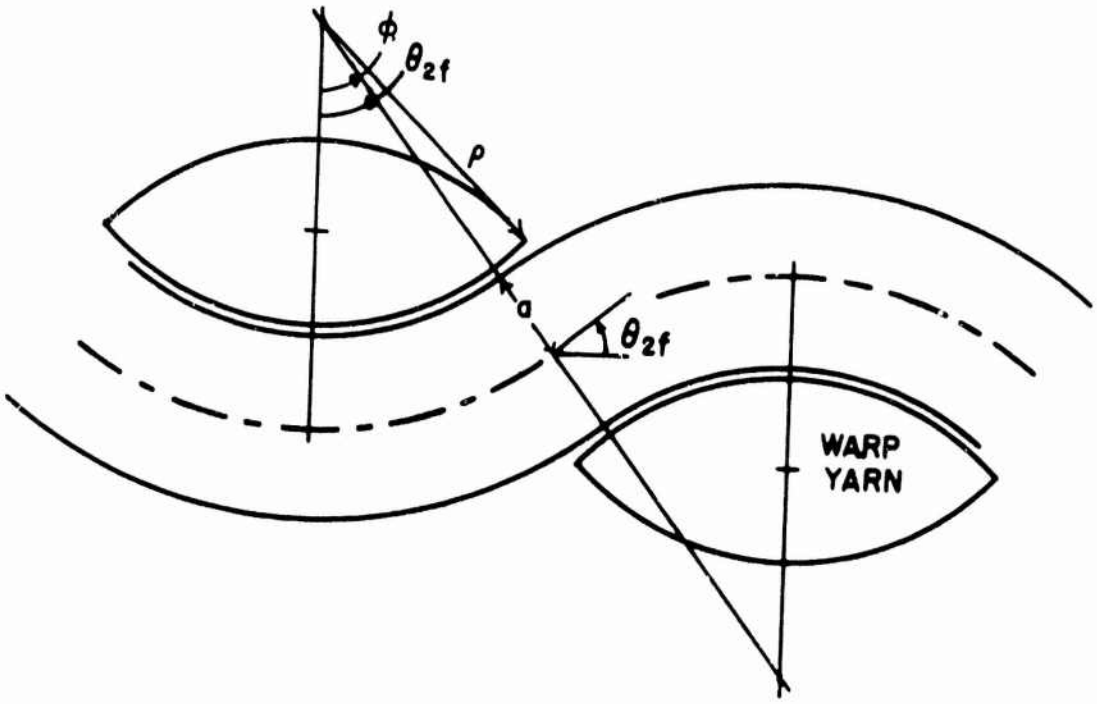

Figure 33. Maximum Filling Yarn Crimp

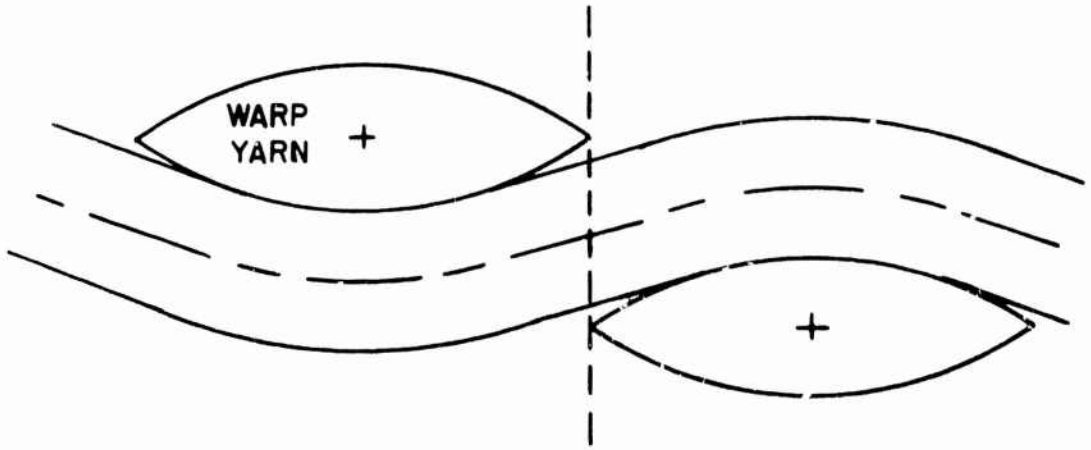

Figure 34. Warp Yarns in Contact at Midplane Between Yarn Crossovers

Combination of the two relationships specifying this condition, namely,

$$\theta_{2f} = \phi$$

$$\theta_{2f} = \frac{L}{2\rho(2-\cos\phi)}$$

yields

$$L/\rho = 2\phi(2-\cos\phi). \tag{49}$$

The above expressions for L/ρ in conjunction with Equations 32 and 33 and 34 may be used to compute boundary values for $L/\sqrt{A/\pi}$ and $N_1\sqrt{A/\pi}$ between types of limiting conditions. These values are listed in Table 3.

For a specified yarn aspect ratio and yarn cross-sectional area, the maximum number of ends which can be accommodated in an initially square fabric can be determined as a special case of the maximum filling contraction limiting condition. A fabric is initially "jammed" when

$$L = 2(\rho+a)\theta_1 = 2\rho(2-\cos\phi)\theta_1. \tag{50}$$

Combining this expression with Equation 33 gives

$$\cos\theta_1 = \frac{1}{2-\cos\phi}. \tag{51}$$

Using the above two relationships and Equations 32 and 34 the maximum value of $N_1\sqrt{A/\pi}$ and minimum value of $L/\sqrt{A/\pi}$ possible in an initially square fabric construction can be computed for various yarn aspect ratios. These values are also given in Table 3.

TABLE 3

TYPE OF LIMITING GEOMETRY ACHIEVABLE
FOR VARIOUS INITIAL FABRIC CONSTRUCTIONS

b/a	$L/\sqrt{A/\pi}$	$N_1\sqrt{A/\pi}$	Limiting Condition
1	$\geq$6.28	0-0.169	Warp yarn pulled straight
	4.19-6.28	0.169-0.289	Maximum filling contraction
	4.19	0.289	Initially jammed construction
2	$\geq$5.99	0.173	Warp yarns pulled straight
	4.87-5.99	0.173-0.218	Maximum filling wrap angle
	4.07-4.87	0.218-0.272	Maximum filling contraction
	4.07	0.272	Initially jammed construction
3	$\geq$6.44	0-0.159	Warp yarns pulled straight
	4.79-6.44	0.159-0.218	Maximum filling wrap angle
	4.36-4.79	0.218-0.244	Maximum filling contraction
	4.36	0.244	Initially jammed construction
5	$\geq$7.67	0-0.132	Warp yarns pulled straight
	5.34-7.67	0.132-0.191	Maximum filling wrap angle
	5.15-5.34	0.191-0.199	Maximum filling contraction
	5.15	0.199	Initially jammed construction
10	$\geq$10.43	0-0.096	Warp yarns pulled straight
	7.04-10.43	0.096-0.143	Maximum filling wrap angle
	6.97-7.04	0.143-0.144	Maximum filling contraction
	7.04	0.144	Initially jammed construction

Superposition of corresponding pairs of maximum values of $N_1\sqrt{A/\pi}$ and b/a on the graph of Figure 8 shows that the same solution space for Equation 32 is defined. This indicates that the maximum values of $N_1\sqrt{A/\pi}$ for which Equation 32 is valid define the initially "jammed" state.

A boundary condition between maximum filling contraction and warp yarns touching, if it exists, is described by the two expressions

$$\theta_{2f} = \frac{L}{2\rho(2-\cos\phi)}$$

and

$$\frac{1}{N_{2w}} = 2b.$$

The latter may be written

$$\frac{1}{N_{2w}\rho} = 2\sin\phi$$

using Equation 28. Substitution in Equation 39 gives

$$\frac{L}{\rho} = 2(2-\cos\phi)\sin^{-1}\left(\frac{\sin\phi}{2-\cos\phi}\right). \qquad (52)$$

Values of $L/\sqrt{A/\pi}$ computed using the above equation and Equation 34 are listed in Table 4. Comparison of these values with the minimum achievable values of $L/\sqrt{A/\pi}$ in Table 3 for an initially jammed construction shows that it is not possible to reach upon loading a situation in which warp yarns touch for aspect ratios of 10 or less. Actually it can be shown that warp yarns cannot touch for any aspect ratio (value of ϕ) by verifying the following inequality: L/ρ (Equation 52) < L/ρ (Equation 50), i.e.,

$$2\rho(2-\cos\phi)\sin^{-1}\left(\frac{\sin\phi}{2-\cos\phi}\right) < 2\rho\theta_1(2-\cos\phi) \qquad (53)$$

where $\cos\theta_1 = 1/(2-\cos\phi)$ (Equation 51).

TABLE 4

YARN LENGTH REQUIRED TO ACCOMMODATE WARP YARNS TOUCHING

b/a	$L/\sqrt{A/\pi}$
1	2.09
2	3.19
3	3.90
5	4.94
10	6.90
20	9.52

The maximum warp extensions and filling contractions attainable from crimp interchange for various initial fabric constructions are given in Table 5 and plotted in Figures 17-26. These were calculated using the appropriate limit expressions in Equations 39, 40 and 41 giving values of $N_{2w}\rho$ and $N_{2f}\rho$ which were then substituted in Equations 25 and 26 to determine the strain levels. No further fabric extension is possible without yarn extension.

Corresponding effective fabric Poisson's ratios are also given in Table 5 as well as values of the loading ratio σ_w/σ_f at which the limiting condition is reached. These loading ratio values were determined by meeting the appropriate limiting values of the various fabric geometric parameters in Equation 38.

A comparison of the information contained in Table 5 with comparable data in Reference 2 shows that in reaching the limiting state fabrics comprised of yarns with a racetrack cross-sectional shape exhibit considerably greater amounts of filling contraction and, therefore, warp extension, for equivalent values of $N_1\sqrt{A/\pi}$ and b/a. This results from the fact that the same yarn cross-sectional area A and aspect ratio b/a, the additional wrap angle, $\theta_{2f}-\theta_1$, required to produce a limiting configuration is considerably greater for the racetrack yarn than for the lenticular yarn. Hence, for the same $N_1\sqrt{A/\pi}$ values, the lenticular yarn fabric is closer to the limiting state initially and therefore cannot exhibit as much extension in reaching it as the racetrack-yarn fabric.

TABLE 5

MAXIMUM EXTENSIONS ACHIEVABLE FROM CRIMP INTERCHANGE

b/a	$N_1\sqrt{A/\pi}$	Warp Extension, ε_w (%)	Filling Contraction, $-\varepsilon_f$ (%)	Effective Poisson's Ratio, μ	Limiting Loading Ratio, σ_w/σ_f	Type of Limiting Condition
1	0.050	0.5	1.5	3.0	∞	warp yarns pulled straight
	0.100	2.0	6.7	3.3	∞	
	0.125	3.2	11.3	3.5	∞	
	0.150	4.7	18.7	4.0	∞	
	0.169	6.0	32.5	5.4	∞	maximum filling contraction
	0.200	7.3	21.8	3.0	37.8	
	0.220	7.0	16.3	2.3	13.8	
	0.240	6.0	11.3	1.9	6.8	
	0.289	0.0	0.0	1.0	1.0	initially jammed construction
2	0.050	0.3	0.9	3.1	∞	warp yarns pulled straight
	0.100	1.1	3.7	3.2	∞	
	0.125	1.8	6.1	3.4	∞	
	0.150	2.7	9.7	3.7	∞	
	0.173	3.6	15.7	4.4	∞	maximum filling wrap angle
	0.200	4.3	11.4	2.7	12.9	
	0.218	4.0	8.5	2.2	7.1	
	0.220	4.0	8.2	2.1	6.4	maximum filling contraction
	0.240	3.1	5.0	1.6	3.5	
	0.272	0.0	0.0	1.0	1.0	initially jammed construction
3	0.050	0.2	0.6	3.1	∞	warp yarns pulled straight
	0.100	0.8	2.5	3.2	∞	
	0.125	1.2	4.2	3.4	∞	
	0.150	1.8	6.9	3.7	∞	
	0.159	2.1	8.3	4.0	∞	maximum filling wrap angle
	0.200	2.3	4.5	1.9	4.8	
	0.218	1.8	2.7	1.5	2.9	maximum filling contraction
	0.220	1.7	2.5	1.5	2.7	
	0.240	0.3	0.4	1.1	1.4	
	0.244	0.0	0.0	1.0	1.0	initially jammed construction

TABLE 5 (Cont.)

MAXIMUM EXTENSIONS ACHIEVABLE FROM CRIMP INTERCHANGE

b/a	$N_1\sqrt{A/\pi}$	Warp Extension, ε_w (%)	Filling Contraction, $-\varepsilon_f$ (%)	Effective Poisson's Ratio, μ	Limiting Loading Ratio, σ_w/σ_f	Type of Limiting Condition
5	0.050	0.1	0.4	3.0	∞	warp yarns pulled straight
	0.100	0.5	1.6	3.3	∞	
	0.125	0.8	2.8	3.6	∞	
	0.132	0.8	3.3	3.9	∞	
	0.150	1.0	2.5	2.4	7.7	maximum filling wrap angle
	0.191	0.4	0.5	1.2	1.2	maximum filling contraction
	0.199	0.0	0.0	1.0	1.0	initially jammed construction
10	0.050	0.1	0.2	3.1	∞	warp yarns pulled straight
	0.096	0.2	0.9	4.0	∞	
	0.100	0.3	0.8	3.1	24.3	maximum filling wrap angle
	0.125	0.4	0.4	1.4	2.9	
	0.143	0.03	0.03	1.0	1.3	maximum filling contraction
	0.144	0.0	0.0	1.0	1.0	initially jammed construction

Effective Fabric Poisson's Ratio

The ratio of the fabric contraction in the filling direction to the corresponding extension in the warp direction, i.e., the effective Poisson's ratio, μ, of the fabric ($\mu = -\varepsilon_f/\varepsilon_w$), is plotted in Figures 35-39. It is recognized that this is a non-standard definition of Poisson's ratio [1] and should be distinguished from the classical Poisson's ratio.

The Poisson's ratios are given in Figures 35(a), 36(a), 37(a), 38(a) and 39(a) as a function of σ_w/σ_f for various values of $N_1\sqrt{A/\pi}$ and b/a. Similarly, they are given in Figures 35(b), 36(b), 37(b), 38(b) and 39(b) as a function of $N_1\sqrt{A/\pi}$ for the various values of σ_w/σ_f and b/a. The Poisson's ratios at the limiting loading ratio are also noted.

The slopes of the curves giving the fabric extension in the warp direction and contraction in the filling direction for $\sigma_w/\sigma_f = \infty$ and each b/a value appear to be equal as $N_1\sqrt{A/\pi}$ approaches the values for the initially jammed construction (see Figures 17(b), 18(b), 18(b), and 20(b) etc.). This indicates (via L'Hôpital's rule) that the Poisson's ratio for $\sigma_w/\sigma_f \to \infty$ at the $N_1\sqrt{A/\pi}$ for which the fabric is initially jammed is 1. Consequently, the limiting σ_w/σ_f curves in Figures 35(b), 36(b), 38(b), 38(b) and 39(b) have been extrapolated to this point.

As shown in Figures 35 through 39, the Poisson's ratio increases with increasing loading ratio. However, it does not vary significantly with increasing $N_1\sqrt{A/\pi}$ for $\sigma_w/\sigma_f \to \infty$. The maximum Poisson's ratio appears to decrease with increasing aspect ratio although μ is approximately the same for all values of b/a when σ_w/σ_f is less than the limiting loading ratio.

Comparison of the foregoing data to that in Reference 2 shows that the effective Poisson's ratio of a fabric comprised of yarns with a racetrack cross-section is roughly the same as that for a similar fabric comprised of yarn with a lenticular cross-section.

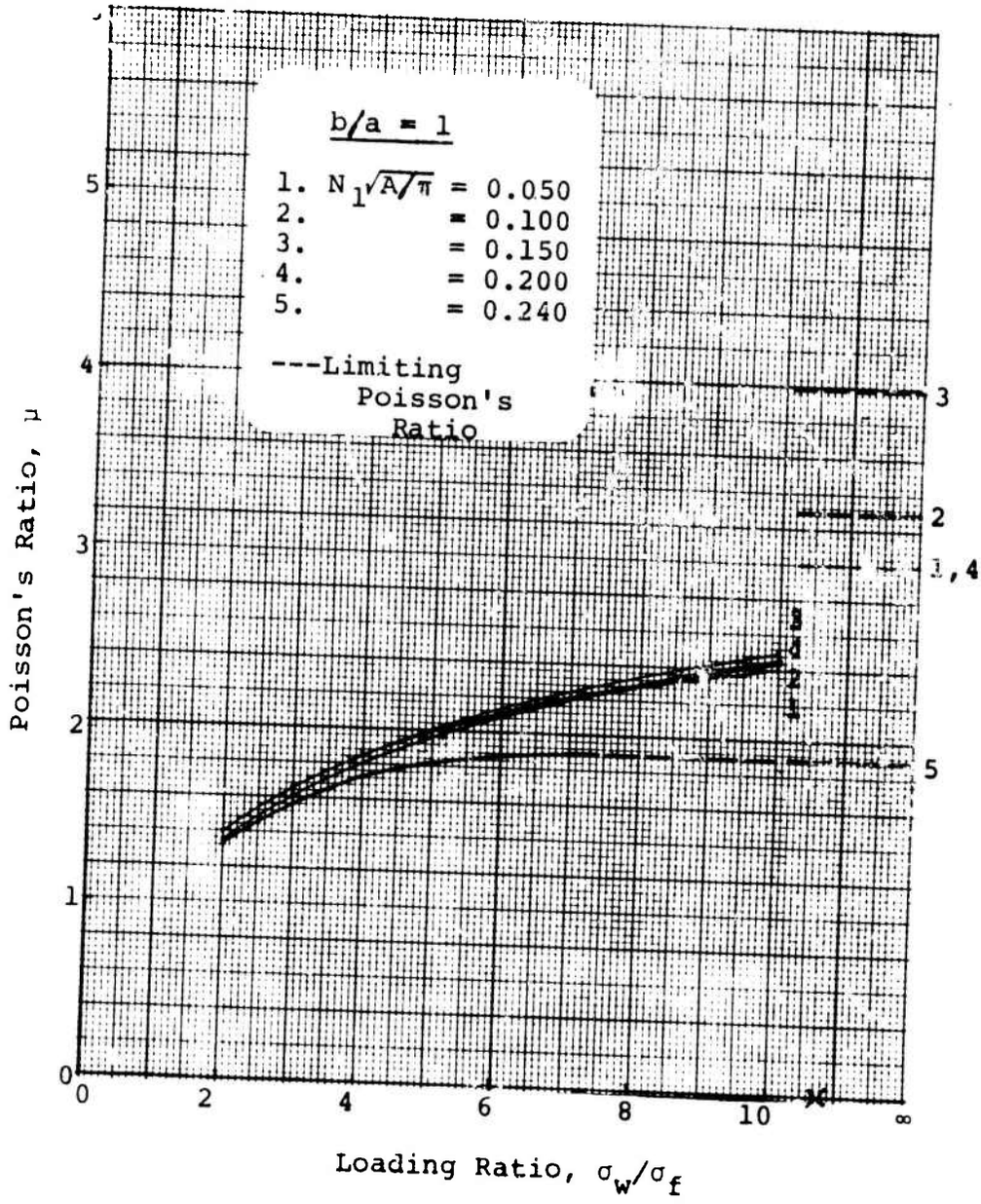

Figure 35(a). Poisson's Ratio: (Aspect Ratio = 1) Inextensible Yarn

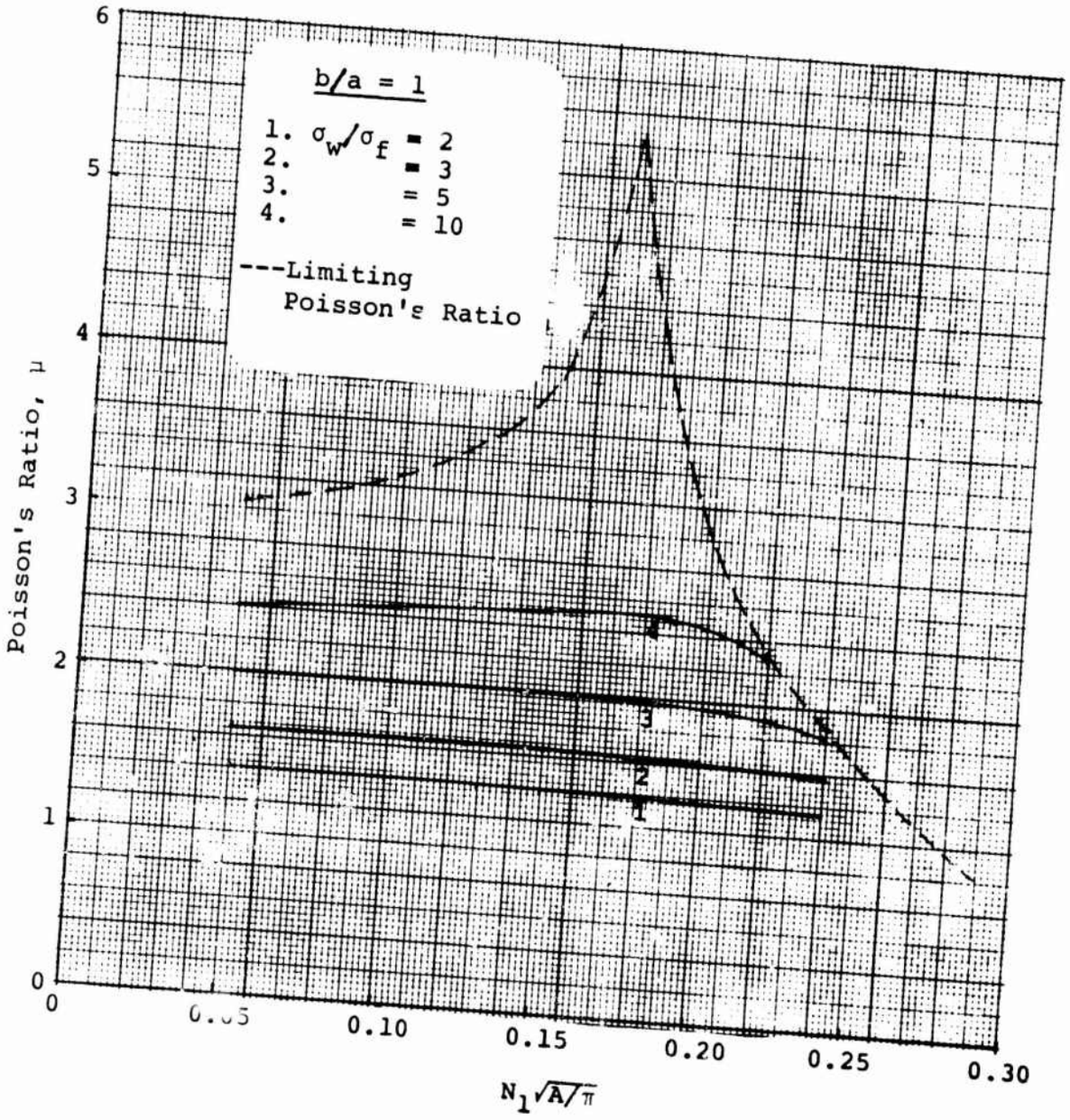

Figure 35(b). Poisson's Ratio: (Aspect Ratio = 1) Inextensible Yarn

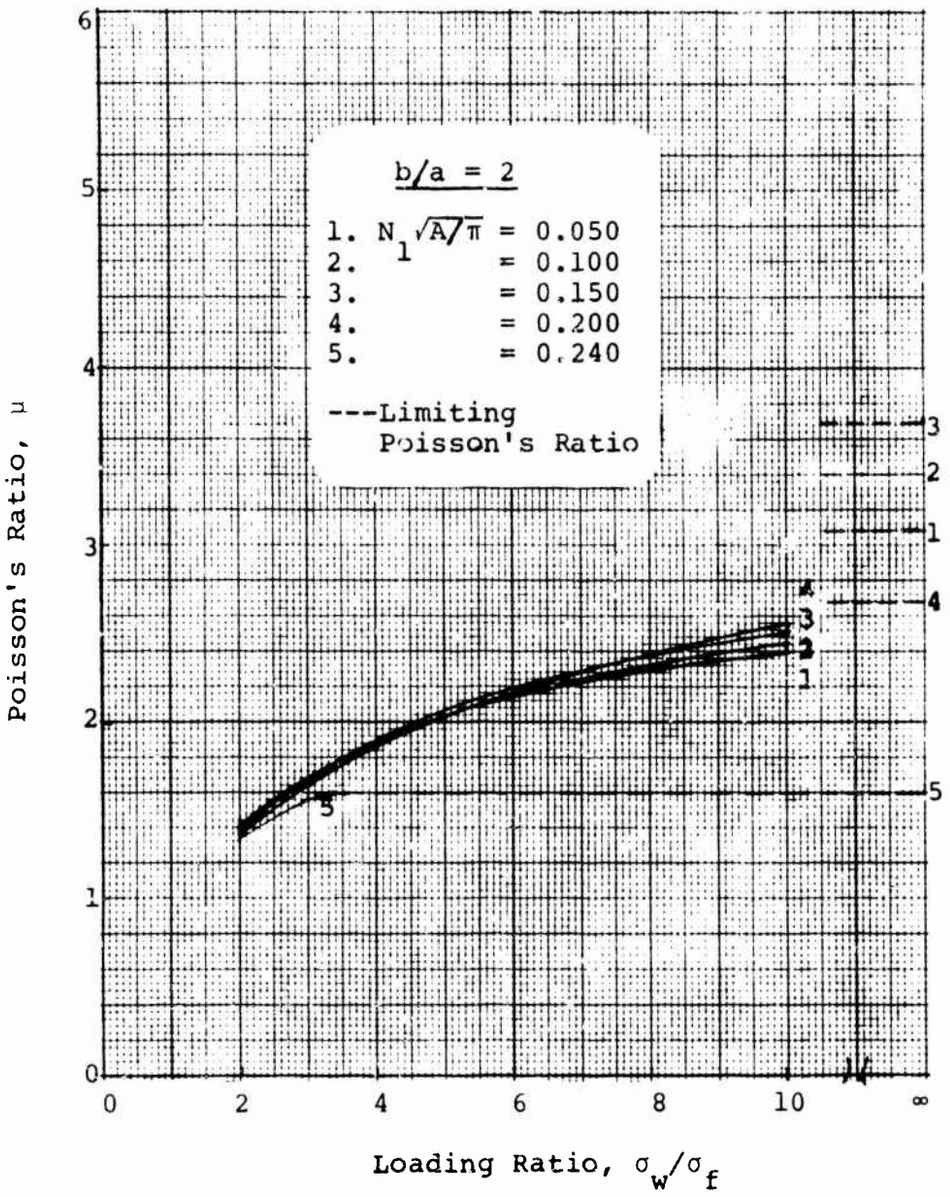

Figure 36(a). Poisson's Ratio (Aspect Ratio = 2) Inextensible Yarn

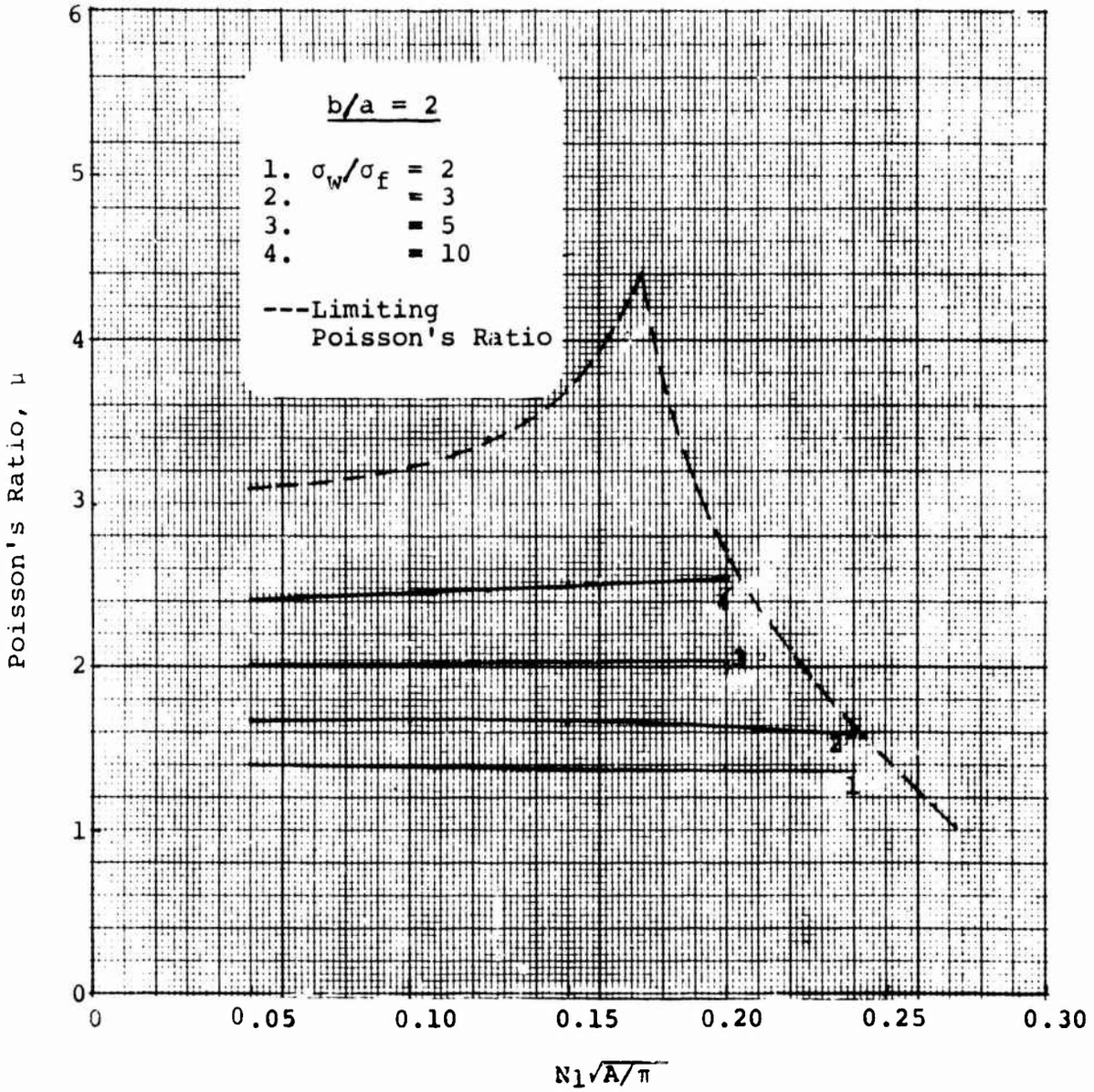

Figure 36(b). Poisson's Ratio (Aspect Ratio = 2) Inextensible Yarn

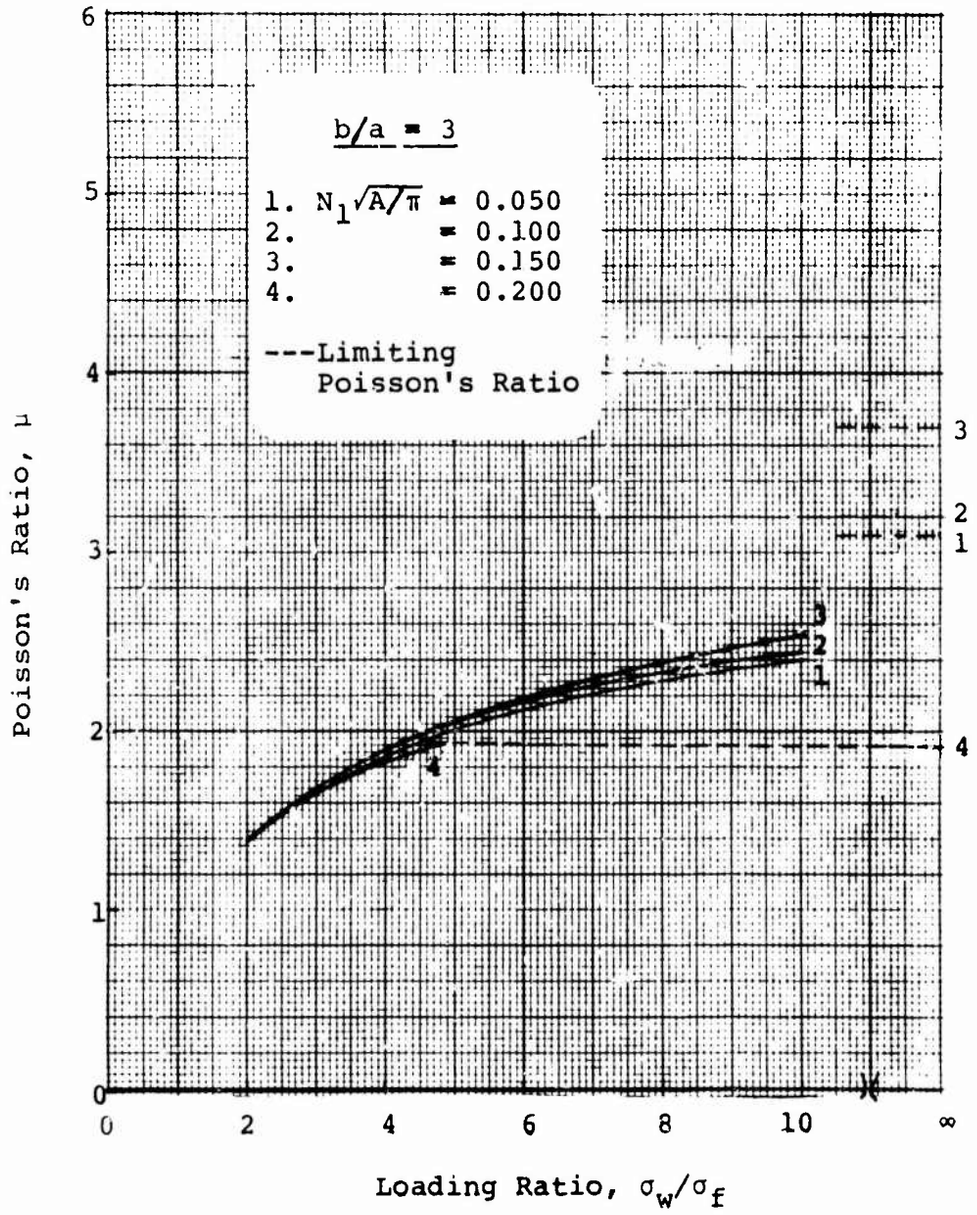

Figure 37(a). Poisson's Ratio (Aspect Ratio = 3) Inextensible Yarn

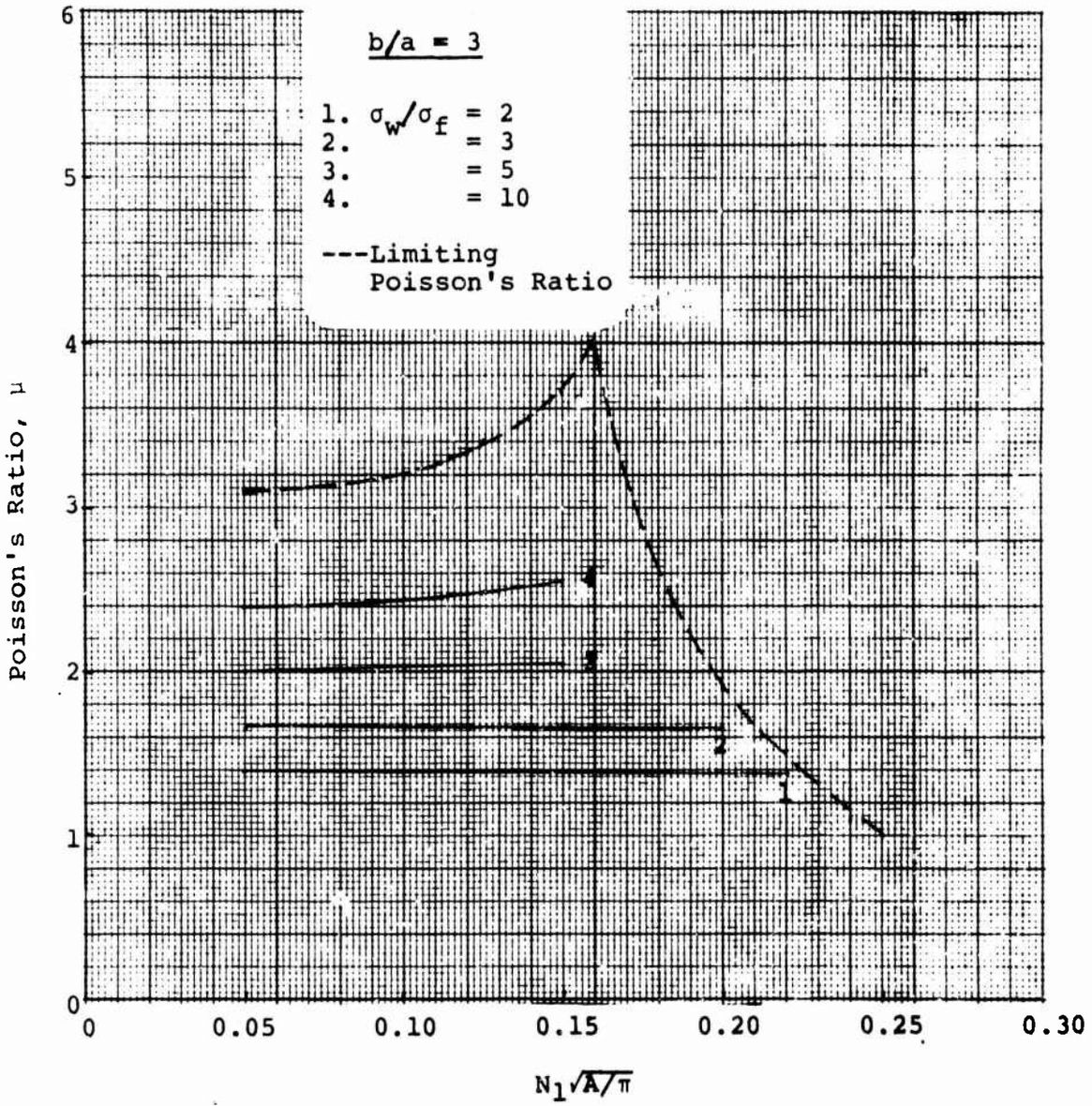

Figure 37(b). Poisson's Ratio (Aspect Ratio = 3) Inextensible Yarn

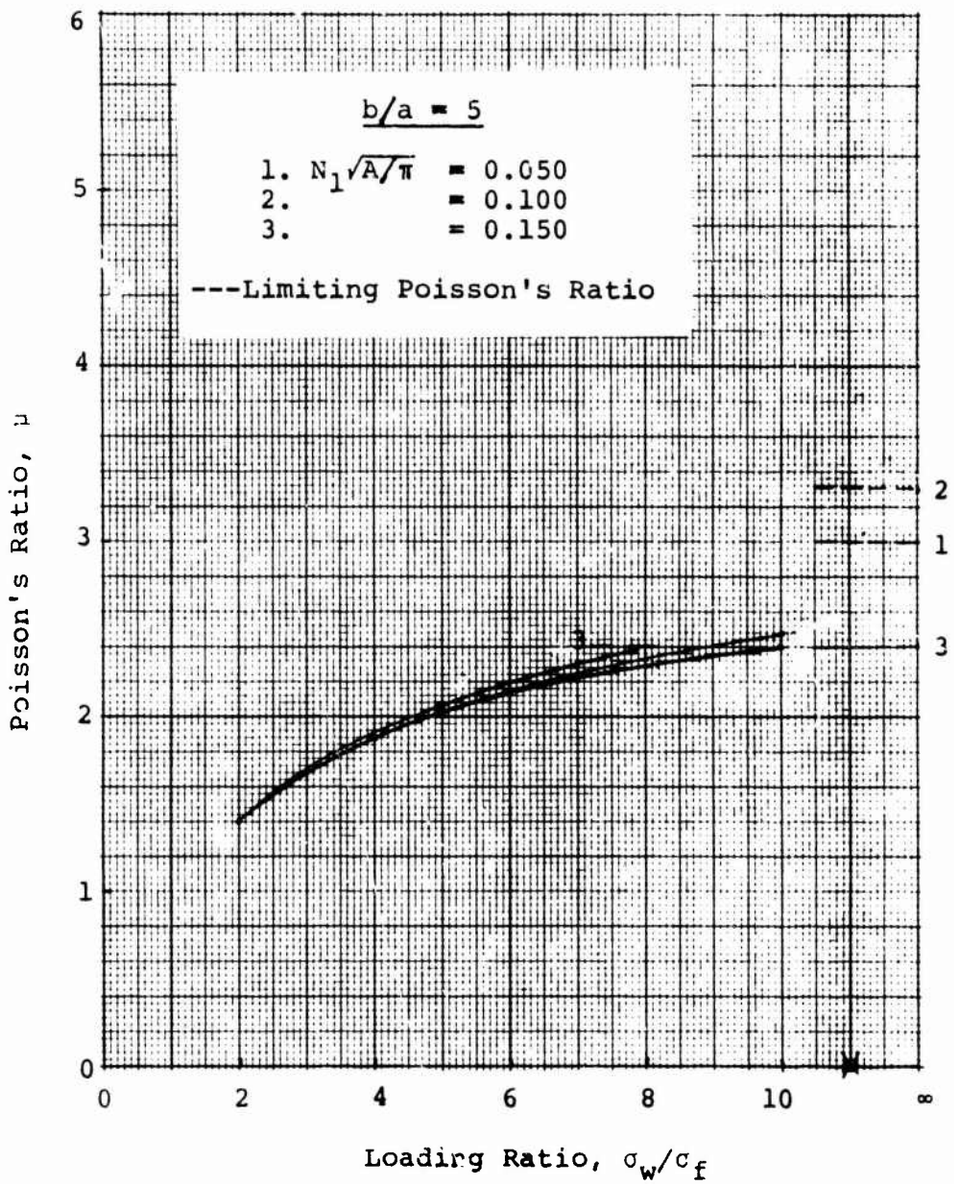

Figure 38(a). Poisson's Ratio (Aspect Ratio = 5) Inextensible Yarn

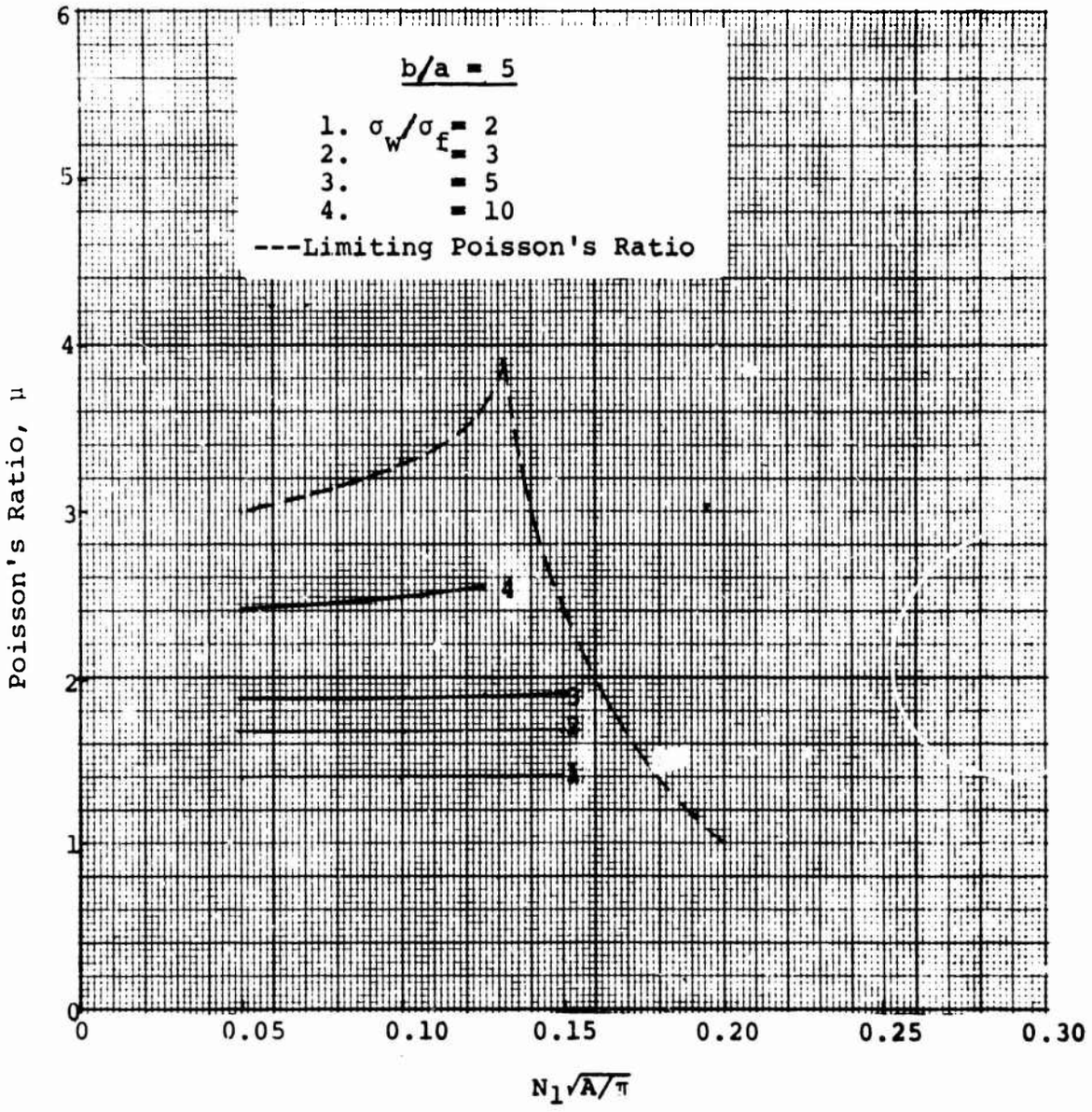

Figure 38(b). Poisson's Ratio (Aspect Ratio = 5) Inextensible Yarn

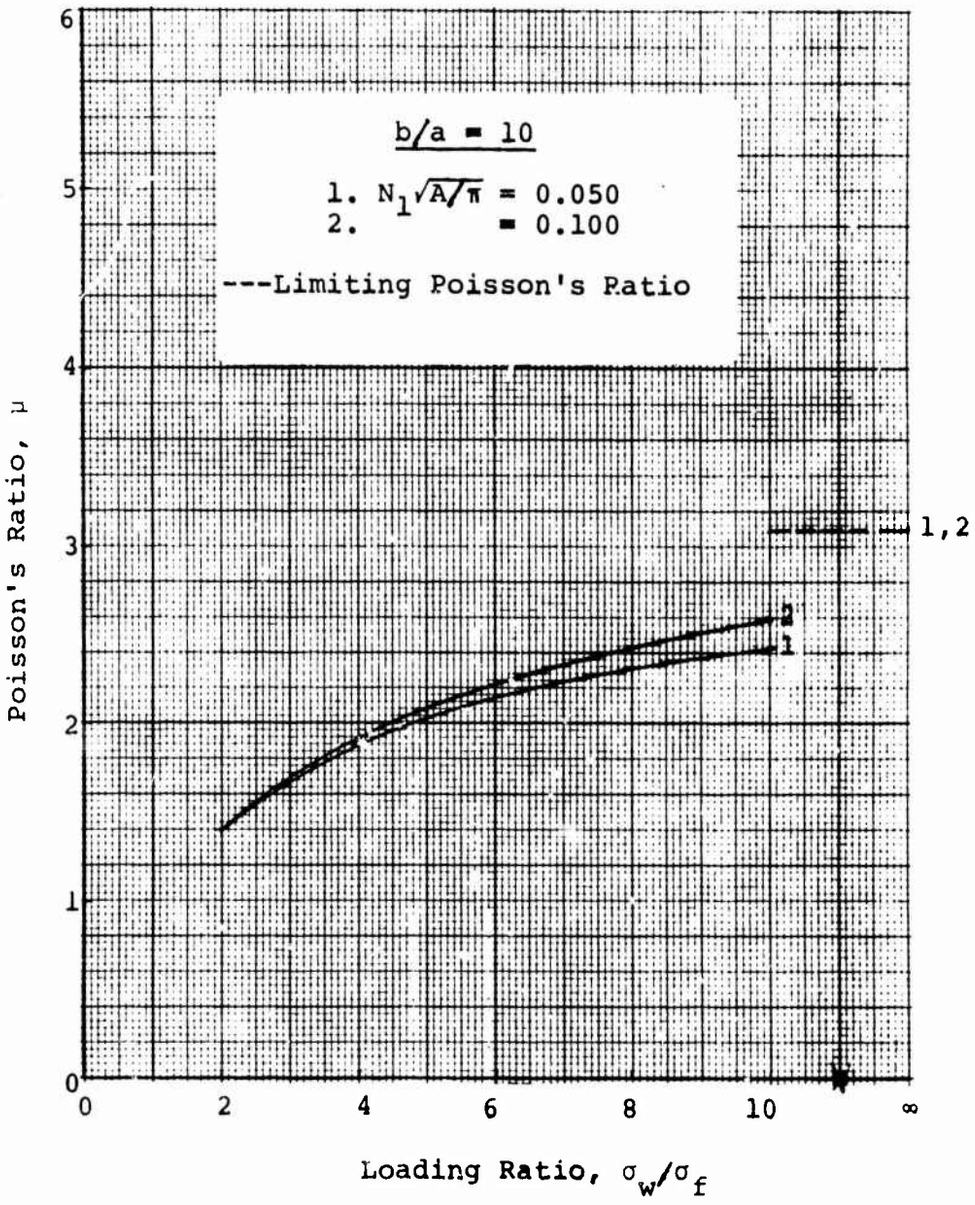

Figure 39(a). Poisson's Ratio (Aspect Ratio = 10) Inextensible Yarn

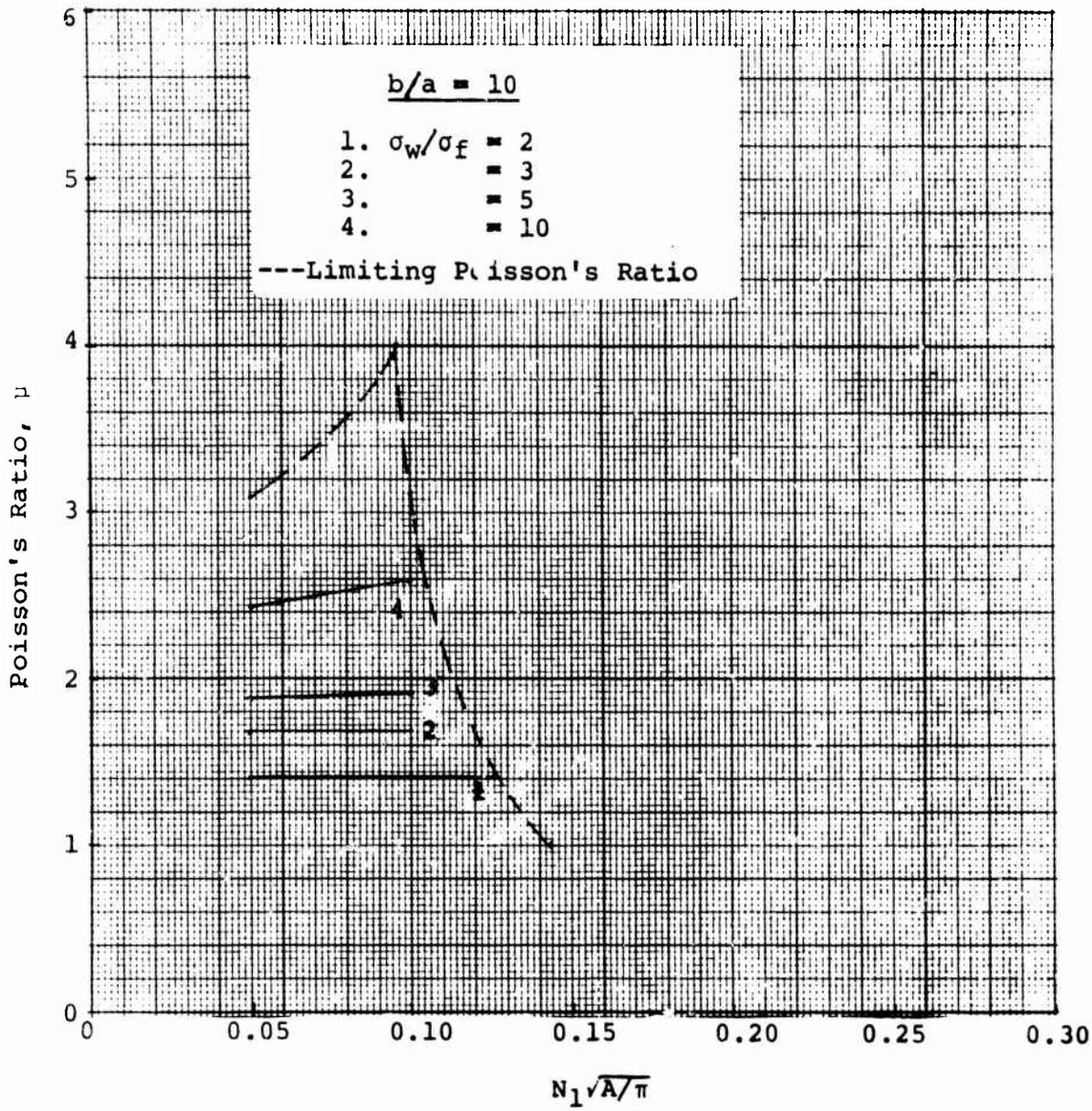

Figure 39(b). Poisson's Ratio (Aspect Ratio = 10) Inextensible Yarn

II. Initially Square Fabric, Infinitely Flexible, Extensible Yarn (Linearly Elastic, $\nu = 0$) $\sigma_w/\sigma_f \geq 1$

An initially square plain-weave fabric with the same infinitely flexible, incompressible but extensible yarn in both directions is assumed. Equations 27 through 33 describe the geometry of the fabric in the unloaded state with L replaced by L_1.

Assuming that the yarn cross-sectional dimensions do not change during loading, i.e., that the Poisson's ratio of the yarn is zero

$$b_{2w} = b_{2f} = b_1 = b$$

$$a_{2w} = a_{2f} = a_1 = a$$

$$A_{2w} = A_{2f} = A_1 = A$$

$$\rho_{2w} = \rho_{2f} = \rho_1 = \rho$$

$$\phi_{2w} = \phi_{2f} = \phi_1 = \phi.$$

The geometry of the deformed fabric is given by the following six equations derived from Equations 11-15 after simplification and replacement of subscript "1" by subscript "2" and Equation 20 and Equations 23 and 24 assuming the fabric is woven from linearly elastic yarns.

$$[L_{2w}/\rho - 2(2-\cos\phi)\theta_{2w}]\sin\theta_{2w} + [L_{2f}/\rho - 2(2-\cos\phi)\theta_{2f}]\sin\theta_{2f} = 2(2-\cos\phi)(\cos\theta_{2w}+\cos\theta_{2f}) - 4 \tag{54}$$

$$\frac{\sigma_w}{K} = \frac{\left(\frac{L_{2w}/\rho}{L_{1w}/\rho} - 1\right)\cos\theta_{2w}}{[L_{2f}/\rho - 2(2-\cos\phi)\theta_{2f}]\cos\theta_{2f} + 2(2-\cos\phi)\sin\theta_{2f}} \tag{55}$$

$$\frac{\sigma_f}{K} = \frac{\left(\frac{L_{2f}/\rho}{L_{1f}/\rho} - 1\right)\cos\theta_{2f}}{[L_{2w}/\rho - 2(2-\cos\phi)\theta_{2w}]\cos\theta_{2w} + 2(2-\cos\phi)\sin\theta_{2w}} \qquad (56)$$

where $K = pE_fA/\rho$

$$\frac{\sigma_w}{\sigma_f} = \frac{\cot\theta_{2w}\{[L_{2w}/\rho - 2(2-\cos\phi)\theta_{2w}]\cos\theta_{2w} + 2(2-\cos\phi)\sin\theta_{2w}\}}{\cot\theta_{2f}\{[L_{2f}/\rho - 2(2-\cos\phi)\theta_{2f}]\cos\theta_{2f} + 2(2-\cos\phi)\sin\theta_{2f}\}} \qquad (57)$$

$$\frac{1}{N_{2w}\rho} = [L_{2f}/\rho - 2(2-\cos\phi)\theta_{2f}]\cos\theta_{2f} + 2(2-\cos\phi)\sin\theta_{2f} \qquad (58)$$

$$\frac{1}{N_{2f}\rho} = [L_{2w}/\rho - 2(2-\cos\phi)\theta_{2w}]\cos\theta_{2w} + 2(2-\cos\phi)\sin\theta_{2w} \qquad (59)$$

$L_{2w}\rho$, L_{2f}/ρ, θ_{2w} and θ_{2f} were obtained from Equations 54 through 57 for a series of values of L_1/ρ, $N_1\rho$, σ_w/σ_f and $\sigma_w/(N_1\rho)K$. (Although results were obtained only for $\sigma_w/\sigma_f \geq 1$, they are also valid for $\sigma_w/\sigma_f < 1$ if the subscripts "w" and "f" are everywhere reversed.) $N_{2w}\rho$ and $N_{2f}\rho$ were then computed for each of the sets of values obtained using Equations 58 and 59, and the corresponding fractional fabric extensions in the warp and filling directions computed with Equations 25 and 26. The results of the computations are plotted in Figures 40 through 63. These results encompass combinations of the following range of values for each of the parameters: aspect ratio b/a = 1-10; $N_1\sqrt{A/\pi}$ = 0.050-0.240; applied load σ_w = ∿0-3200 pounds per inch width; yarn cross-sectional area A = 0.785×10^{-4} - 3.14×10^{-4} square inches (for circular yarns this is a yarn radius of 0.005-0.010 inch; fiber modulus $E_f = 2 \times 10^5$-30×10^6 pounds per square inch; packing factor p = 0.75.

The fabric extensions in the warp and filling direction are given in Figures 40 through 59 as a function of the load applied in the warp direction for specific loading ratios and yarn aspect ratios and various values of $N_1\sqrt{A/\pi}$. Similarly, the fabric extensions are given in Figures 60 through 63 as a function of the load applied in the warp direction for specific values of b/a and $N_1\sqrt{A/\pi}$, and the various values of σ_w/σ_f. All the filling load-extension diagrams are terminated at the point corresponding to either 50% extension in the warp direction or a value of the loading parameter equal to 0.4.

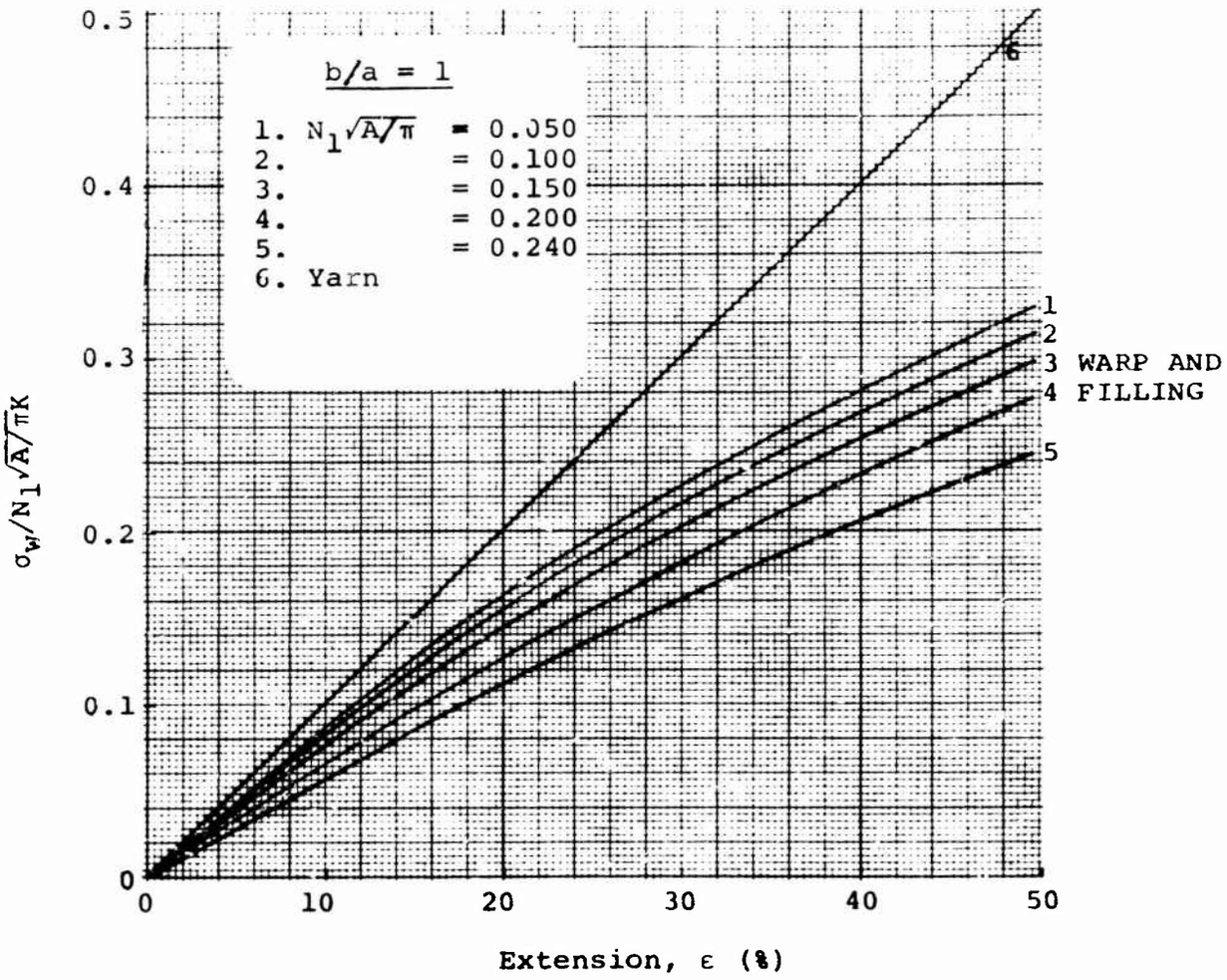

Figure 40. Fabric Extension: Linearly Elastic Yarn $\sigma_w/\sigma_f = 1$, b/a = 1

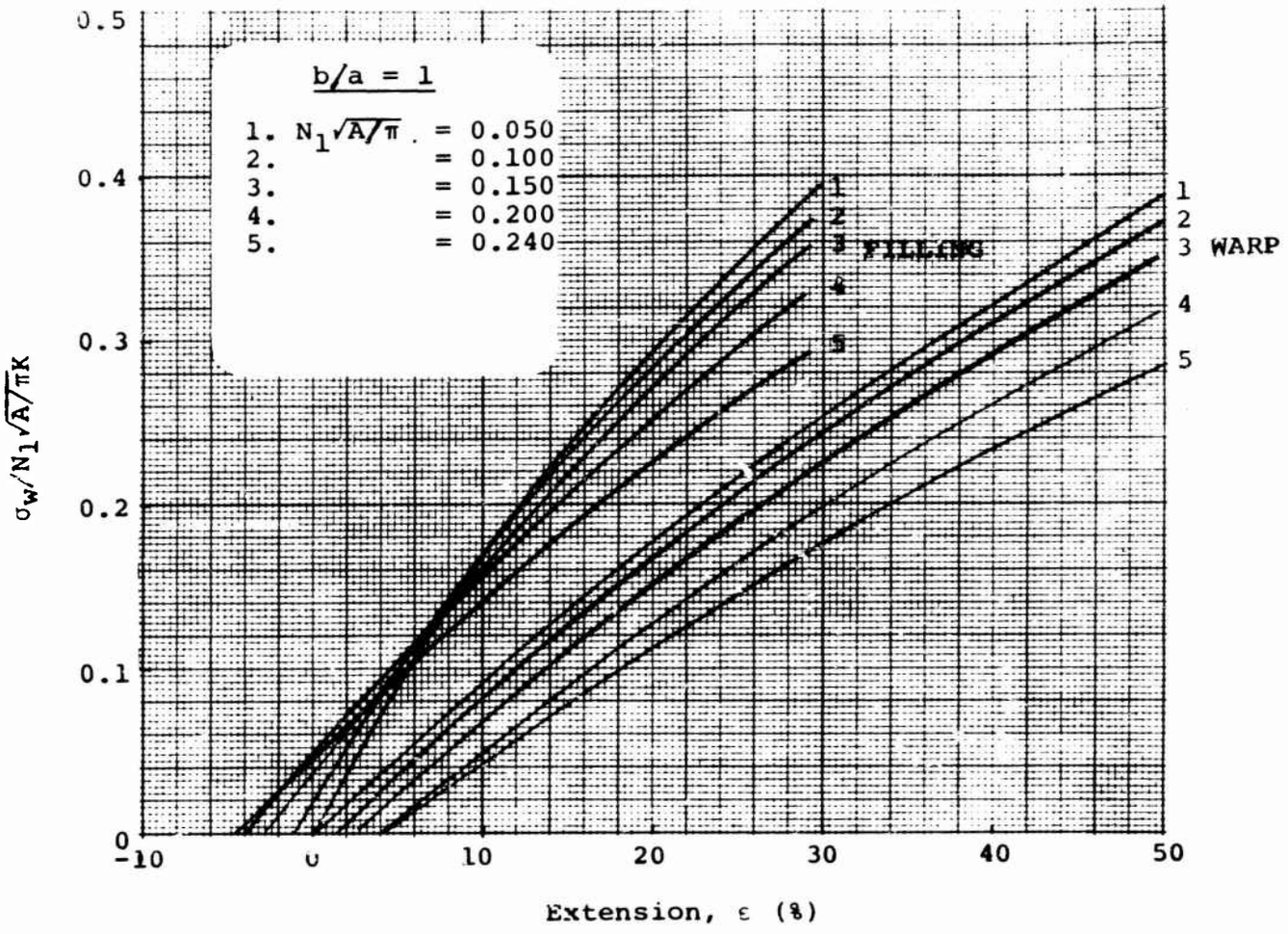

Figure 41. Fabric Extension: Linearly Elastic Yarn
$\sigma_w/\sigma_f = 2$, b/a = 1

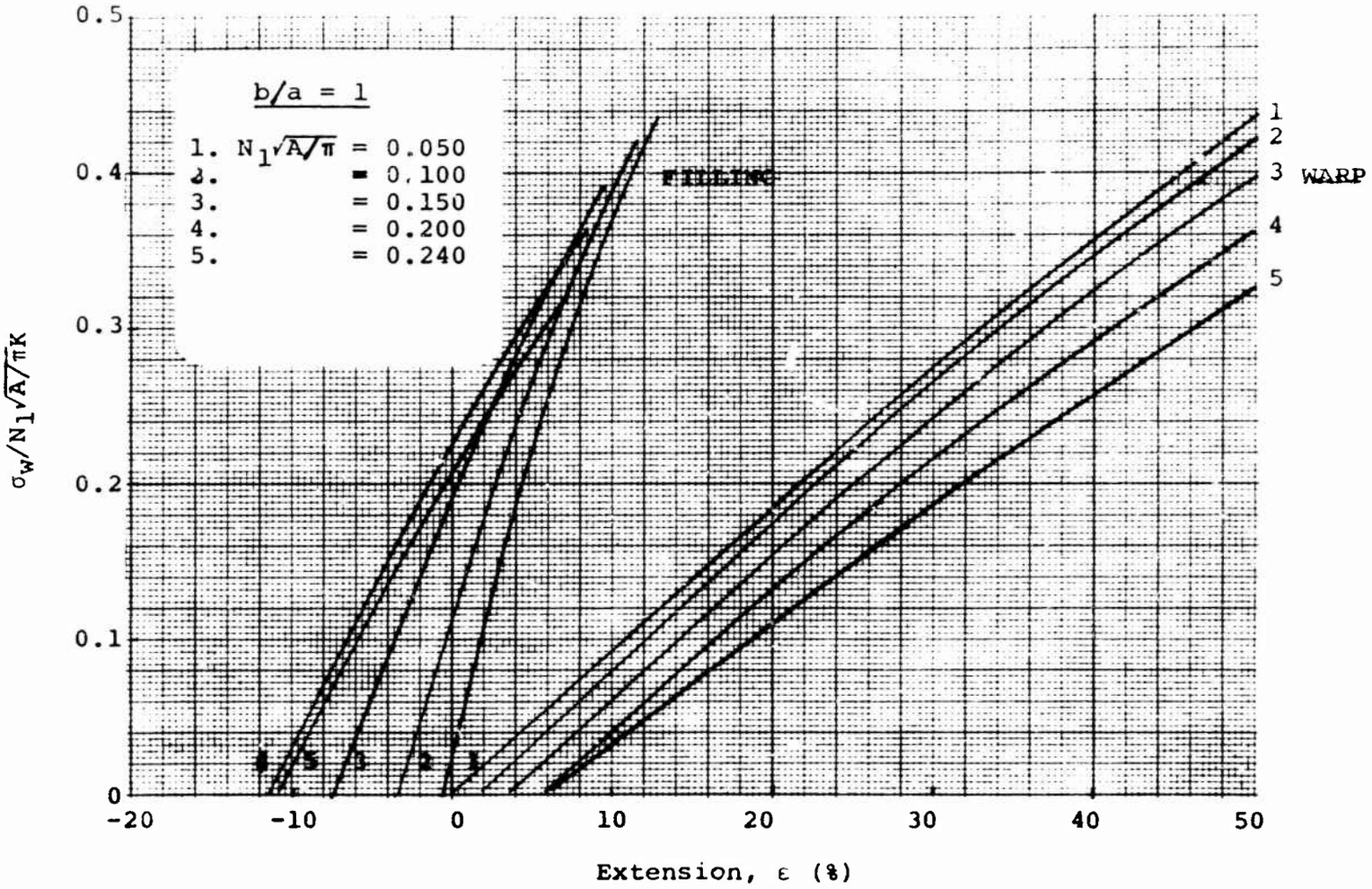

Figure 42. Fabric Extension: Linearly Elastic Yarn
σ_w/σ_f = 5, b/a = 1

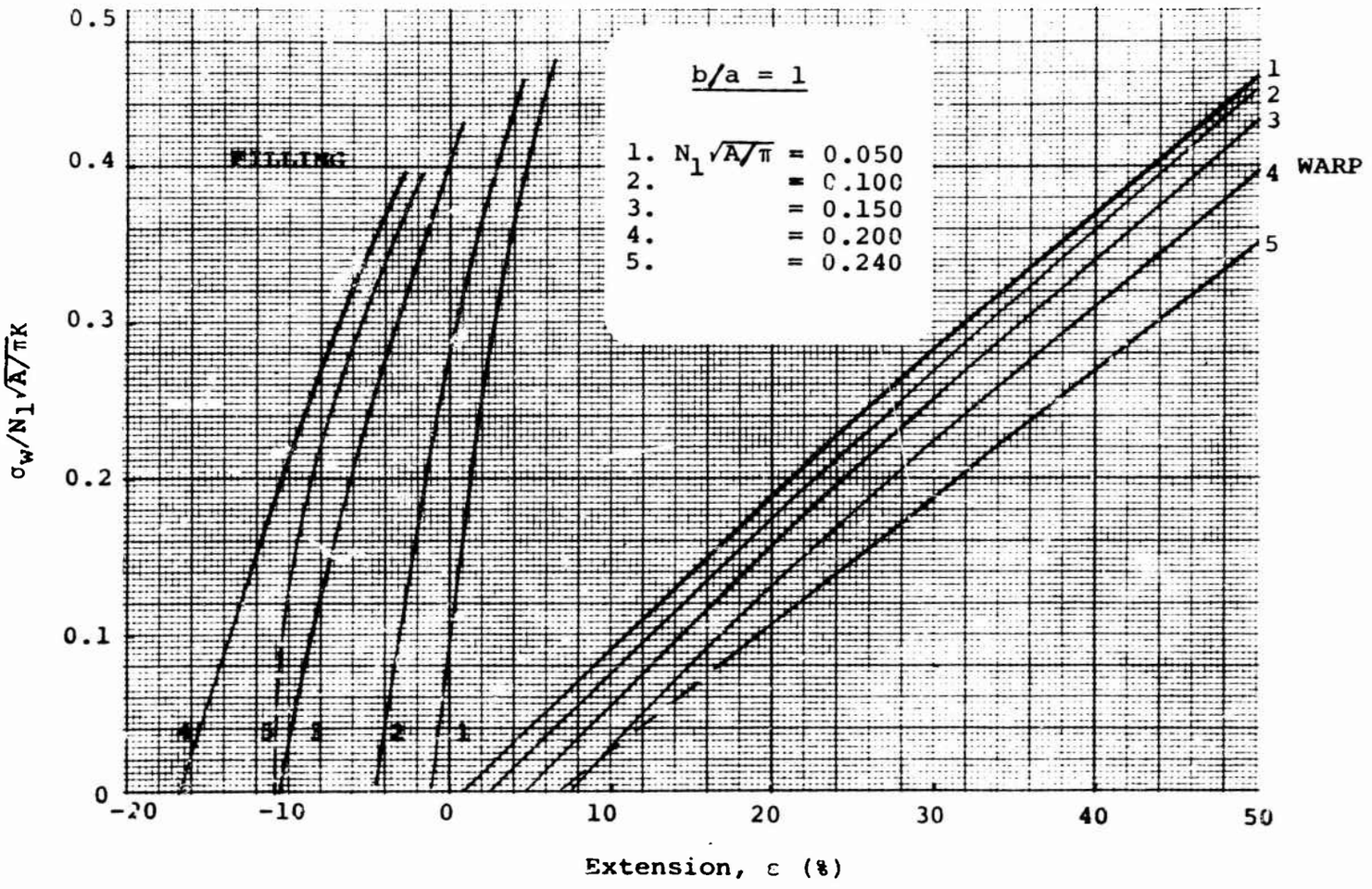

Figure 43. Fabric Extension: Linearly Elastic Yarn
σ_w/σ_f = 10, b/a = 1

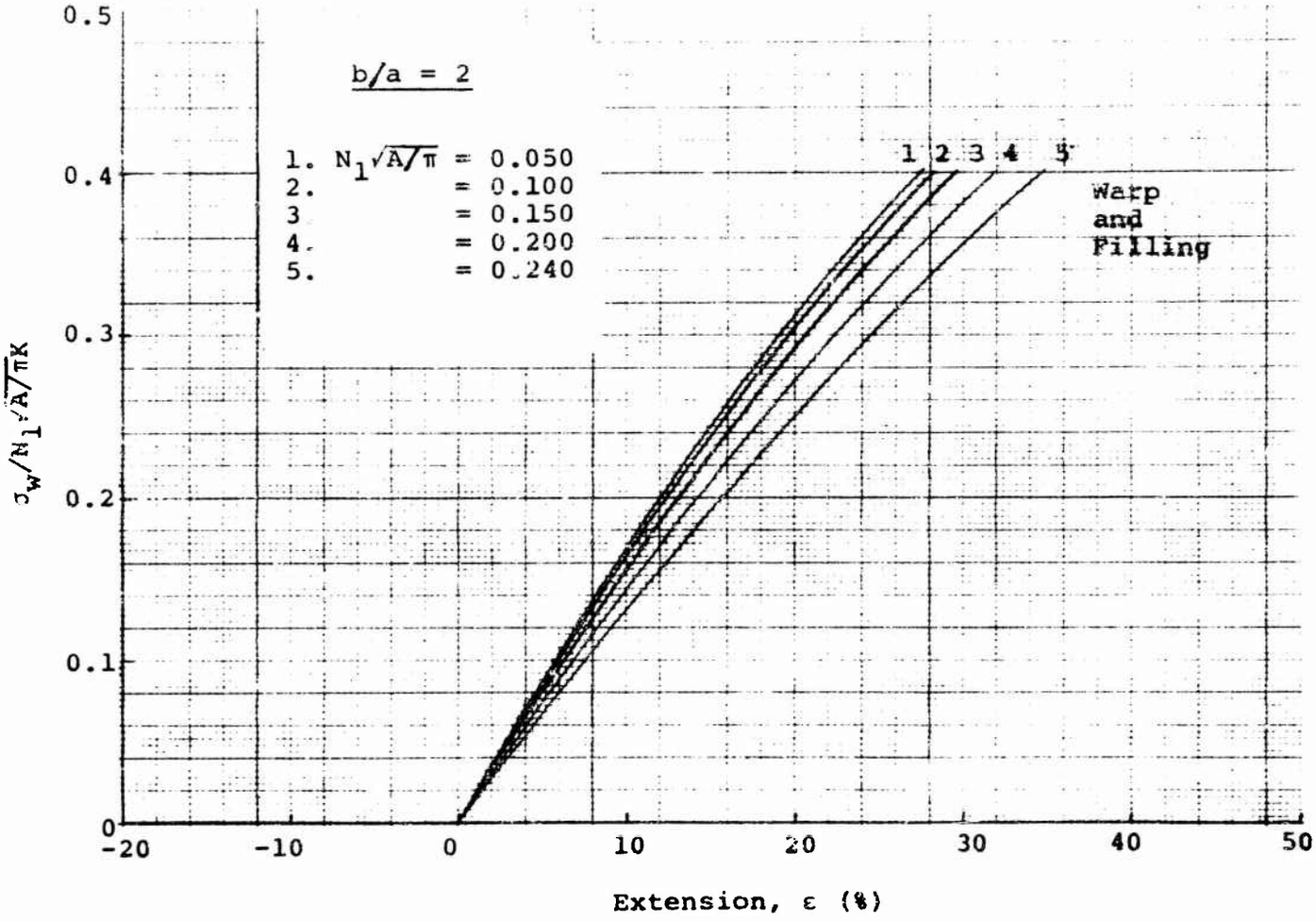

Figure 44. Fabric Extension: Linearly Elastic Yarn $\sigma_w/\sigma_f = 1$, b/a = 2

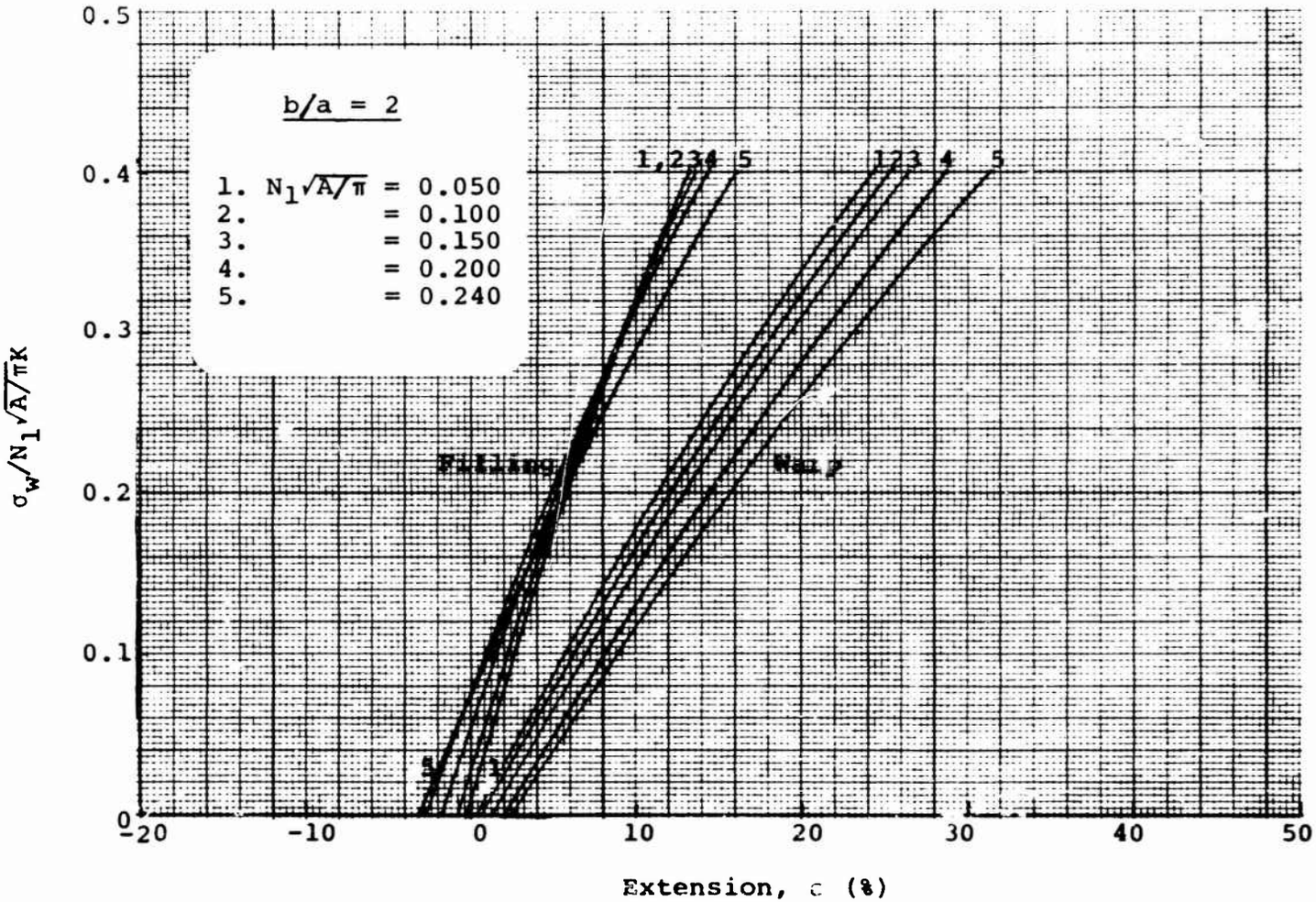

Figure 45. Fabric Extension: Linearly Elastic Yarn
$\sigma_w/\sigma_f = 2$, b/a = 2

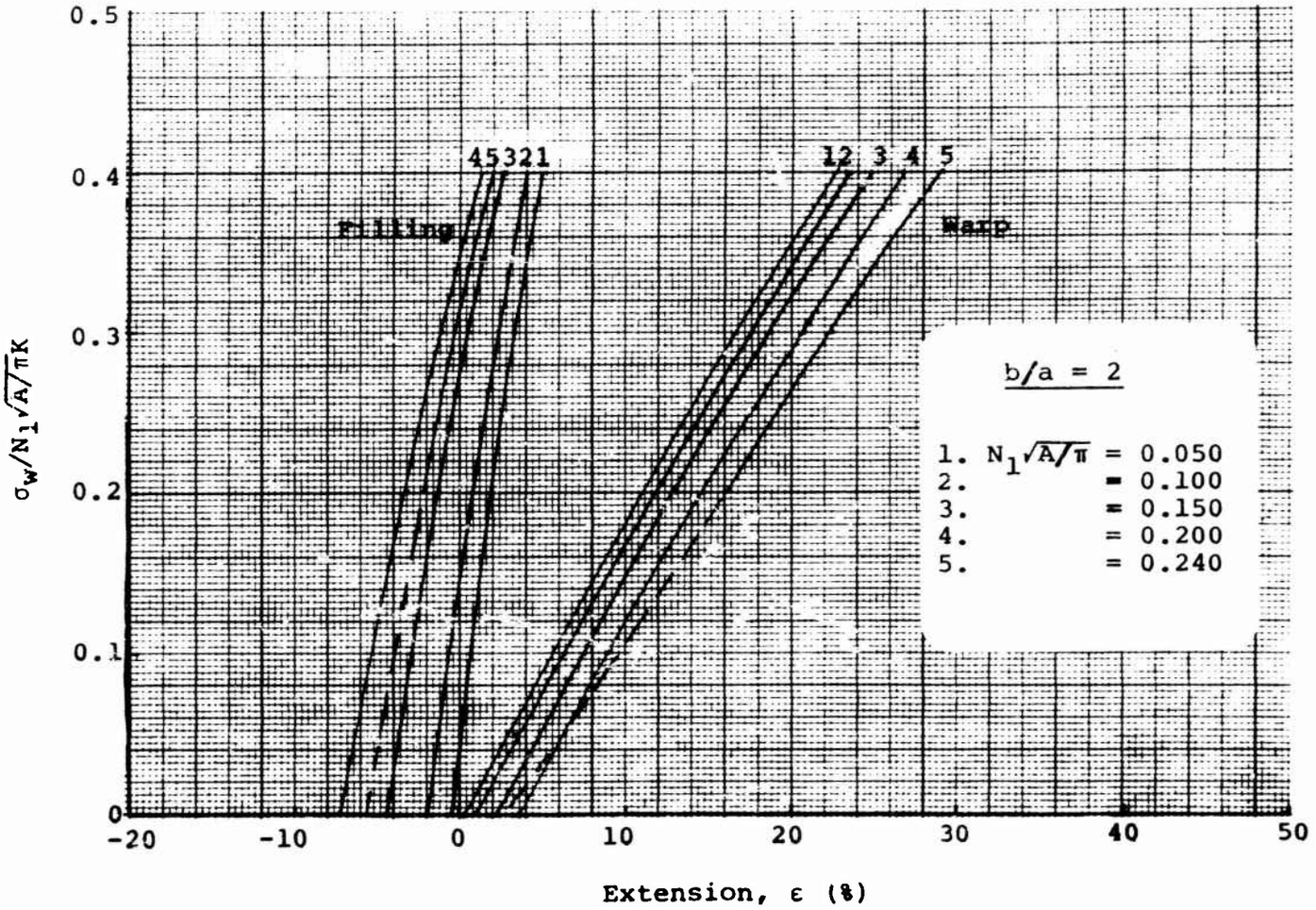

Figure 46. Fabric Extension: Linearly Elastic Yarn
$\sigma_f/\sigma_E = 5$, b/a = 2

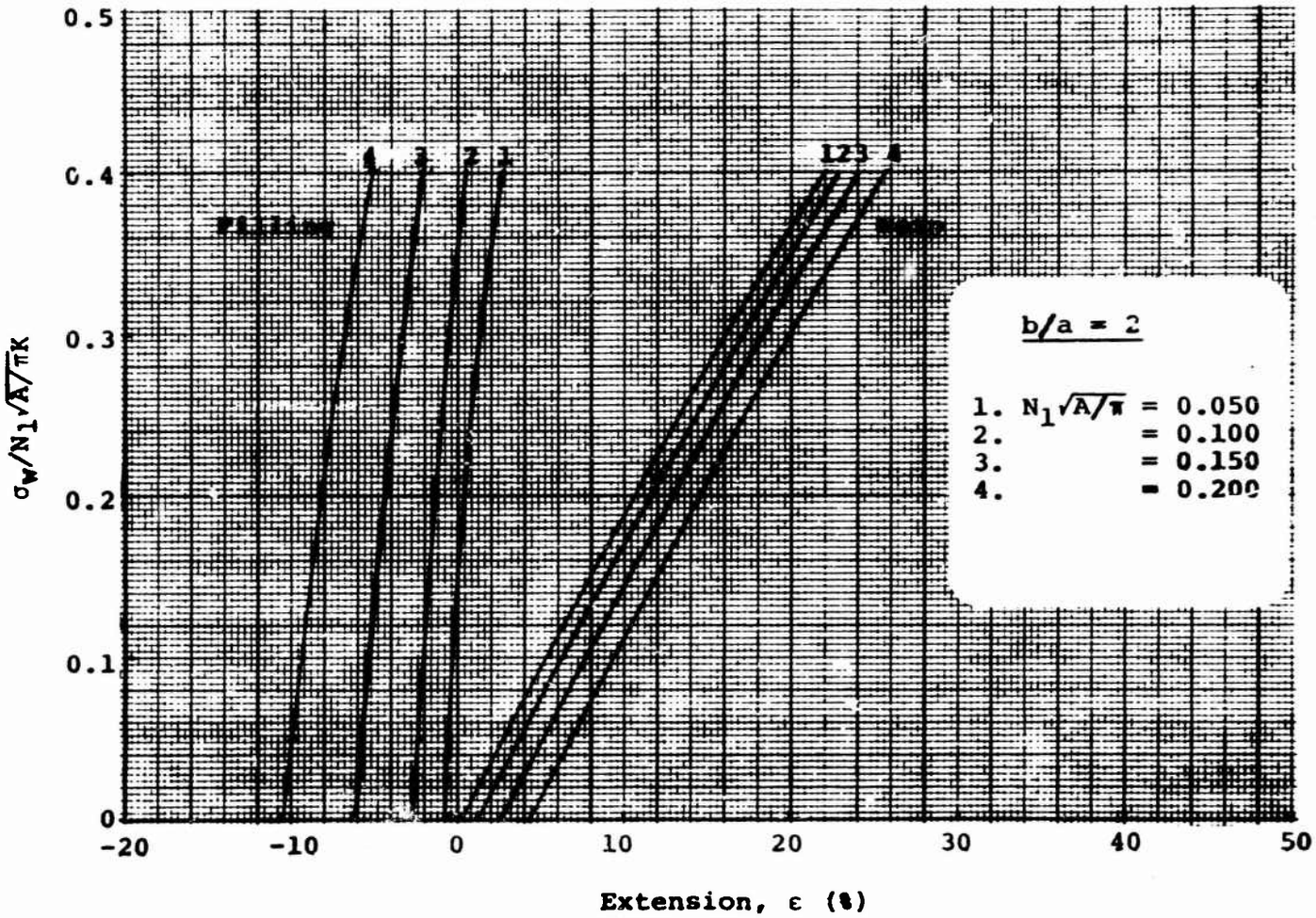

Figure 47. Fabric Extension: Linearly Elastic Yarn
$\sigma_w/\sigma_f = 10$, b/a = 2

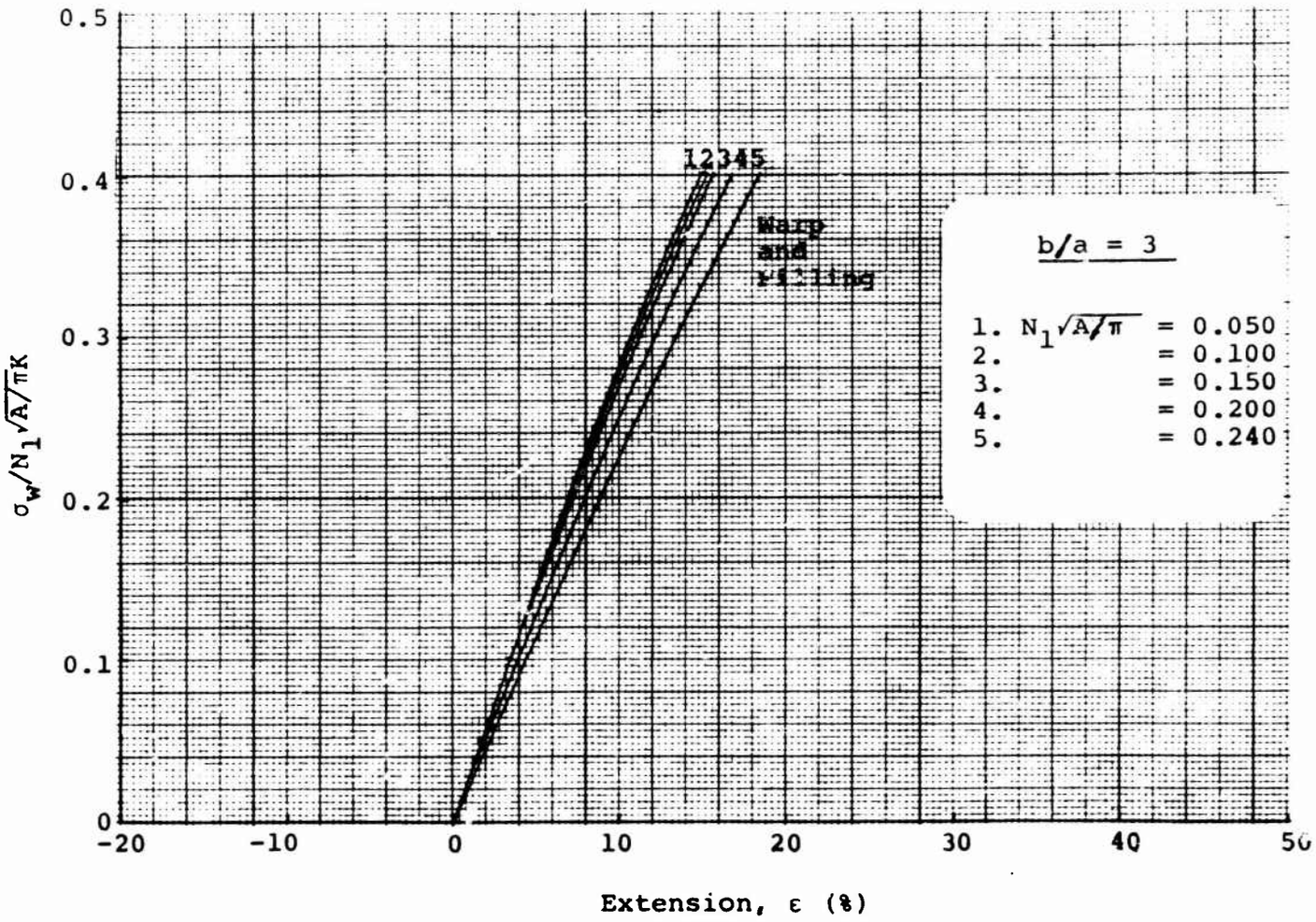

Figure 48. Fabric Extension: Linearly Elastic Yarn
σ_w/σ_f = 1, b/a = 3

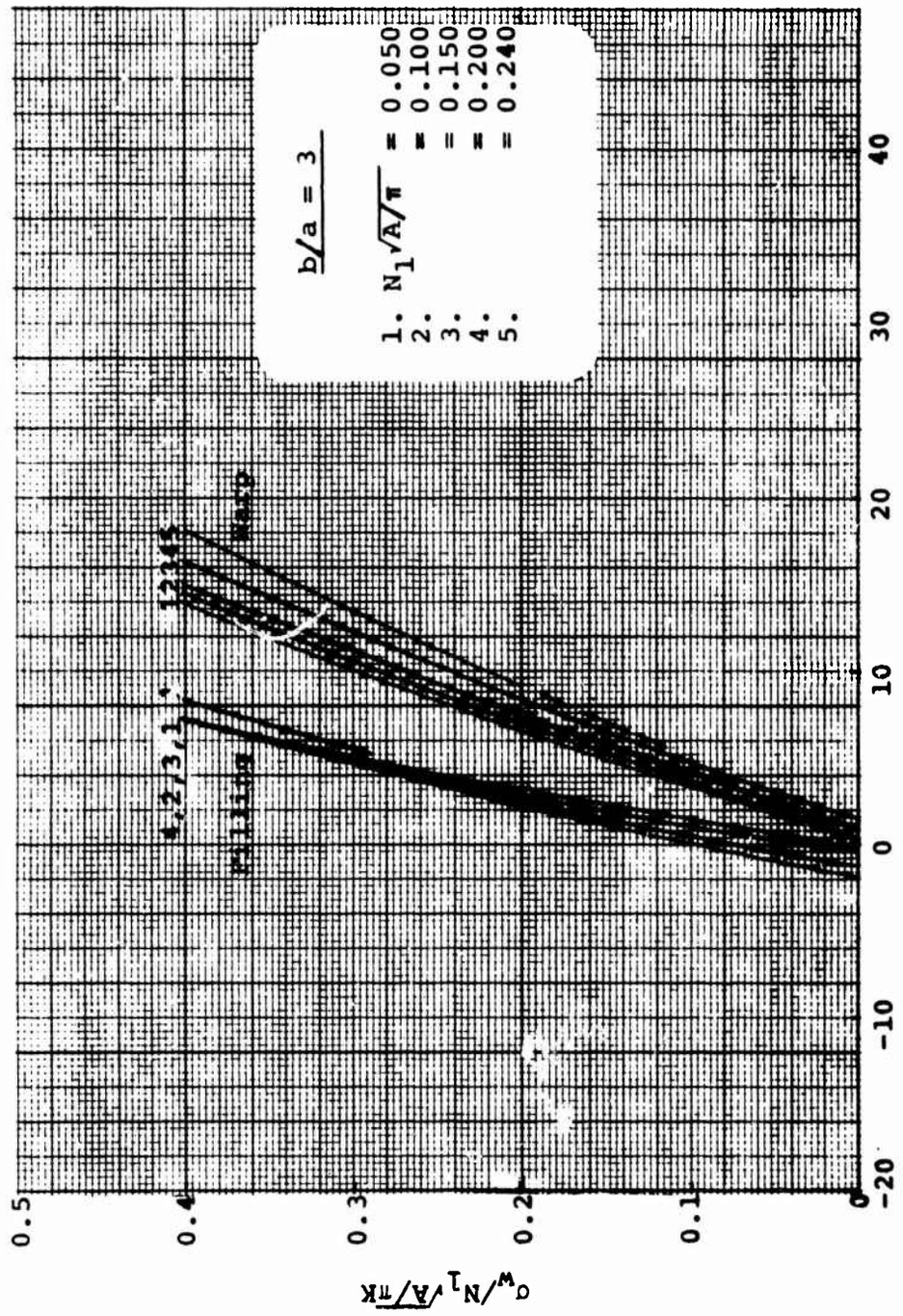

Figure 49. Fabric Extension: Linearly Elastic Yarn
$\sigma_w/\sigma_f = 2$, b/a = 3

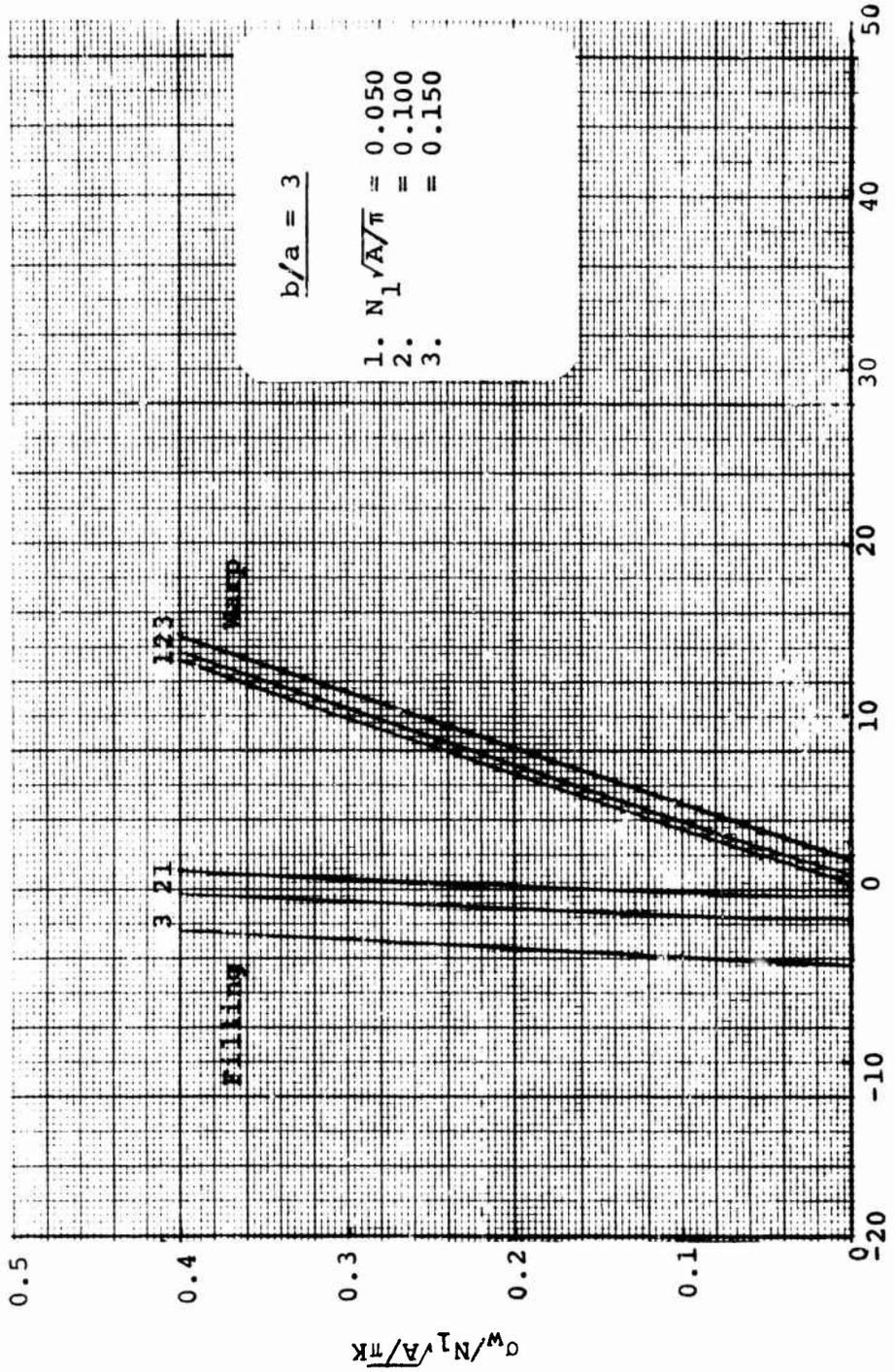

Figure 50. Fabric Extension: Linearly Elastic Yarn
$\sigma_w/\sigma_f = 5$, b/a = 3

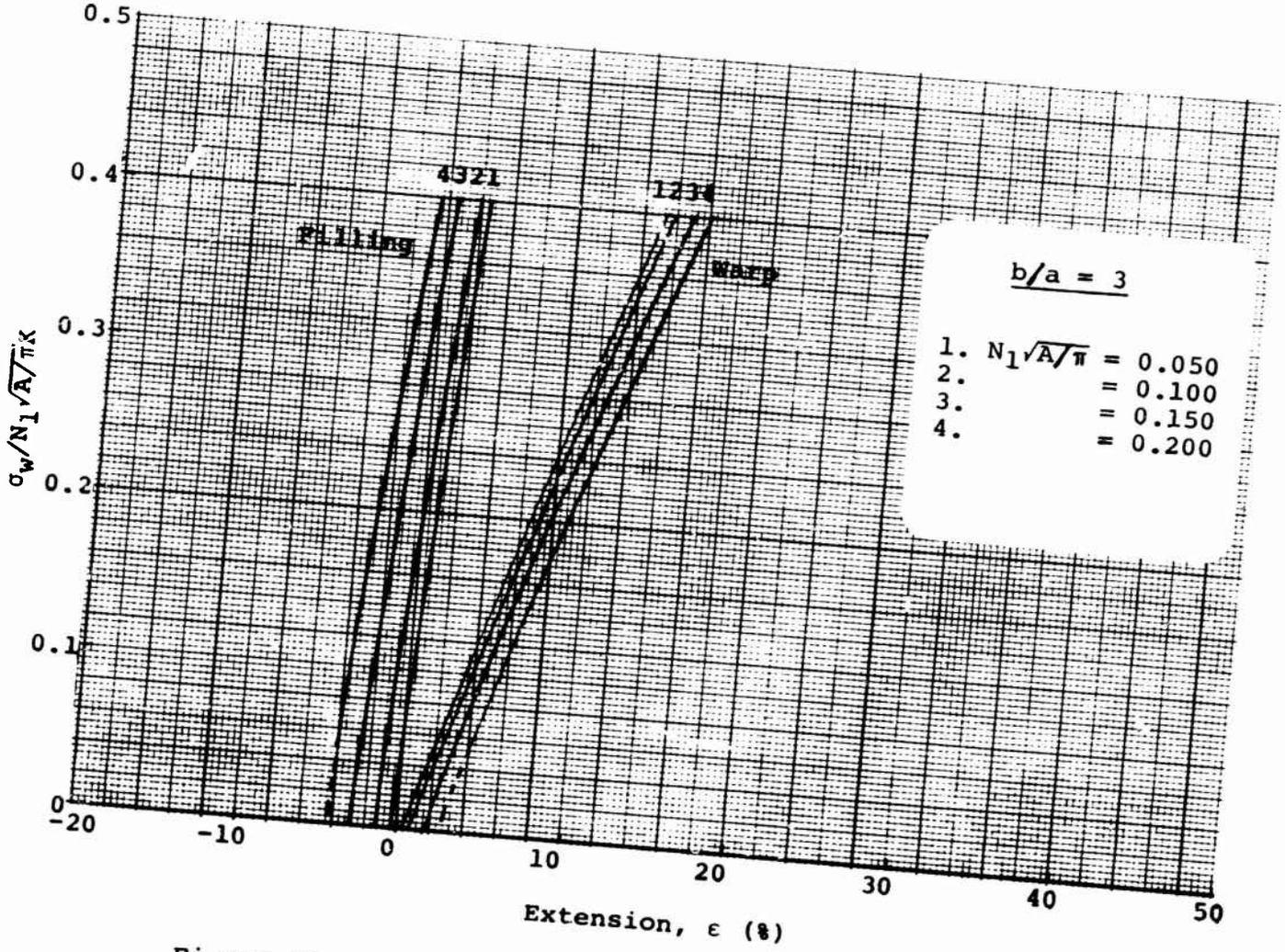

Figure 51. Fabric Extension: Linearly Elastic Yarn
σ_w/σ_f = 10, b/a = 3

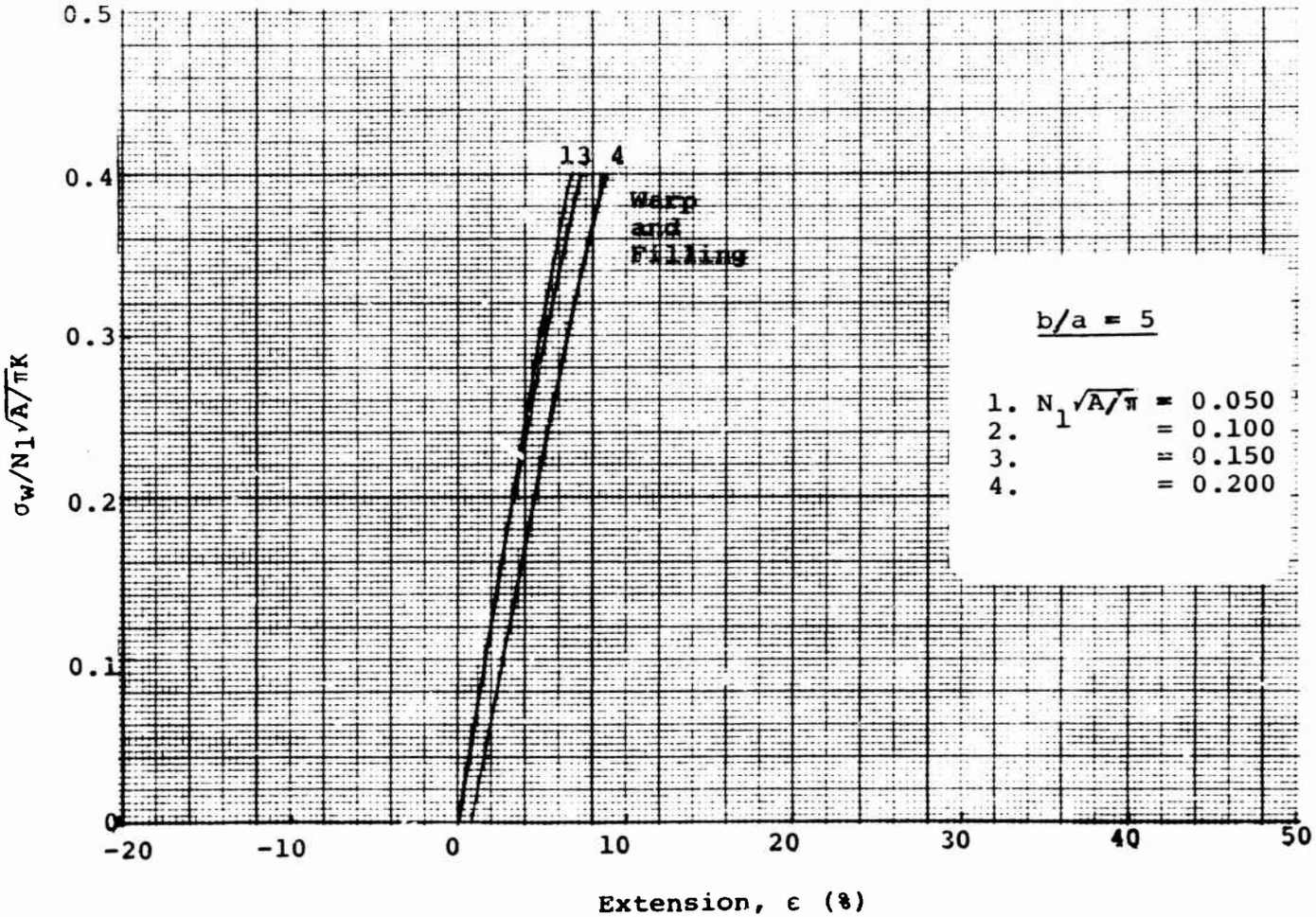

Figure 52. Fabric Extension: Linearly Elastic Yarn
$\sigma_w/\sigma_f = 1$, b/a = 5

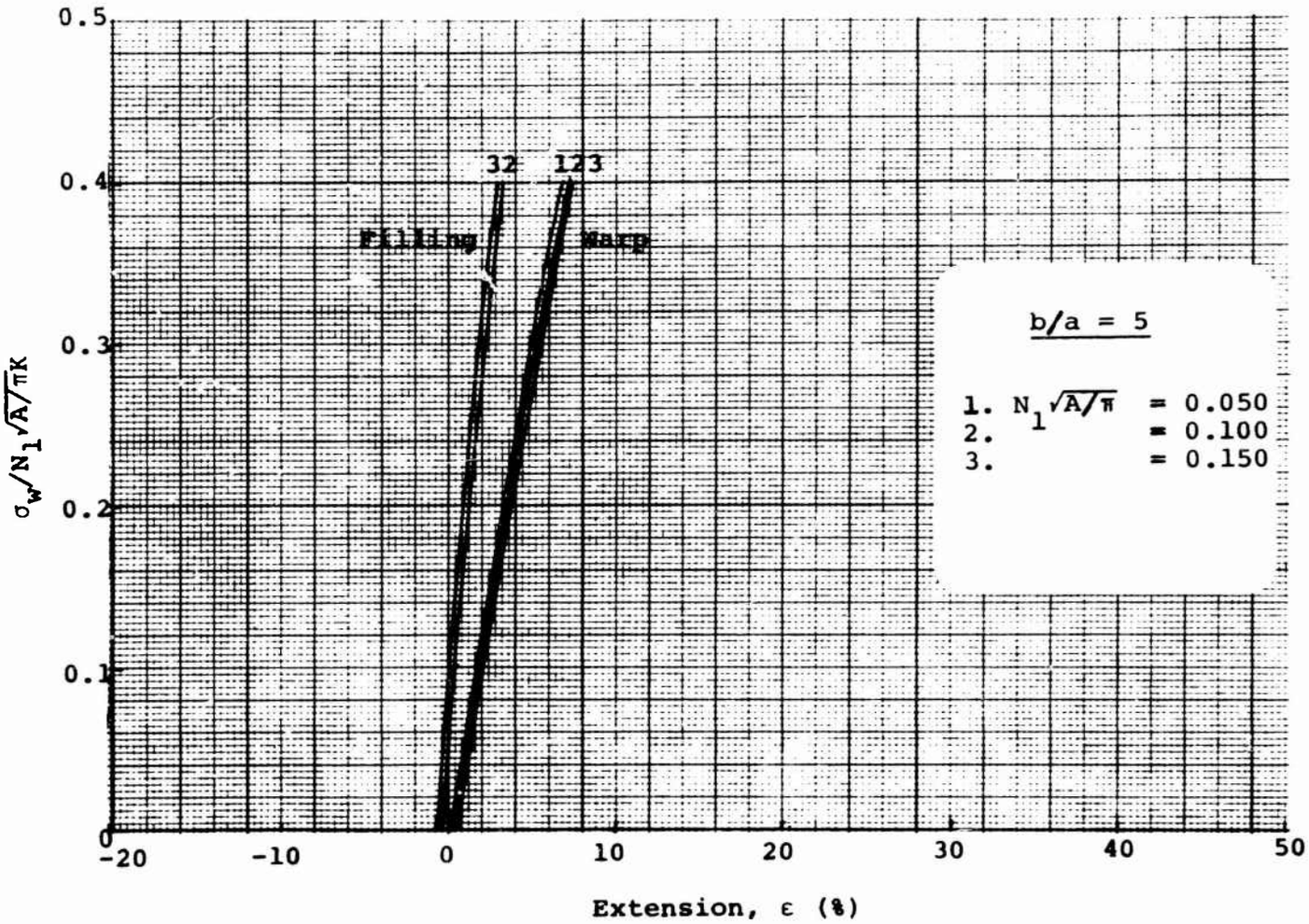

Figure 53. Fabric Extension: Linearly Elastic Yarn
$\sigma_w/\sigma_f = 2$, b/a = 5

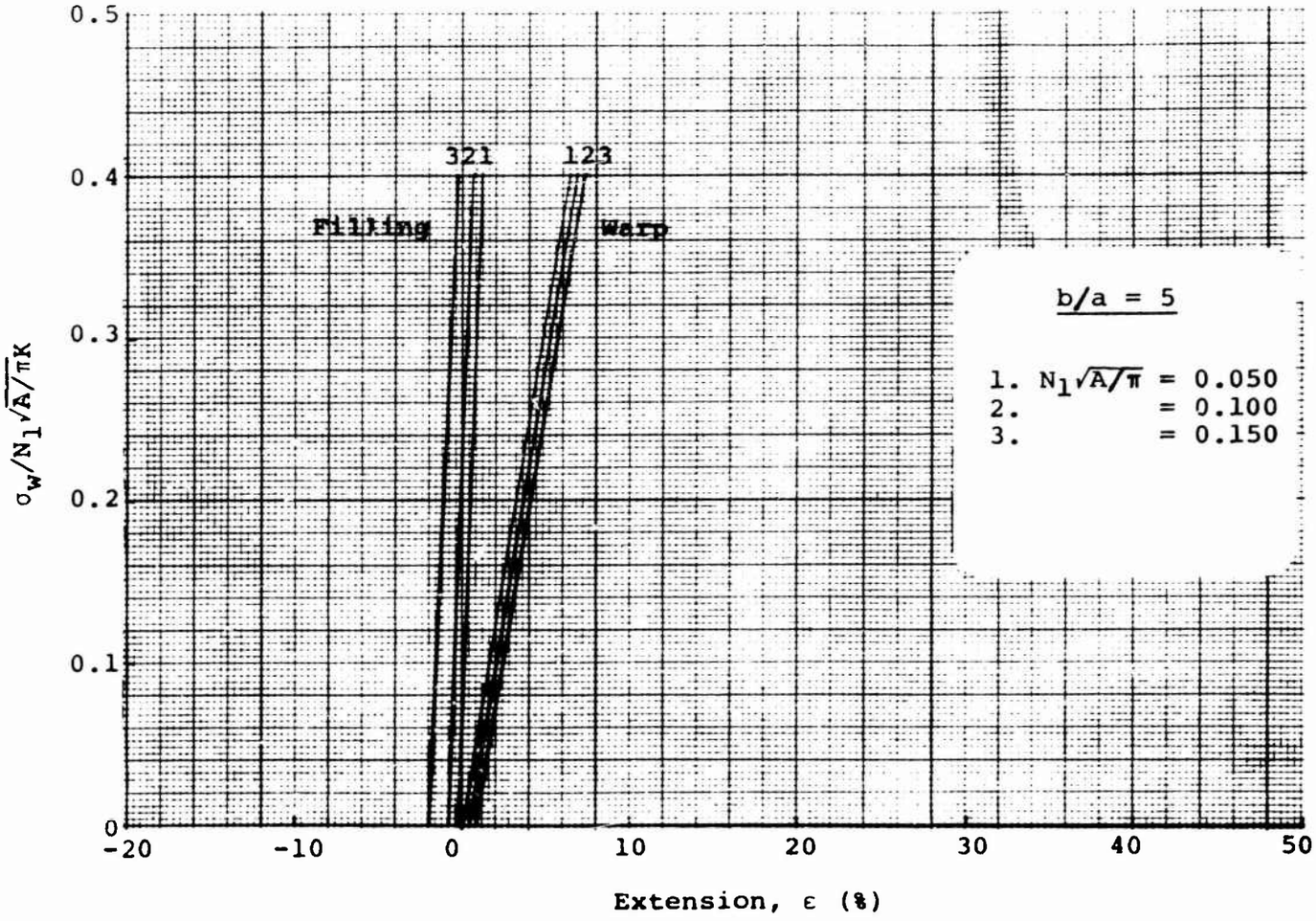

Figure 54. Fabric Extension: Linearly Elastic Yarn
σ_w/σ_f = 5, b/a = 5

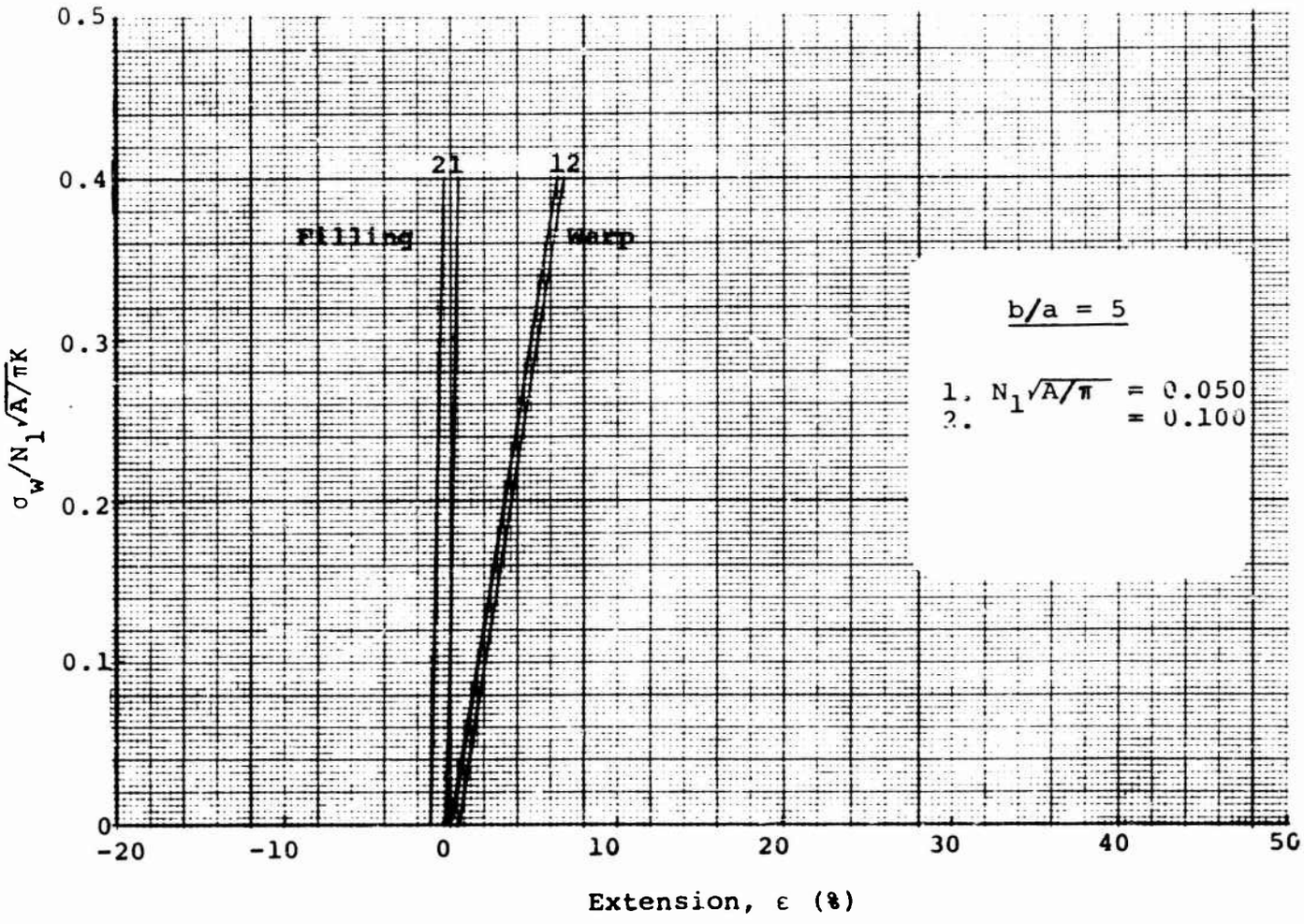

Figure 55. Fabric Extension: Linearly Elastic Yarn
$\sigma_w/\sigma_f = 10$, b/a = 5

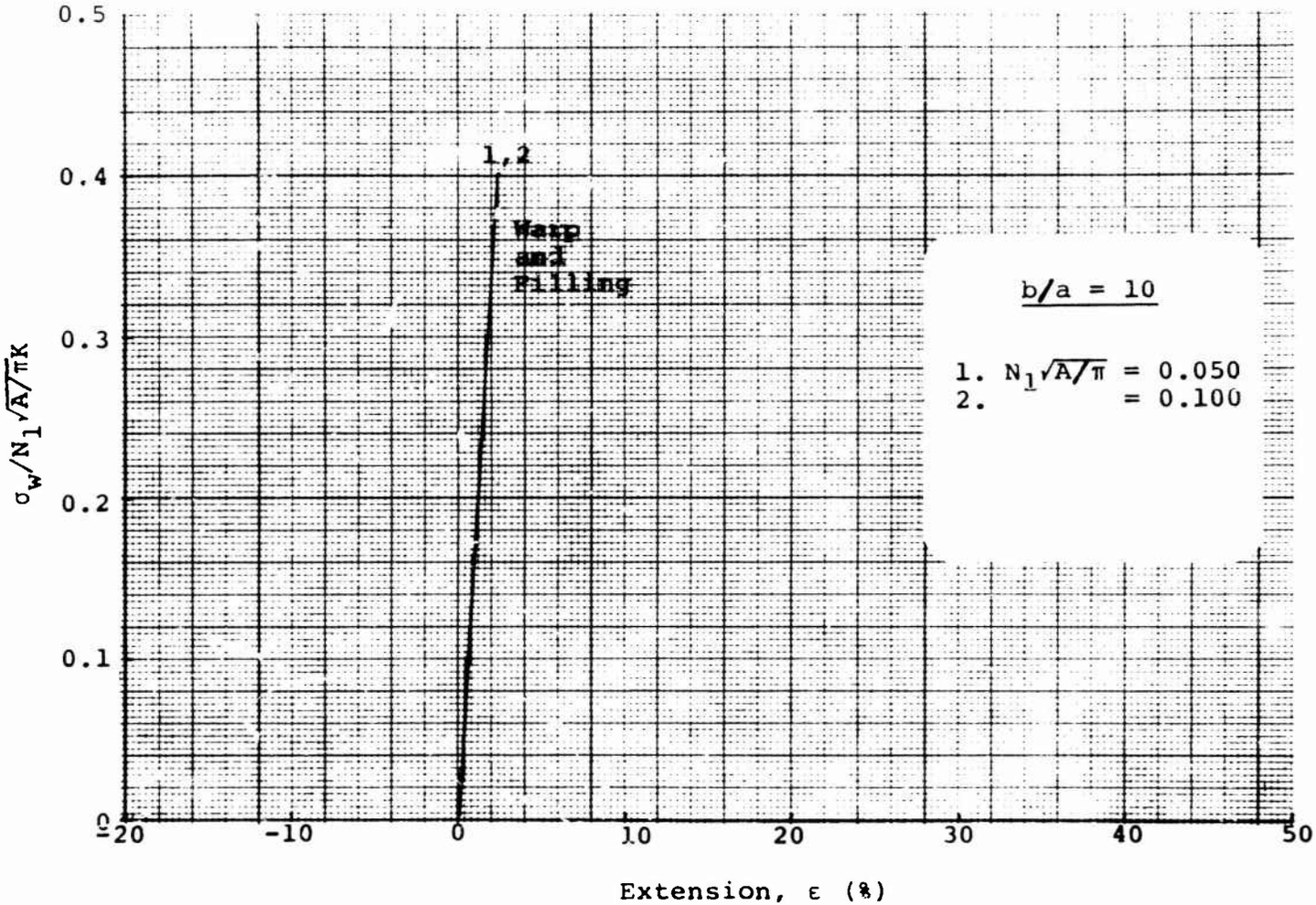

Figure 56. Fabric Extension: Linearly Elastic Yarn
σ_w/σ_f = i, b/a = 10

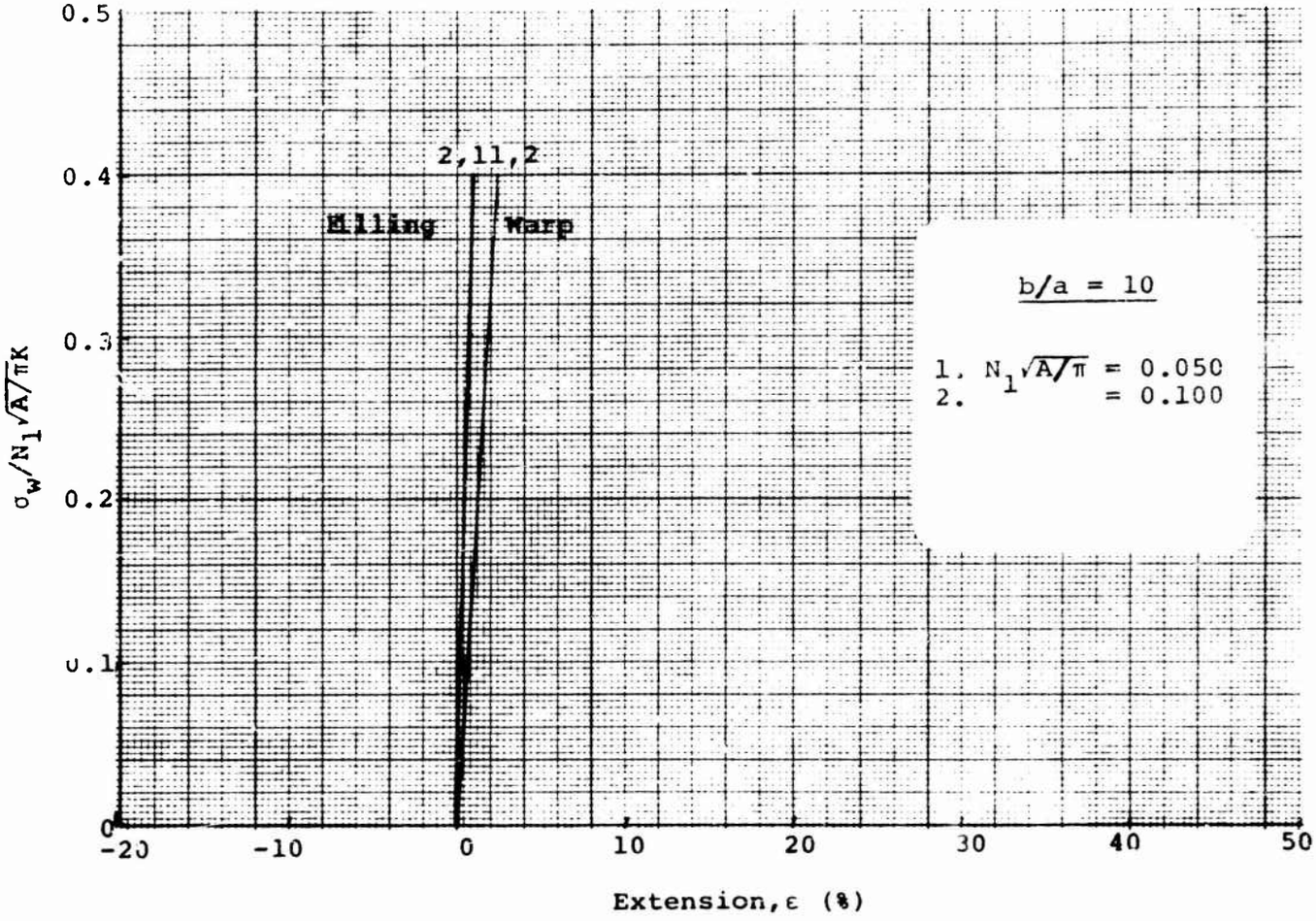

Figure 57. Fabric Extension: Linearly Elastic Yarn
σ_w/σ_f = 2, b/a = 10

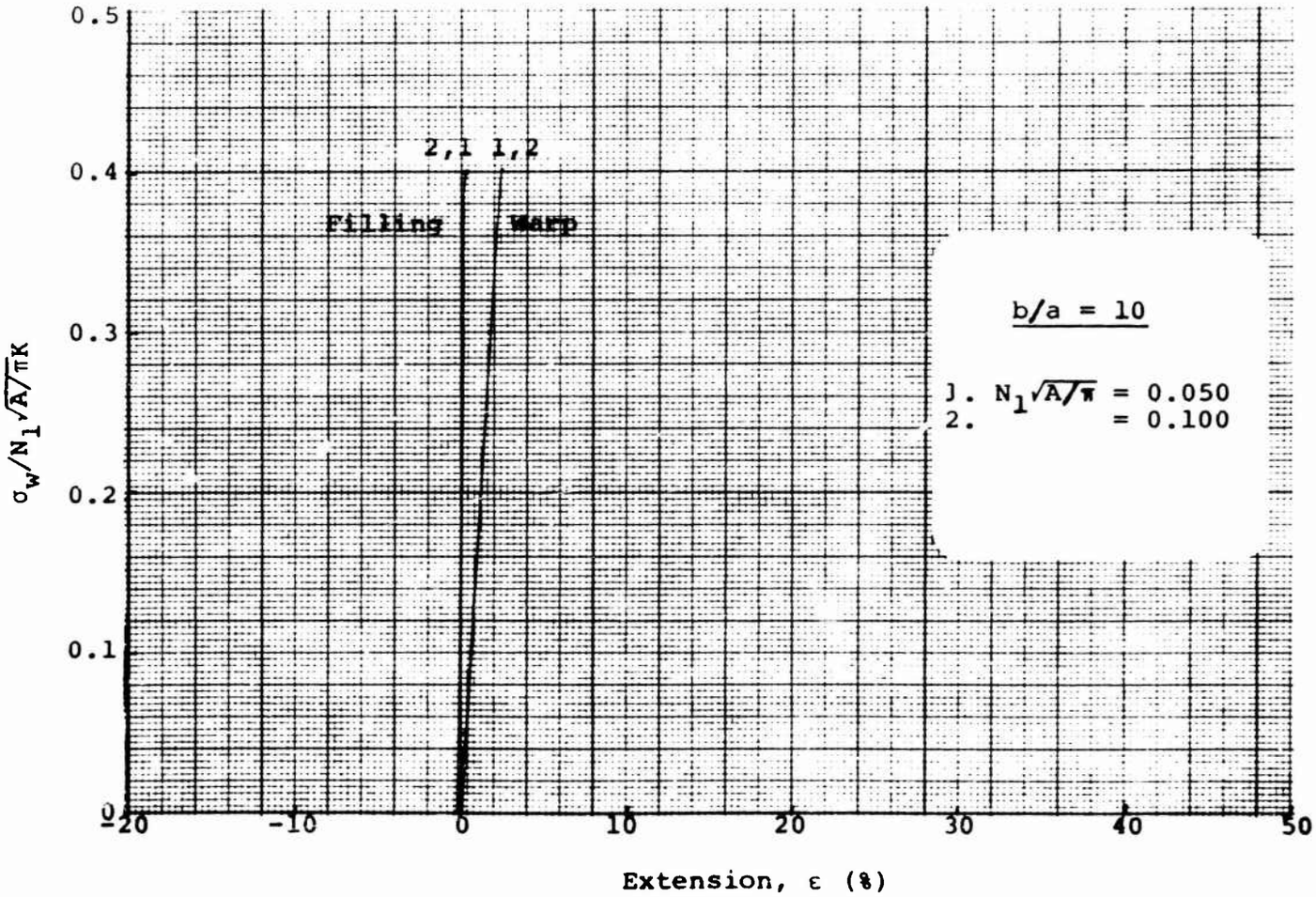

Figure 58. Fabric Extension: Linearly Elastic Yarn $\sigma_w/\sigma_f = 5$, b/a = 10

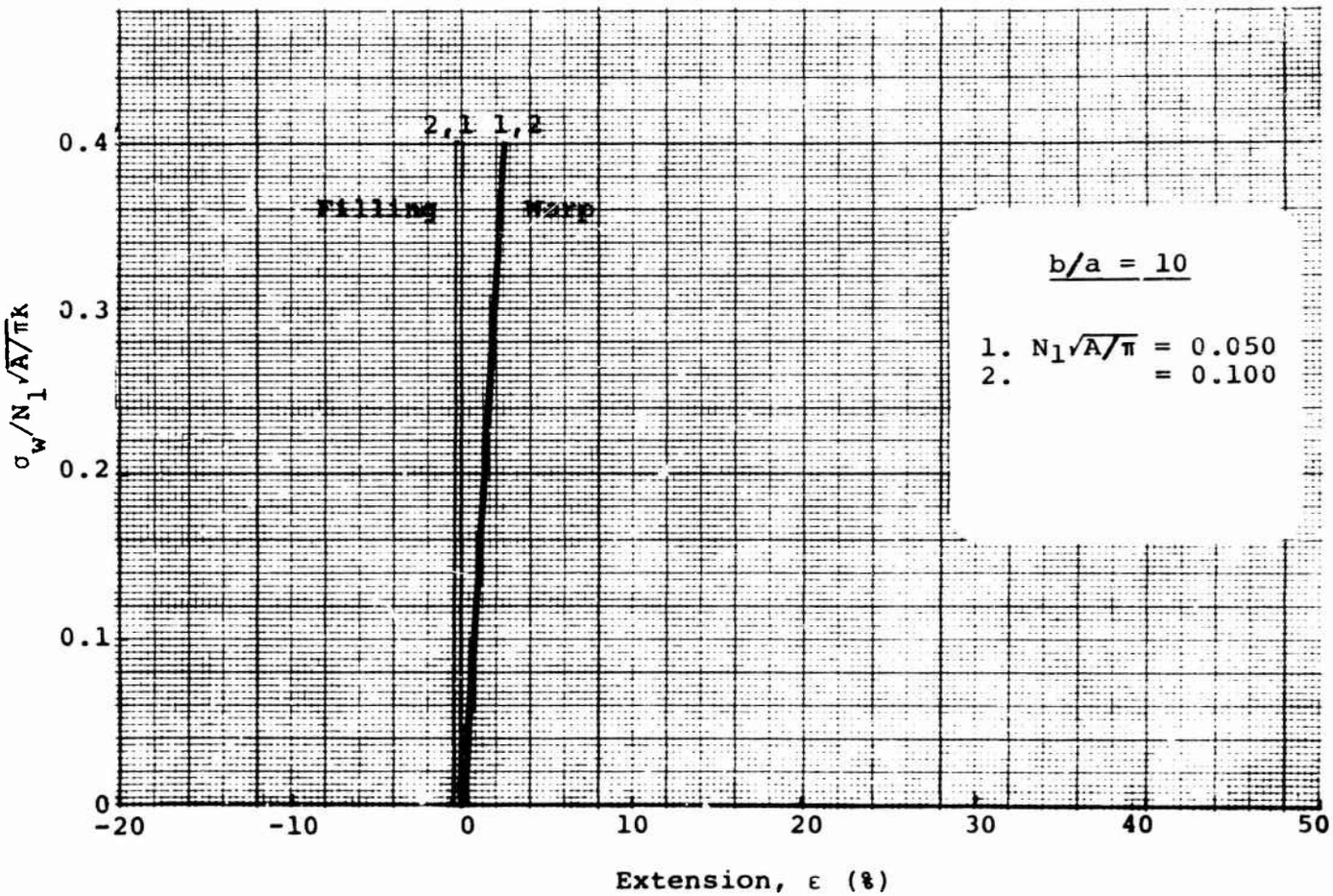

Figure 59. Fabric Extension: Linearly Elastic Yarn σ_w/σ_f = 10, b/a = 10

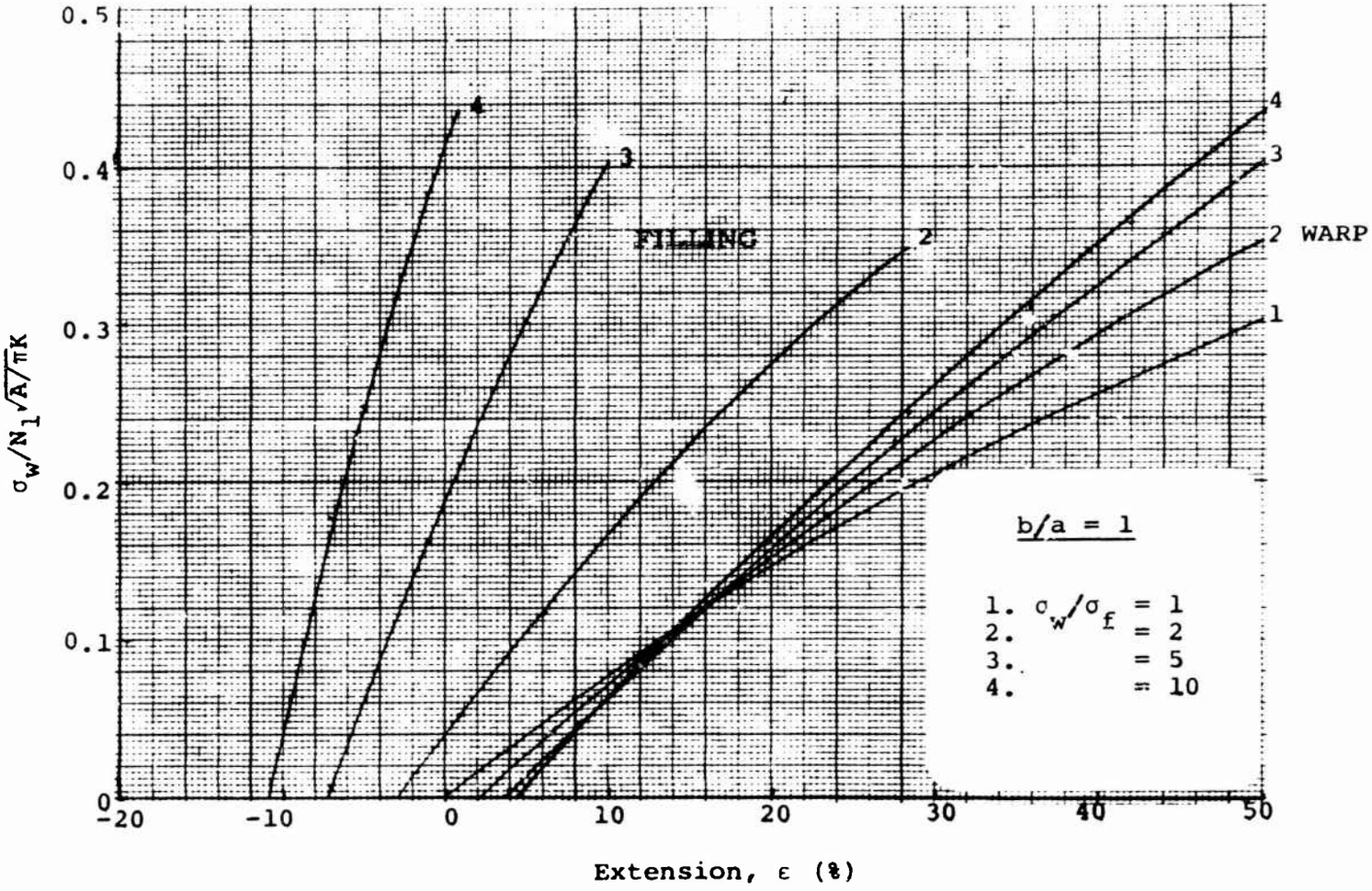

Figure 60. Fabric Extension: Linearly Elastic Yarn
$N_1\sqrt{A/\pi}$ = 0.15, b/a = 1

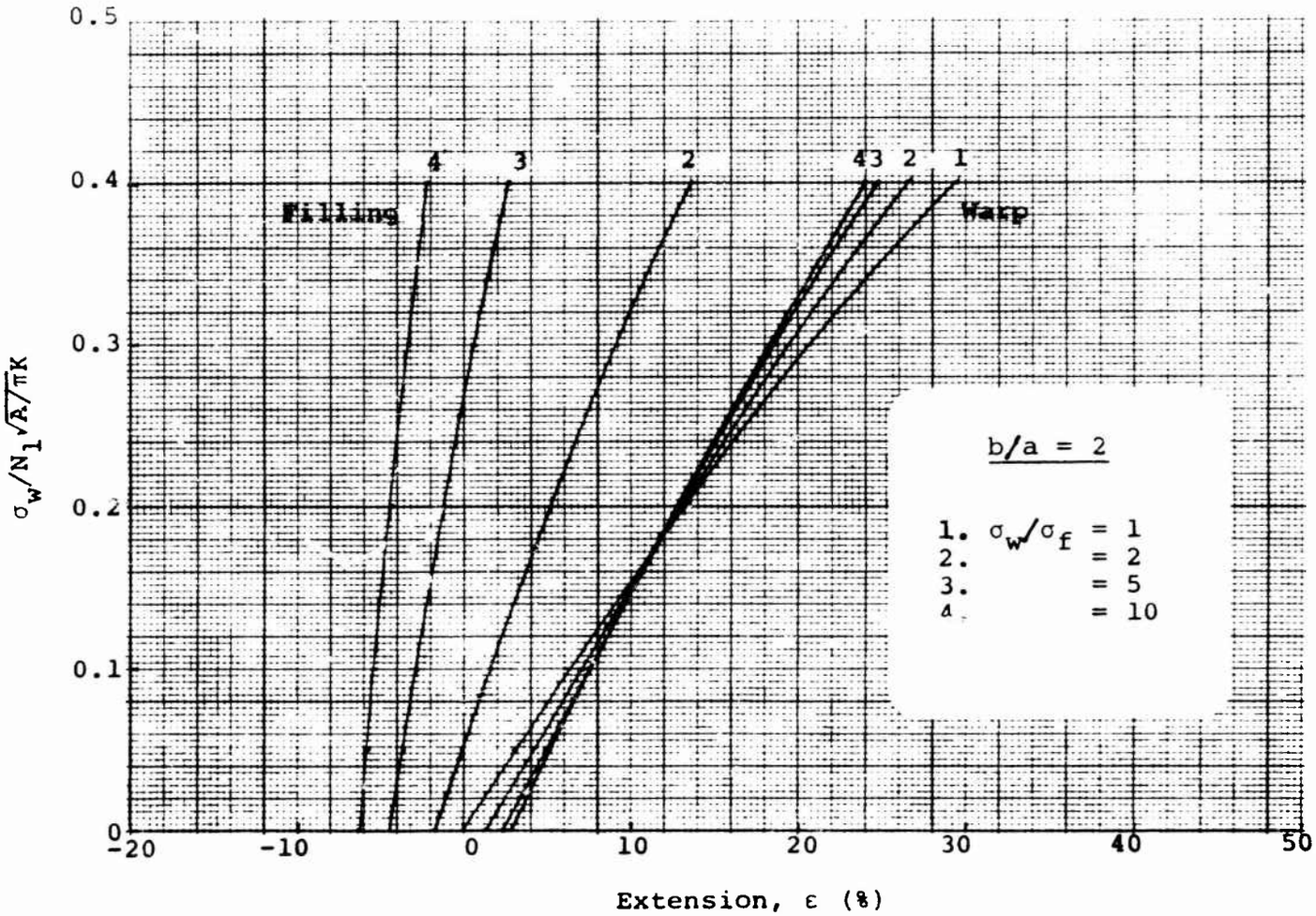

Figure 61. Fabric Extension: Linearly Elastic Yarn
$N_1\sqrt{A/\pi}$ = 0.15, b/a = 2

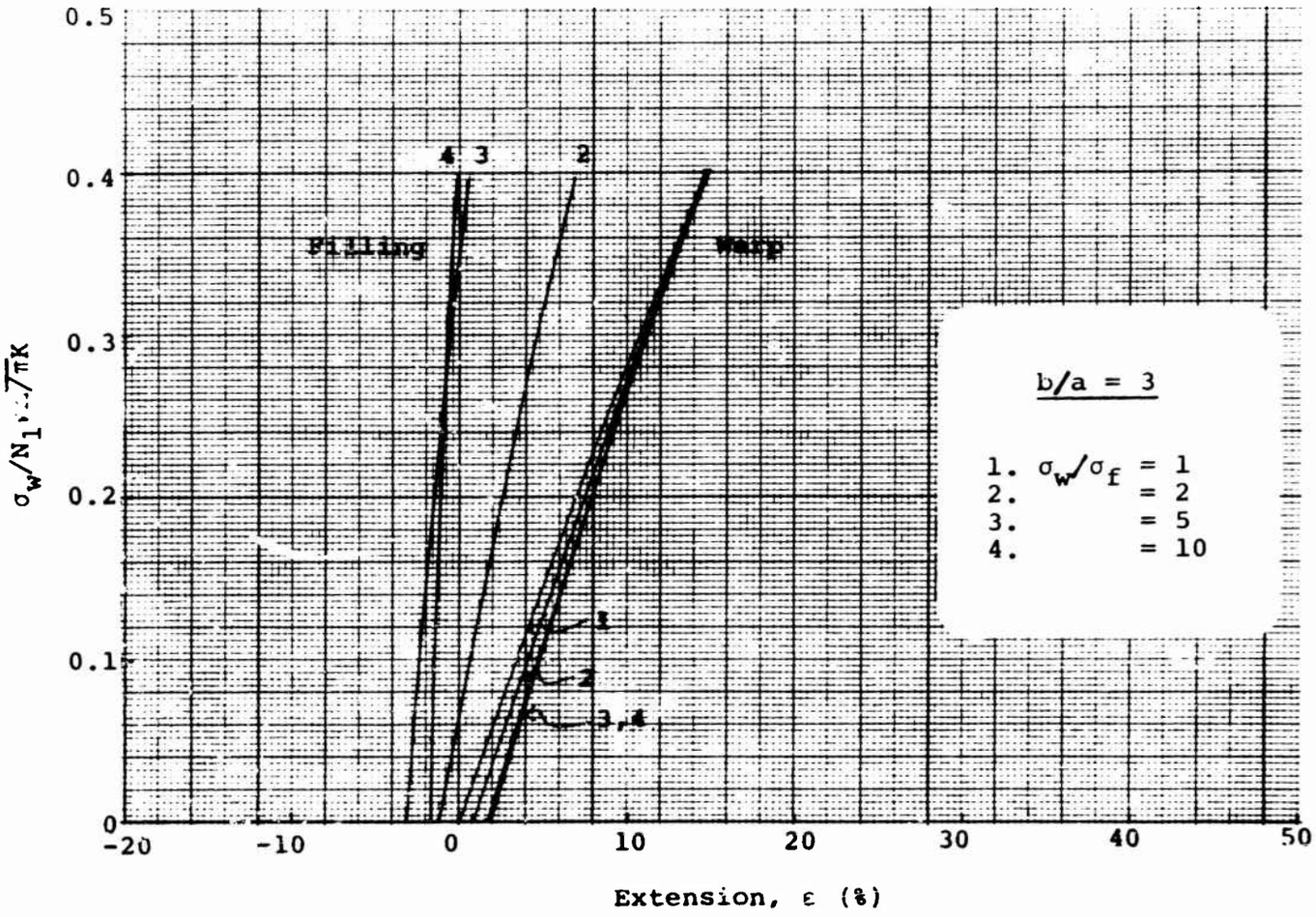

Figure 62. Fabric Extension: Linearly Elastic Yarn
$N_1\sqrt{A/\pi}$ = 0.15, b/a = 3

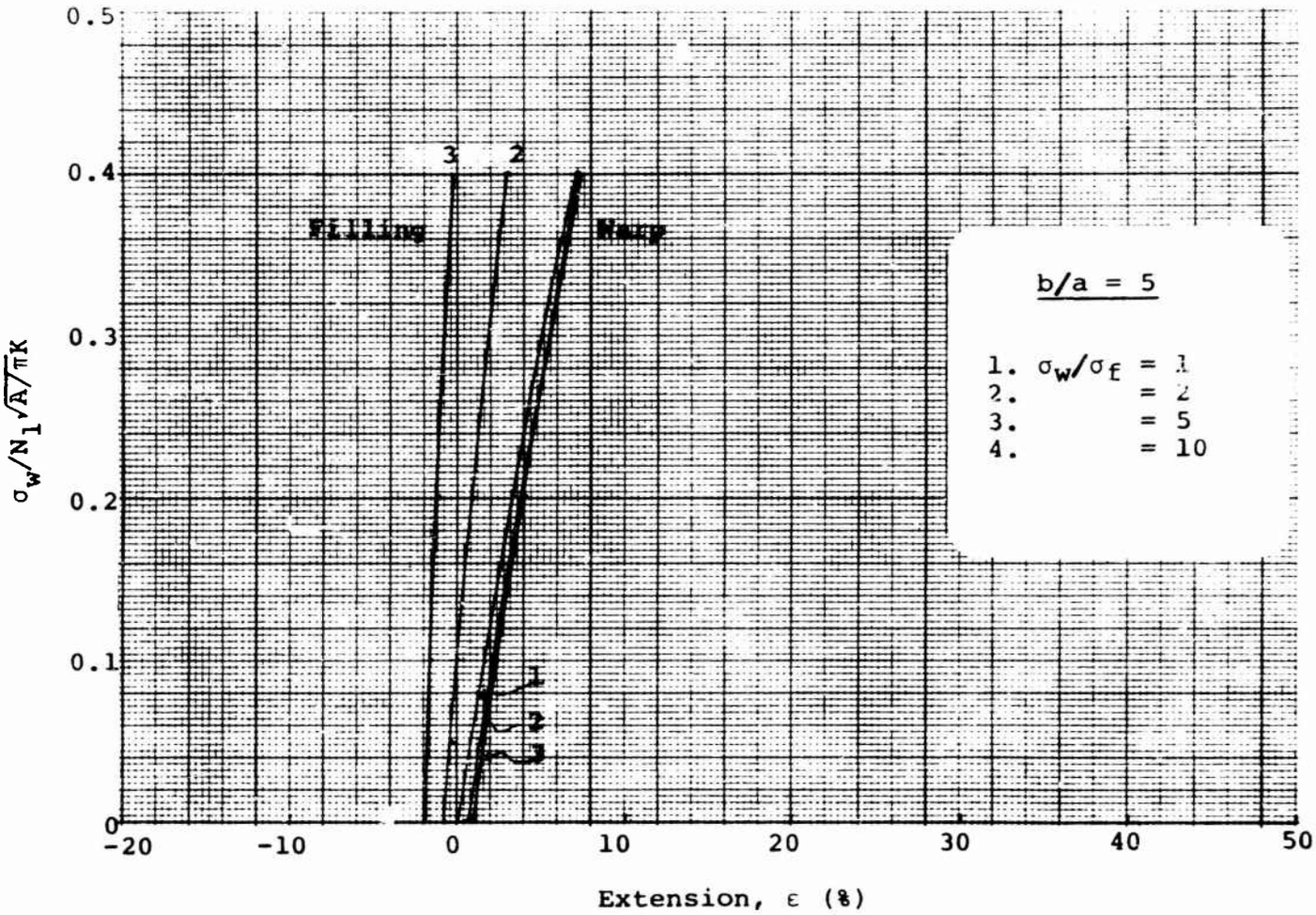

Figure 63. Fabric Extension: Linearly Elastic Yarn
$N_1\sqrt{A/\pi}$ = 0.15, b/a = 5

The extension at constant radius of a straight, linearly elastic, twisted yarn is also given in Figure 40 as a function of the same parameters. This can be done since σ/N_1 represents the load applied to each yarn in the fabric and, from Equation 22, the extension, ε_y, of a linearly elastic yarn is given by

$$\varepsilon_y = \frac{P_y}{pE_fA} = \frac{\sigma}{N_1 pE_f A} = \frac{\sigma}{(N_1\rho)K}$$

where P_y is the load applied to the yarn. The parameter $\sigma/(N_1\rho)K$ is transformed into the parameter $\sigma/(N_1\sqrt{A/\pi})K$ used in Figures 40 through 63 via Equation 34. As shown in Figure 40 the fabric is more easily extended than a straight yarn identical to those from which the fabric is woven. This is because of the crimp in the fabric yarns.

In Figures 40 through 59, curves are given only for the lower values of $N_1\sqrt{A/\pi}$ at the larger yarn aspect ratios, i.e., for those values of $N_1\sqrt{A/\pi}$ for which the fabric is neither initially jammed, nor reaches the jammed state at low levels of load.

All the analytical results were examined to check that none of the solutions gave a physically impossible fabric deformation, i.e., a deformation that violated the second or third types of limiting geometries discussed previously. The dotted portions of some of the curves in Figures 43, 46, 49 and 51 indicate regions of the loading parameter where no solutions exist; as the applied load increases, however, it becomes possible to obtain solutions. In each of the cases where no solution was found Table 5 indicates that for the particular aspect ratio and value of $N_1\sqrt{A/\pi}$ involved, maximum filling yarn contraction occurs at a lower value of the loading ratio than that in question for similar fabrics in which no yarn extension takes place. Evidently, in these instances, the yarn extension, as indicated by the value of the loading parameter, must reach a magnitude such that the fabric becomes "unjammed" before solutions are possible.

Since touching of adjacent warp yarns was not possible for square fabric constructions in which no yarn extension was allowed, it cannot occur in fabrics where yarn extension increases the length of yarn between yarn crossovers.

As shown in Figures 40 through 50, the fabric load-extension curves appear to intersect the zero-load axes at finite strains. This results from the assumption that the yarns are infinitely flexible, i.e., have zero bending rigidity. The strain values at these apparent intercepts are roughly the same as those given for initially square fabrics woven from inextensible yarn at the corresponding loading ratios (see Figures 17 through 26).

It can be shown that for any specific load, σ, (pounds per inch width of fabric) applied to the fabric, the fabric extension increases with decreasing $N_1\sqrt{A/\pi}$. The smaller $N_1\sqrt{A/\pi}$, the fewer are the number of yarns available for supporting the applied load and thus, the greater the yarn's share of the total load applied to the fabric. The fabric extension also increases with decreasing yarn cross-sectional area and decreasing yarn modulus.

The fabrics contract in the filling direction at low levels of applied loads; the contraction is greater at the higher loading ratios and lower yarn aspect ratios. However, the fabric extends from the contracted state as the applied load is increased. The level of load that must be applied in the warp direction to eliminate the filling contraction increases with increasing loading ratio and decreasing yarn aspect ratio. For a given applied load and loading ratio, the magnitude of the fabric extension in the warp direction is considerably greater than the extension (or contraction) in the filling direction; the difference increases with increasing loading ratio and increasing yarn aspect ratio.

The slope of the fabric warp and filling load-extension curves subsequent to the extension that occurs instantaneously upon application of infinitesimal loads (when $\sigma_w/\sigma_f > 1$) increases as the yarn aspect ratio increases. Thus the fabric extension decreases with increasing yarn aspect ratio. This occurs because,

in general, the initial angulation of the fabric yarns to the fabric midplane decreases with increasing yarn aspect ratio.

Additionally, the slopes of the fabric load-extension curves increase with increasing loading ratio. The reason for this trend is not readily apparent.

As also shown in the figures the initial "instantaneous" fabric extension in the warp direction increases with increasing loading ratio. However, for the smaller values of b/a, the extension at the lower loading ratios increases at a faster rate with increasing applied load so that the curves cross. At load levels resulting in extensions larger than those at which the curves cross the fabric extension in the warp direction increases with decreasing loading ratio; the loading ratio $\sigma_w/\sigma_f = 1$ gives the greatest fabric extension. The latter evidently is the result of the greater filling extension that occurs when the load applied in the filling direction approaches that applied in the warp direction. Increased filling yarn extension permits a decrease in filling yarn crimp, and, consequently, through the balance of the vertical components of the forces in the two orthogonal systems of yarns, a decrease in warp yarn crimp, thereby permitting increased fabric extension in the warp direction.

Comparison of the foregoing data to the results given in Reference 2 for a fabric woven from yarns with a racetrack cross-section shows that fabrics woven from yarns with a lenticular cross-section are considerably stiffer in tension. Thus, for a given applied load, lenticular-yarn fabrics exhibit less extension. This probably occurs because for fabrics comprised of yarns with a lenticular cross-section, the average angle of the yarn to the fabric midplane and the yarn length between yarn crossovers is less than for fabrics comprised of yarns with a racetrack cross-section.

The magnitude of the radial separation or GAP between the node of the lenticular cross-section and the crossing yarn after loading is illustrated in Figures 64 through 79. The GAP is given as a percent of one half the yarn thickness as a function of the load parameter for various yarn aspect ratios and initial fabric constructions. Results are given for both the warp and filling directions.

As shown in these figures both GAP_{2w} and GAP_{2f} increase moderately with increasing values of the loading parameters. Also, the GAP_{2w} between the node of the warp yarn cross-section and the crossing filling yarn decreases with increasing loading ratio for particular aspect ratios and $N_1\sqrt{A/\pi}$. However, the GAP_{2f} between the node of the filling yarn cross-section and the crossing warp yarn increases with increasing loading ratio. Both GAP_{2w} and GAP_{2f} decrease with increasing yarn aspect ratio for particular loading ratios and $N_1\sqrt{A/\pi}$. As is evident in these figures, the GAP is large for all but the most tightly woven fabric constructions at each yarn aspect ratio.

Effective Poisson's Ratio

The effective fabric Poisson's ratio, μ, is given in Figures 80 through 98 as a function of the dimensionless loading parameter $\sigma_w/(N_1\sqrt{A/\pi})K$ for various values of initial fabric geometry $N_1\sqrt{A/\pi}$, yarn aspect ratio b/a and loading ratio σ_w/σ_f. The curves have been terminated at a value of 0.4 for the loading parameter. For a loading ratio of one, $\mu = -1$ at all loads and for all initial fabric geometries. A fabric that is initially square extends the same amount in both principal directions when equal loads are applied parallel to these directions.

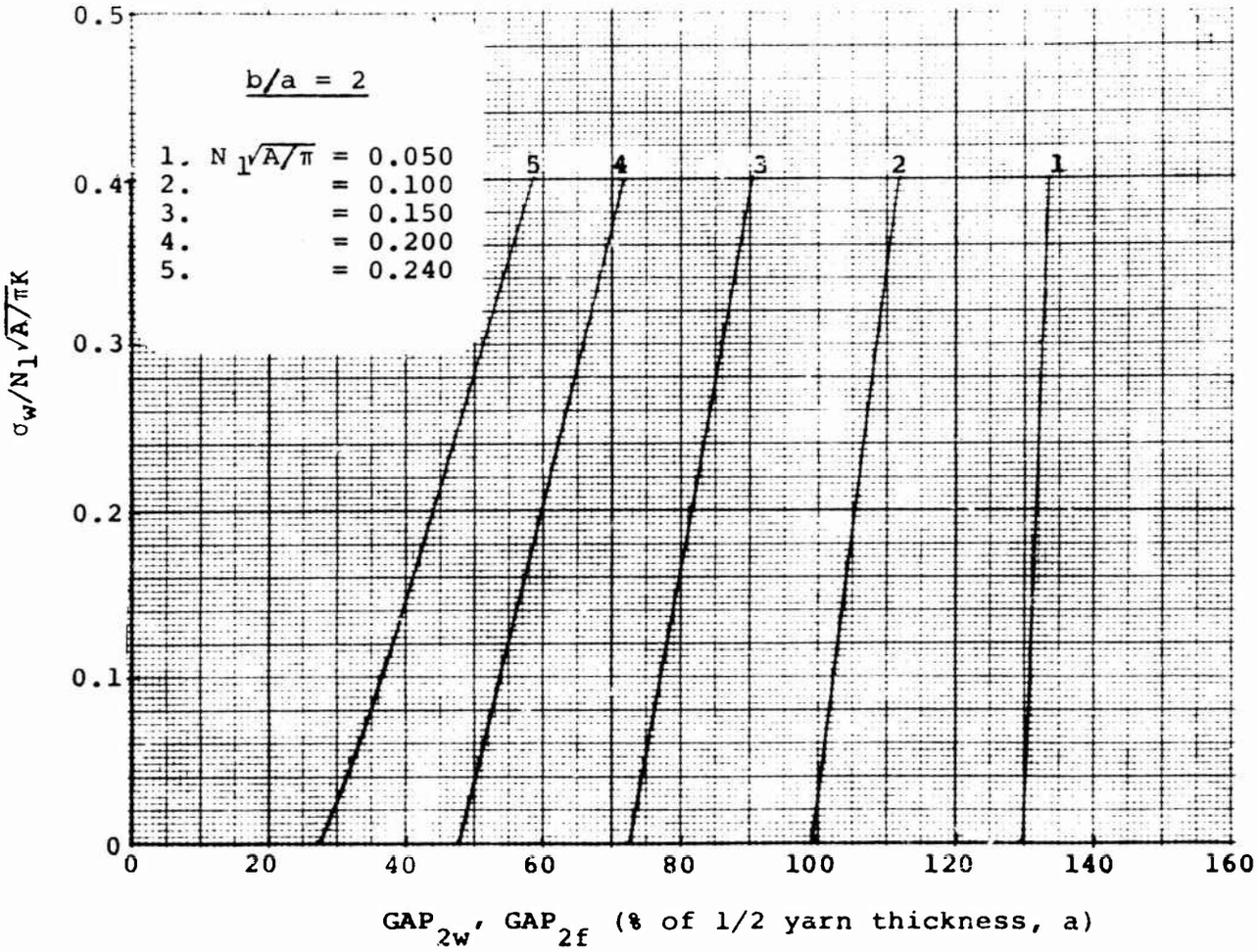

Figure 64. Radial Separation Between One Crossing Yarn and the Node of the Cross-Section of the Other Yarn (Aspect Ratio = 2), Linearly Elastic Yarn, $\sigma_w/\sigma_f = 1$

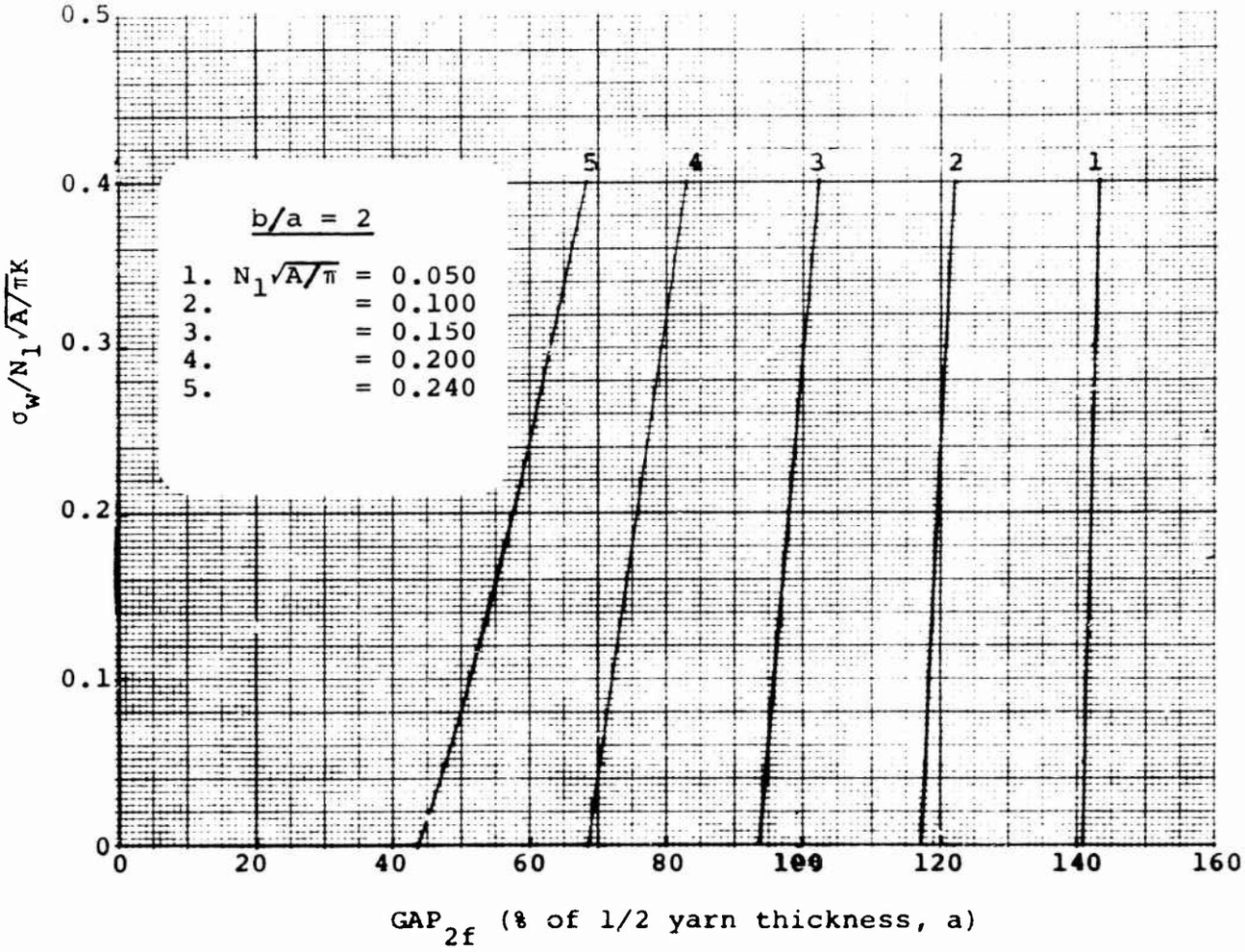

Figure 65(a). Radial Separation Between the Crossing Warp Yarn and the Node of the Filling Cross-Section (Aspect Ratio = 2): Linearly Elastic Yarn, $\sigma_w/\sigma_f = 2$

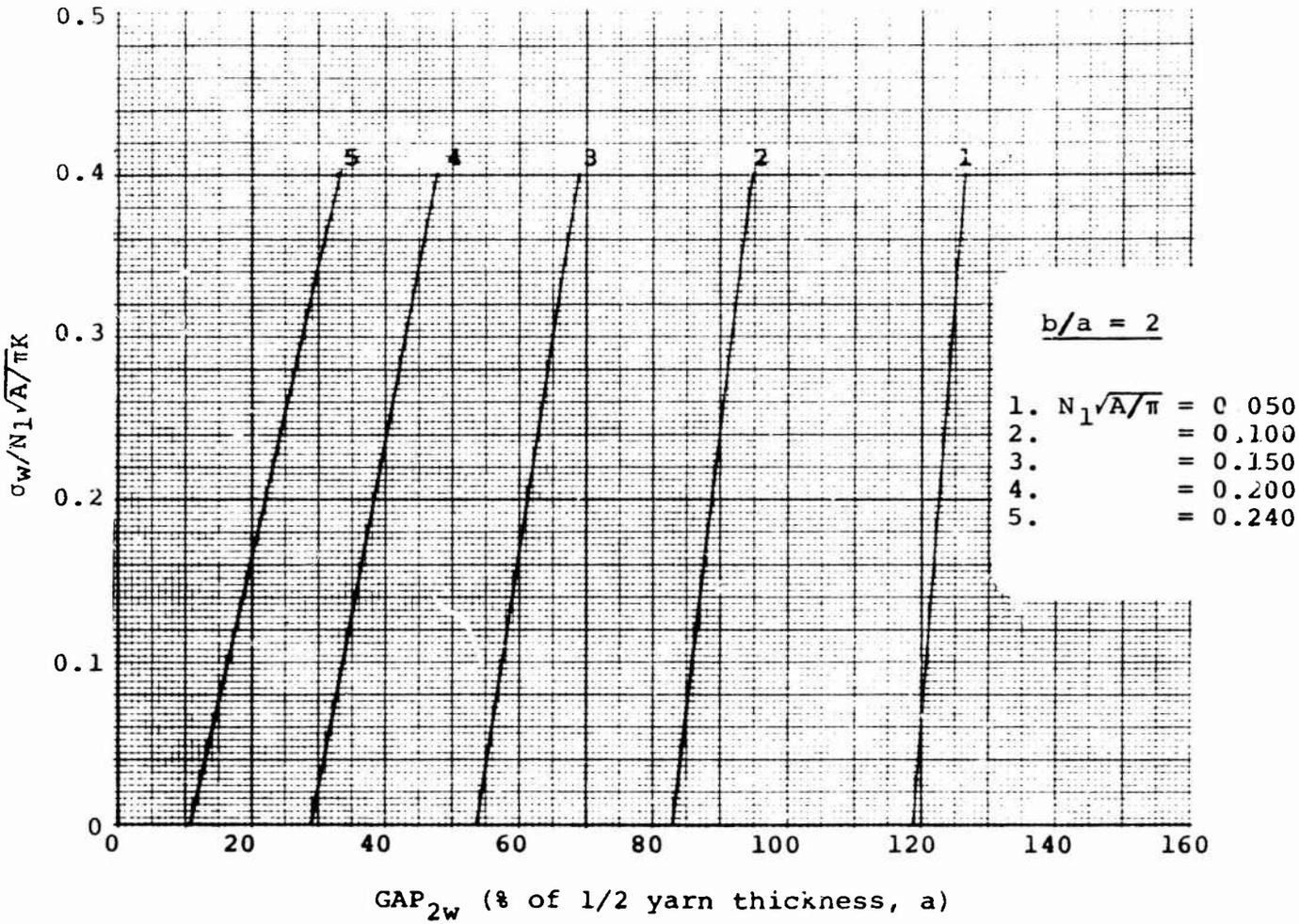

Figure 65(b). Radial Separation Between the Crossing Filling Yarn and the Node of the Warp Cross-Section (Aspect Ratio = 2): Linearly Elastic Yarn, $\sigma_w/\sigma_f = 2$

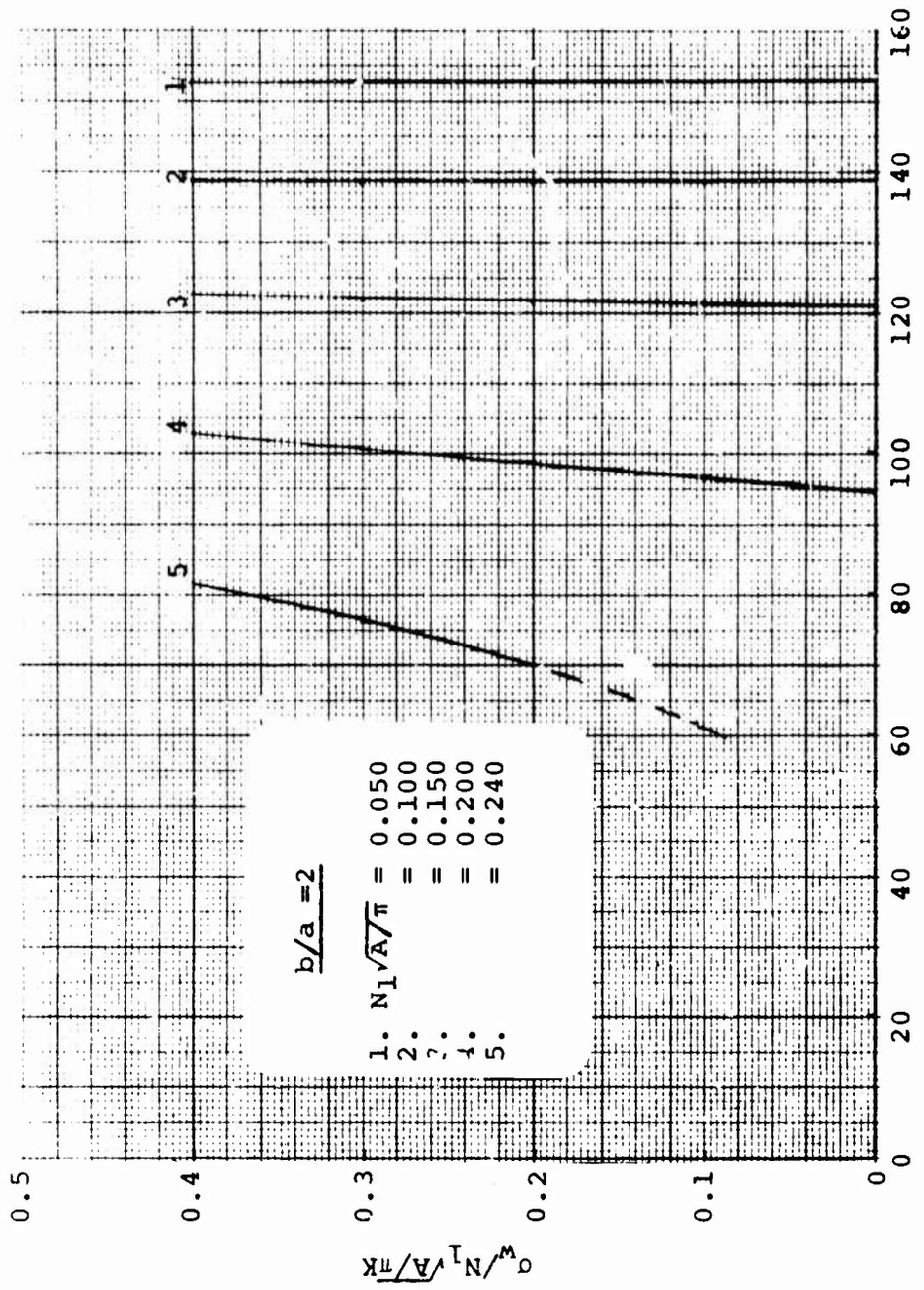

Figure 66(a). Radial Separation Between the Crossing Warp Yarn and the Node of the Filling Cross-Section (Aspect Ratio = 2): Linearly Elastic Yarn, $\sigma_w/\sigma_f = 5$

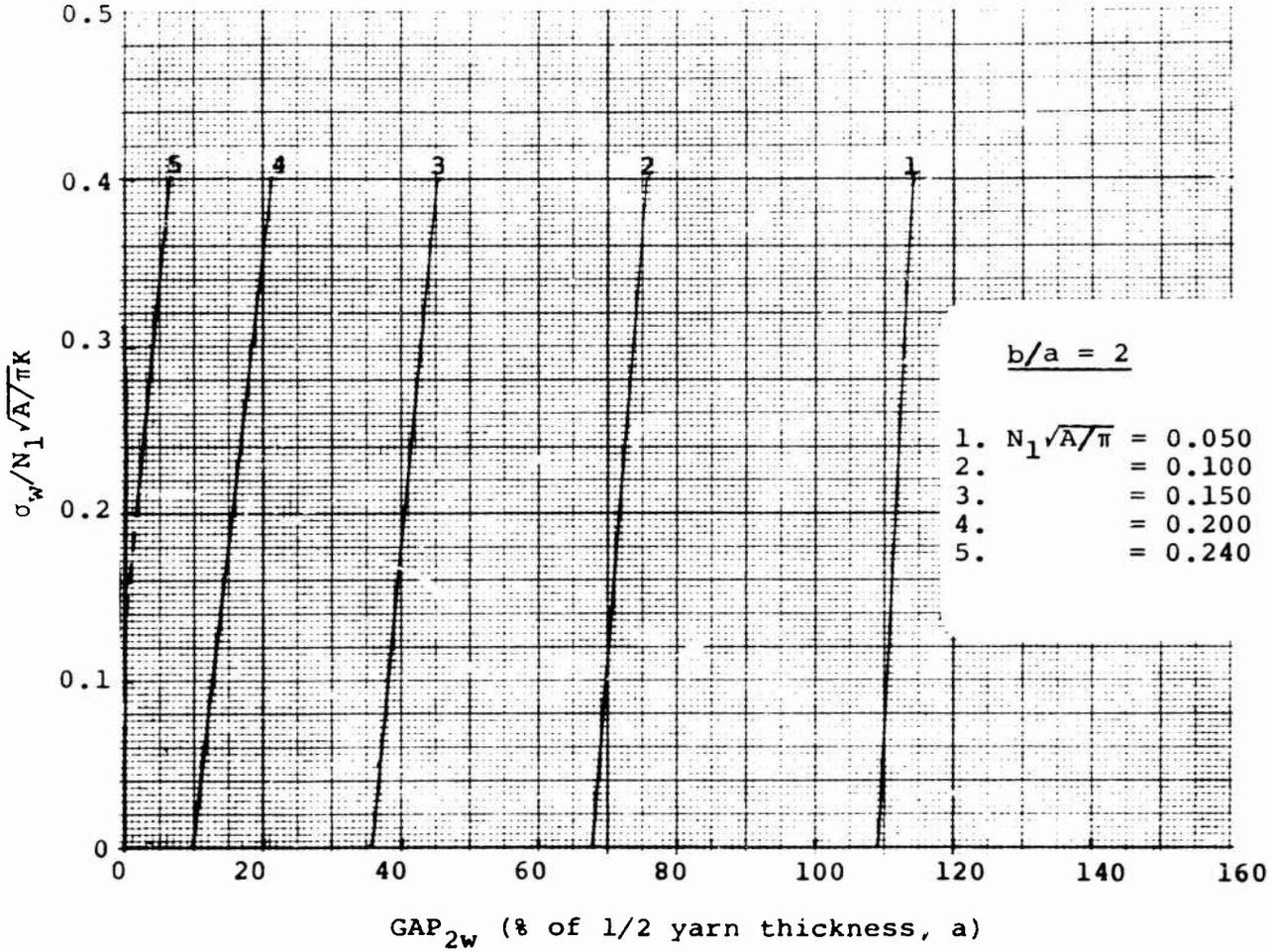

Figure 66(b). Radial Separation Between the Crossing Filling Yarn and the Node of the Warp Cross-Section (Aspect Ratio = 2): Linearly Elastic Yarn, $\sigma_w/\sigma_f = 5$

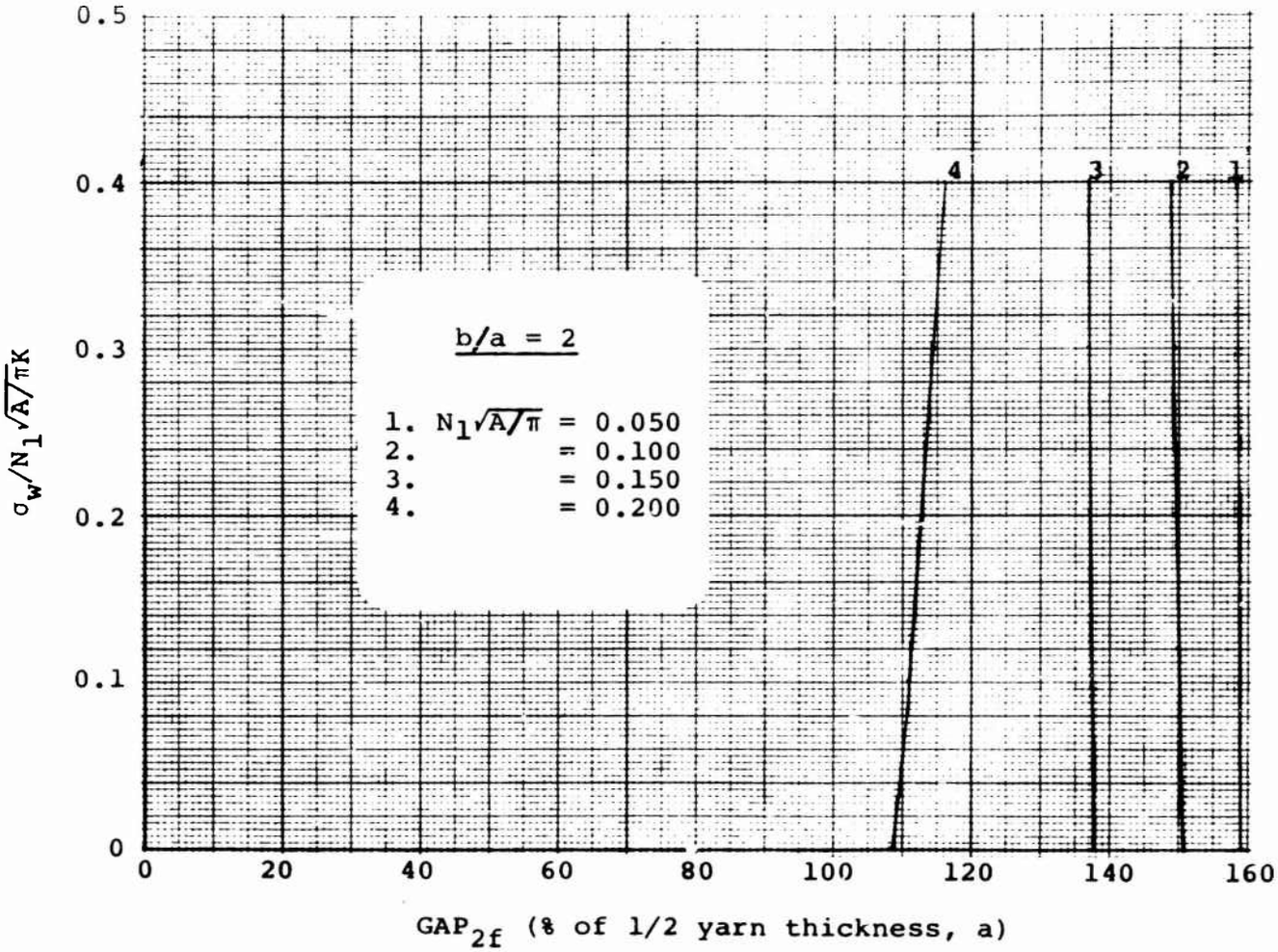

Figure 67(a). Radial Separation Between the Crossing Warp Yarn and the Node of the Filling Cross-Section (Aspect Ratio = 2): Linearly Elastic Yarn, σ_w/σ_f = 10

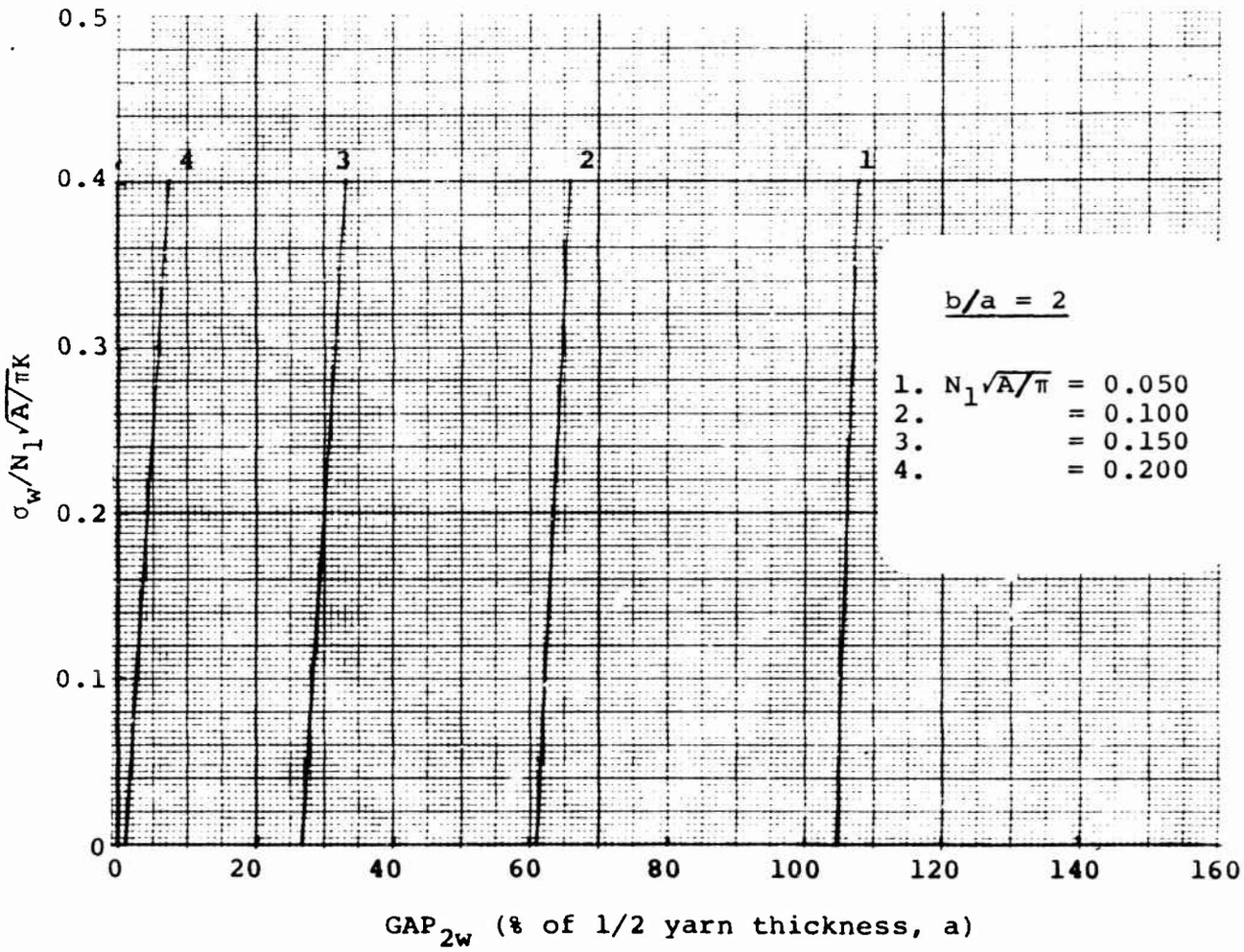

Figure 67(b). Radial Separation Between the Crossing Filling Yarn and the Node of the Warp Cross-Section (Aspect Ratio = 2): Linearly Elastic Yarn, $\sigma_w/\sigma_f = 10$

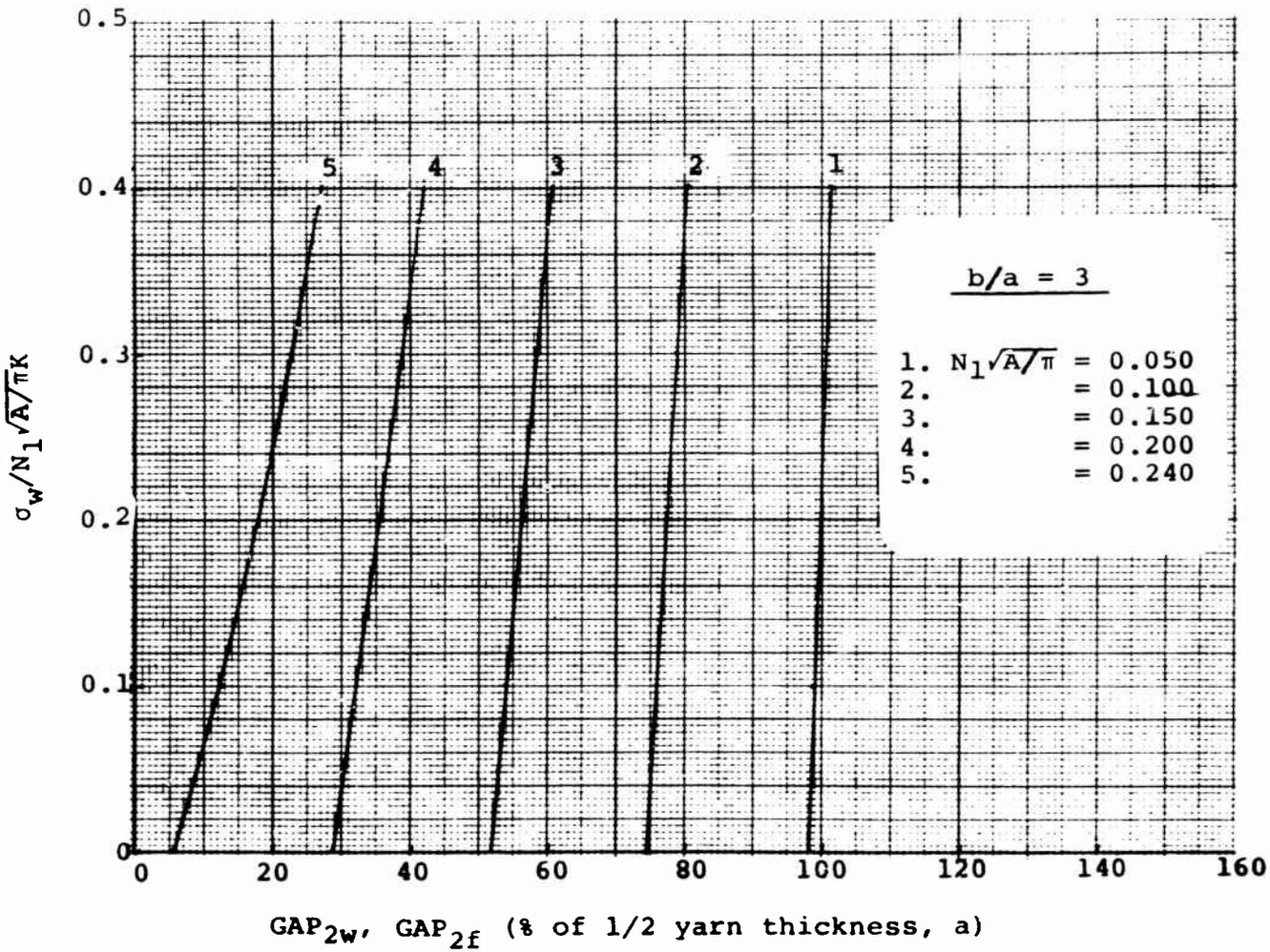

Figure 68. Radial Separation Between One Crossing Yarn and the Node of the Cross-Section of the Other Yarn (Aspect Ratio = 3): Linearly Elastic Yarn, $\sigma_w/\sigma_f = 1$

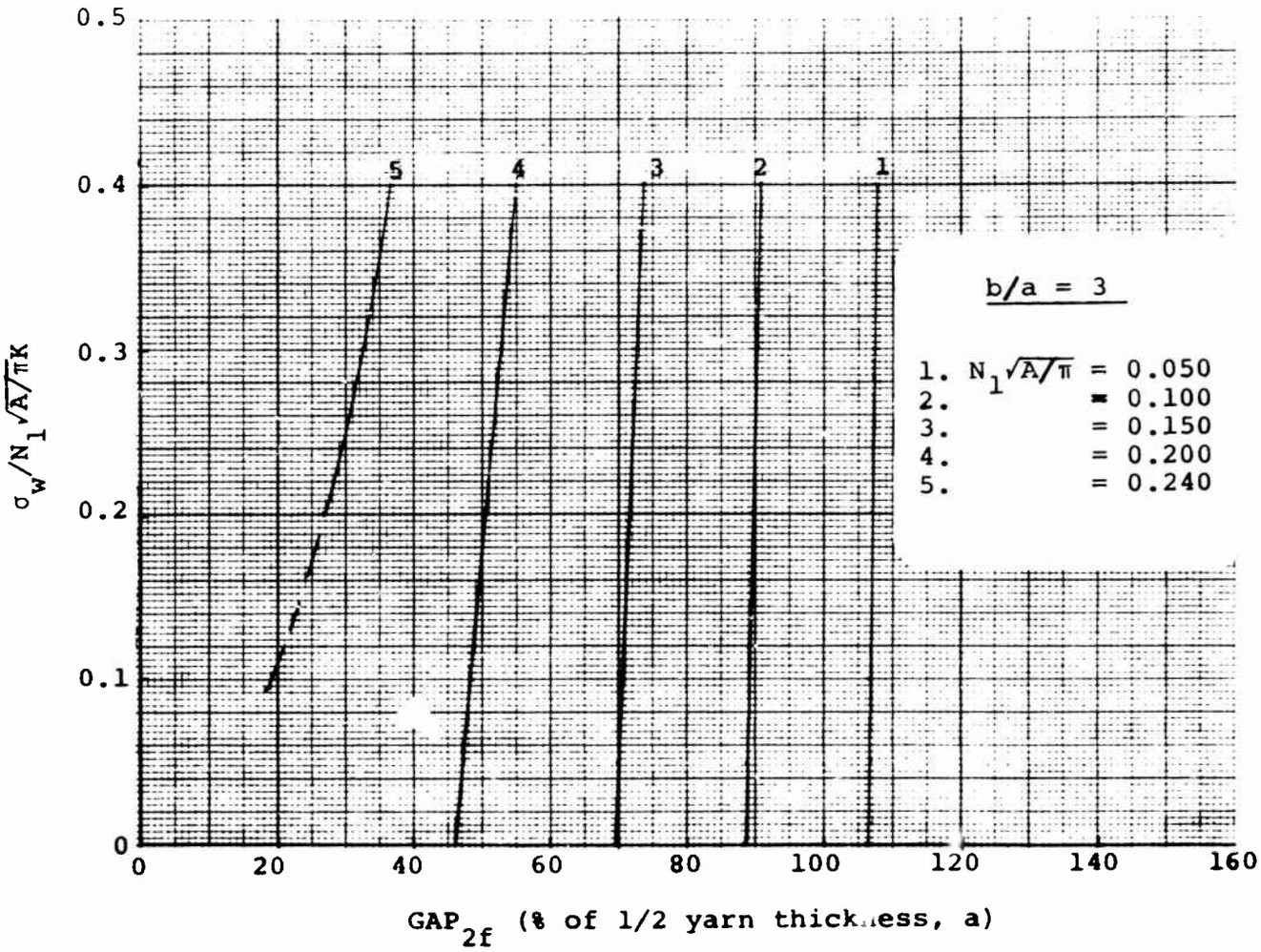

Figure 69(a). Radial Separation Between the Crossing Warp Yarn and the Node of the Filling Cross-Section (Aspect Ratio = 3): Linearly Elastic Yarn, $\sigma_w/\sigma_f = 2$

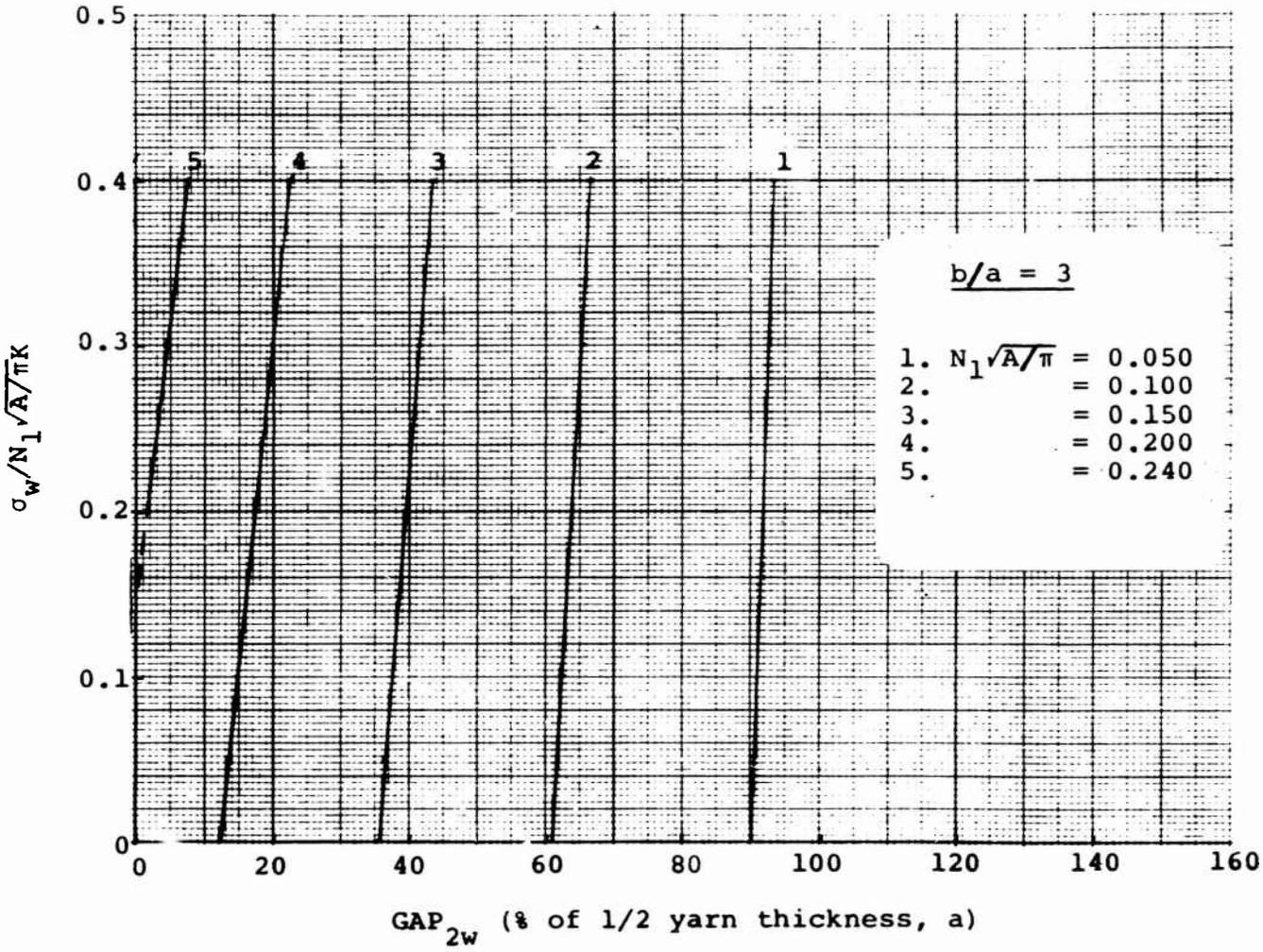

Figure 69(b). Radial Separation Between the Crossing Filling Yarn and the Node of the Warp Cross-Section (Aspect Ratio = 3): Linearly Elastic Yarn, $\sigma_w/\sigma_f = 2$

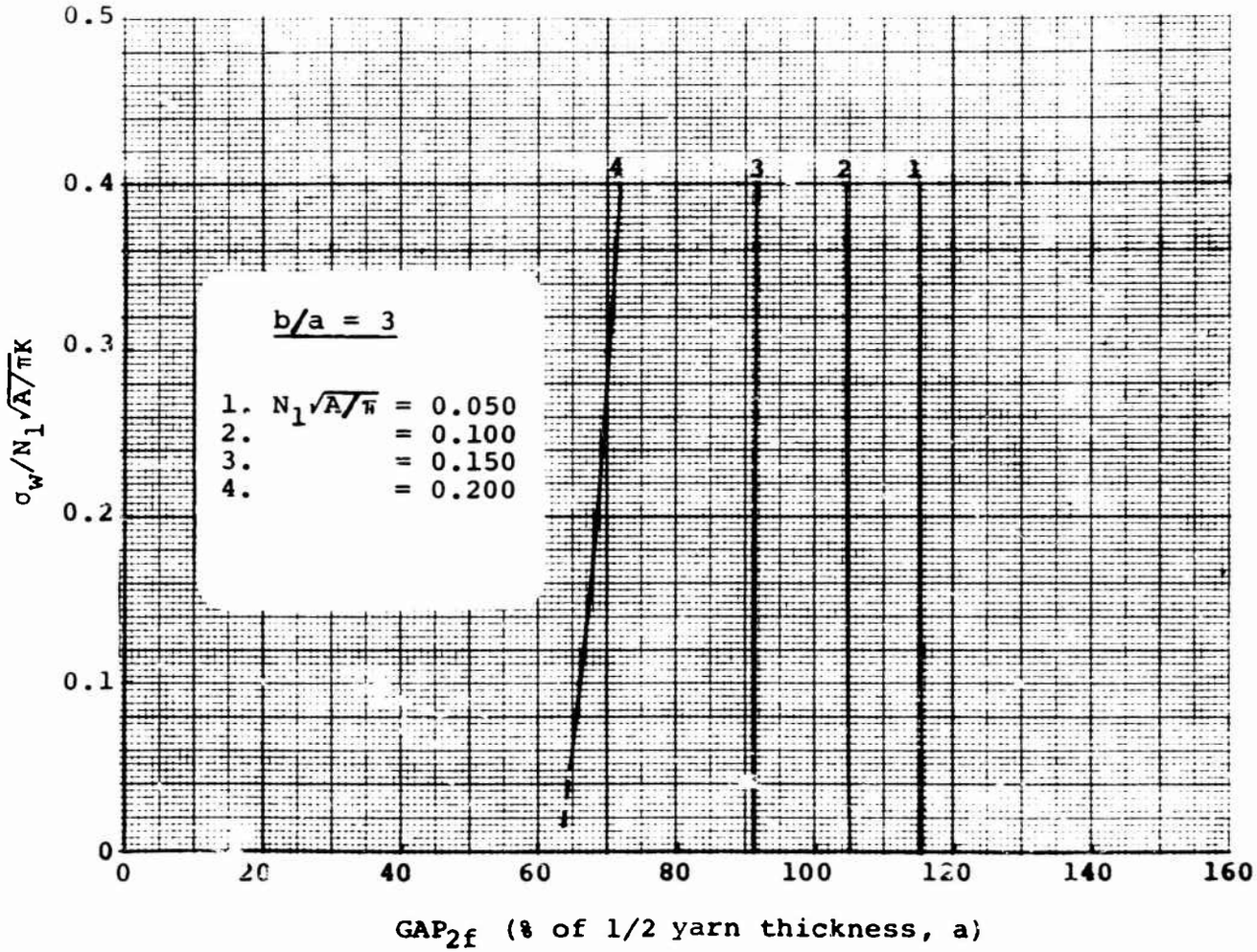

Figure 70(a). Radial Separation Between the Crossing Warp Yarn and the Node of the Filling Cross-Section (Aspect Ratio = 3): Linearly Elastic Yarn, $\sigma_w/\sigma_f = 5$

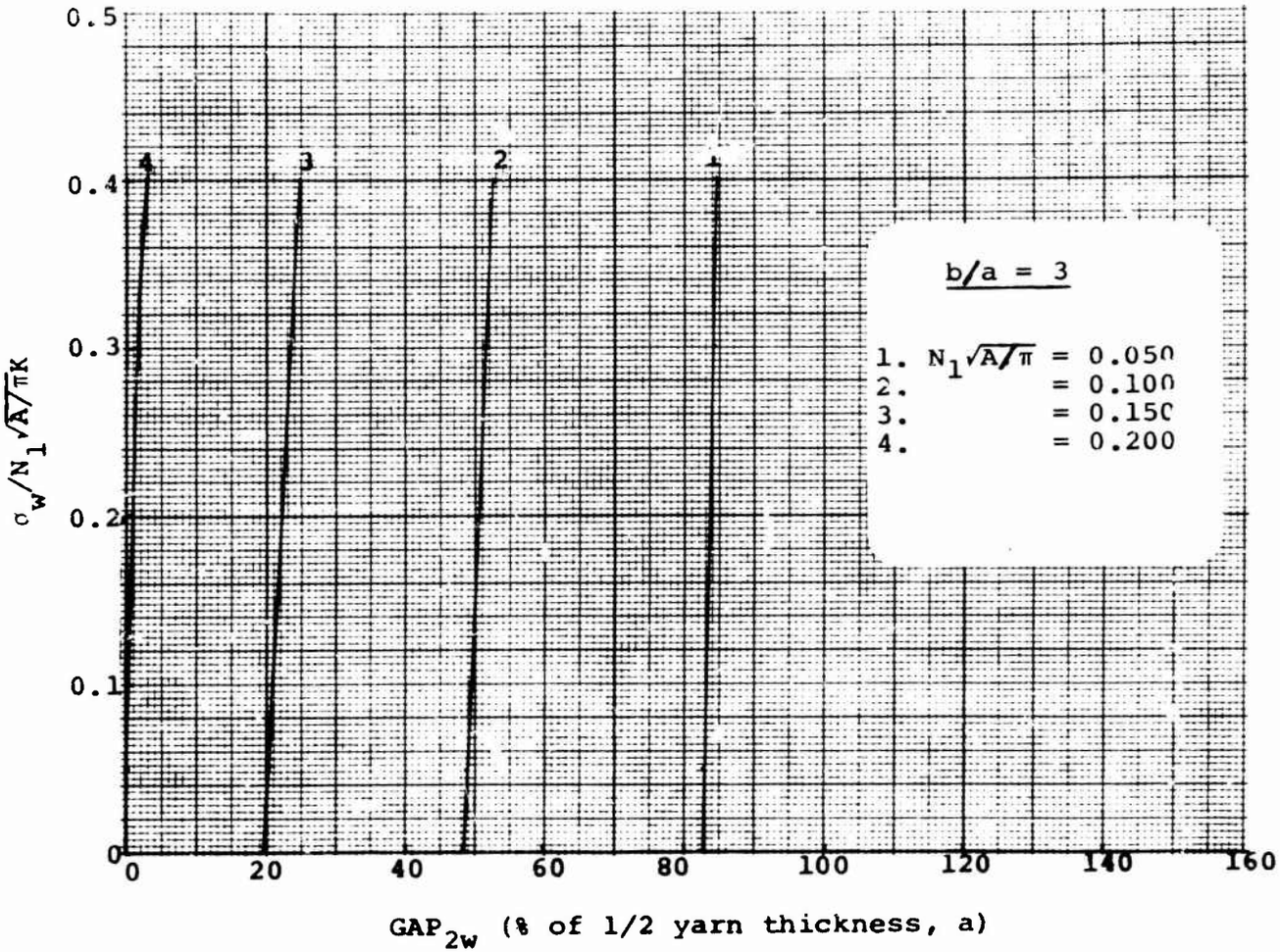

Figure 70(b). Radial Separation Between the Crossing Filling Yarn and the Node of the Warp Cross-Section (Aspect Ratio = 3): Linearly Elastic Yarn, $\sigma_w/\sigma_f = 5$

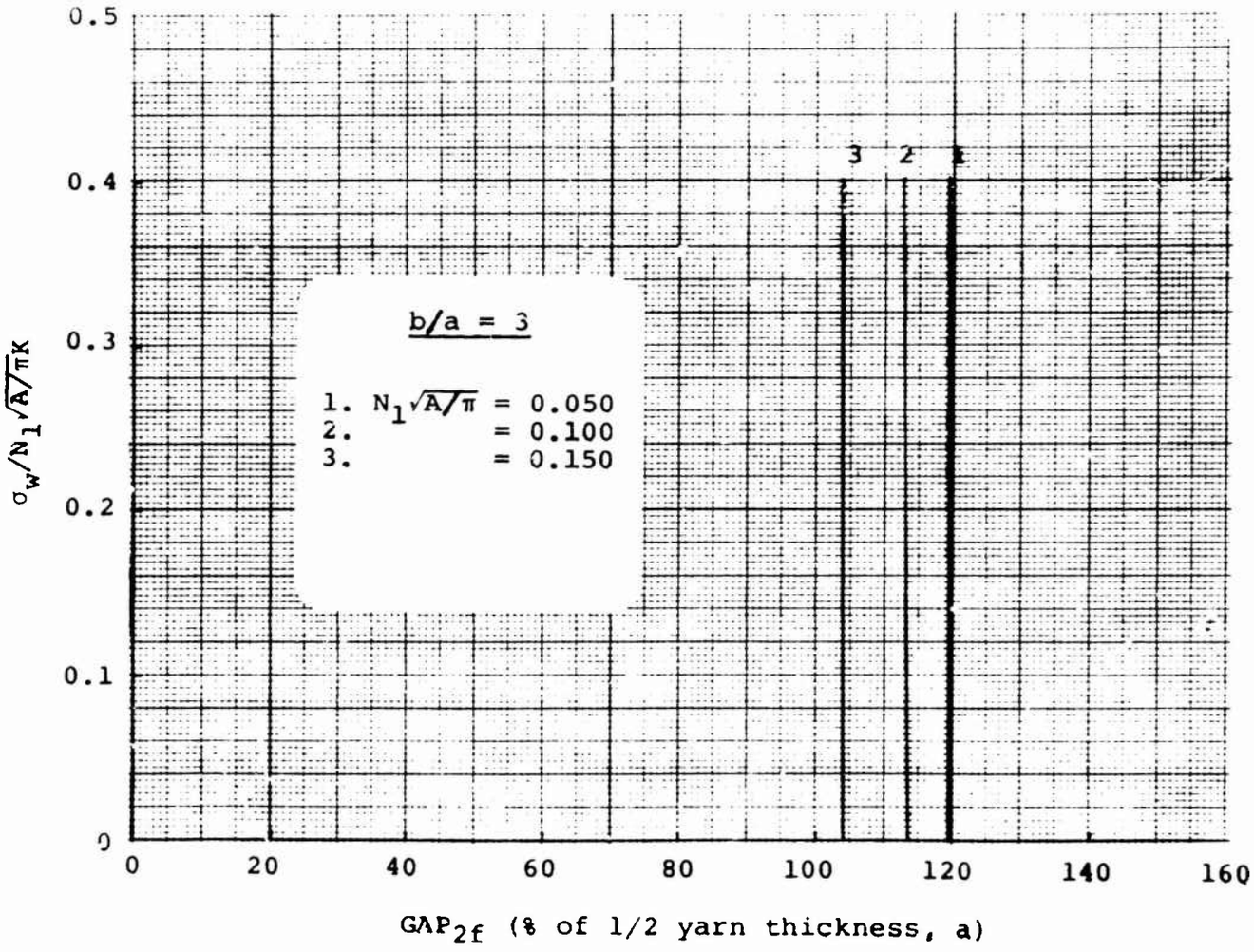

Figure 71(a). Radial Separation Between the Crossing Warp Yarn and the Node of the Filling Cross-Section (Aspect Ratio = 3): Linearly Elastic Yarn, σ_w/σ_f = 10

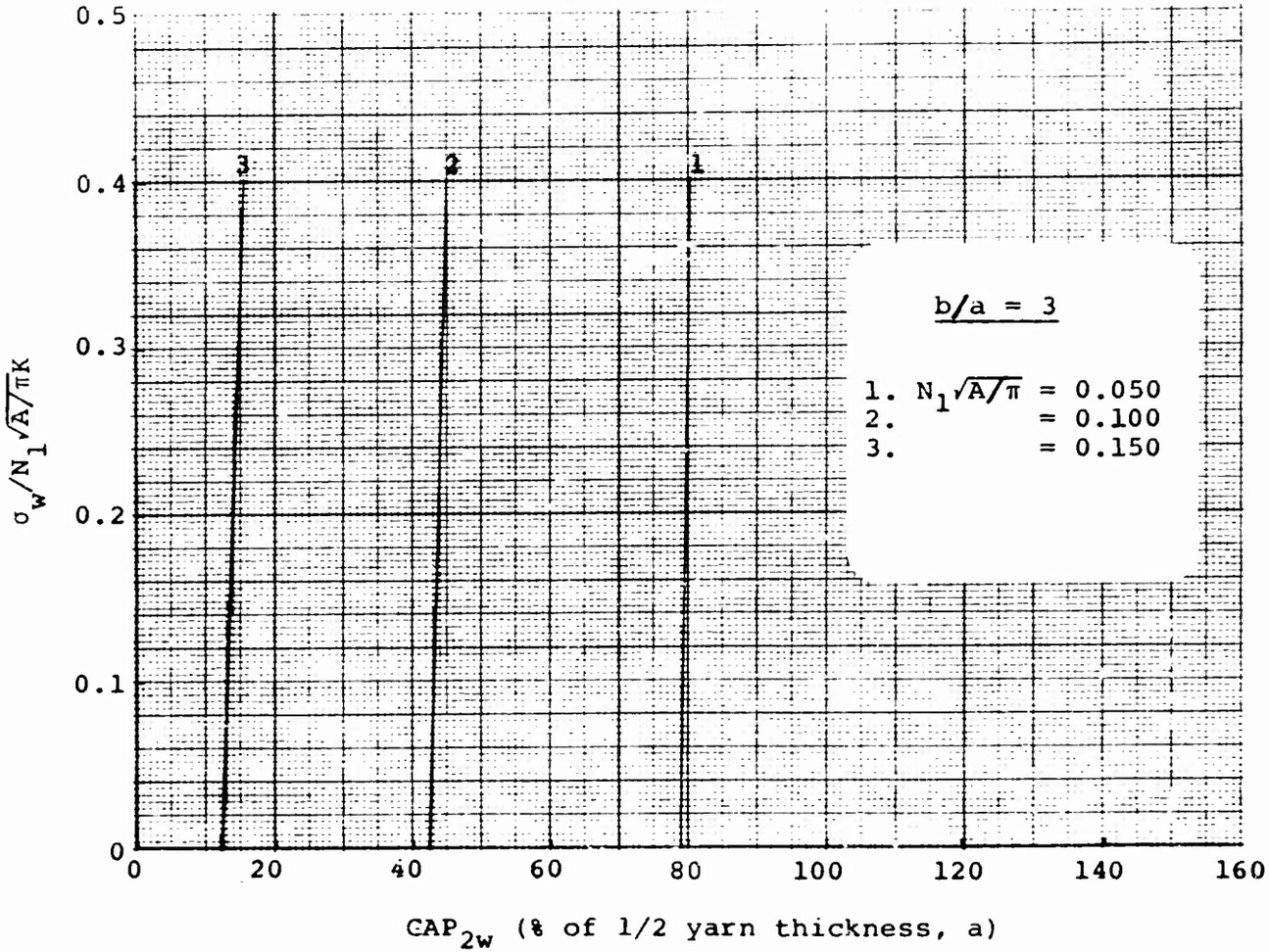

Figure 71(b). Radial Separation Between the Crossing Filling Yarn and the Node of the Warp Cross-Section (Aspect Ratio = 3): Linearly Elastic Yarn, σ_w/σ_f = 10

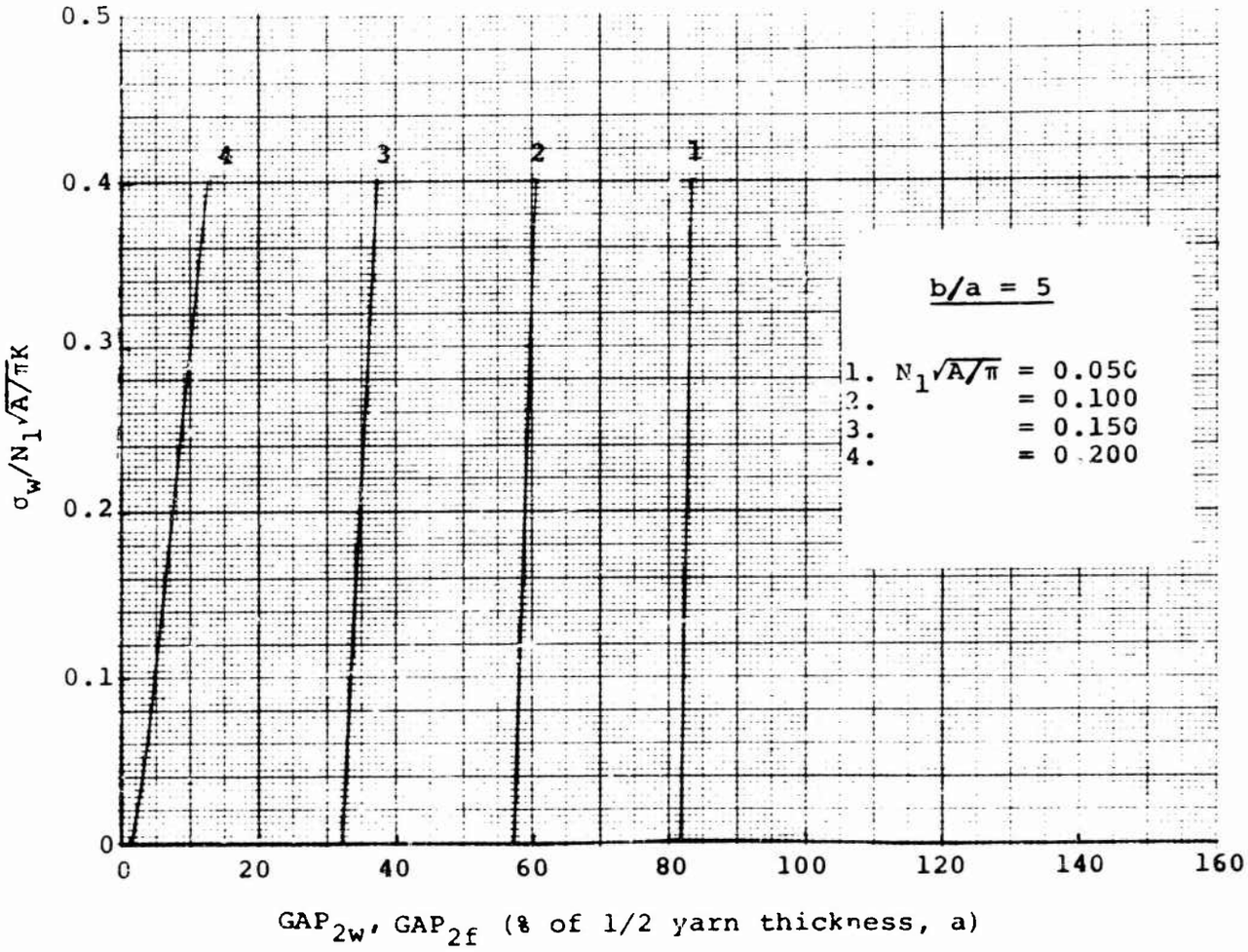

Figure 72. Radial Separation Between One Crossing Yarn and the Node of the Cross-Section of the Other Yarn (Aspect Ratio = 5), Linearly Elastic Yarn, $\sigma_w/\sigma_f = 1$

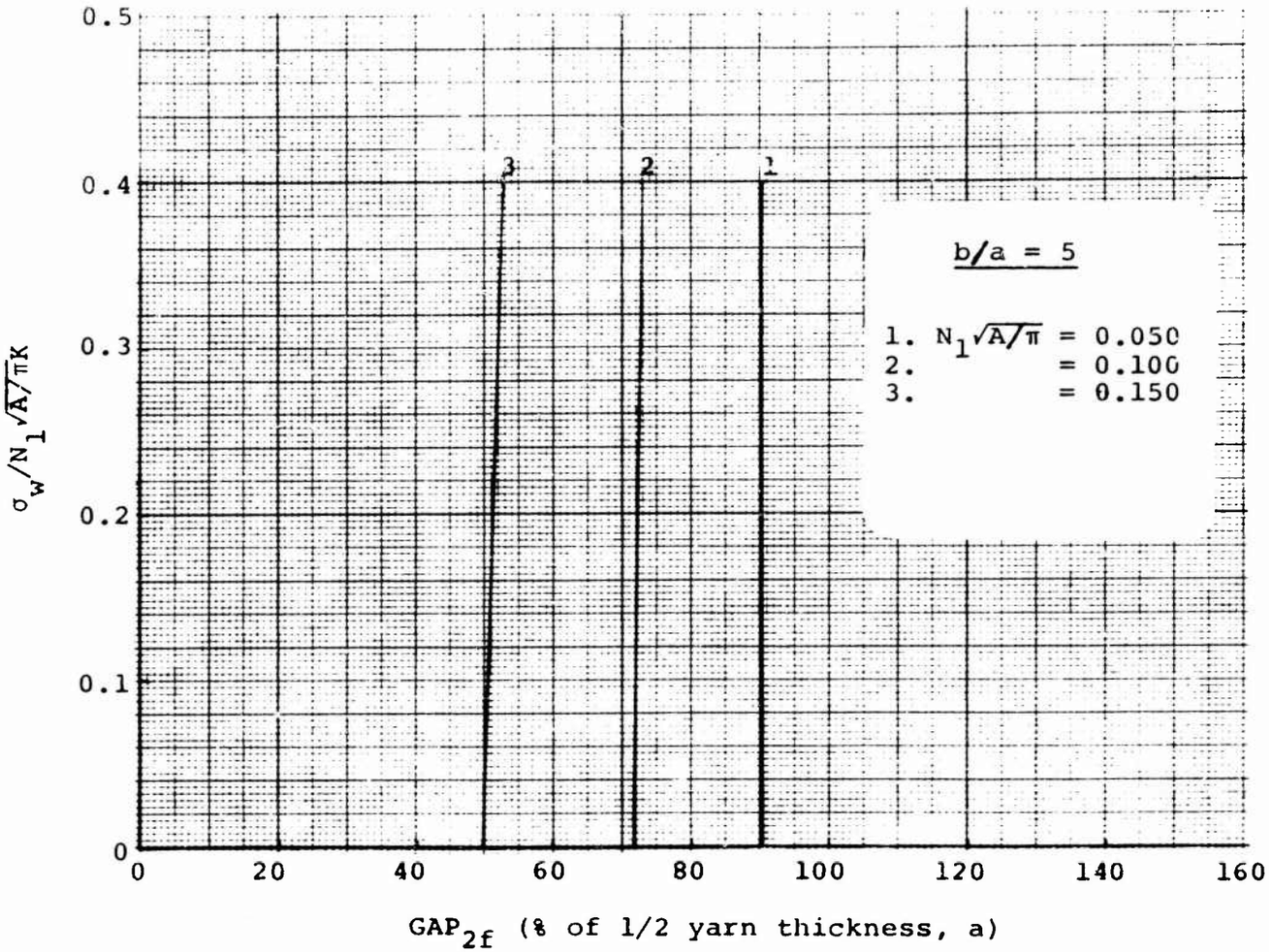

Figure 73(a). Radial Separation Between the Crossing Warp Yarn and the Node of the Filling Cross-Section (Aspect Ratio = 5): Linearly Elastic Yarn, $\sigma_w/\sigma_f = 2$

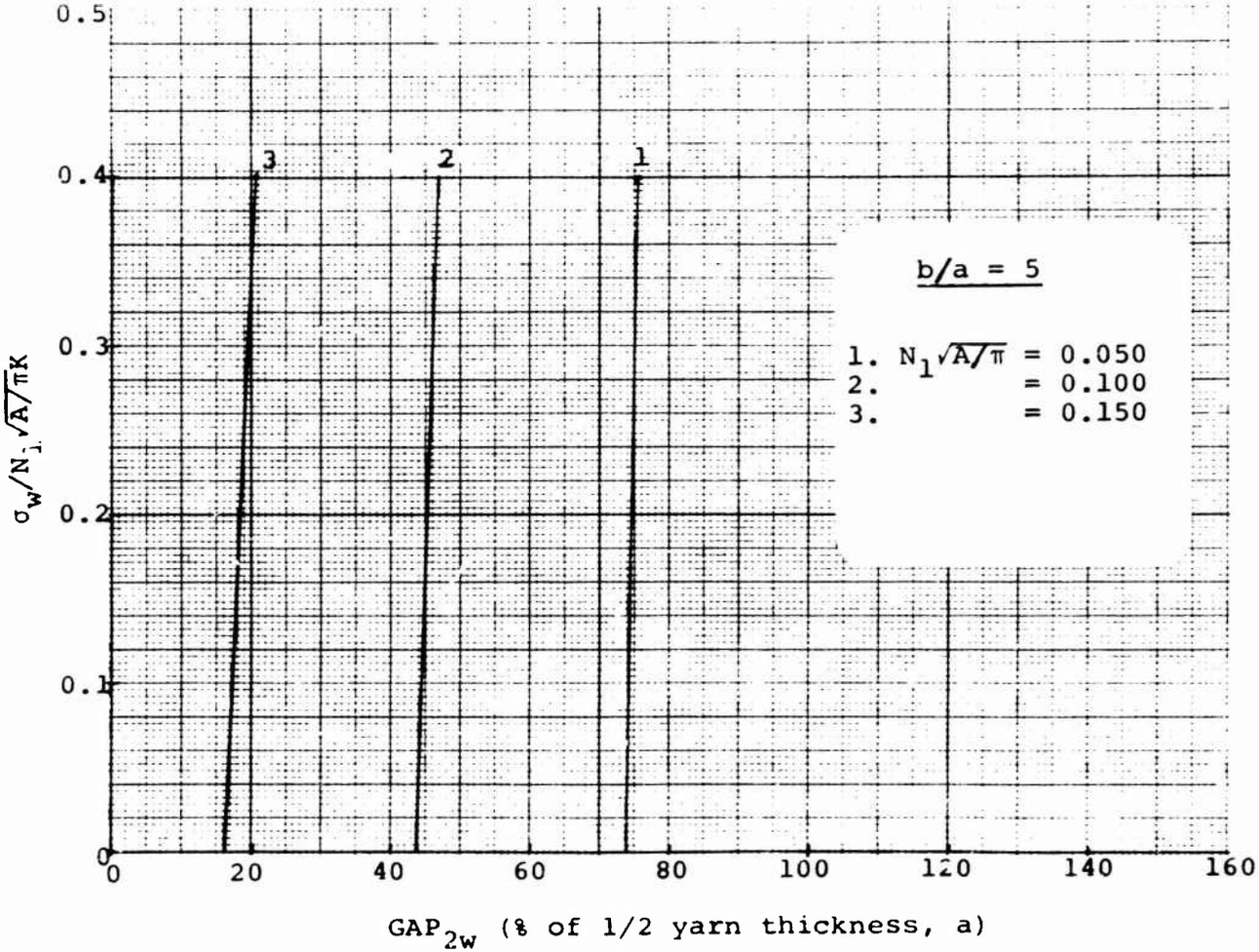

Figure 73(b). Radial Separation Between the Crossing Filling Yarn and the Node of the Warp Cross-Section (Aspect Ratio = 5): Linearly Elastic Yarn, $\sigma_w/\sigma_f = 2$

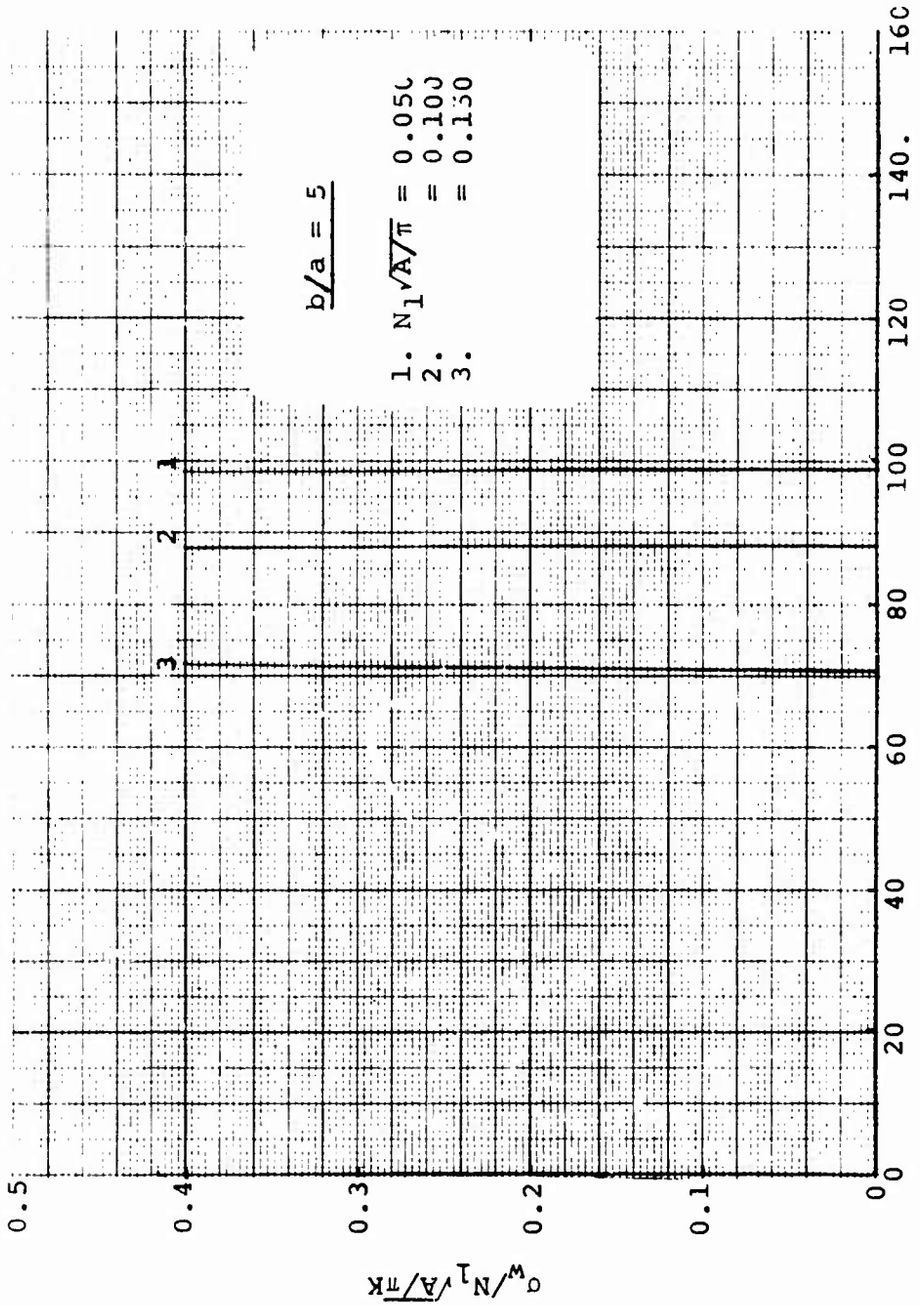

Figure 74(a). Radial Separation Between the Crossing Warp Yarn and the Node of the Filling Cross-Section (Aspect Ratio = 5): Linearly Elastic Yarn, $\sigma_w/\sigma_f = 5$

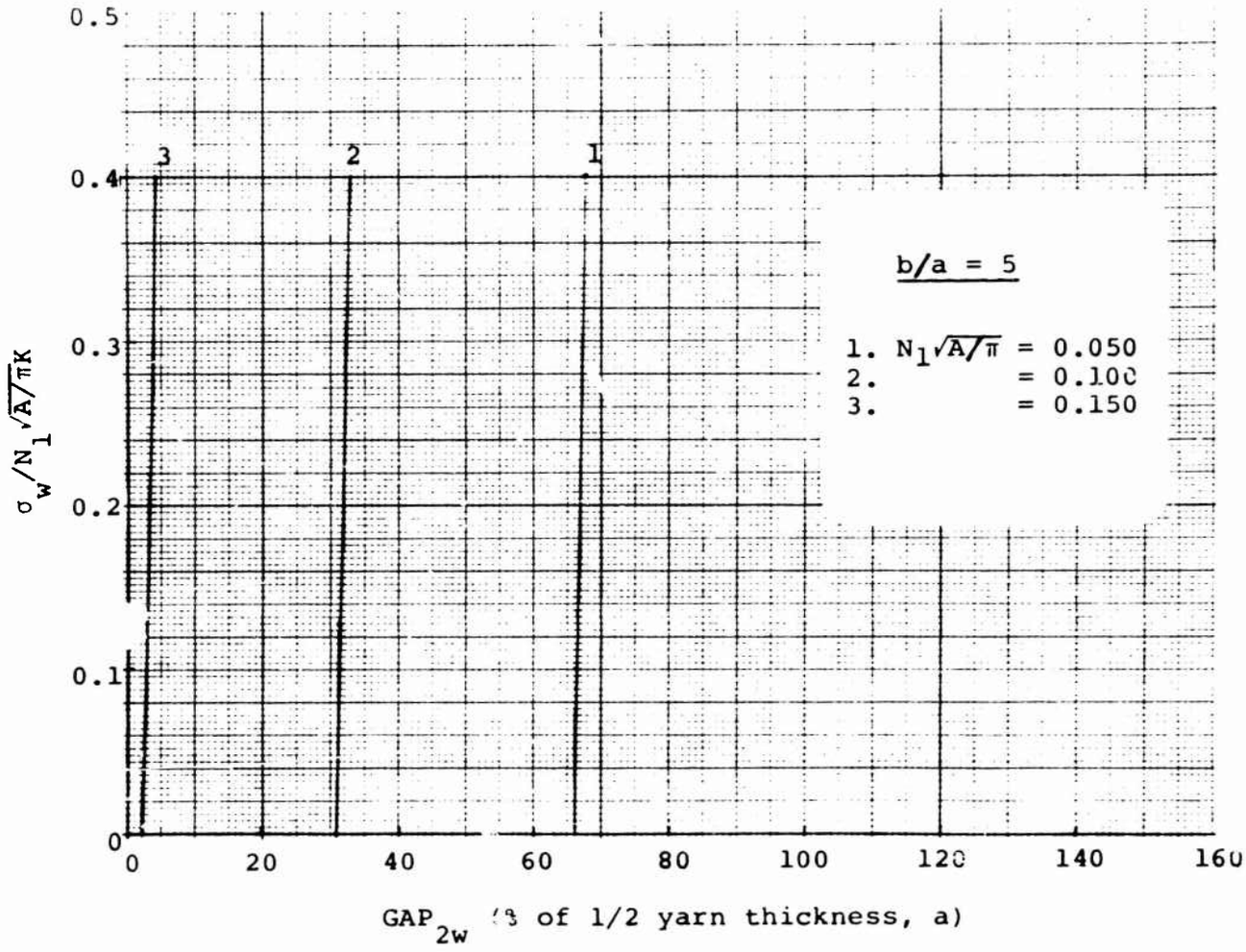

Figure 74(b). Radial Separation Between the Crossing Filling Yarn and the Node of the Warp Cross-Section (Aspect Ratio = 5): Linearly Elastic Yarn, $\sigma_w/\sigma_f = 5$

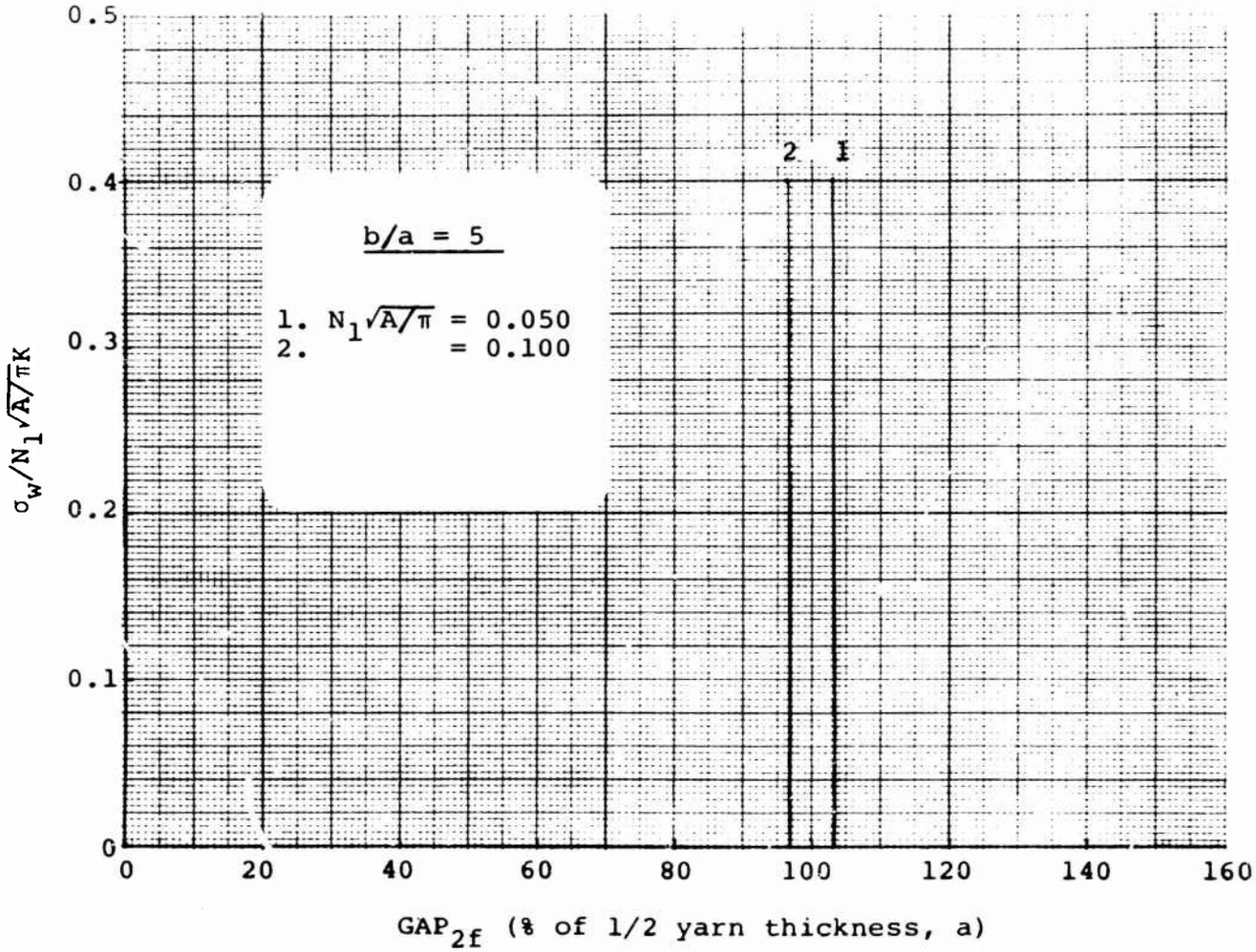

Figure 75(a). Radial Separation Between the Crossing Warp Yarn and the Node of the Filling Cross-Section (Aspect Ratio = 5): Linearly Elastic Yarn, σ_w/σ_f = 10

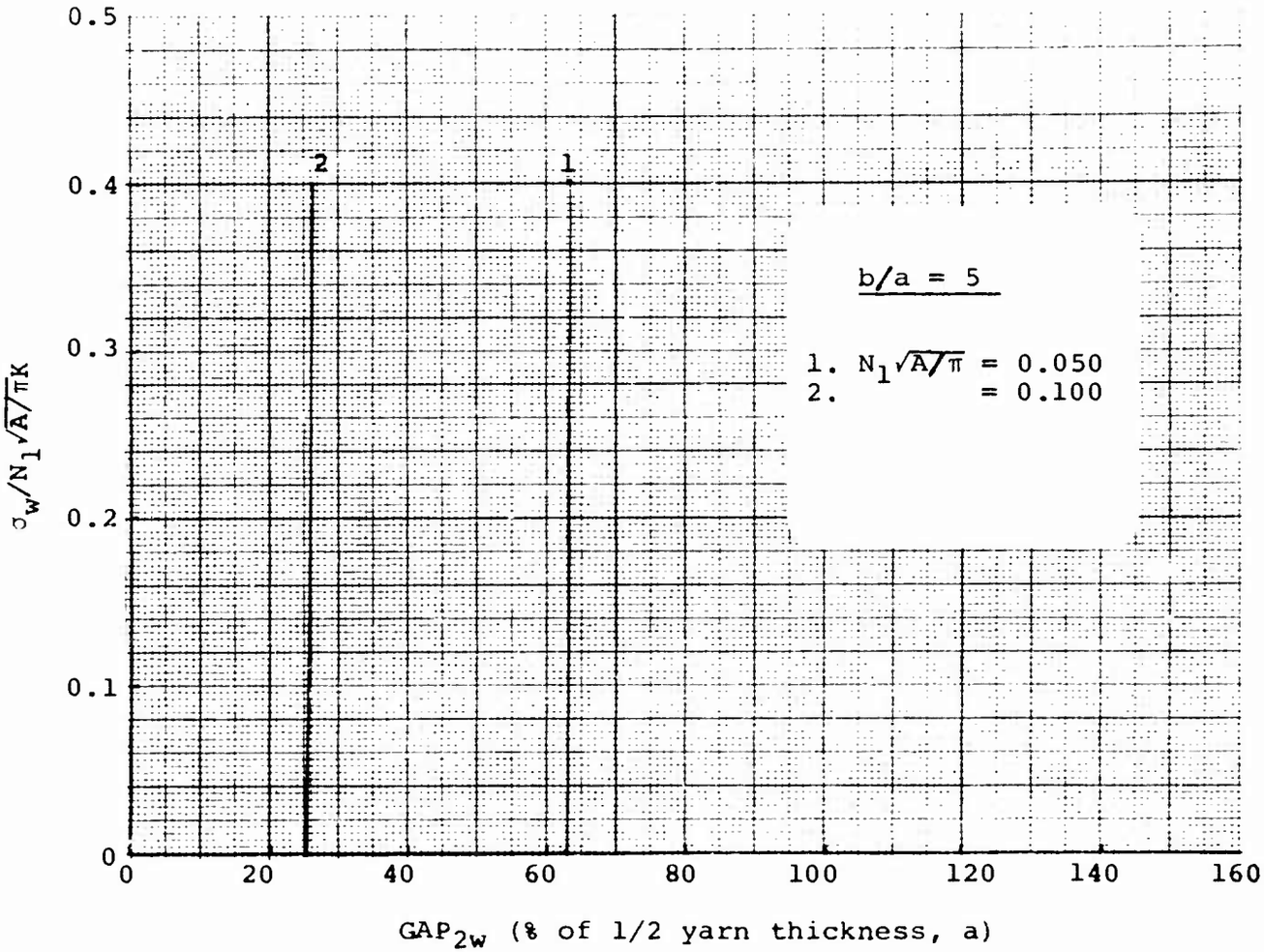

Figure 75(b). Radial Separation Between the Crossing Filling Yarn and the Node of the Warp Cross-Section (Aspect Ratio = 5): Linearly Elastic Yarn, σ_w/σ_f = 10

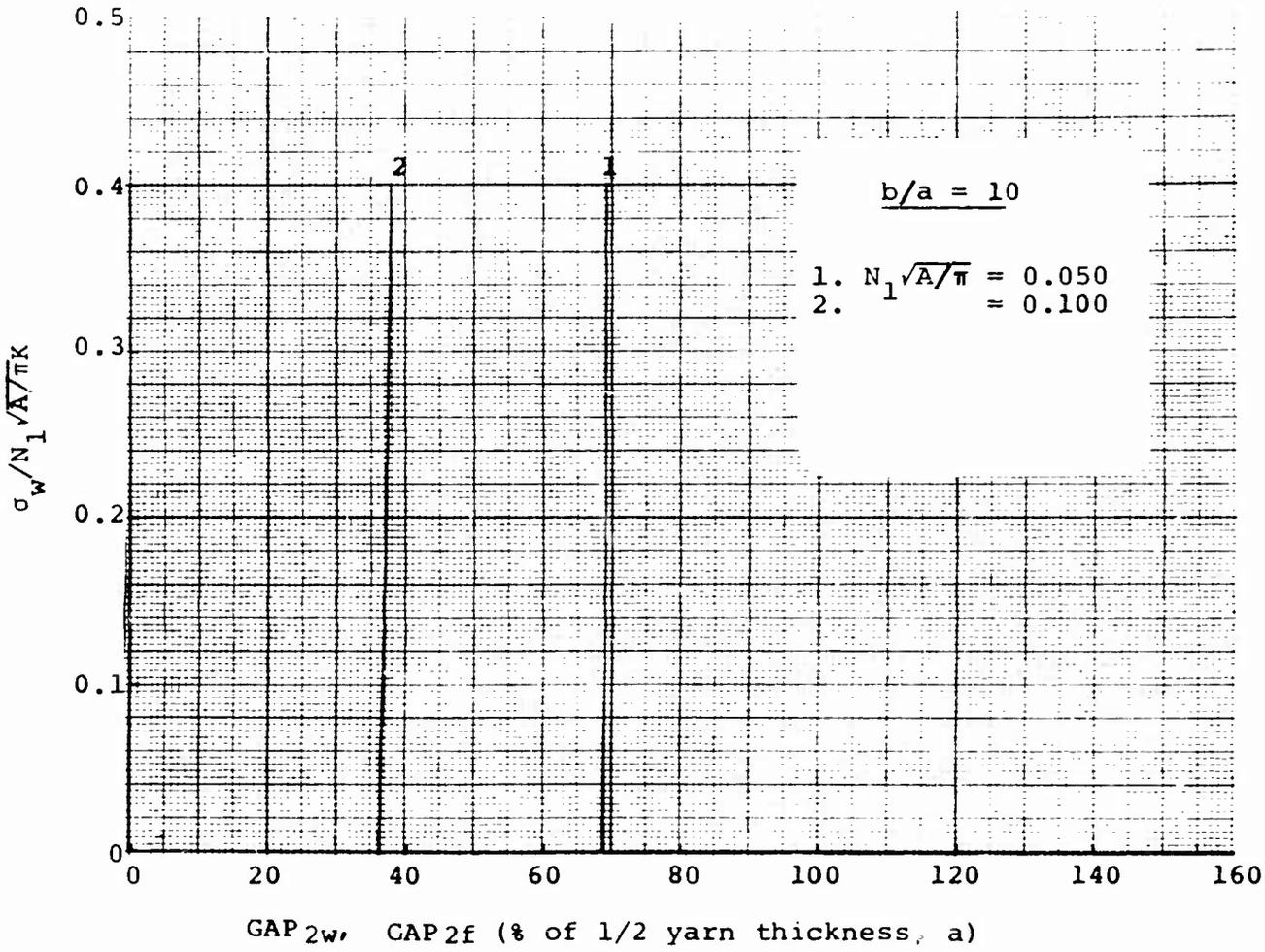

Figure 76. Radial Separation Between One Crossing Yarn and the Node of the Cross-Section of the Other Yarn (Aspect Ratio = 10): Linearly Elastic Yarn $\sigma_w/\sigma_f = 1$

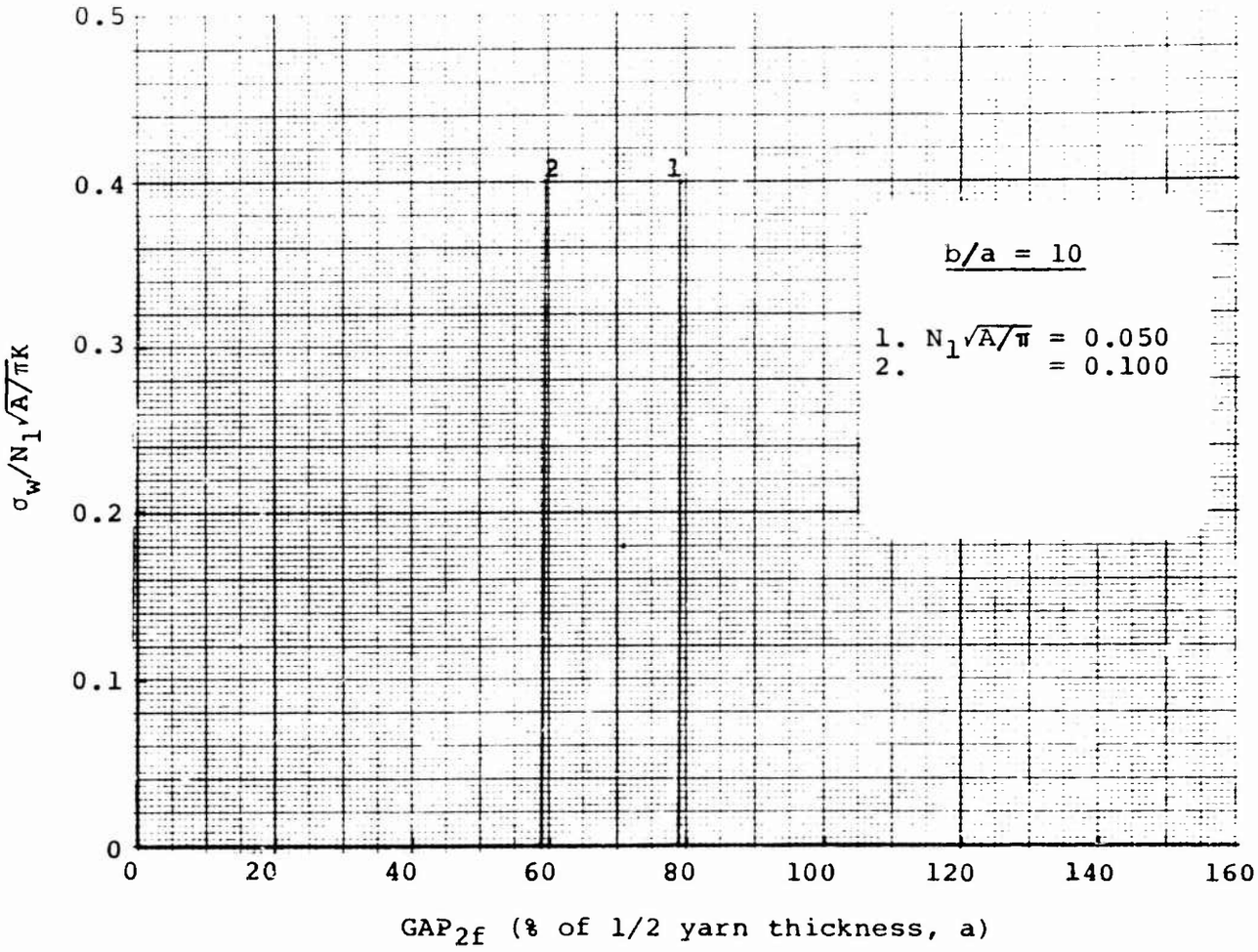

Figure 77(a). Radial Separation Between the Crossing Warp Yarn and the Node of the Filling Cross-Section (Aspect Ratio = 10): Linearly Elastic Yarn, $\sigma_w/\sigma_f = 2$

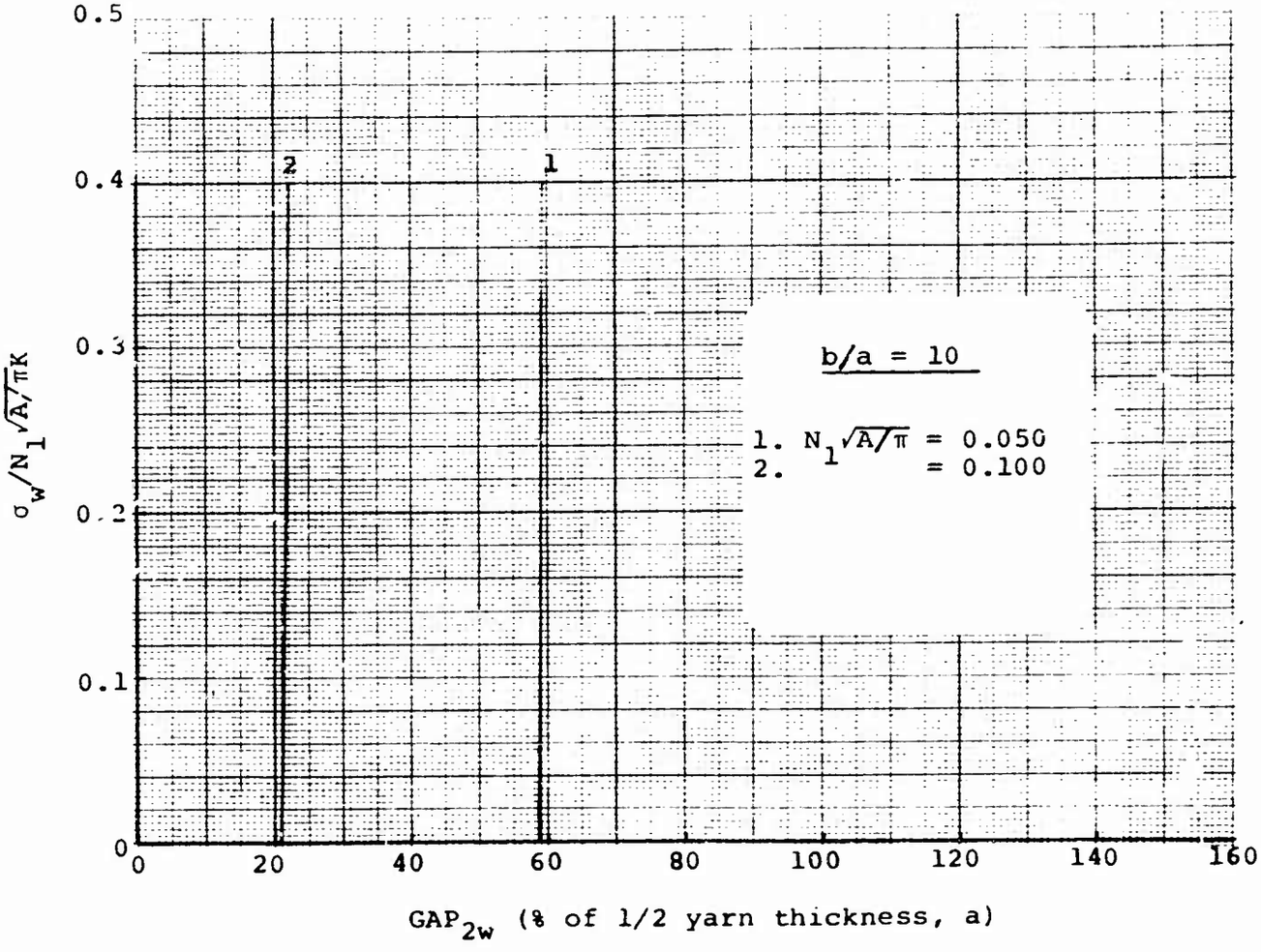

Figure 77(b). Radial Separation Between the Crossing Filling Yarn and the Node of the Warp Cross-Section (Aspect Ratio = 10): Linearly Elastic Yarn. $\sigma_w/\sigma_f = 2$

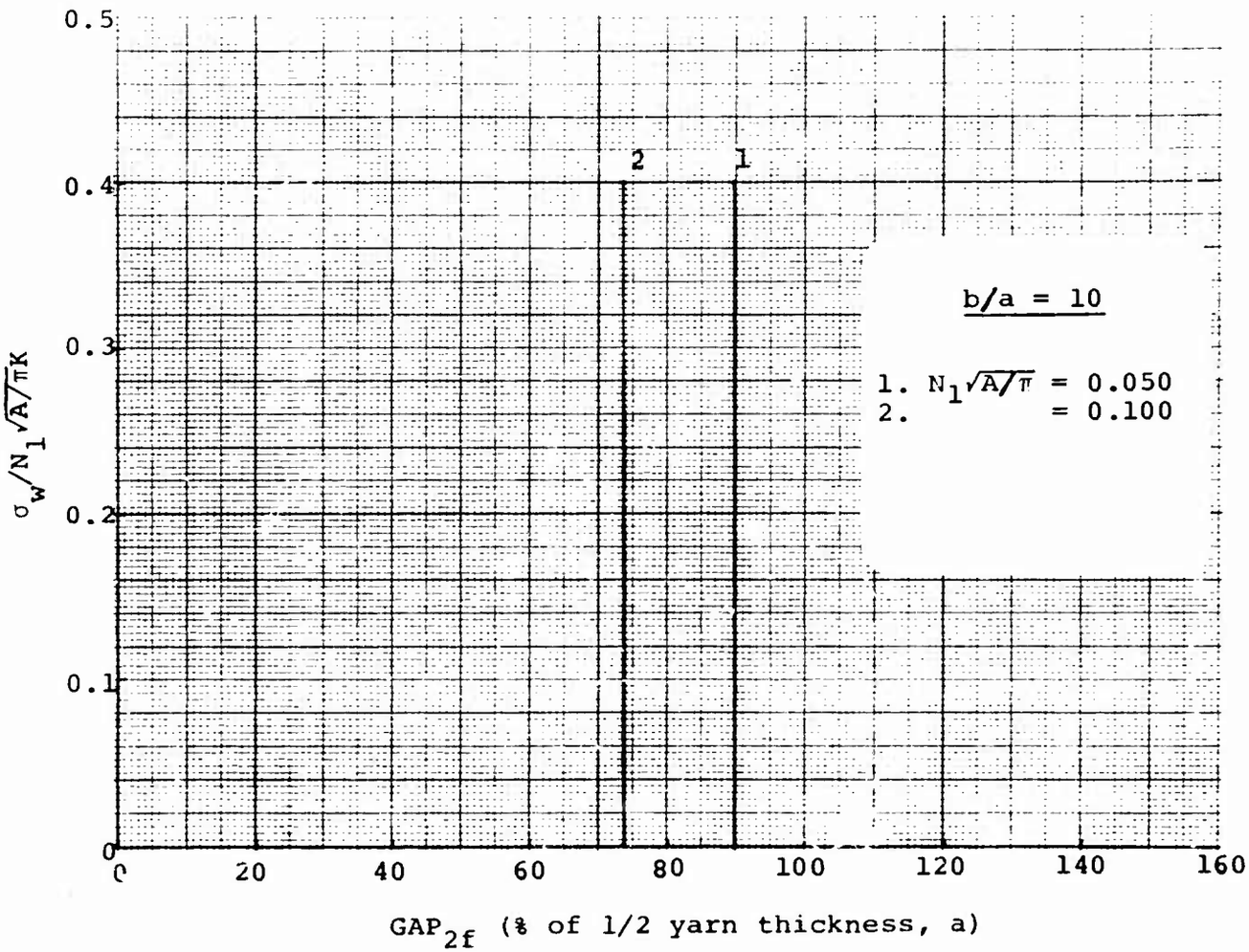

Figure 78(a). Radial Separation Between the Crossing Warp Yarn and the Node of the Filling Cross-Section (Aspect Ratio = 10): Linearly Elastic Yarn, σ_w/σ_f = 5

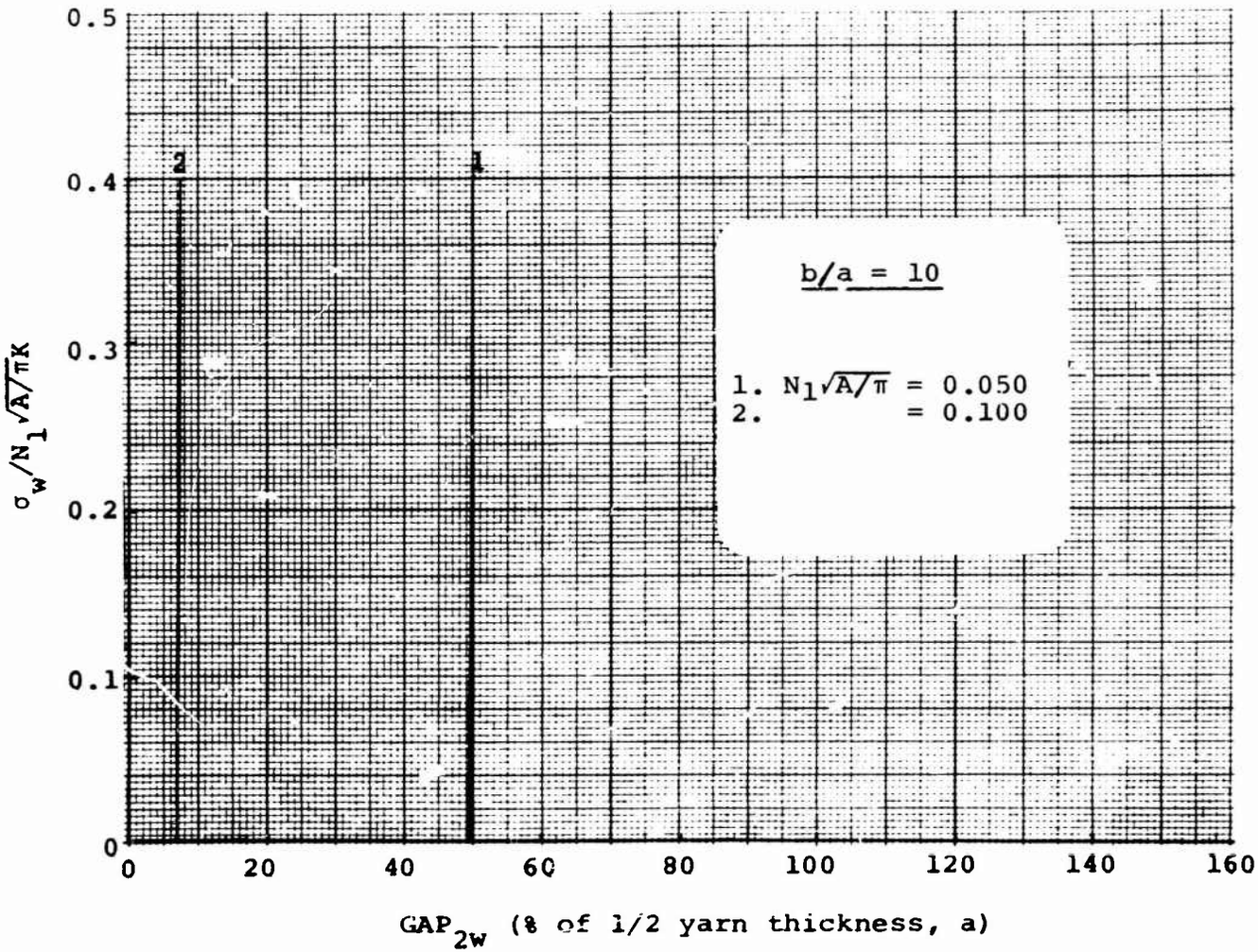

Figure 78(b). Radial Separation Between the Crossing Filling Yarn and the Node of the Warp Cross-Section (Aspect Ratio = 10): Linearly Elastic Yarn, $\sigma_w/\sigma_f = 5$

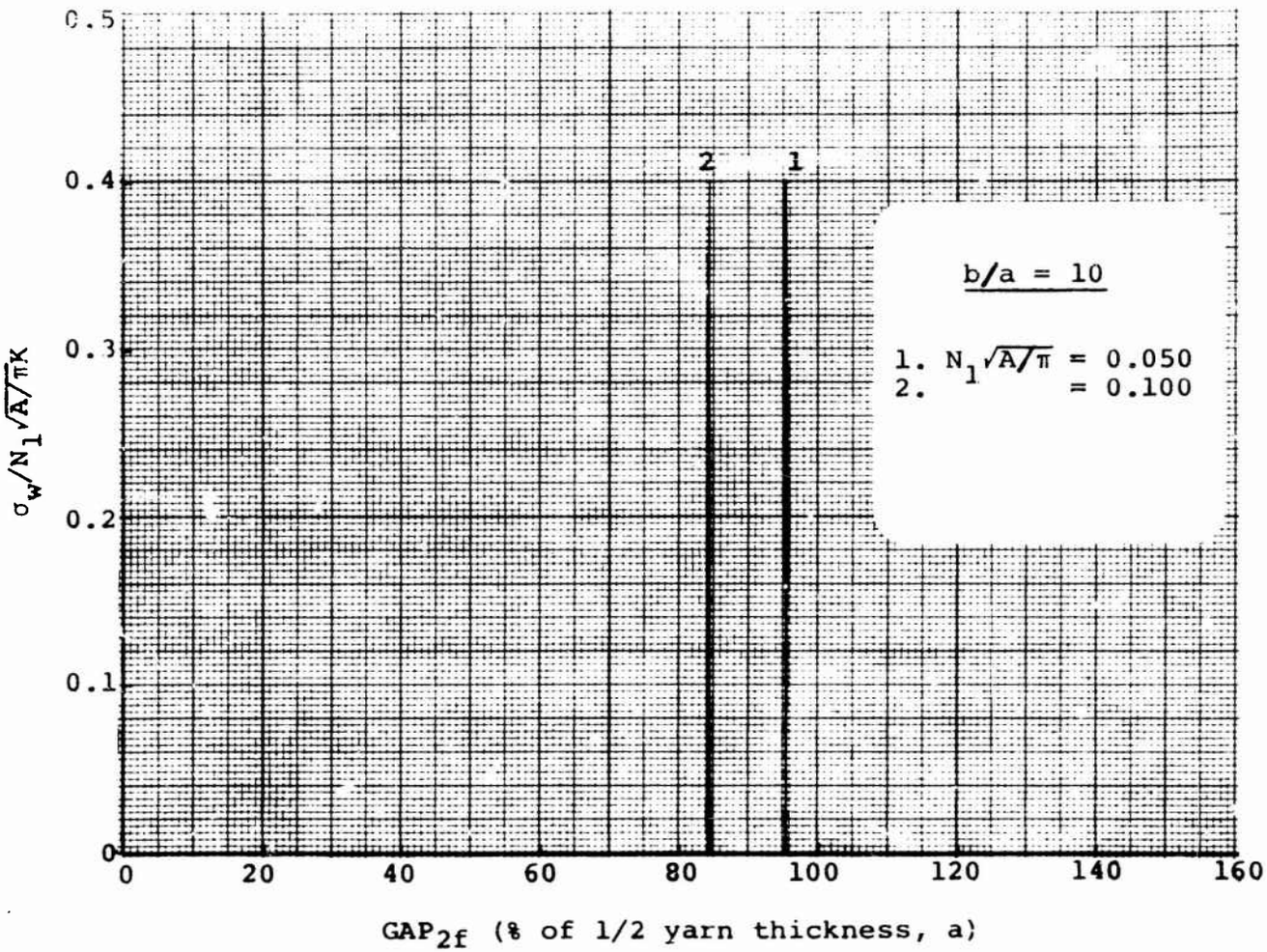

Figure 79(a). Radial Separation Between the Crossing Warp Yarn and the Node of the Filling Cross-Section (Aspect Ratio = 10): Linearly Elastic Yarn, $\sigma_w/\sigma_f \simeq 10$

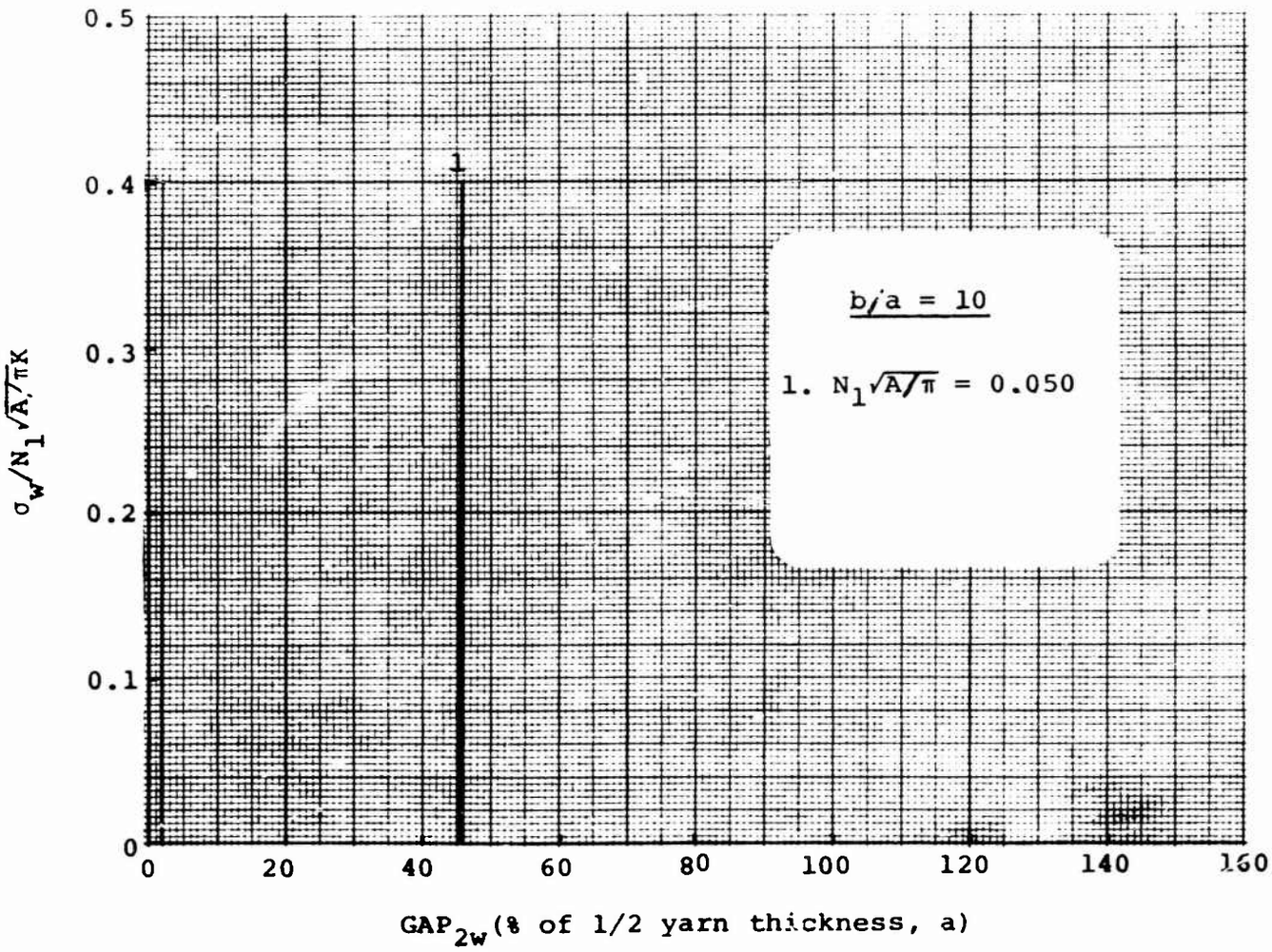

Figure 79(b). Radial Separation Between the Crossing Filling Yarn and the Node of the Warp Cross-Section (Aspect Ratio = 10): Linearly Elastic Yarn, $\sigma_w/\sigma_f = 10$

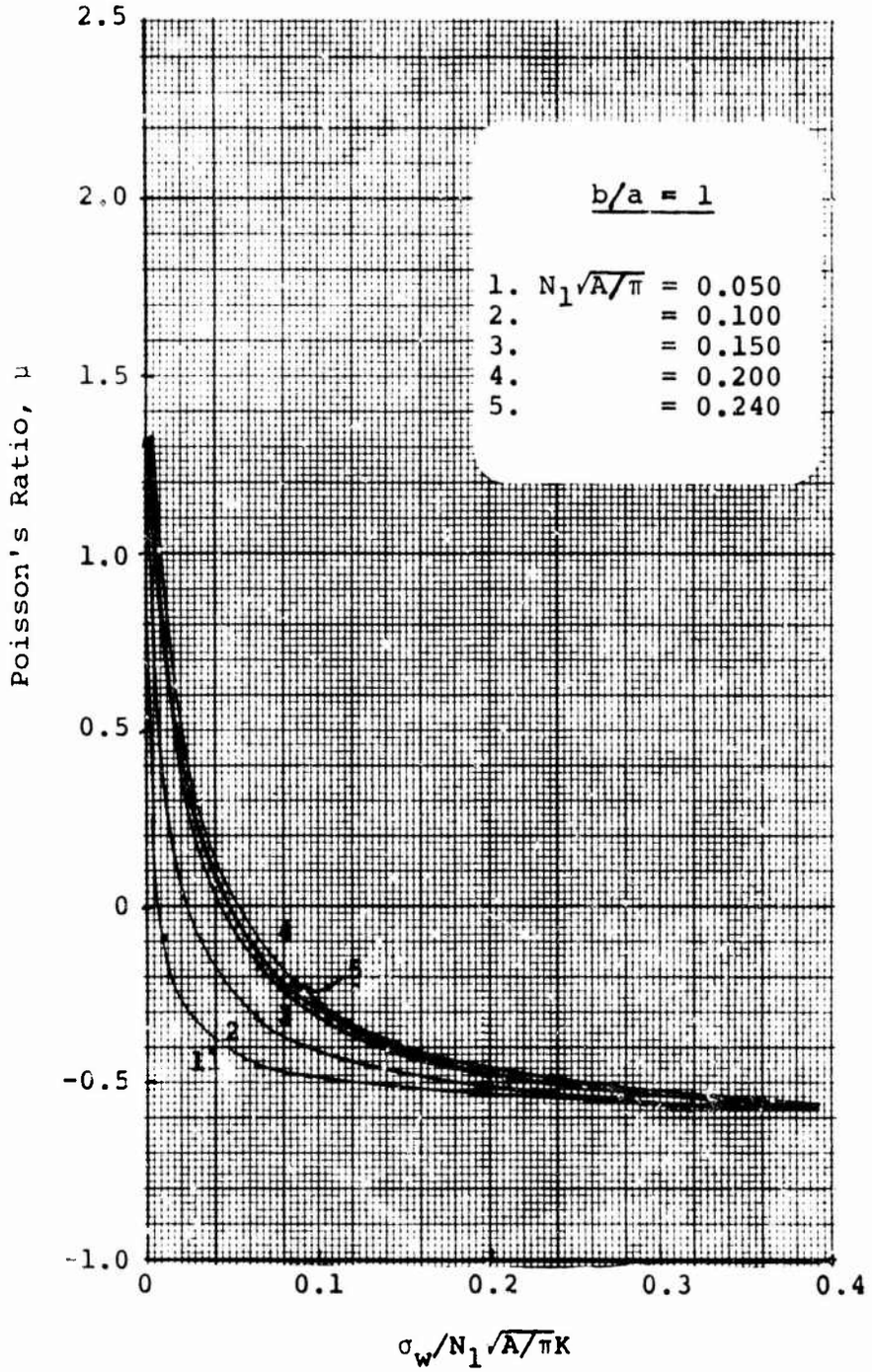

Figure 80. Poisson's Ratio (Aspect Ratio = 1): Linearly Elastic Yarn, $\sigma_w/\sigma_f = 2$

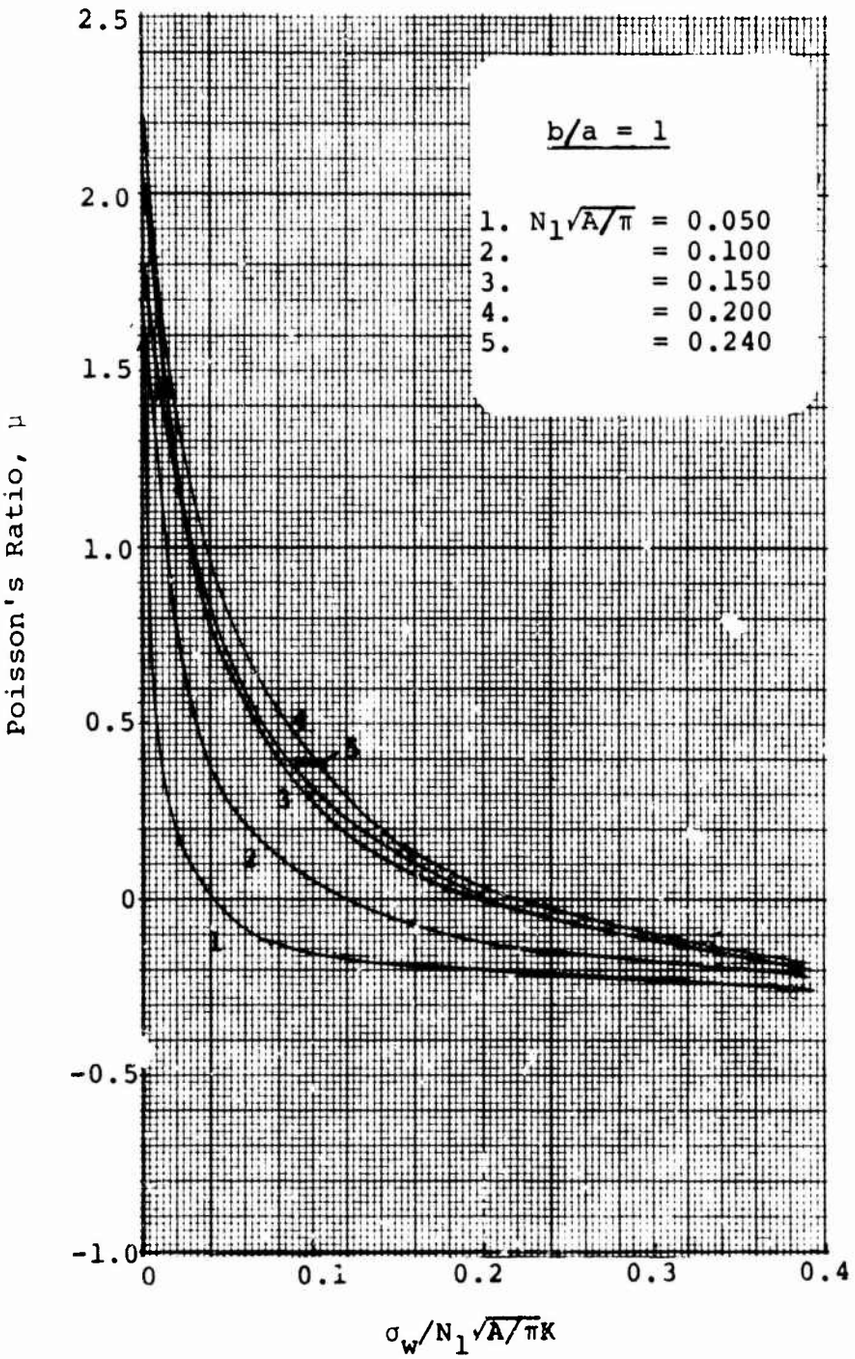

Figure 81. Poisson's Ratio (Aspect Ratio = 1): Linearly Elastic Yarn, $\sigma_w/\sigma_f = 5$

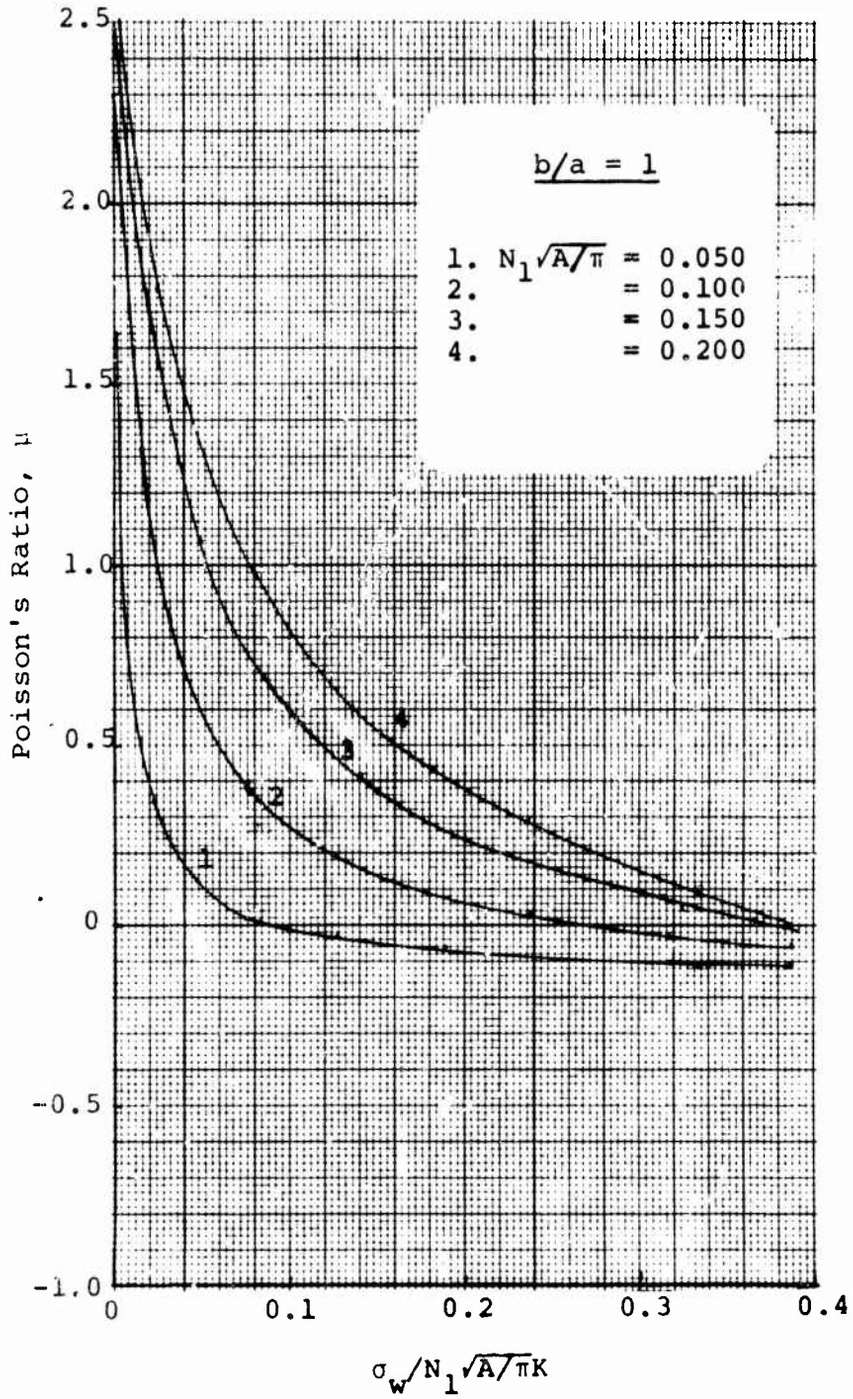

Figure 82. Poisson's Ratio (Aspect Ratio = 1): Linearly Elastic Yarn, $\sigma_w/\sigma_f = 10$

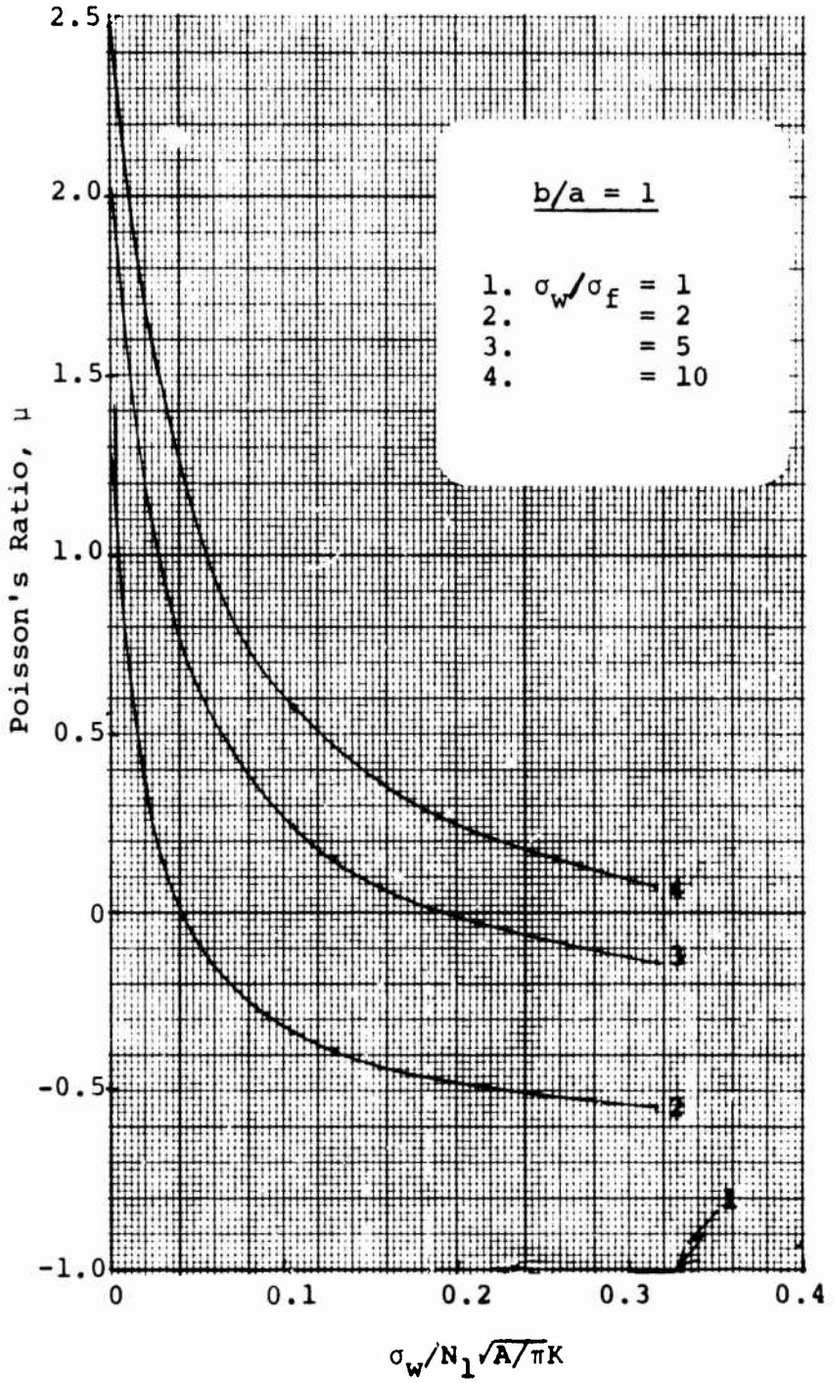

Figure 83. Poisson's Ratio (Aspect Ratio = 1): Linearly Elastic Yarn, $N_1\sqrt{A/\pi}$ = 0.15

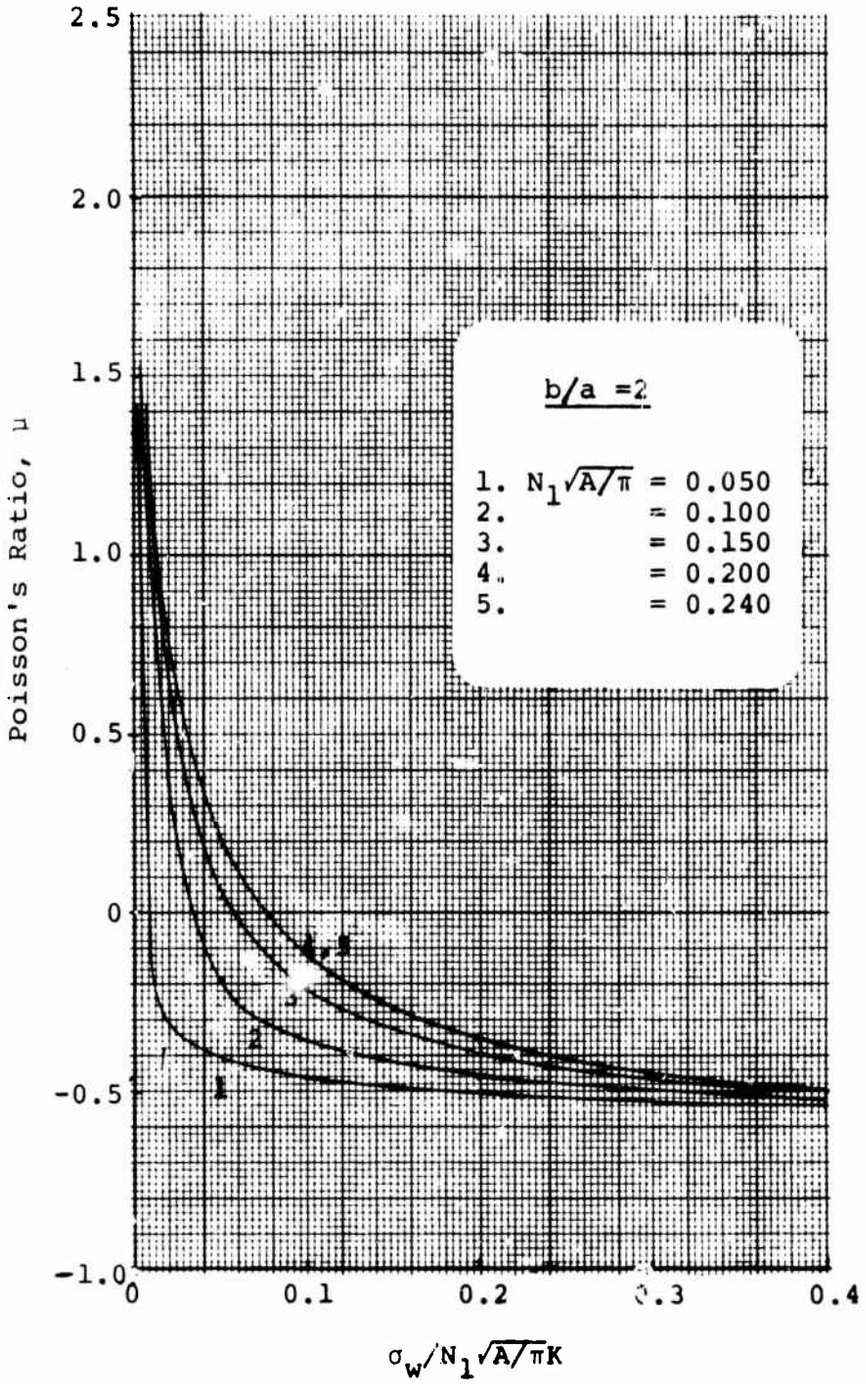

Figure 84. Poisson's Ratio (Aspect Ratio = 2): Linearly Elastic Yarn, $\sigma_w/\sigma_f = 2$

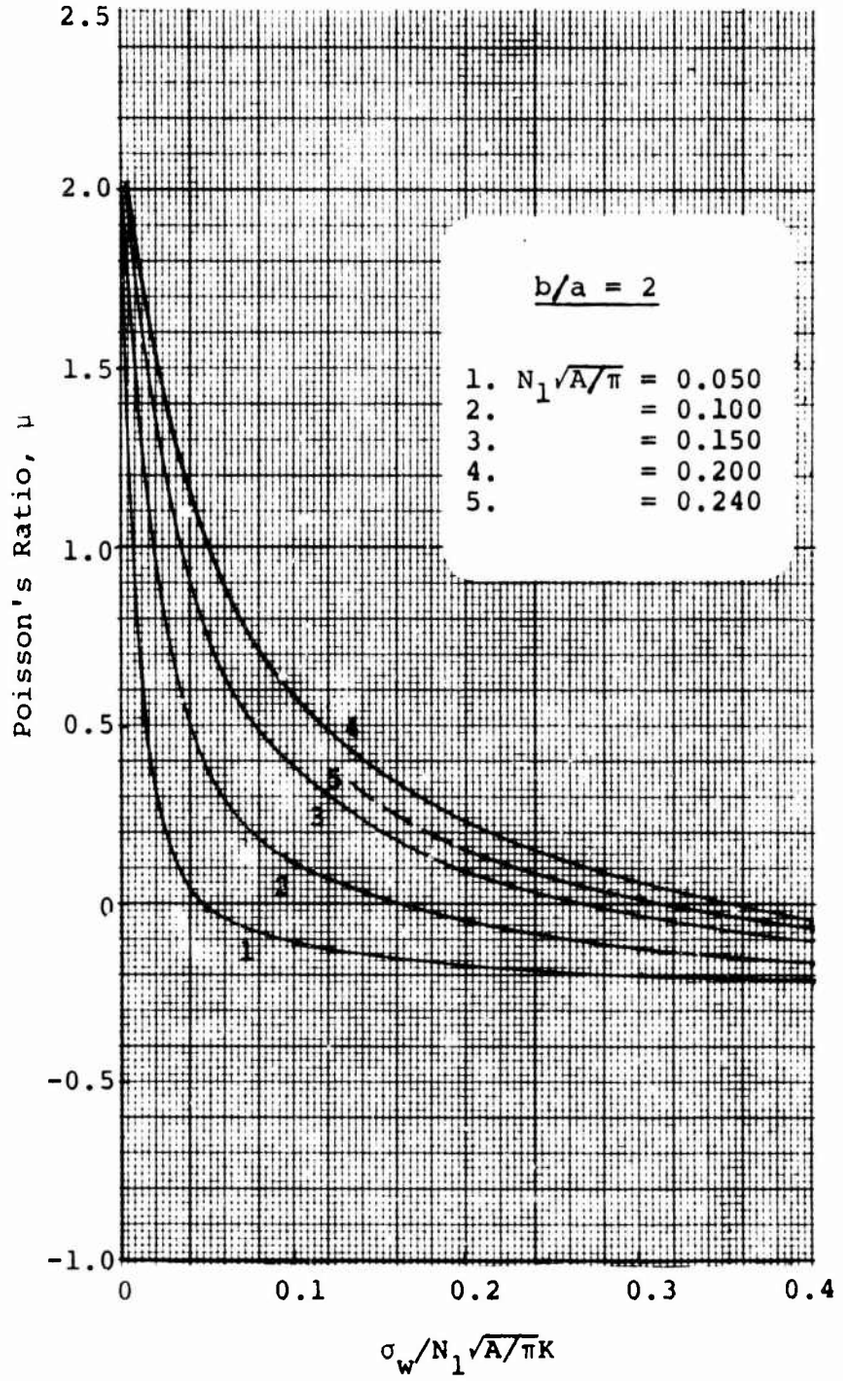

Figure 85. Poisson's Ratio (Aspect Ratio = 2): Linearly Elastic Yarn, $\sigma_w/\sigma_f = 5$

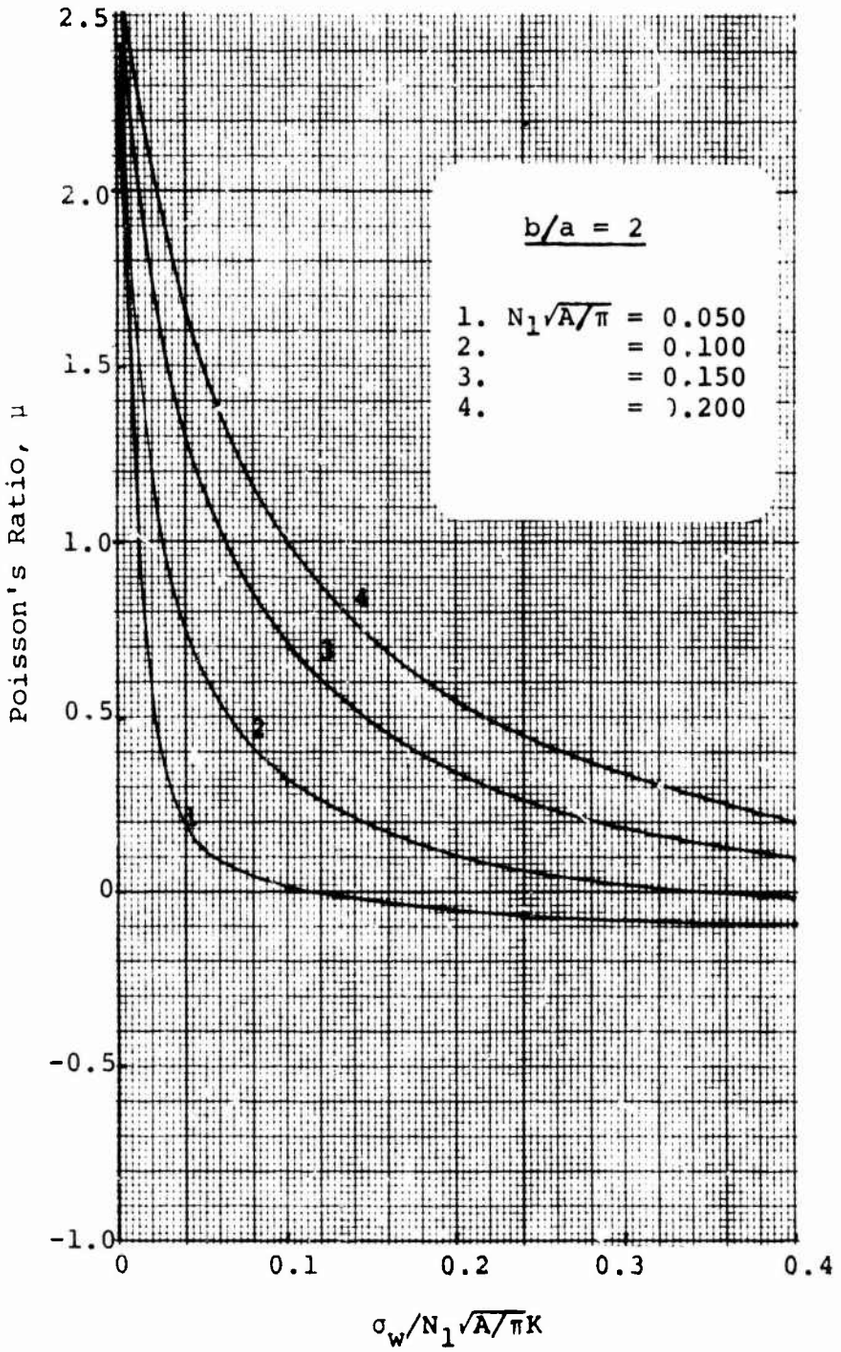

Figure 86. Poisson's Ratio (Aspect Ratio = 2): Linearly Elastic Yarn, $\sigma_w/\sigma_f = 10$

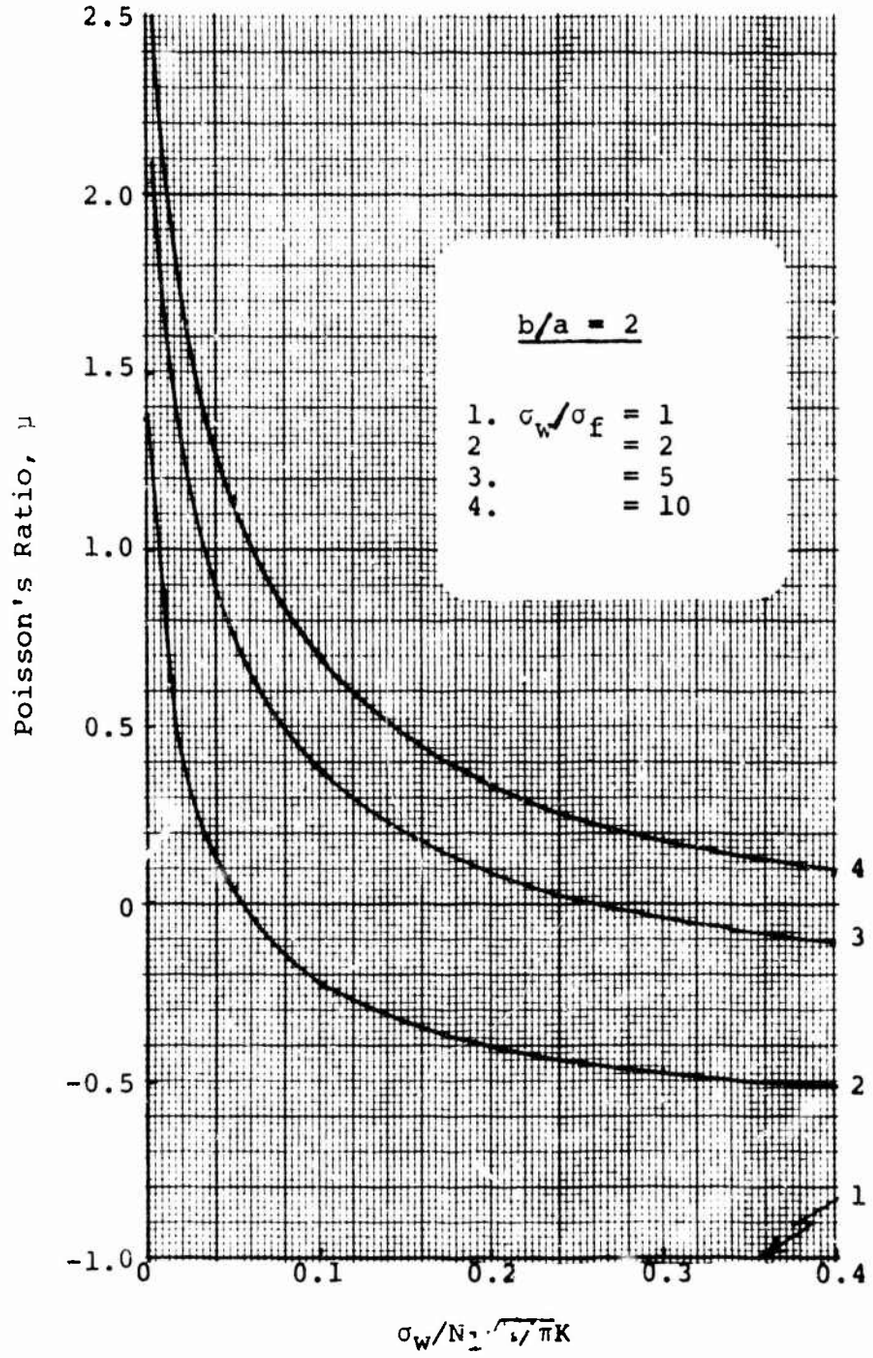

Figure 87. Poisson's Ratio (Aspect Ratio = 2): Linearly Elastic Yarn, $N_1\sqrt{A/\pi} = 0.15$

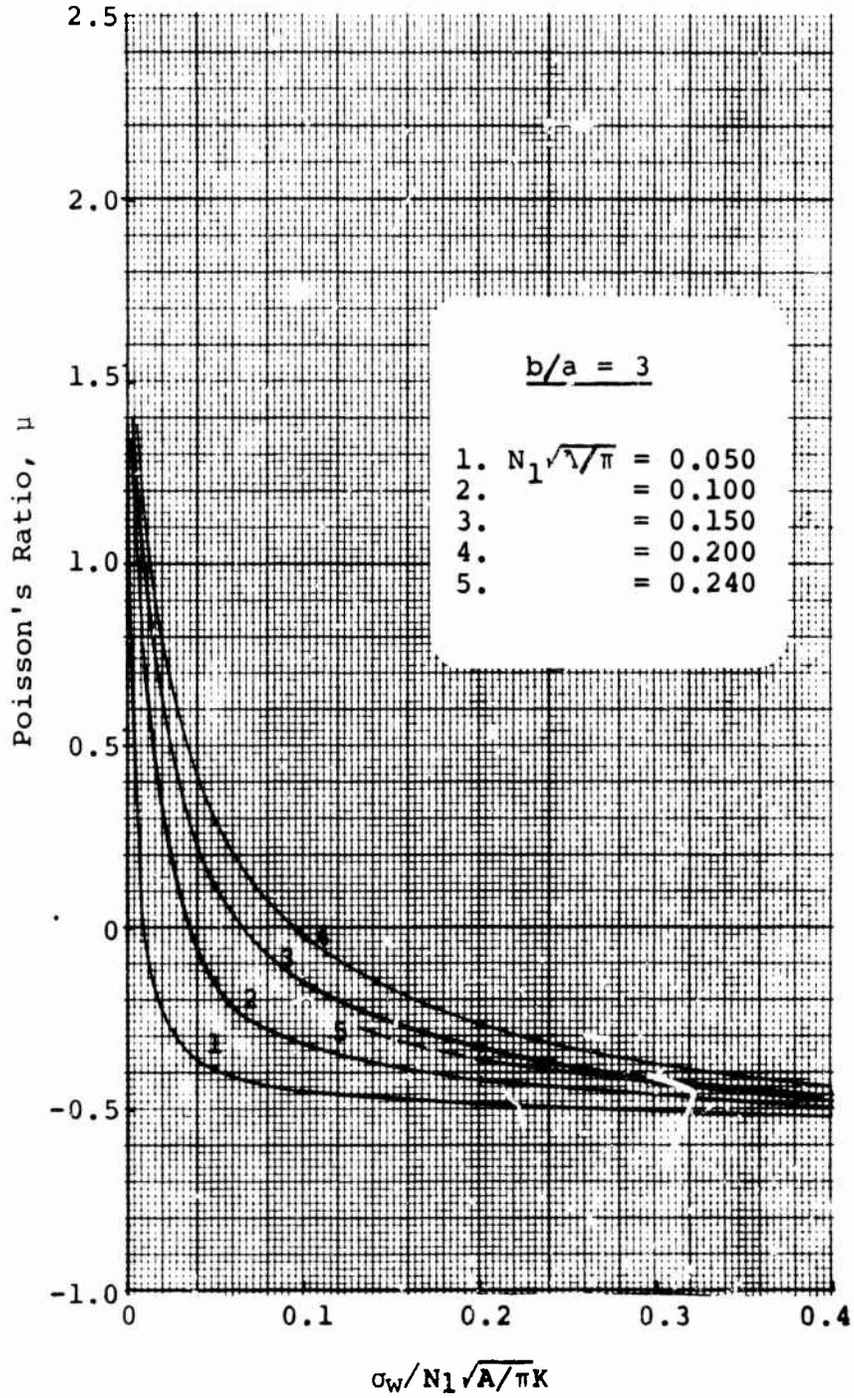

Figure 88. Poisson's Ratio (Aspect Ratio = 3): Linearly Elastic Yarn, $\sigma_w/\sigma_f = 2$

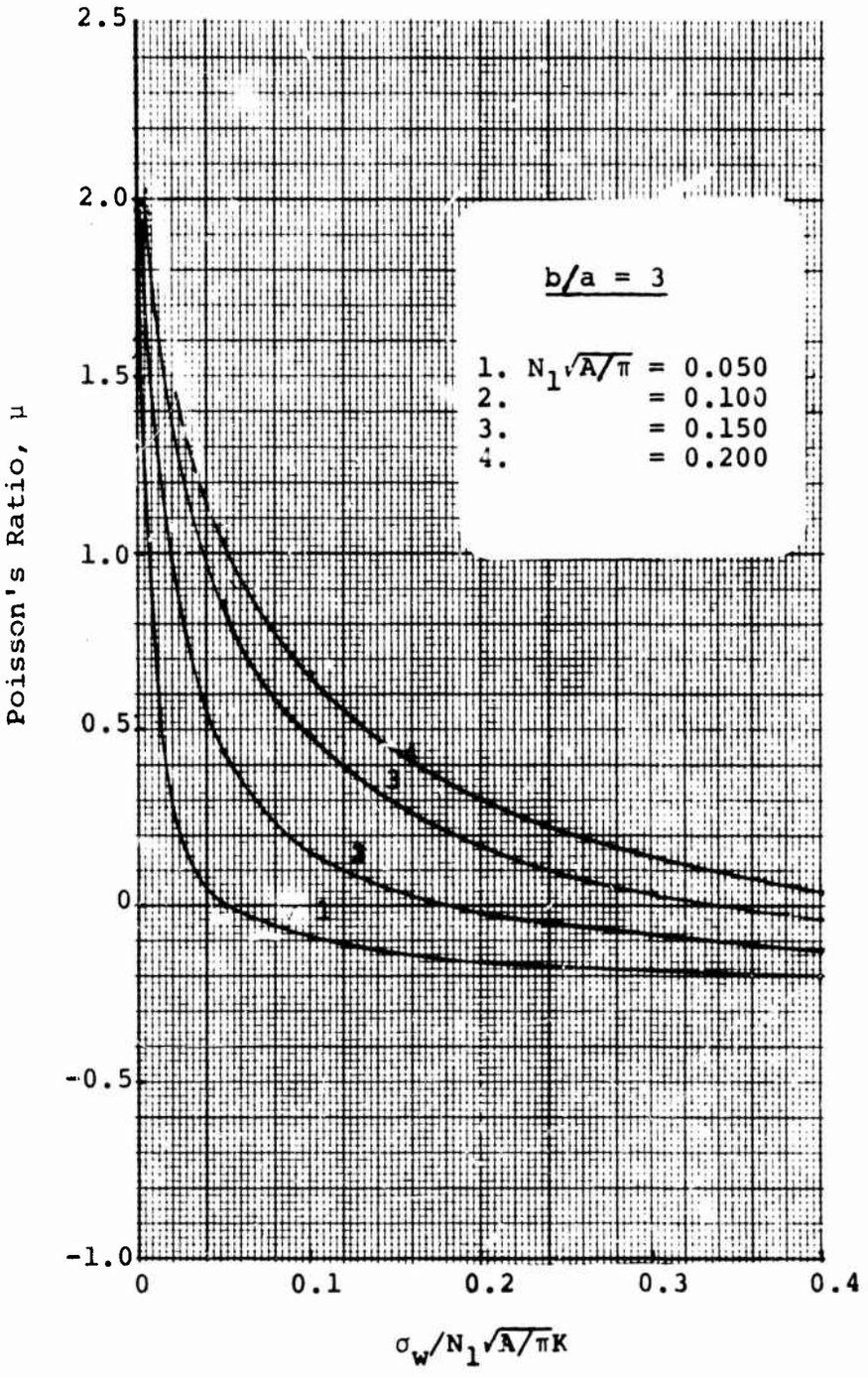

Figure 89. Poisson's Ratio (Aspect Ratio = 3): Linearly Elastic Yarn, $\sigma_w/\sigma_f = 5$

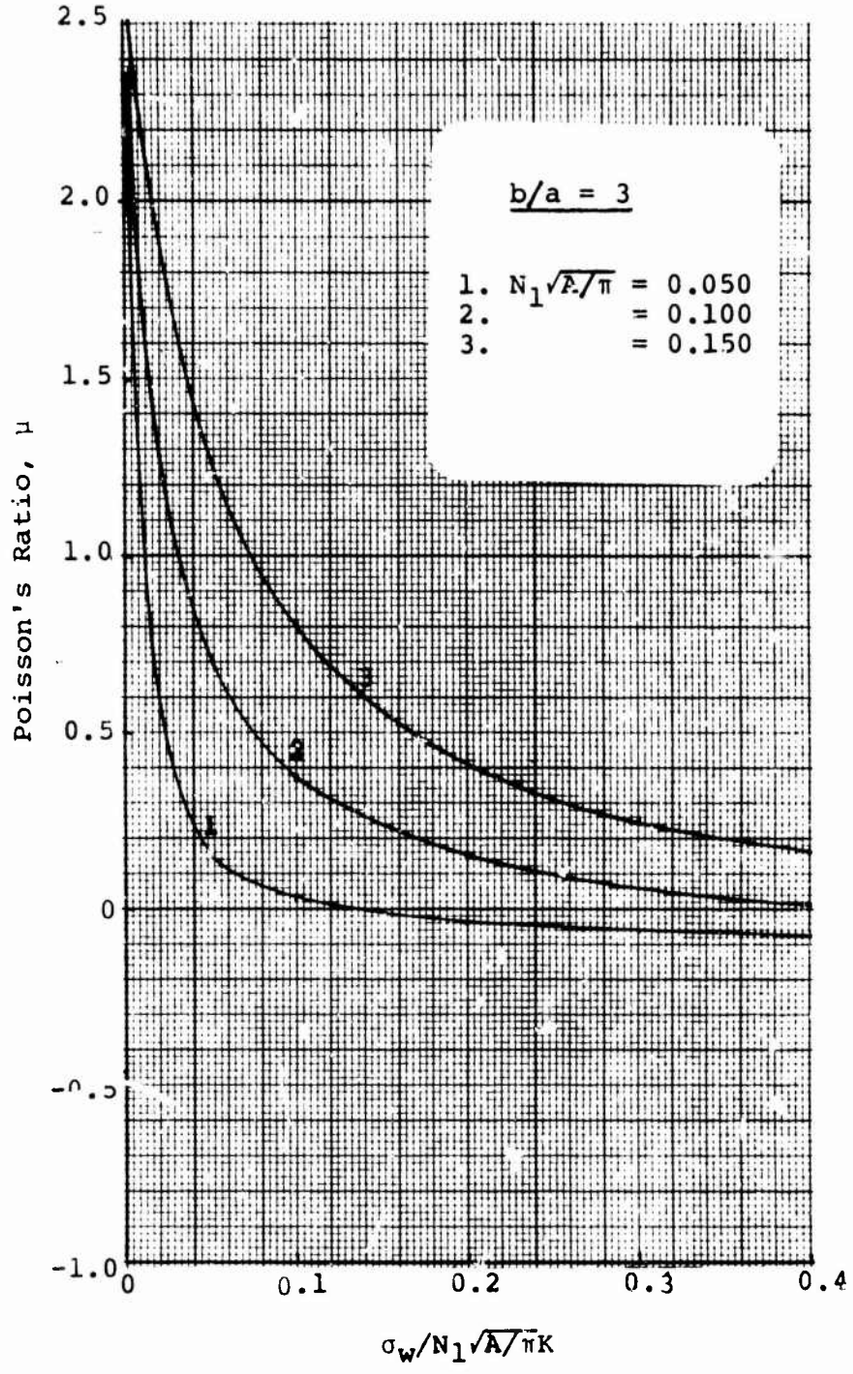

Figure 90. Poisson's Ratio (Aspect Ratio = 3): Linearly Elastic Yarn, σ_w/σ_f = 10

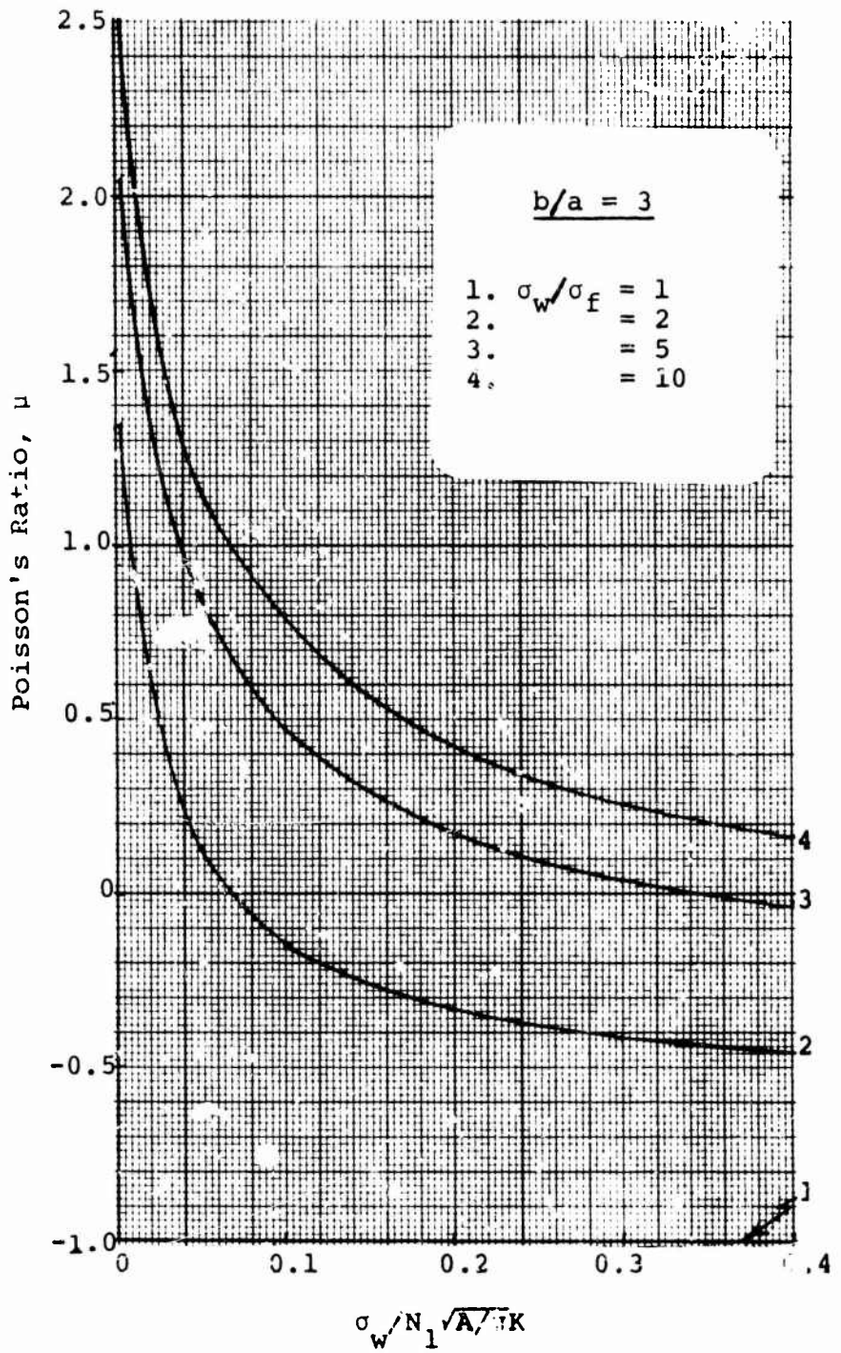

Figure 91. Poisson's Ratio (Aspect Ratio = 3): Linearly Elastic Yarn, $N_1\sqrt{A/\pi} = 0.15$

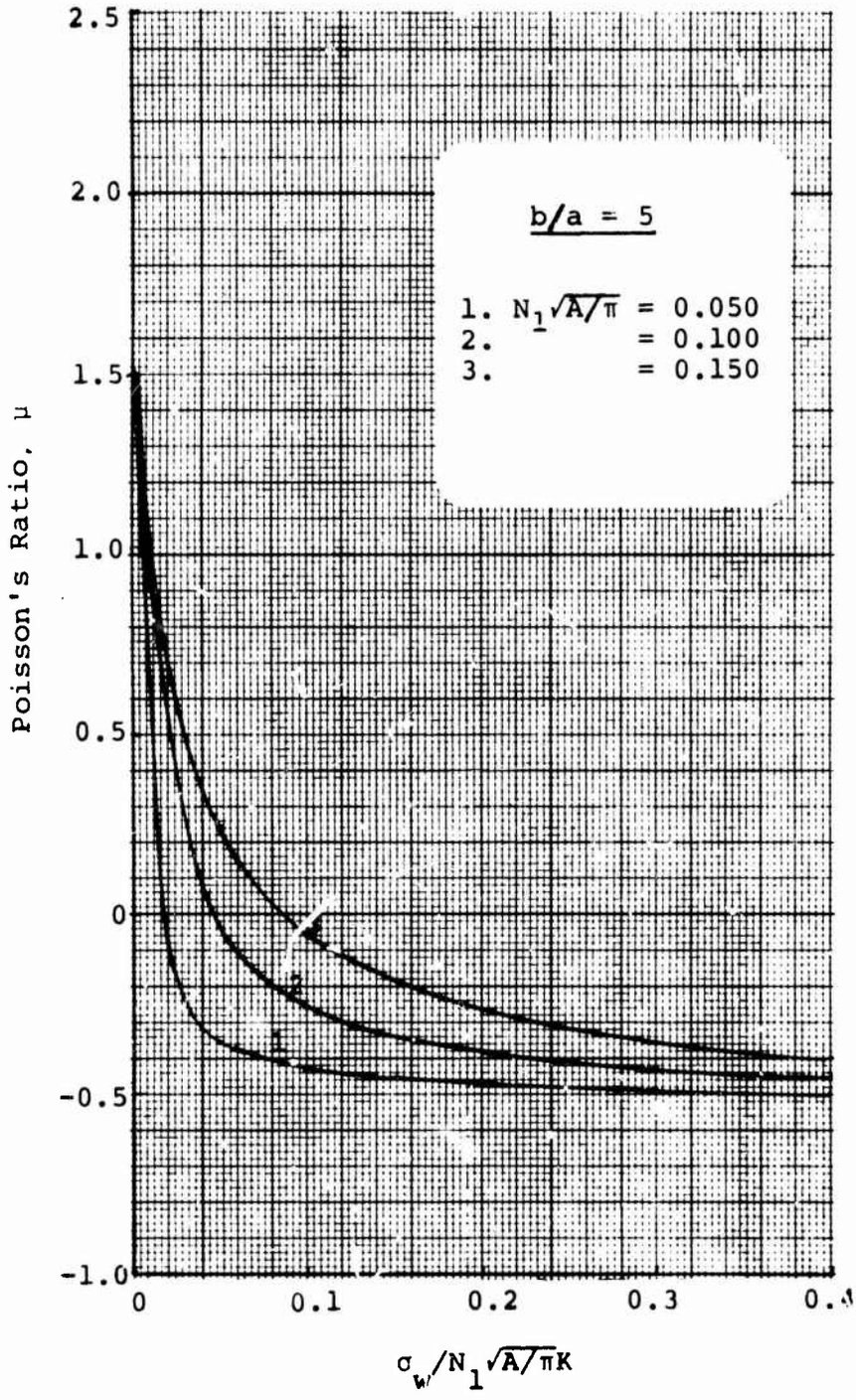

Figure 92. Poisson's Ratio (Aspect Ratio = 5): Linearly Elastic Yarn, $\sigma_w/\sigma_f = 2$

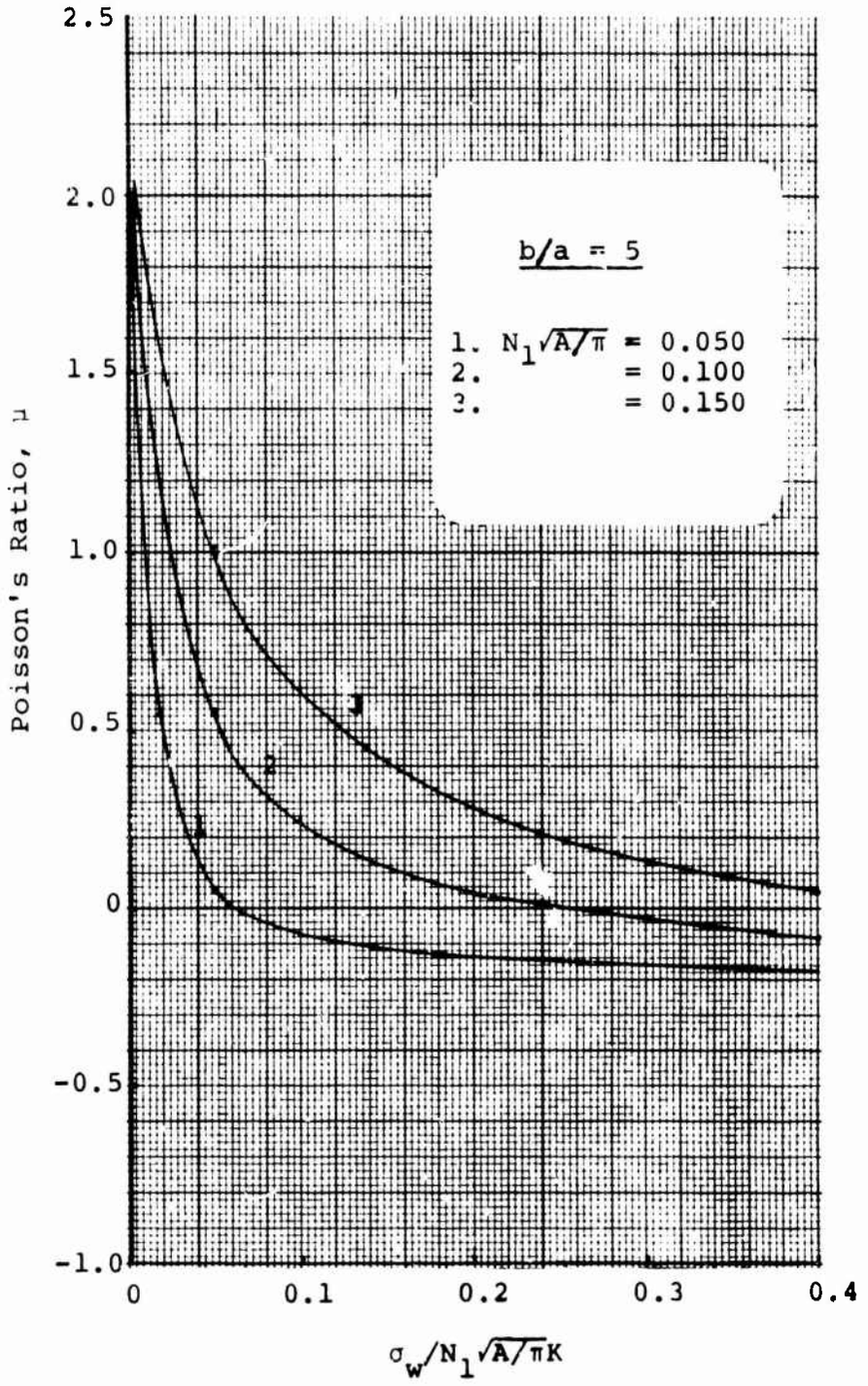

Figure 93. Poisson's Ratio (Aspect Ratio = 5): Linearly Elastic Yarn, $\sigma_w/\sigma_f = 5$

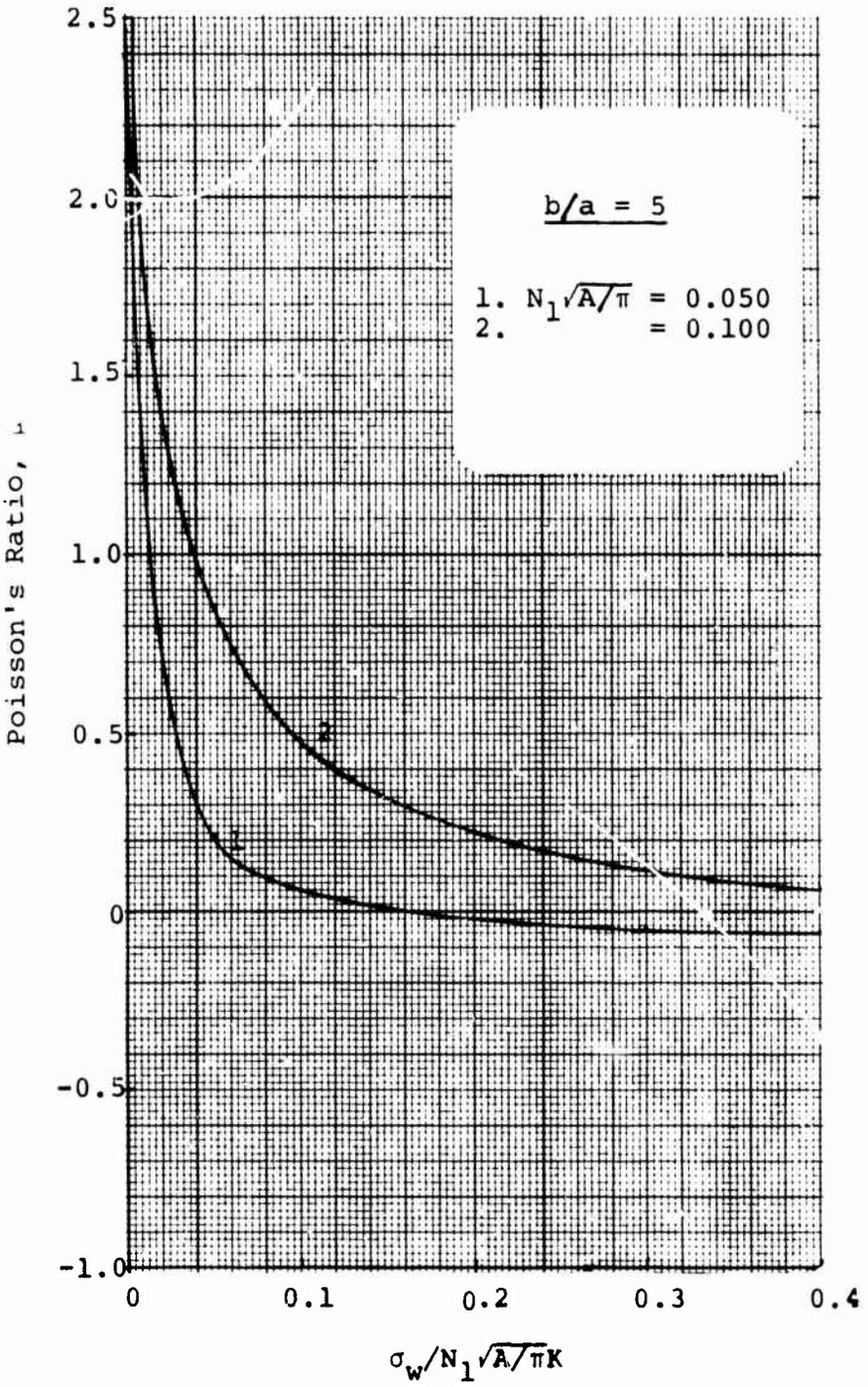

Figure 94. Poisson's Ratio (Aspect Ratio = 5); Linearly Elastic Yarn, σ_w/σ_f = 10

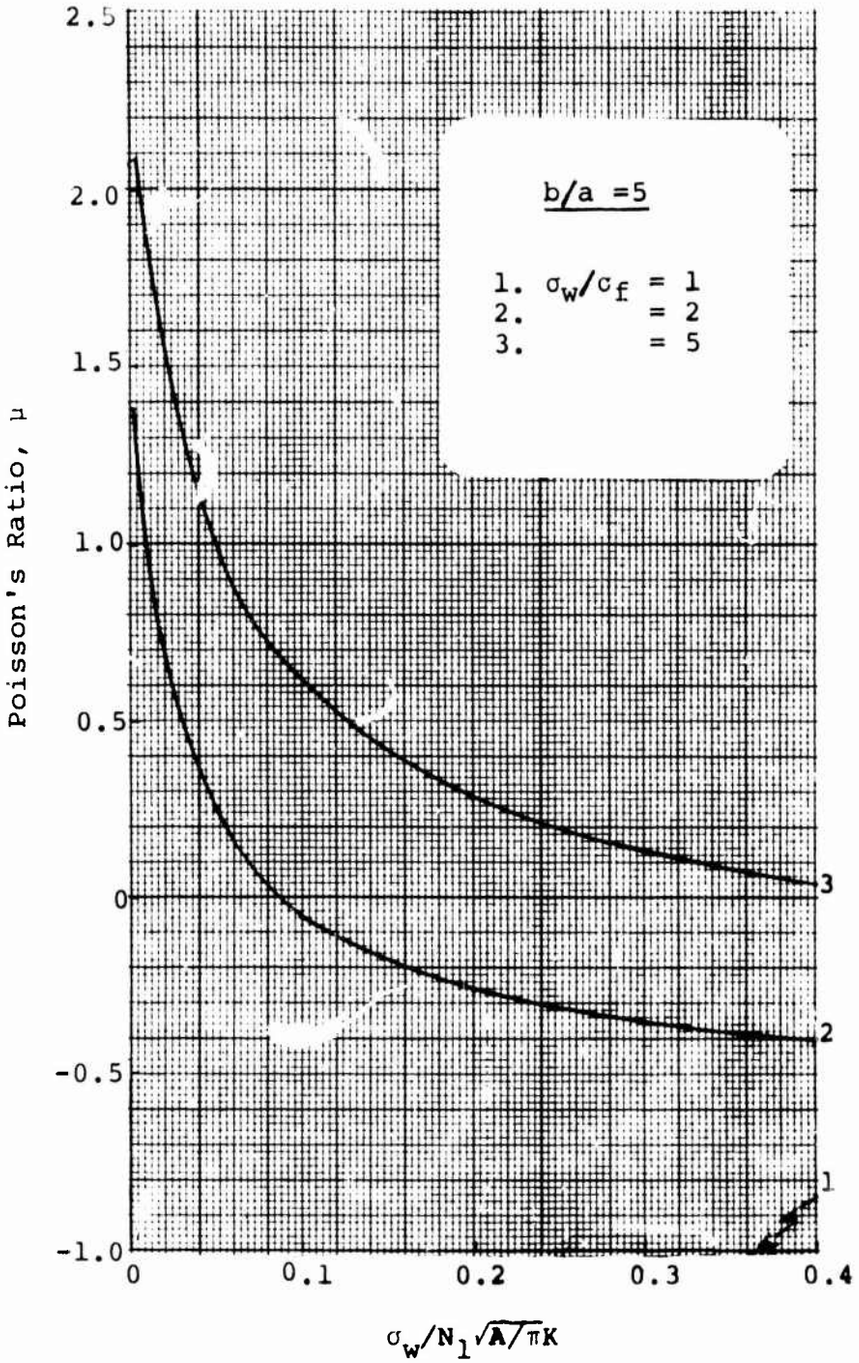

Figure 95. Poisson's Ratio (Aspect Ratio = 5): Linearly Elastic Yarn, $N_1\sqrt{A/\pi} = 0.15$

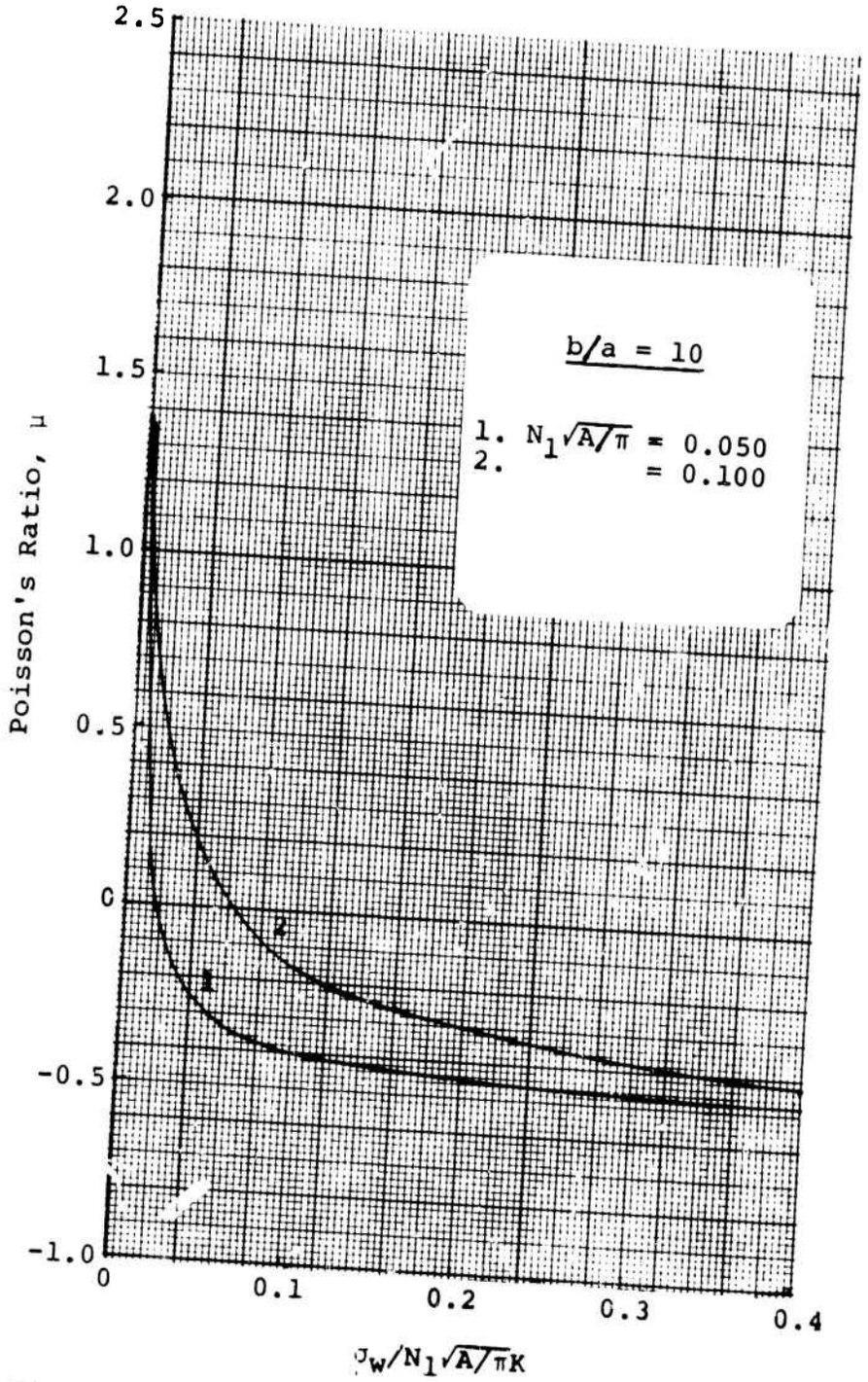

Figure 96. Poisson's Ratio, (Aspect Ratio = 10): Linearly Elastic Yarn, $\sigma_w/\sigma_f = 2$

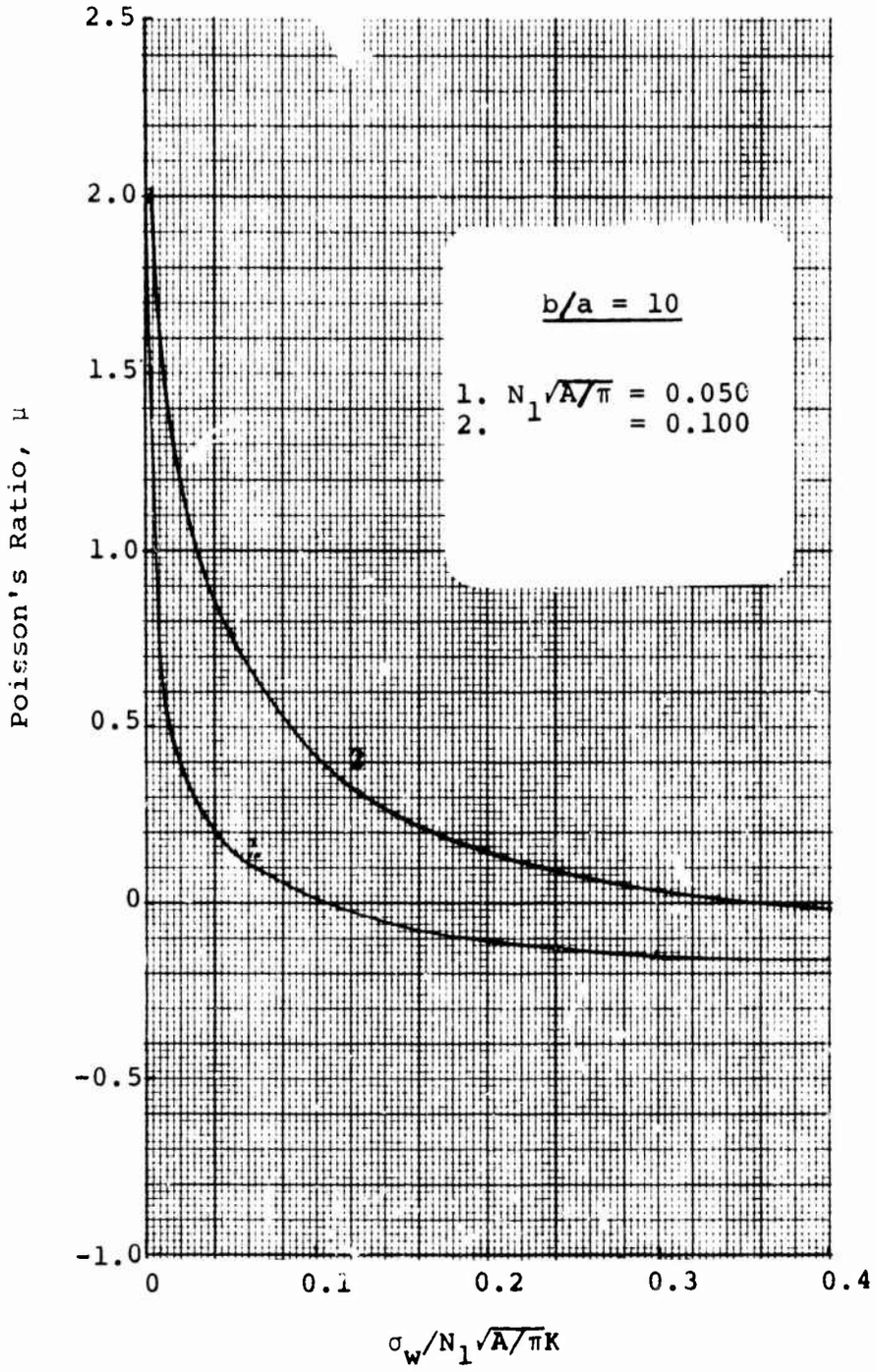

Figure 97. Poisson's Ratio (Aspect Ratio = 10): Linearly Elastic Yarn, $\sigma_w/\sigma_f = 5$

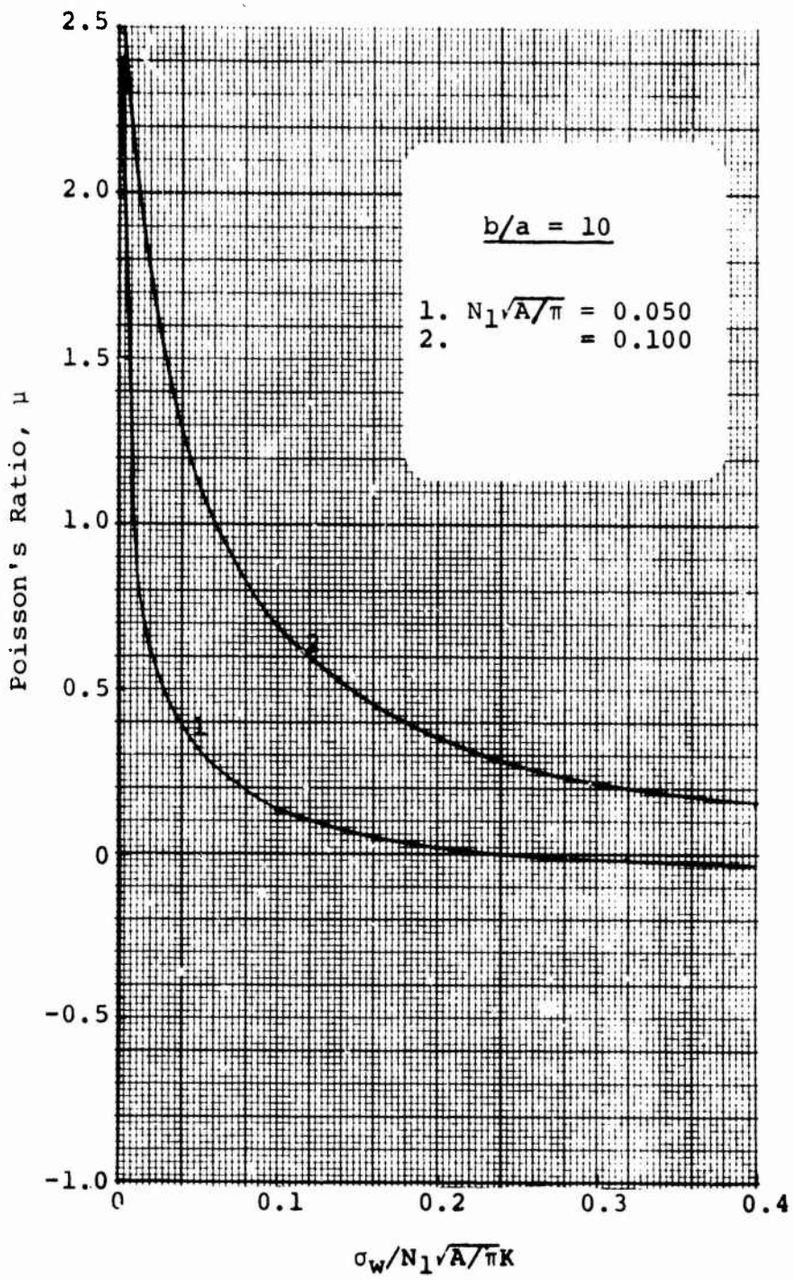

Figure 98. Poisson's Ratio (Aspect Ratio = 10): Linearly Elastic Yarn, σ_w/σ_f = 10

For $\sigma_w/\sigma_f \geq 2$ the Poisson's ratio is positive and greater than one at small values of the loading parameter, decreases with increasing values of the loading parameter becoming negative over a large portion of the load-parameter range. Also, μ increases somewhat with increasing $N_1\sqrt{A/\pi}$. The Poisson's ratio also increases positively with increasing loading ratio for particular aspect ratios and $N_1\sqrt{A/\pi}$. The trend with increasing yarn aspect ratio is not clear.

The Poisson's ratio for fabrics comprised of lenticular yarns and fabrics comprised of racetrack yarns follow the same trends and are nearly equal for low values of $N_1\sqrt{A/\pi}$. However, the Poisson's ratio for fabrics comprised of lenticular yarns increases more rapidly with increasing $N_1\sqrt{A/\pi}$ for a particular aspect ratio and loading ratio.

III. Experimental Study of Yarn Flattening

Experimental investigation shows that the degree of yarn flattening changes considerably from fabric to fabric. The geometry of yarns distorted by transverse yarns at the crossover points is indeed complex. In order to check the dependence of the cross-sectional shape on filament denier, yarn twist and fabric structure, a series of experimental fabrics was woven. Yarns of a total denier of 530 with twists of 1.75 and 4.35 turns per inch were prepared from yarns containing 2.0, 2.5 and 5 denier filaments. These yarns were woven into fabrics with 30, 40 and 50 warp ends per inch width and a wide range of pickspacing. Construction details of the yarns and fabrics are given in Tables 6 and 7 respectively. This series of fabrics encompasses constructions in which the warp yarn is essentially straight and the filling yarn highly crimped, the filling yarn essentially straight and the warp yarn highly crimped, and many combinations between these two extremes.

TABLE 6

YARN CONSTRUCTION

Material	Singles Yarn	Number of Plies	Total Yarn Denier	Denier per Filament	Yarn Ply Twist (tpi)
Enka Polyester Semi-dull	50/24 1/2tpi*Z	10	550	2.0	1.75Z
	120/48 1/2tpiZ	4	530	2.5	
	120/24 1/2tpiZ	4	530	5.0	4.35Z
	70/14 1/2tpiZ	7	535	5.0	

*turns per inch.

TABLE 7

FABRIC CONSTRUCTION

Yarn Ply Twist (tpi)	Warp Ends per Inch	Picks per Inch
1.75Z	30	24, 30, 34, 40, 44, 50
	40	24, 30, 34, 40, 44
	50	24, 30, 34, 40, 44
4.35Z	30	20, 24, 30, 34, 40, 44, 50
	40	24, 30, 34, 40
	50	24, 30, 34, 40, 44

All yarn was steam set to reduce twist liveliness and no size was used in the warp preparation. Samples of each fabric were set in embedding medium and sections were cut along the center lines of warp and filling yarns. Photographs were prepared of each section from which measurements of the yarn spacing and the major and minor axis of each yarn cross-section were made, in order to assess the relative importance of the various factors in determining the shape of the yarn cross-section.

In general the yarn cross-sections are represented very closely by the lenticular shape. The results are summarized in Figures 99 and 100 which show the aspect ratios, b_{lw}/a_{lw} and b_{lf}/a_{lf}, of the yarns as a function of the number of picks per inch width for the various fabrics. As shown in Figure 99, the aspect ratio for the fabrics woven from high twist yarns varies between 2.0 and 4.0. Detailed study of the individual results shows no significant difference between yarns with different denier per filament; neither is there any significant difference between the results for the warp yarns of all the fabrics. Thus the broken line in Figure 99 represents reasonablly well the experimental results for the warp yarns for all the fabrics woven from the high twist yarns. In contrast, the filling yarn aspect ratio depends very markedly both on number of warp and filling yarns per inch width.

The curves for both warp and filling yarns in Figure 99 show a decrease in aspect ratio with increasing number of picks per inch following an initial increase for very open fabrics. The decrease for increasing picks per inch is associated with the high crimp found in tight fabrics, which forces the crossing yarn to become more circular. In very open fabrics the yarns are influenced by the transverse forces applied by the crossing yarns over a smaller fraction of their length and tend to revert to a stable, more closely circular configuration.

The results for the fabrics woven from low-twist yarns are summarized in Figure 100. Study of these results shows, as anticipated, that the low-twist yarns are flattened to a greater extent than the high-twist yarns in comparable fabrics. For the low-twist yarns, the aspect ratio occasionally falls below 3.0 and rises as high as 6.0 in certain fabric constructions. The warp yarn aspect ratio is not very sensitive to changes in the number of warp yarns per inch, as was the case for the high-twist yarns. However, the filling yarn aspect ratio is very sensitive to changes in the number of picks per inch in the low-twist fabrics, and there is no real evidence of a maximum aspect ratio in these fabrics.

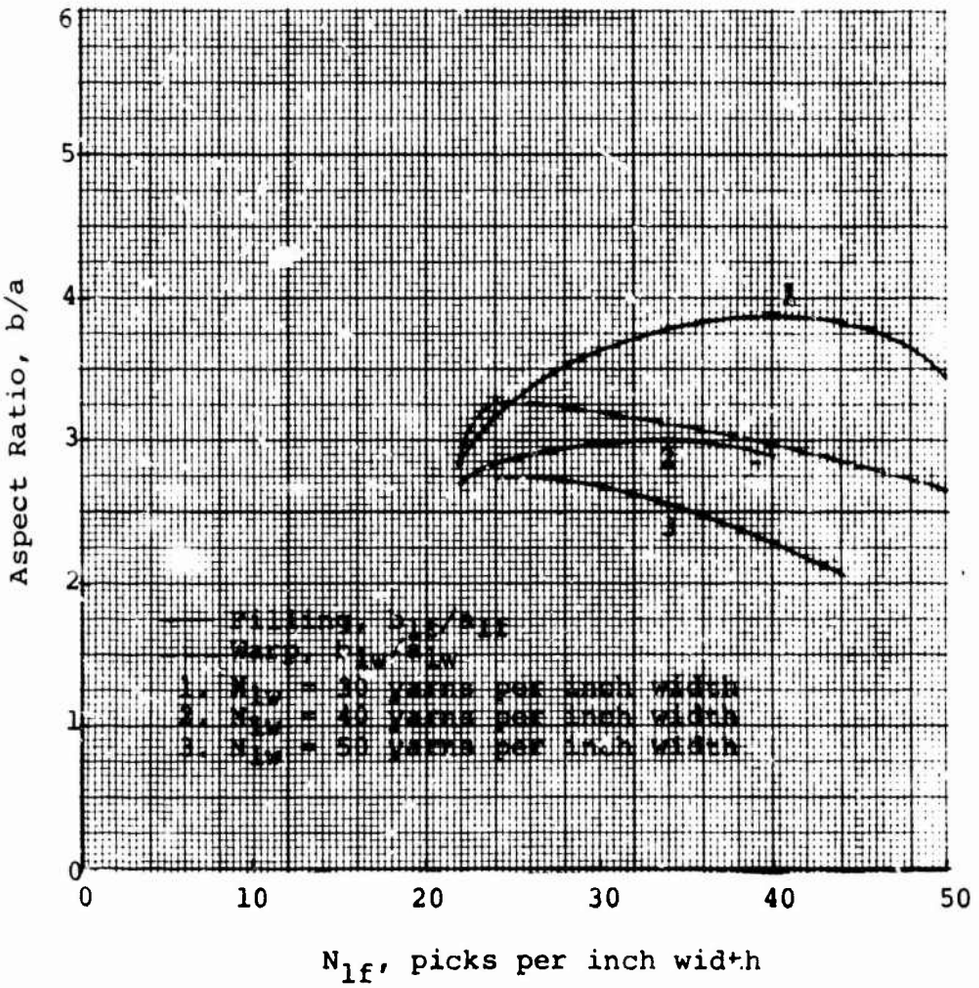

Figure 99. Yarn Aspect Ratio as a Function of N_{lf} and N_{lw} (4.3 tpi yarn ply twist)

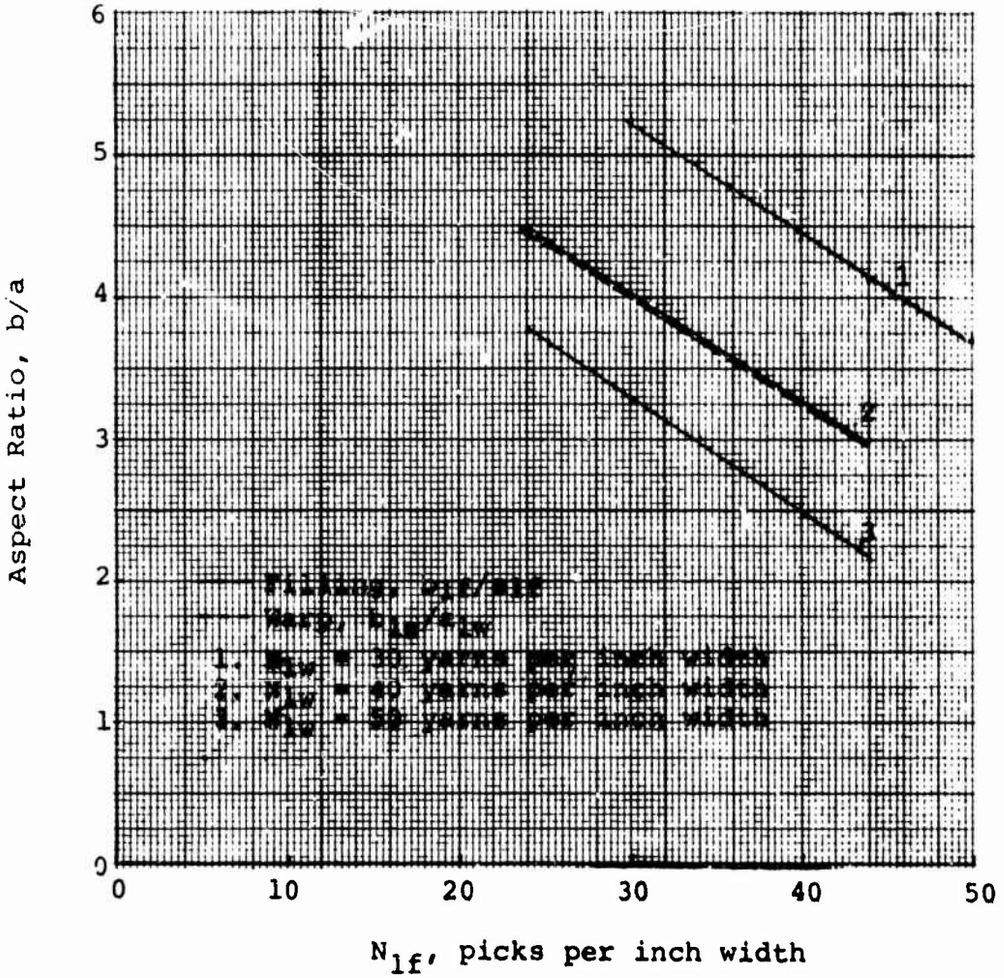

Figure 100. Yarn Aspect Ratio as a Function of N_{lf} and N_{lw} (1.8 tpi yarn ply twist)

The vast majority of the fabrics that are used in industrial applications where strength is important are tightly woven fabrics comprised of low-twist yarns. The foregoing experimental study indicates that the aspect ratio of the yarns in these types of fabrics is in the 3.5 to 5.0 range. Additionally, the value of the parameter $N_1\sqrt{A/\pi}$ for a tightly woven fabric is large. As shown in Figures 27 through 30, the radial separation between the node of the yarn cross-section and the crossing yarn in the lenticular yarn fabric model is not large for such fabrics; thus, it appears that the model is a worthwhile one to use in theoretical analyses of the load-extension response of such fabrics. Ultimate justification for the use of the model will depend upon experimental justification.

IV. Fabric Strength

The design engineer is usually concerned with predicting not only the load-extension behavior of the fabric but also the ultimate strength of the fabric. Assuming the load applied in the warp direction is greater than or equal to that applied in the filling direction, $\sigma_w \geq \sigma_f$, the fabric strength is given by the following expression (see Equation 17).

$$(\sigma)_{ult} = N_2 \cos\theta_2 (P_y)_{ult} \tag{60}$$

where $(P_y)_{ult}$ is the rupture strength of the yarn from which the fabric is woven. If it is assumed that the fabric is comprised of linearly elastic yarns having a modulus E_y and known rupture extension $(\varepsilon_y)_{rupt}$

$$(P_y)_{ult} = E_y(\varepsilon_y)_{rupt} = pE_f A(\varepsilon_y)_{rupt}. \tag{61}$$

The extended length of the yarn between crossovers in the fabric can be determined from the following expression

$$L_2 = (1+\varepsilon_y)L_1. \tag{62}$$

For the case of initially square fabrics with $\sigma_w \geq \sigma_f$, the load and also the yarn extensions are greater in the warp direction. Therefore, the ultimate strength of the fabric is governed by the load σ_w and the fabric will fail in the warp direction. For this case L_{1w} is determined from Equations 27 through 33 for specific initial parameters $N_1\sqrt{A/\pi}$ and b/a. Then $\sigma_{w(ult)}$ can be found from Equations 54 through 57 for a specific loading ratio.

Although the design engineer may only be interested in the strength or strength-to-weight ratio of a fabric, industrial fabrics are often rated by the efficiency with which the yarn strength is translated into fabric strength. This efficiency, E_w, in the warp direction is given in percent by (see Equation 60)

$$E_w = \frac{(\sigma_w)_{ult}}{N_{2w}(P_y)_{ult}} \times 100 = \cos\theta_{2w} \times 100. \qquad (63)$$

This quantity is plotted for initially square fabric woven from linearly elastic yarns in Figures 101 through 111 as a function of yarn rupture strain determined according to Equation 62 for various initial fabric constructions, degrees of yarn flattening and loading ratios. Results are not plotted for $\sigma_w/\sigma_f = 10$ with b/a = 2 and 3, nor for $\sigma_w/\sigma_f = 5$ and 10 with b/a = 5 and no results are given for b/a = 10 because the efficiency in these cases is greater than 99.5% for all values of $N_1\sqrt{A/\pi}$. As shown, the efficiency increases with increasing loading ratio, yarn aspect ratio, and yarn rupture strain. Additionally, the more open the fabric, i.e., the lower $N_1\sqrt{A/\pi}$, the higher the efficiency. All of these trends toward increased efficiency are the result of decreasing warp yarn crimp - yarn angulation with the fabric midplane - with increasing loading ratio, aspect ratio, yarn rupture strain and decreasing $N_1\sqrt{A/\pi}$.

The efficiency of translation of yarn strength into fabric strength is moderately greater for fabrics comprised of yarns with a lenticular yarn cross-section than for fabrics comprised of yarns with a racetrack cross-section: the angle the yarns make with the fabric midplane is less for fabrics composed of lenticular yarns.

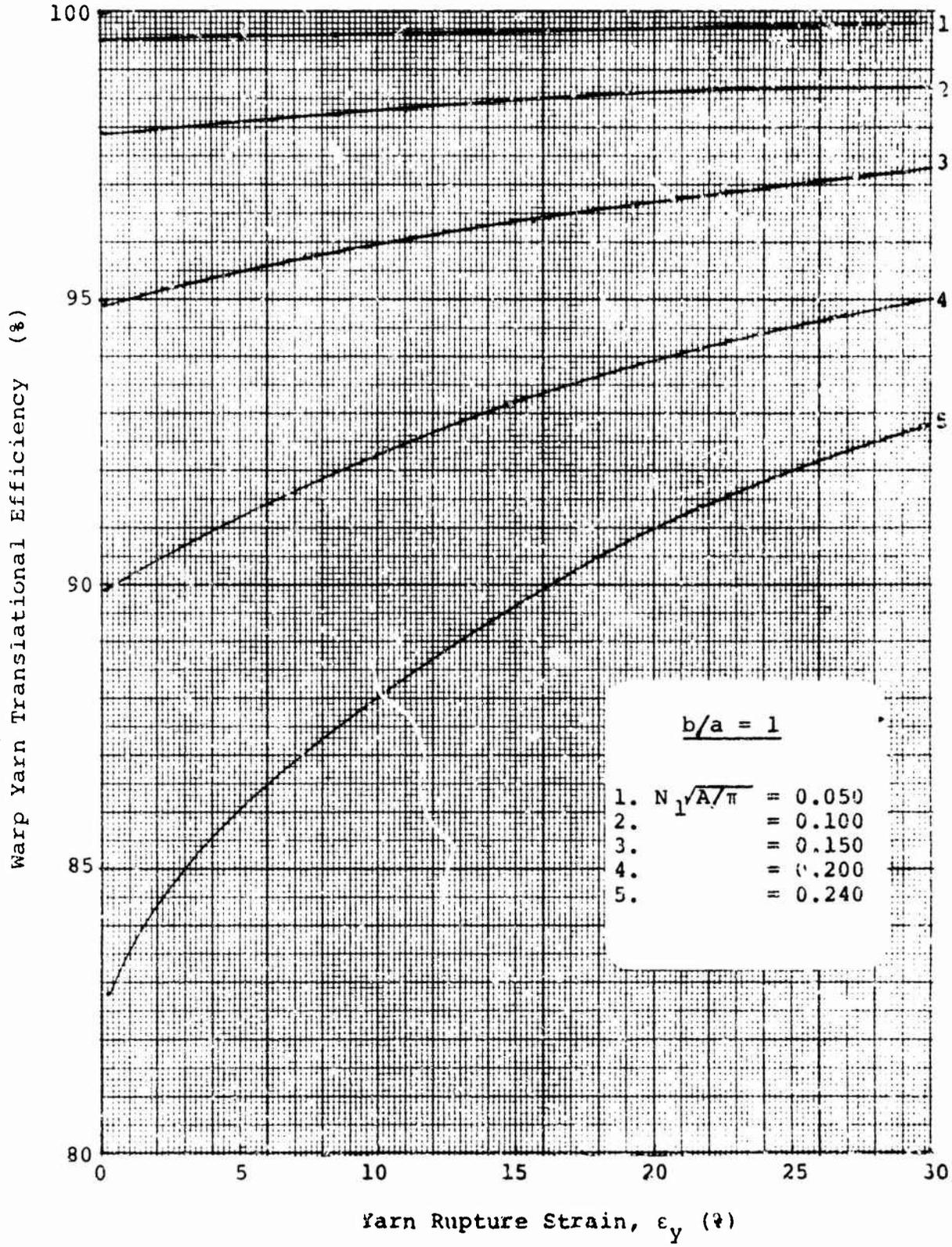

Figure 101. Yarn Translation Efficiency (Aspect Ratio = 1): Linearly Elastic Yarn, $\sigma_w/\sigma_f = 1$

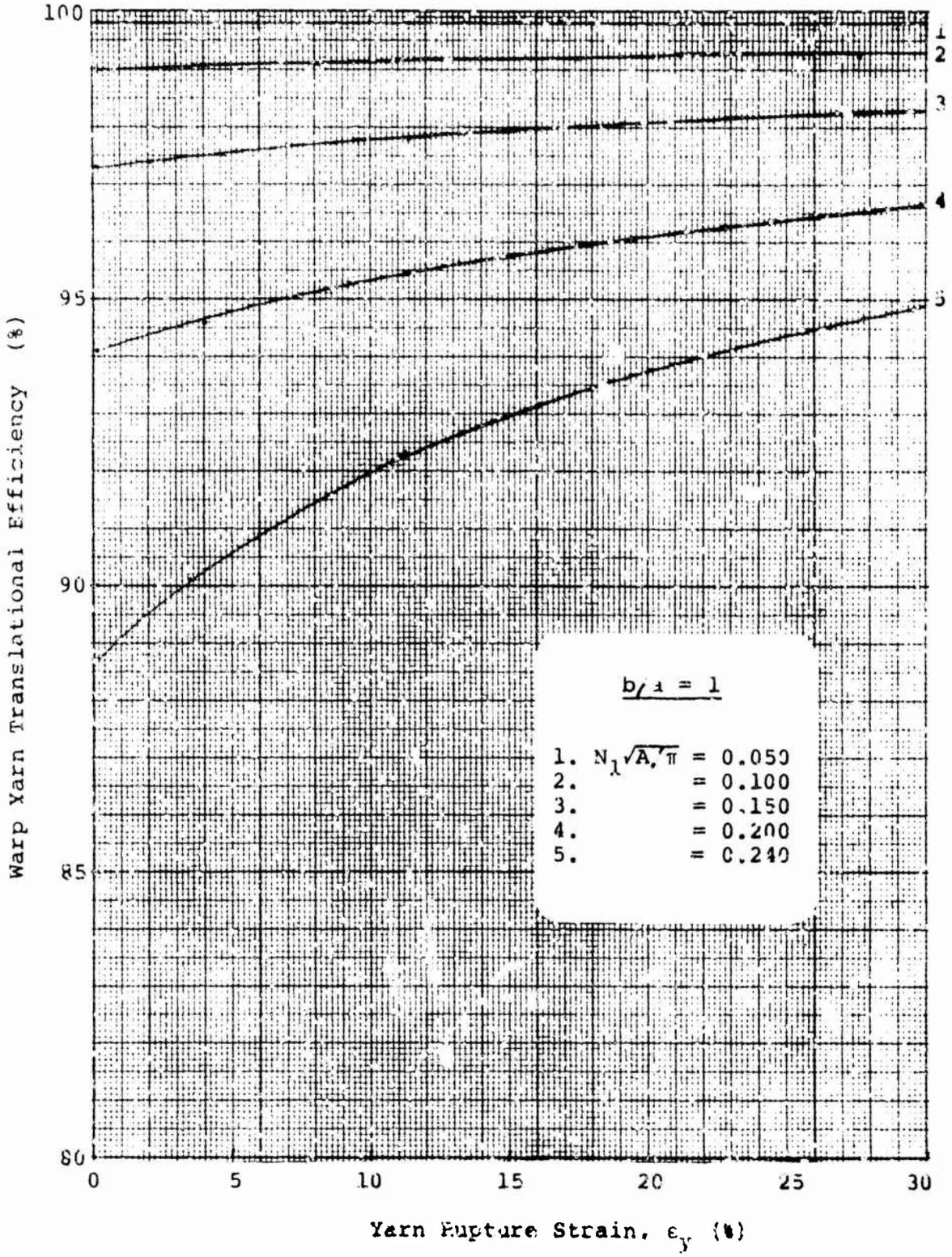

Figure 102. Yarn Translational Efficiency (Aspect Ratio = 1); Linearly Elastic Yarn, $\sigma_w/\sigma_\ell = 2$

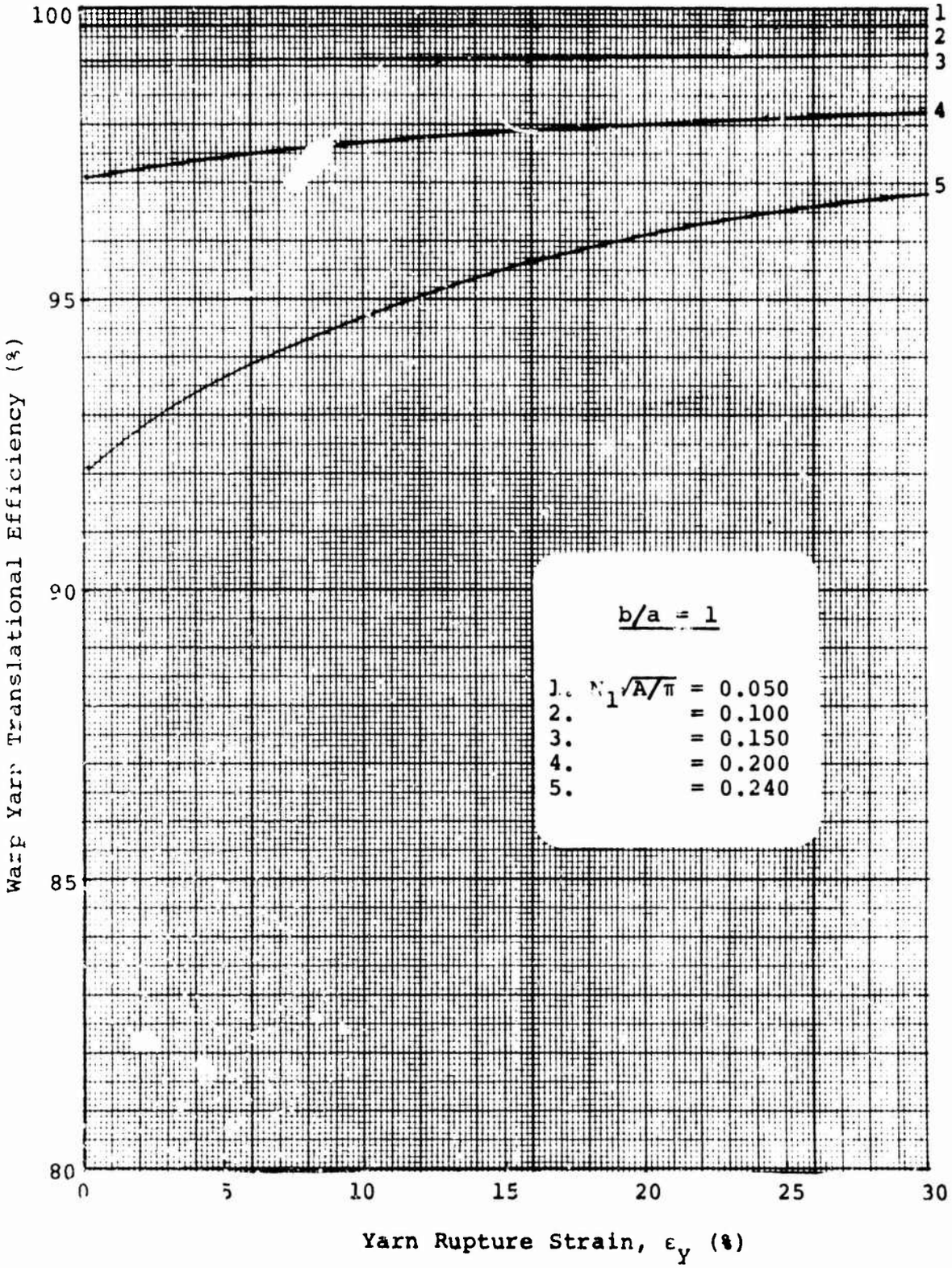

Figure 103. Yarn Translational Efficiency (Aspect Ratio = 1): Linearly Elastic Yarn, $\sigma_w/\sigma_f = 5$

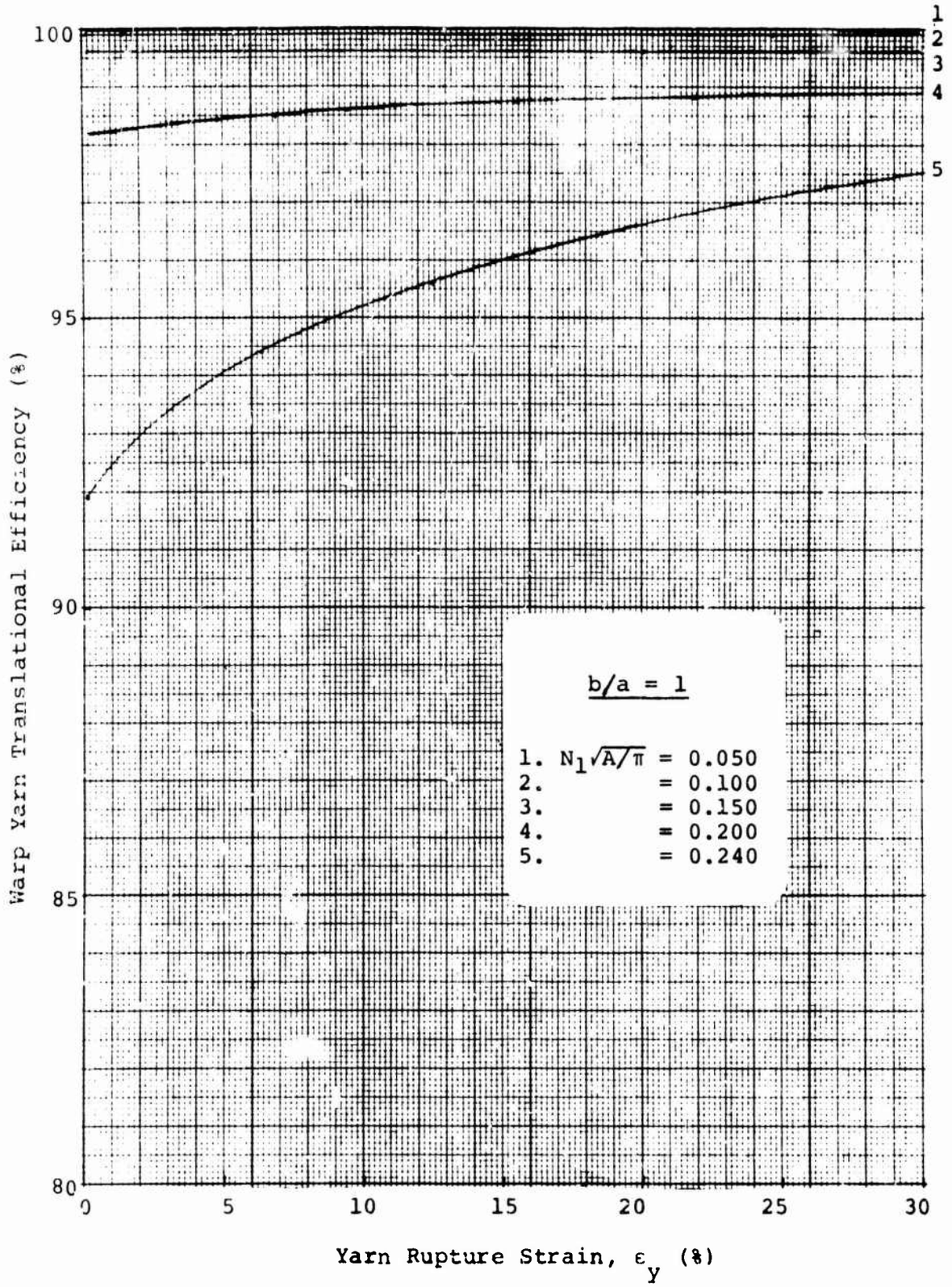

Figure 104. Yarn Translational Efficiency (Aspect Ratio = 1): Linearly Elastic Yarn, $\sigma_w/\sigma_f = 10$

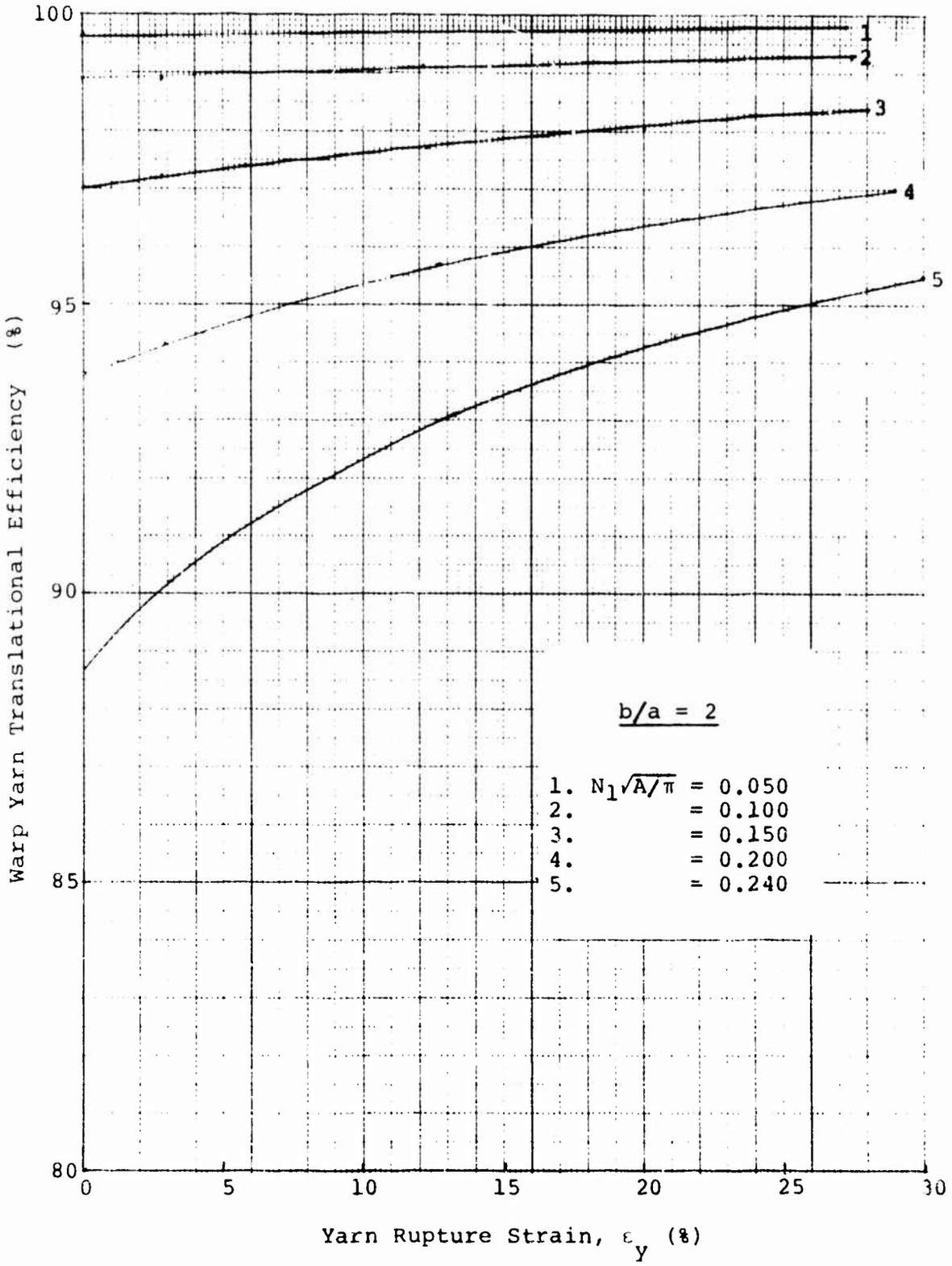

Figure 105. Yarn Translational Efficiency (Aspect Ratio = 2): Linearly Elastic Yarn, $\sigma_w/\sigma_f = 1$

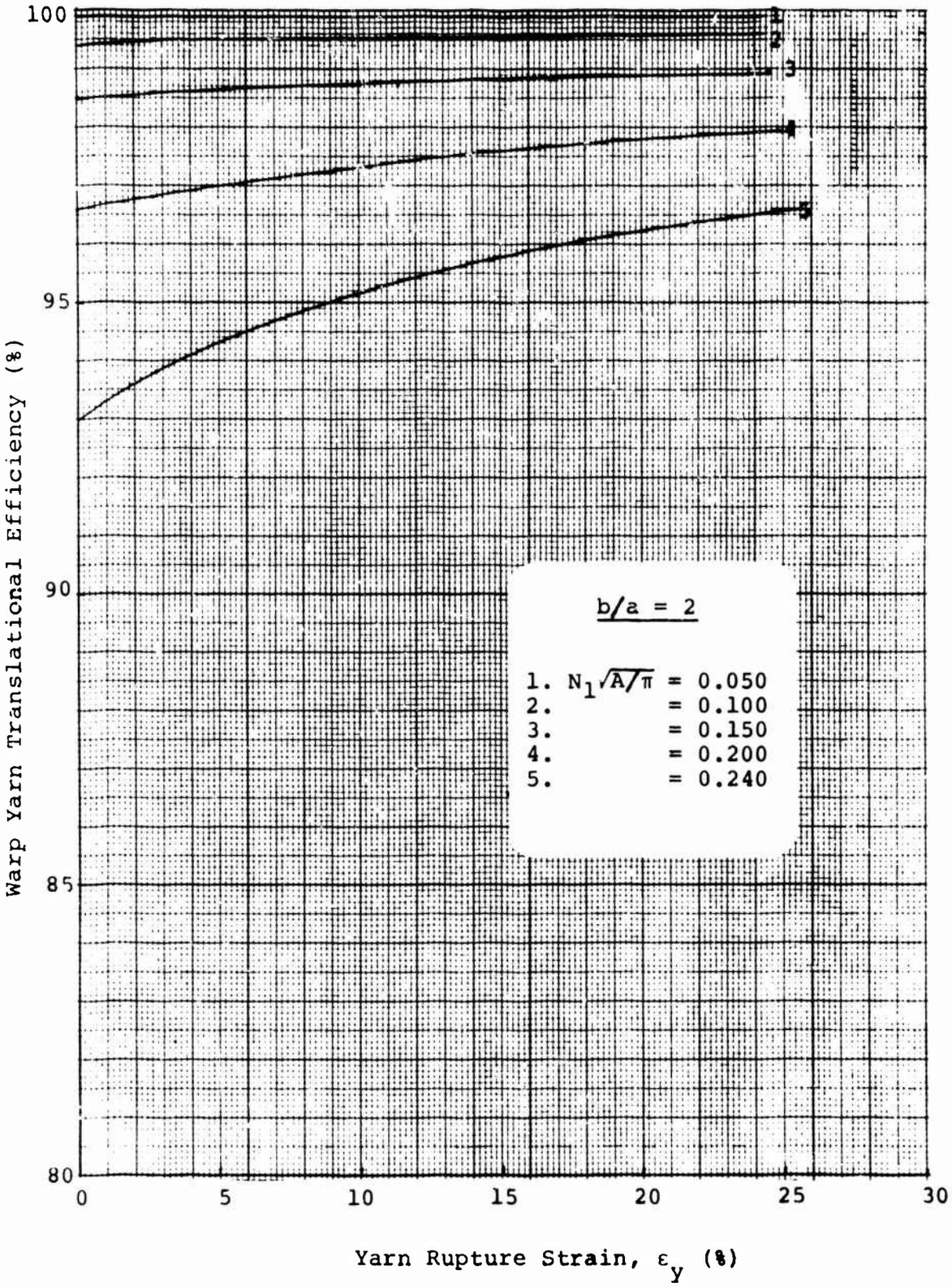

Figure 106. Yarn Translational Efficiency (Aspect Ratio = 2): Linearly Elastic Yarn, $\sigma_w/\sigma_f = 2$

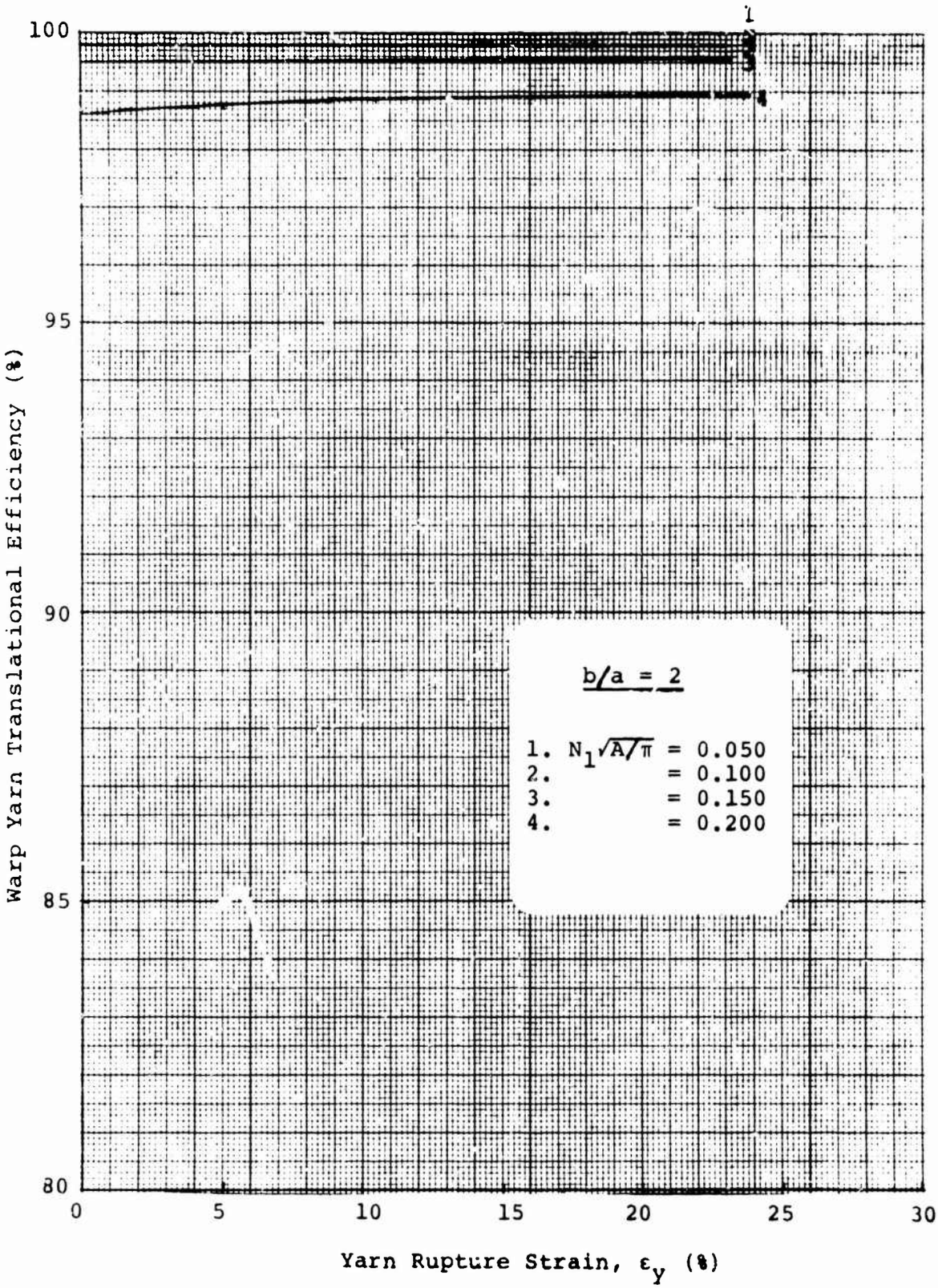

Figure 107. Yarn Translational Efficiency (Aspect Ratio = 2): Linearly Elastic Yarn, $\sigma_w/\sigma_f = 5$

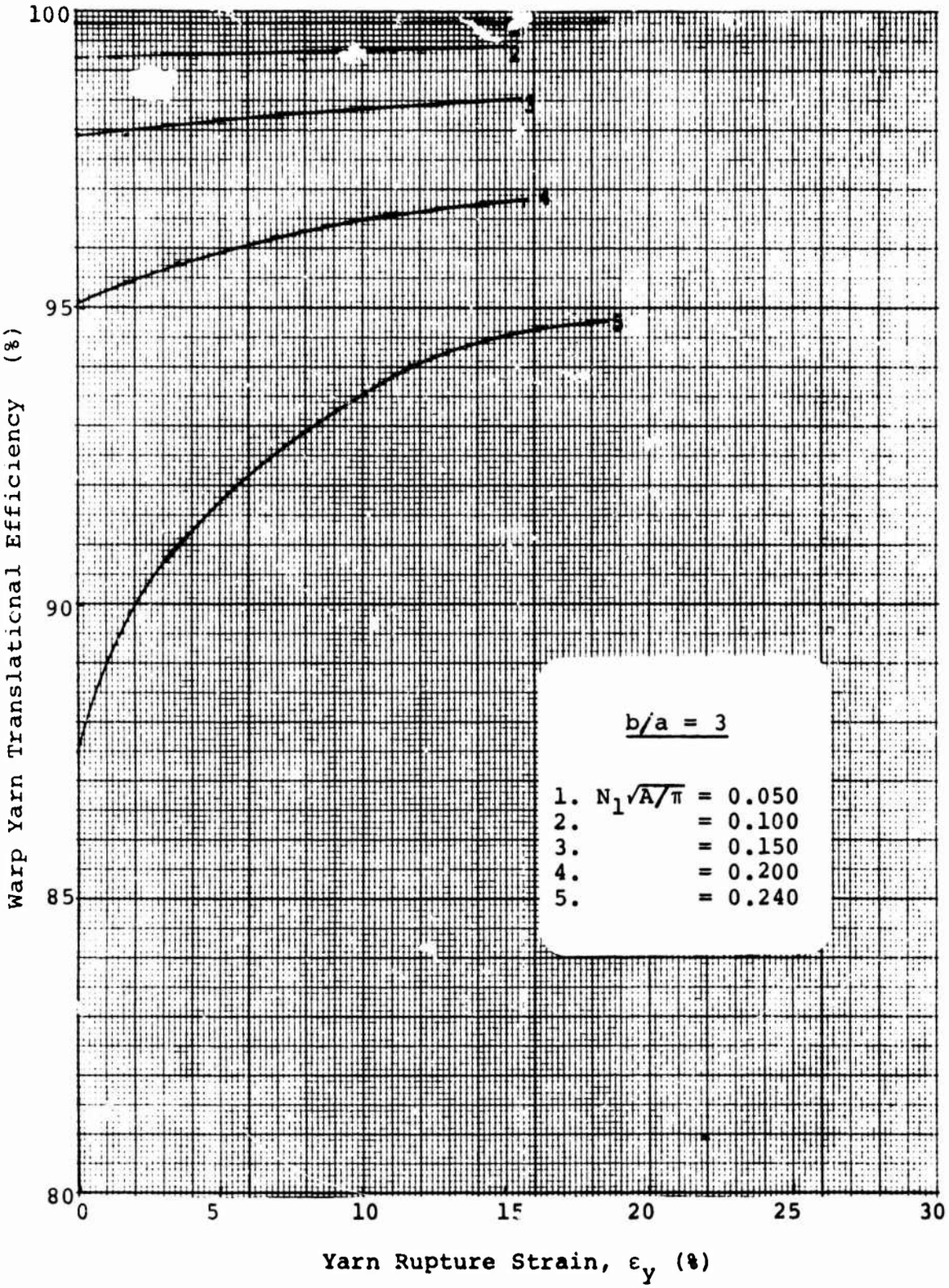

Figure 108. Yarn Translational Efficiency (Aspect Ratio = 3): Linearly Elastic Yarn, $\sigma_w/\sigma_f = 1$

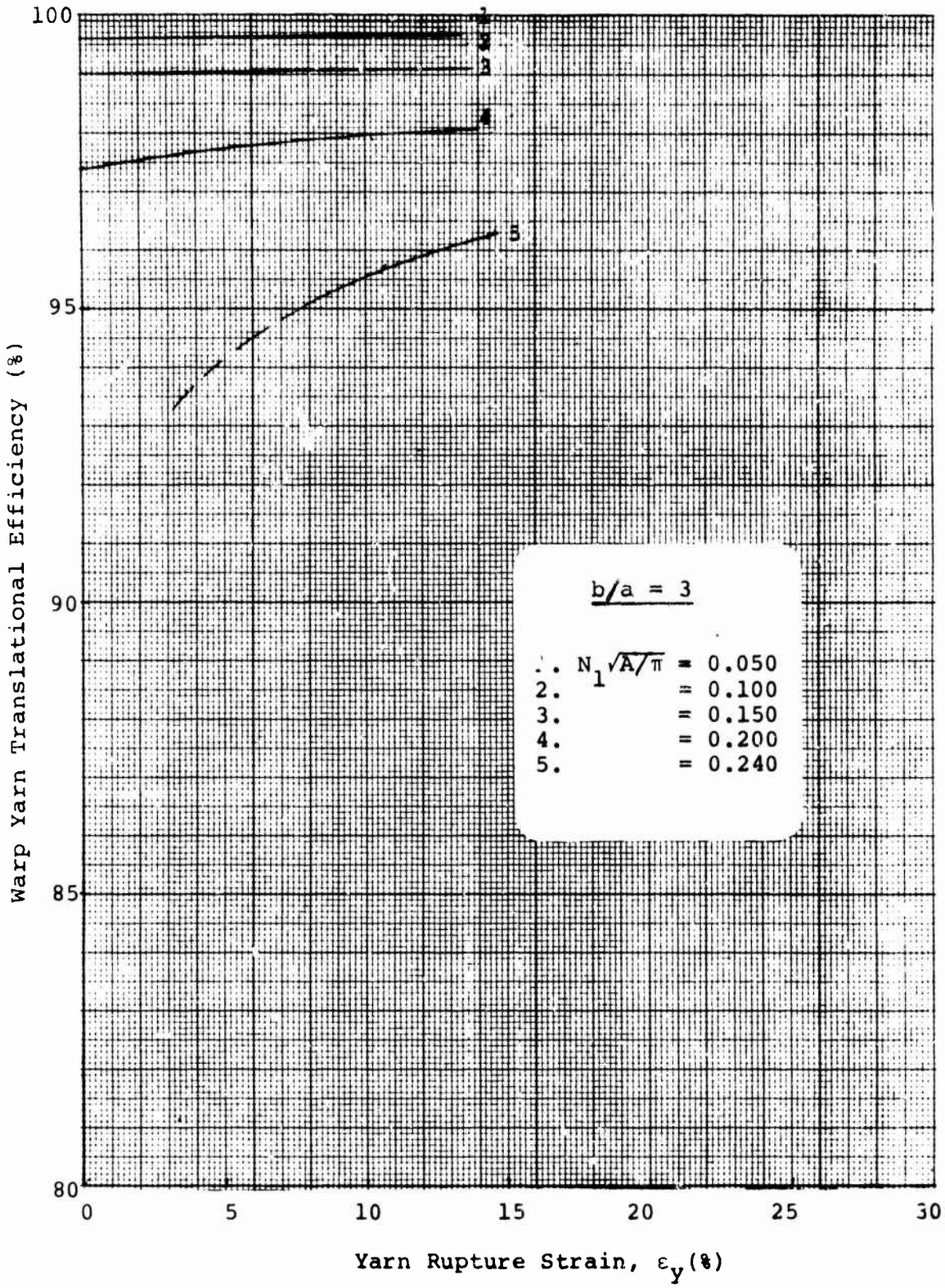

Figure 109. Yarn Translational Efficiency (Aspect Ratio = 3): Linearly Elastic Yarn, $\sigma_w/\sigma_f = 2$

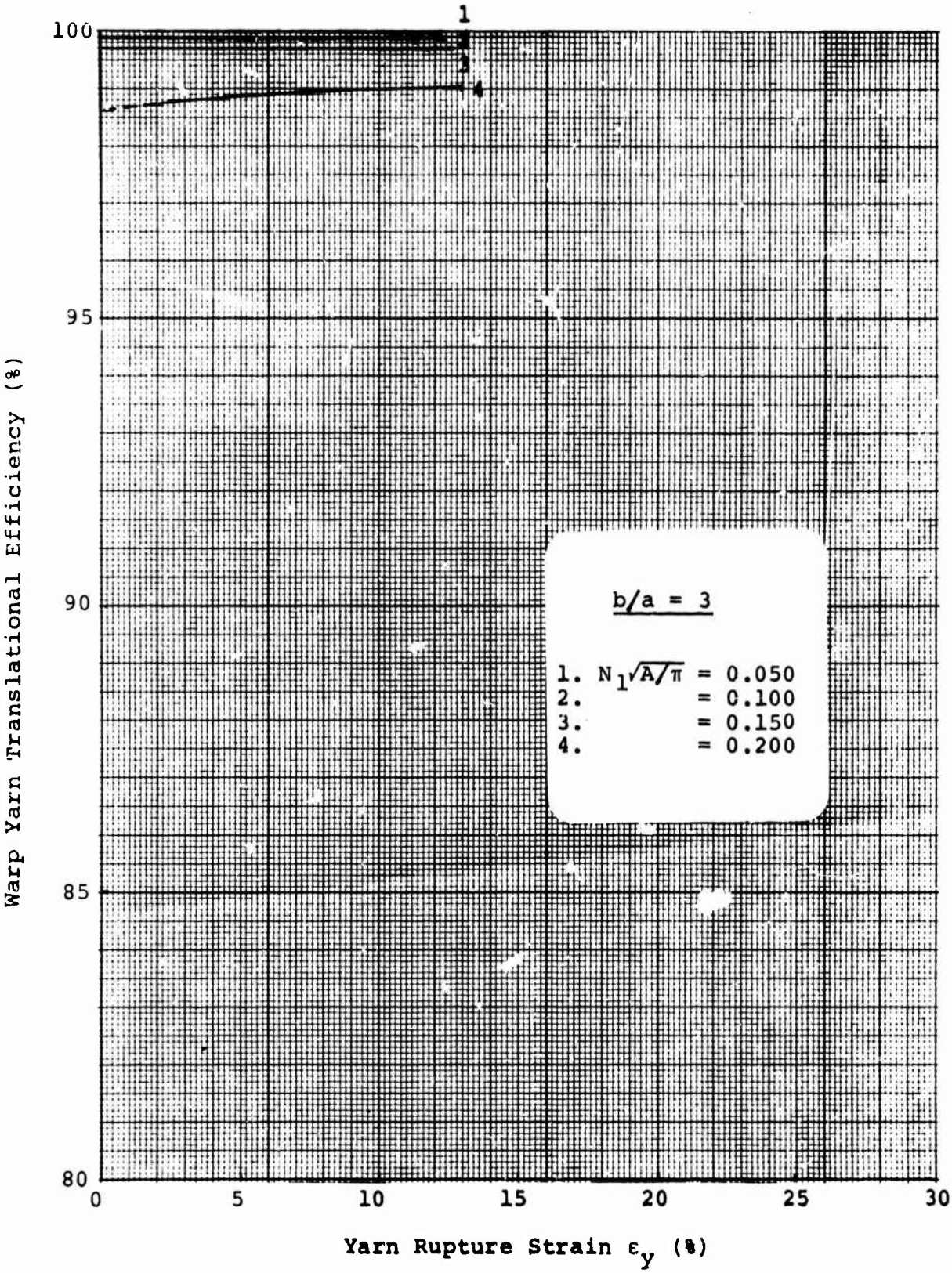

Figure 110. Yarn Translational Efficiency (Aspect Ratio = 3): Linearly Elastic Yarn, $\sigma_w/\sigma_c = 5$

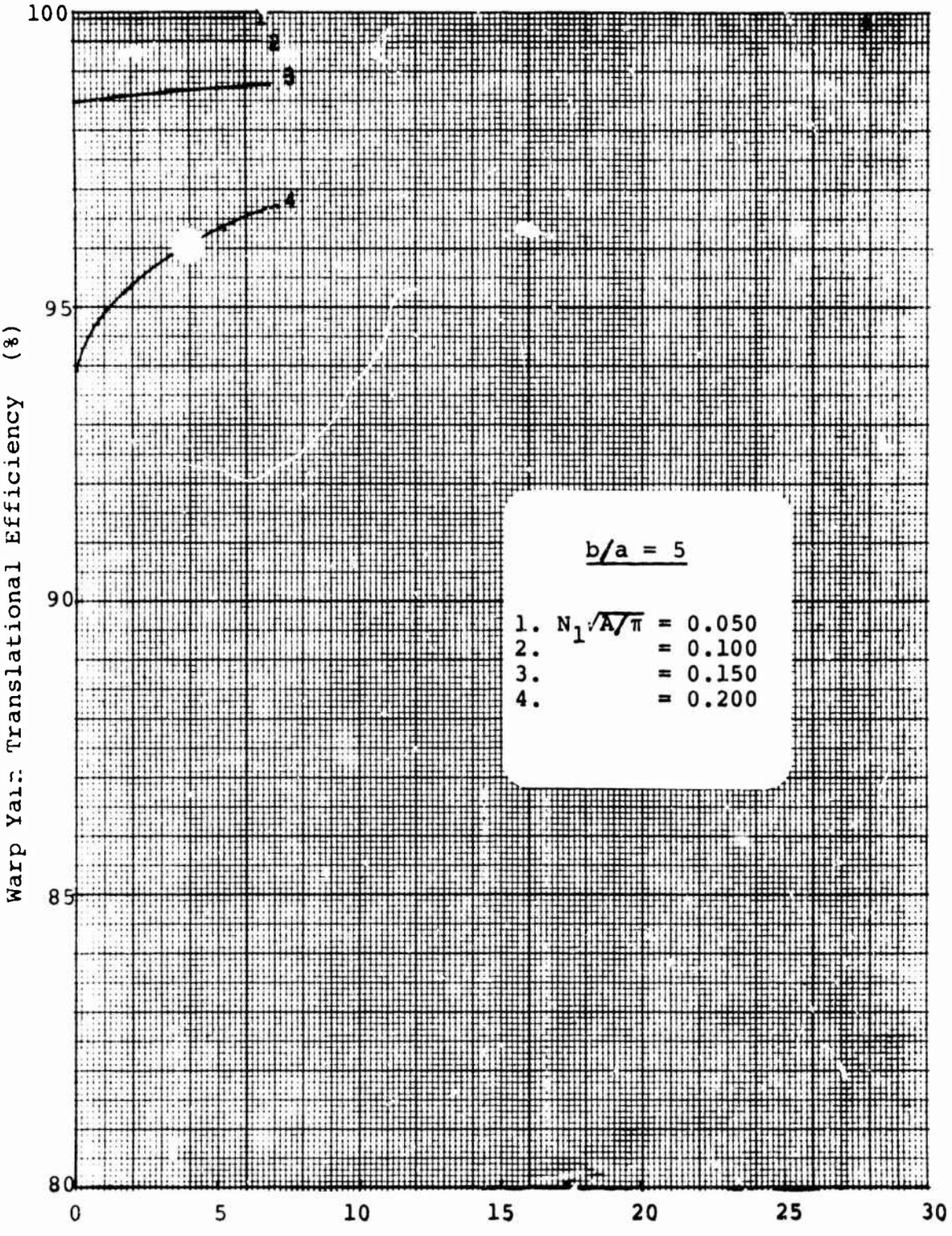

Figure 111. Yarn Translational Efficiency (Aspect Ratio = 5); Linearly Elastic Yarn, $\sigma_w/\sigma_f = 1$

Investigation of the yarn cross-section in fabrics woven from yarns twisted to low-to-moderate levels that have not been calendered indicates that it is best described by a lenticular shape. The foregoing analysis shows that the stress-strain response of plain-weave fabric comprised of such yarn and subjected to biaxial loading can be computed theoretically with an as yet unknown degree of accuracy.

For fabric woven from infinitely flexible, inextensible yarn, the amount of warpwise extension and filling contraction - crimp interchange - resulting from the application of a particular ratio of loads in the two directions decreases as the degree of yarn flattening increases. Additionally, the effective fabric Poisson's ratio is approximately the same for all yarn aspect ratios.

For initially square fabric woven from infinitely flexible, linearly elastic yarn, the slope of the fabric warp and filling load-extension diagrams subsequent to the extension that occurs instantaneously upon application of infinitesimal loads ($\sigma_w/\sigma_f > 1$) increases with increasing yarn aspect ratio.

EXTENSIONS OF THE ANALYSIS

As discussed in Reference 1, the divergence between the predicted and measured response of some types of real fabrics becomes quite large at low levels of applied load when the loading ratio is greater than one This is because the load-deformation behavior of fabrics at low-to-moderate loads - in the crimp interchange region - is strongly dependent upon the yarn bending rigidity, which has not been included in the analyses developed to date. However, attempts at doing so are being made in the continuation of the present work.

The analyses to date have assumed the yarns to be incompressible. In reality the yarn cross-section deforms - flattens further - as the applied tensile load increases due to the transverse forces at yarn crossovers. Efforts are underway to include this effect in future analyses.

REFERENCES

1. Freeston, W. D., Jr., Platt, M. M. and Schoppee, M. M. "Mechanics of Elastic Performance of Textile Materials, Part XVIII: Stress-Strain Response of Fabrics Under Two-Dimensional Loading," TRJ, Vol. 37, No. 11, November 1967.

2. Freeston, W. D., Jr., Schoppee, M. M. and Wall, M. A., "Stress-Strain Response of Fabrics under Two-Dimensional Loading Part I: Racetrack Yarn Cross-Section," U. S. Natick Laboratories, TR 73-24-GP, March 1971.

3. Hamburger, W. J., Platt, M. M., Morgan, H. M., "Mechanics of Elastic Performance of Textile Materials Part X: Some Aspects of Elastic Behavior at Low Strains," TRJ, Vol. 22, No. 11, November 1952.

4. Peirce, F. T., "The Geometry of Cloth Structure," J. Text. Inst. 28, T45 (1937).

5. Popper, P., "A Theoretical Investigation of Crimp-Interchange in a Woven Fabric Under Biaxial Stress," ASD-TDR-26-457 (1962).

APPENDIX

NUMERICAL PROCEDURE

FOR

SOLVING SIMULTANEOUS NONLINEAR EQUATIONS

APPENDIX

The angle associated with each value of b/a was obtained using Equation 30 by a simple iteration procedure. Since ϕ must be in the first quadrant, the iteration procedure was started with a guess of 0.1. As ϕ increased the ratio b/a decreased. If the calculated ratio was smaller than the desired ratio the increment was halved. The process was continued until the calculated ratio agreed with b/a to within 0.000001.

The angle θ_1 was also determined by a simple iteration procedure using Equation 32. The value of $N_1\rho$ increases as θ_1 increases to a maximum and then decreases. θ_1 cannot be determined for some values of $N_1\rho$ and b/a. Iteration was continued until the calculated ratio agreed with $N_1\sqrt{A/\pi}$ to within 0.000001.

L/R and GAP_i were determined by simple substitution using Equations 33 and 37 respectively

The two simultaneous equations, Equations 38 and 39, were solved for θ_{2w} and θ_{2f} by the Newton-Raphson method for simultaneous equations. This procedure is as follows: represent the two simultaneous equations by the expressions:

$$f(x,y) = 0$$
$$g(x,y) = 0 \qquad \text{(A1)}$$

where $x = \theta_{2f}$ and $y = \theta_{2w}$

Let

$$h_i = \Delta(x)_i = x_{i+1} - x_i$$
$$k_i = \Delta(y)_i = y_{i+1} - y_i \qquad \text{(A2)}$$

where

$$h_i = \frac{\begin{vmatrix} -f(x_i,y_i) & \partial f/\partial y_i \\ -g(x_i,y_i) & \partial g/\partial y_i \end{vmatrix}}{D}$$

$$k_i = \frac{\begin{vmatrix} \partial f/\partial x_i & -f(x_i,y_i) \\ \partial g/\partial x_i & -g(x_i,y_i) \end{vmatrix}}{D} \qquad \text{(A3)}$$

$$D = \begin{vmatrix} \partial f/\partial x_i & \partial f/\partial y_i \\ \partial g/\partial x_i & \partial f/\partial y_i \end{vmatrix}$$

Then:

1) Make an initial guess for x and y and designate these guesses by (x_0) and (y_0);

2) Calculate h_0 and k_0;

3) Determine

$$x_1 = x_0 + h_0$$

and

$$y_1 = y_0 + k_0 \qquad \text{(A4)}$$

4) If x_1 and y_1 satisfy Equations A1 to the desired number of decimal places, the solution has been obtained. If they do not satisfy Equation A1, substitute x_1 and y_1 for x_0 and y_0, h_1 and k_1 for h_0 and k_0 and go through the procedure again, etc.

The original guesses made for the angles θ_{2w} and θ_{2f} were $\vartheta_1 - 0.02$ for θ_{2w} and $\theta_1 + 0.02$ for ϑ_{2f}. Initially this procedure failed for many of the conditions. Placing restrictions on the guesses at each step of the iteration procedure forced convergence in most of these cases. These restrictions were as follows:

$$0 < \theta_{2w} < \theta_1, \; \theta_1 < \theta_{2f} \leq \phi.$$

$N_{2w}\rho$, $N_{2f}\rho$, ε_w and ε_f were then determined by direct substitution using Equations 40, 41, 25 and 26 respectively.